# DESIGN AND DEVELOPMENT OF CD205 TARGETED PLGA NANOPARTICLES AND EVALUATION OF ANTIGEN SPECIFIC IMMUNE RESPONSES

A Thesis Submitted to the College of Graduate and Postdoctoral Studies

in Partial Fulfillment of the Requirements for the

Doctor of Philosophy

in the College of Pharmacy and Nutrition, University of Saskatchewan

Saskatoon, Saskatchewan, Canada

By

Sheikh Tasnim Jahan

# PERMISSION TO USE

In presenting this thesis in partial fulfillment of the requirements for a postgraduate degree from the University of Saskatchewan, I agree that the Libraries of this University may make it freely available for inspection. I further agree that permission for copying this thesis in any manner, in whole or in part, for scholarly purposes may be granted by the professor who supervised my thesis work or, in their absence, by the Head of the Department or the Dean of the College in which my thesis work was done. It is understood that any copying, publication or use of this thesis or parts thereof for financial gain shall not be allowed without my written permission. It is also understood that due recognition shall be given to me and to the University of Saskatchewan in any scholarly use which may be made of any material in my thesis.

Requests for permission to copy or make any other use of material in this thesis in whole or in part should be addressed to:

Dean, of the College of Pharmacy & Nutrition
University of Saskatchewan
Saskatoon, Saskatchewan, Canada
OR
Dean, College of Graduate and Postdoctoral Studies
University of Saskatchewan
107 Administration Place
Saskatoon, Saskatchewan, Canada

# ABSTRACT

Stimulation of a patient's immune system to fight cancer is the underlying mechanism of immunotherapy. Cancer immunotherapy manipulates the dendritic cells (DCs) to identify the non-self present in the immunosuppressive microenvironment. This vaccination strategy based on nanoparticulate drug delivery system has the potential to treat cancer through packaging of therapeutic cargoes and delivering them to target immune cells (DCs). FDA approved poly-(D, L-lactic-co-glycolide) is approved for use in human due to its widely accepted properties such as low immunogenicity, minimal toxicity, biocompatibility and biodegradability. The goal of this project is to develop an understanding of a comprehensive relationship between nanoparticle (NP) structure and activity; and address the important requirements of NP structure and chemistry to selectively target specific markers. Plain NPs were prepared by emulsification solvent evaporation method with number of preparation variables. Double emulsification solvent evaporation method was used to prepare ovalbumin (OVA) and/or adjuvant loaded NPs. The DC targeting ligand (anti-CD205 monoclonal antibody) was attached to the NPs through two methods: covalent binding in presence of spacer molecule and physical adsorption method. Infra-red (IR) spectroscopy was performed to ensure the structural modification of NPs. Formulations were evaluated in respect to particle size, polydispersity index, zeta potential, surface display, cytotoxicity assay, OVA release studies, structural integrity of OVA in formulations, DC uptake study, DC maturation study, T cell proliferation study, estimation of total IgG and cytokine secretion profile. Results indicated that different formulation groups of NPs with different viscosity grades had desirable physicochemical properties. In case of the ligand (anti-CD205 antibody) conjugated NP's spectrum, there was presence of amide-I vibrations resulted from C=O stretching vibration near 1610 $cm^{-1}$ and N-H stretching of high intensity between 3310 to 3250 $cm^{-1}$. These characteristic IR peak reflects the

antibody conjugation with the NPs. DC uptake study shows when ligand was adsorbed onto the surface, these NPs were better uptaken compared to covalently attached formulations. No significant correlation was observed in uptake due to change of polymer viscosity and type. Highest expression of markers CD40, CD86 and MHCII molecules were observed with adjuvant (monophosphoryl lipid A)-antigen loaded targeted NPs. Though, high viscosity grade polymers (ester or COOH terminated) had higher OVA loading, they expressed lower percentage of markers compared to low viscosity formulations. These could be attributed to the release mechanism of the respective PLGA NP formulation. In addition, sufficient secretion of T helper cell 1 (Th1) and Th2 cytokines was observed. This confirmed the maturation of DCs as well as activation of the T cells. The T cell proliferation study confirmed the proliferation of cells *in-vitro* for both wild type balb/c and TCR transgenic (OT1) mice. Results from OT1 mice confirmed the OVA-specific immune response. Secretion of higher level of OVA-specific IgG by the formulations confirms the antigen specific immune response. Therefore, a comprehensive evaluation of effect of formulation parameters (polymer viscosity, polymer end group, conjugation methods) was performed to modulate the antigen specific immune response. These findings would be insightful when designing a vaccine formulation for a specific type of cancer.

# ACKNOWLEDGEMENTS

First and foremost I would like to thank Allah Almighty, Who gave me the strength and patience to bear with all the difficult time I have faced during this incredible journey.

I would like to express my sincere appreciation to my supervisor Dr. Azita Haddadi for her constant guidance and support. Without her help and assistance this thesis would not be possible. For her unwavering support, I am and will be grateful. Thank you for all the positive vibes that motivated me throughout my studies.

I would like to extend my thanks to the extraordinary members of my advisory committee, Dr. Adil J. Nazarali, Dr. Jim Xiang, Dr. Jian Yang and Dr. Edward S. Krol for their helpful suggestions, encouragement and support. I specially remember Dr. Adil Nazarali with great condolence as he passed away just a week before my thesis defence. I also thank Dr. David Blackburn, graduate chair of Pharmacy for his helpful contribution. Thank to all of my colleagues for their kind supports whenever needed.

I would thank College of Pharmacy and Nutrition for providing me financial support through New Faculty Graduate Student Support scholarship, graduate student service awards and travel awards. Thanks to Government of Saskatchewan for providing me Saskatchewan Innovation and Opportunity Scholarship for consecutive three years. Thanks to College of Graduate studies and Research (CGSR) for providing George and Arlene Loewen family bursary and travel award. Special thanks to Dr. Azita Haddadi for generously supporting me with stipend from Natural science and engineering research council of Canada and Canadian Breast Cancer Foundation grant.

Finally, I would like to thank my friends and family who helped contribute this thesis. I am grateful for your encouragement that I could be successful in the area of graduate studies. I would like to specially thank my husband Sams Mohammad Anowar Sadat for helping me throughout my research. Last but not the least; I would like to thank my daughter, Alina Zafreen for being true inspiration. Thanks for keeping me company on long walks.

# DEDICATIONS

*To my parents,*

*Hasna Hena Begum and Sirazul Hoque*

*&*

*Parents-in-law*

*Mohammad Abdus Salam and Salma Akter*

## TABLE OF CONTENTS

## LIST OF FIGURES

## TABLES

## LIST OF ACRONYMS AND ABBREVIATIONS

| | |
|---|---|
| Ab | Antibody |
| AD | Adsorption |
| Anti-CD 205 | Antibody against CD-205 receptor |
| APC | Antigen presenting cell |
| BCA | Bicinchoninic acid assay |
| BSS/BS3 | Bis-sulfosuccinimidyl suberate |
| CD | Cluster Differentiation |
| CFSE | Carboxyfluorescein succinimidyl ester |
| CpG | Cytosine triphosphate Guanine |
| CTL | Cytotoxic T lymphocyte |
| CTLA-4 | Cytotoxic T lymphocyte antigen-4 |
| COV | Covalent |
| DC | Dendritic cell |
| EDC/EDAC | 1-Ethyl-3-(3-dimethylaminopropyl) carbodiimide |
| EGFR | Endothelial growth factor receptor |
| ELISA | Enzyme Linked Immunosorbent Assay |

| | |
|---|---|
| ELISPOT | The Enzyme-Linked ImmunoSpot |
| FDA | Food and Drug Administration |
| FOXP3 | Forkhead box P3 |
| GM-SCF | Granulocyte-macrophage colony stimulating factor |
| HER | Human epidermal growth factor receptor |
| HGF | Hepatocyte growth factor |
| HLA | Human leukocyte antigen |
| ICAM | Intercellular cell adhesion molecule |
| Ig | Immunoglobulin |
| IL | Interleukin |
| INF | Interferon |
| IS | Immunological synapse |
| i.v./iv | Inherent viscosity |
| MAb | Monoclonal antibody |
| MCF | Michigan Cancer Foundation |
| MHC | Major histocompatibility complex |
| MPLA | Monophosphoryl lipid A |

| | |
|---|---|
| MPS | Mononuclear phagocyte system |
| MUC 1 | Mucin 1 |
| NaOH | Sodium hydroxide |
| NCR | Natural cytotoxic receptor |
| NHS | N-hydroxy succinimide |
| NK | Natural killer |
| NP | Nanoparticle |
| OVA | Ovalbumin |
| O/W | Oil in water |
| PAMP | Pathogen associated molecular pattern |
| PDGF | Platelet derived growth factor |
| PE | Phycoerythrin |
| PEG | Polyethylene glycol |
| PLGA | Poly lactic co-glycolic acid |
| PD-1 | Programmed death |
| PRRs | Pattern recognition receptors |
| PSMA | Prostate specific membrane antigen |

| | |
|---|---|
| PVA | Polyvinyl alcohol |
| ScFv | Single chain variable fragment |
| SDS | Sodium dodecyl sulfate |
| SUC | Sucrose |
| TCR | T cell receptor |
| TGF | Tumor growth factor |
| TH-1 | T helper cell-1 |
| TLR | Toll-like receptor |
| Treg | Regulatory T cells |
| TAA | Tumor associated antigen |
| TSA | Tumor specific antigen |
| TNF | Tissue necrosis factor |
| VEGF | Vascular endothelial growth factor |
| W/O/W | Water-in-oil-in-water |

# General overview

In this ‘manuscript style’ of thesis, the entire project work is presented in Chapters 2 to 5, each of which has its own hypothesis and objectives leading to achieve a common goal of the thesis.

In the beginning, an introduction and a general literature review pertaining to the subject of the thesis leading to overall hypothesis and objectives of the thesis in its entirety are given.

Subsequently, each chapter containing relevant literature review, introduction, materials and methods, results and discussion is presented. The style of all these chapters has been uniformly maintained irrespective of the journals considered for publication. At the end, a general discussion of the thesis in its entirety is given.

# CHAPTER 1

## 1 Literature review

### 1.1 Overview of immune system

The immune system consists of intricate structures designated to protect the body against attack by non-self intruder.(1) The immune system protects against pathogens and ensures tolerance for self-antigens.(2) The innate components act rapidly, but in a non-specific manner. And the adaptive components act specifically, but need time for clonal expansion and subsequent differentiation to effector cells. Adaptive immune response is relatively late since both the B cells and T cells undergo some progression before migrating to the site of infection.(3) Thus, two types of immunity are obtained, namely innate and acquired/adaptive immunity.(4)

### 1.2 Immune system components

#### 1.2.1 Innate defense components

The components of innate defense are epithelial barriers, leukocytes, circulating proteins (complement, collectins) and cytokines (interferons, chemokines, interleukins).(5) Innate defense composes mainly of phagocytic cells such as macrophages, B cells and interdigiting dendritic cells.(6),(7) Granulocytic cells such as eosinophils, basophils, mast cells also protect host from parasitic infection. In addition, natural killer (NK) cells work by antibody-dependent cell mediated cytotoxicity (ADCC), killer activating signal (when target cell do not express MHCI molecules) and killer inhibiting signal (when self-cell express MHCI molecules).(7)

#### 1.2.2 Acquired immune components

It is composed of humoral and cellular immunity.

Humoral immunity: This type of immunity involves B cells produced ‘antibodies’ in response to certain antigen. The functions of antibodies include: neutralisation of antigens, prevention of infectivity,

phagocytosis, utilizing products of complement activation and antibody dependent cell mediated cytotoxicity (ADCC).(8), (9)

Cellular immunity: It is mainly performed by B and T cells. Here, discussions will specifically focus on CD4 and CD8 T cells. Immune response occurs through several steps, starting from antigen recognition by naive cells' to differentiation into activated T cells. Antigen specific T cells are able to recognize non-self epitopes of foreign antigens on their surface. T cells recognize antigen presented on MHC molecule with the help of T cell receptor (TCR). The human MHC locus encodes three human leukocyte antigen (HLA) class-1 and three HLA class-2 molecules. These HLA molecules are highly polymorphic in nature. Thus, different T cells from individuals are able to recognize a specific epitope.(8), (10)

#### 1.2.2.1 CD4 T cells

CD4 T cells are subdivided into T helper 1 (Th1) and T helper 2 (Th2) subsets. Both the subsets are responsible for producing different types of cytokines.(11) The memory T cell proliferation depends on the production of IL-2. Cells capable of producing both IFNγ and IL-2 are considered as the precursor of CD4 T cell memory.(12) There are some mutually inhibitory functions of the cytokines. It is found that, IL-10 can inhibit cytokine synthesized by Thl cells. On contrary, the proliferation of Th2 cells is inhibited by IFNγ. Thus, a bias towards either Thl or Th2 responses are observed during many infections. In addition, Th0 cells are capable of secreting mixed types of cytokines such as IL-4, IL-5, IFNγ and IL-10.(13)

Th17 is another type of CD4 cell that requires TGF-β and IL-6 cytokines for induction. Thus, the involvement of Th1 cells in auto-immune diseases was excluded.(14)

Regulatory T cells (Tregs) are important to maintain self-tolerance and immune response. They have beneficial role in treating auto-immune diseases. TGF-β induces RORγt expression in both Th17 and Treg cells, whereas Foxp3 is only found in Treg cells. Both IL-2 and TGF-β are required for Treg differentiation, survival and action.(12) CD4 T cells recognize pathogen by MHCII molecules. Thus, the functions of CD4 T cells are restricted.(5), (15)

#### 1.2.2.2 CD8 T cells

CD8 T cells recognize infected and altered cells upon epitope expression on MHCI molecules. These MHC1 molecules are present in all types of cells. The naïve T cells take about 72 hours to recruit after infection.(16) CD8 positive CTLs are group of T cells that release cytotoxic granules upon recognition of the infected cells and thereby directly kills that cell. They kill pathogen by lethality (perforin and nuclear fragmentation) and IFNγ secretion. Activation of antigen presenting cells (APC) can then prime cytotoxic CD8 T cells directly.(17) The interaction of DC costimulatory molecules with the ligands present on CD4 T cells increases the efficacy of these APCs to generate effector and memory CD8 T cells.(18)

### 1.3 Mechanism of innate immune recognition

Multicellular organisms have the capacity to recognize patterns unique to microorganisms. These molecular structures are known as pathogen associated molecular patterns (PAMPs). The host organism has receptors that can easily recognize these molecular patterns. C-type lectins, leucine rich proteins, scavenger receptors are some of the members of pathogen recognition receptors (PRRs). Therefore, the PRRs are capable of initiating immune responses.(19)

Microorganisms upon entering the body come across the immune cells. The PAMPs on organisms being recognized results in secretion of biologically active cytokines and chemokines. This inflammation process can also be triggered by the activation of the microorganisms own system. Neutrophils are the first sentinels recruited at the site of inflammation. The later events of this inflammation involve lymphocytes that have been activated by an antigen.(20)

### 1.4 Interface between innate and adaptive immunity

DCs are the unique immune cells capable of linking innate and adaptive immunity. DCs can promote adaptive immune response or control overactive immune response. Immature DCs upon pathogen encounter undergo the process of maturation. This pathogen recognition occurs by the toll-like receptors (TLRs) present abundantly on the surface of DCs. This process leads to synthesis and release of cytokines. This secretion of interleukins creates the interface between the two types of immunity.

Therefore, the cross-talk exists; the innate system alerts the adaptive system for dangers and the adaptive system triggers the innate response.(21), (22)

### 1.5 Mechanism of immune response produced by CD4 and CD8 T cells

Upon antigen attack, T cells are activated via signal through TCR. The receptor for costimulatory molecules (CD40, CD80) also needs to be activated to avoid the clonal anergy process. Unless, unresponsive state is created, rendering the T cells to produce its own growth hormone (IL-2). Therefore, signals through both the receptors are necessary to produce effector molecules and consequential T cell multiplication. CD4 or CD8 molecules are also present in the TCR complex. CD4 binds MHC class II molecules, whereas CD8 binds MHC class I molecules to show responses to antigen.(23)

The ability to produce an immune response upon reinfection depends on the presence of large number of antigen specific memory T cells. Primary CD8 immune response to acute infections does not depend on CD4 T cell help. In this case, recognition of microbial products through TLR directly activates APCs bypassing CD4 help. But, CD8 response to non-inflammatory immunogens requires CD4 T cell help. This involves activation of both APCs and CD40 molecules.(24)

### 1.6 Regulation of T cell activity

T cell activity is dependent on costimulatory signals provided by TCR. The specificity of T cell response depends on the interaction between 'MHC: peptide complex' and 'TCR'.(25) This interaction is known as immunological synapse (IS). The stability of IS depends on:(26)

- The duration of interaction between APC and T cell. For example, when DCs are mature the durability of IS is long-lasting and leads to immunity. When the DCs are immature they lead to shorter durability, leading to tolerance development.
- The receptors present in IS region helps to maintain stability and organization of IS region.
- Pre-activation of T cells is required to obtain complementary response from DC to form stable IS.

Surface proteins present on DCs and T cells in an IS are represented in Figure 1.1.(26) This synapse is required for MHC molecules to present antigen to T cell. This induces T cell to produce T cell effector function. Thus, expression of costimulatory molecules through this co-stimulation as well as secretion of cytokines that regulate T cell activity can be obtained.(27)

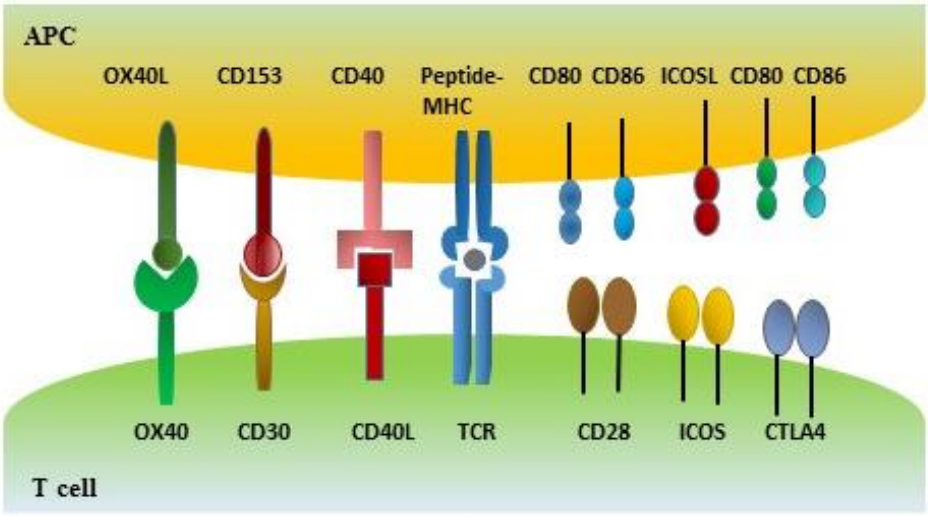


**Figure 1.1: Immunological synapse formed between APC and T cell (27)**

### 1.7 Organs/tissues of immune system

Bone marrow, thymus, lymph node, spleen are specialized organs where lymphocytes interact with non-lymphoid cells either for their maturation or initiation of adaptive immune response. Lymphatic tissues have numerous lymphocytes.(7) Thus, the immune system provides protection from any type of pathogens or neoplastic changes. Utilizing the immune system for cancer is attracting scientists for new treatment development.(28)

### 1.8 Immune system and cancer

The immune system identifies the tumor cells through immunosurveillance before their progression. In spite of continuous observation of the immune system, tumor cells escape the immune defense, instigating the scientists to discover various mechanisms to treat cancer. Thus, Paul Ehrlich's concept of immunosurveillance came to a refined hypothesis elaborated by Brunet as 'immunoediting'. Elimination,

equilibrium and escape are the three Es' of immunoediting to balance between immune system and developing tumor. In addition, elimination phase occurs during early tumor growth and destroy the cells before further tumor occurs. In the escape phase, tumor cells become resistant to the effect of adaptive immunity. The immunoediting theory suggests that the immune system can eradicate suboptimal tumors, but when equilibrium is reached tumor burden starts to increase and enters escape phase.(29), (30)

### 1.8.1 Tumor development, recognition by immune system, tumor microenvironment

#### 1.8.1.1 Tumor development

The major challenge for the immune system is to eliminate cells undergoing neotransformation. The development of malignant cells is a multi-step process. The immune system applies some tumor-suppressor mechanisms to prevent the capability of abnormal cell proliferation.(29), (31) But, progression of tumors escape such controls due to mutation of the genes. This occurs due to breakdown of one or several components of the genomic integrity. Cancer cells are self-sufficient and evade all the control mechanism of the immune system allowing continuous growth of cells.(32)

#### 1.8.1.2 Tumor recognition by the immune system

A mutated or new protein can express their fragments on their surface as a target for immune cell, especially CD8 positive T cells. Several methods have been utilized to identify the tumor antigens recognised by T cells. There are about 11,000 mutations found in tumors. These mutations undergo immunogenic selection in the early stage of cancer and might not be present at advanced stage of disease.(33)

Previously mentioned, NK cells kill target lacking MHCI molecules, an underlying fact for many cancer cells. Recently it has been found that, receptors like natural cytotoxicity receptor (NCR) of NKs can lyse tumor cells. However, though these activating NCRs are present still there is limited tumor regression. The underlying reason is the immunosuppressive environment operating within the tumor manifesting tumor progression.(34)

#### 1.8.1.3 The tumor microenvironment

The tumor is considered as organ having complex biology. The tumor epithelial cells form a unique compartment named parenchyma. And the mesenchymal cell forms the tumor stroma. The stromal cell changes in abundance, histology, phenotypic characterization. A solid tumor is a collection of distinctive cells such as cancer stem cell, cancer cell, cancer associated fibroblast, pericytes, immune inflammatory cells, endothelial cells and invasive cancer cells.(32)

There are several immune cells present in tumor mediating immunity such as T cells, DCs, B cells, macrophages, NKs, polymorphonuclear leukocytes. CD4+CD25$^{high}$ FoxP3 + cells, subset of CD4 T cells, are also expanded in that environment. These cells are Tregs capable of suppressing proliferation of effector T cells through secretion of IL-10 and TGF-β cytokines. Cytotoxic T lymphocyte antigen 4 (CTLA-4), an immune-inhibitory molecule, is expressed by CD8 and CD4 T cells and FoxP3 Tregs. Programmed death (PD-1) receptor is also expressed on Tregs, monocytes and T cells. Macrophages present in tumor secret inhibitory cytokines such as IL-10, prostaglandin, reactive oxygen species.(35) Myeloid suppressor cells (CD34+CD33+CD13+CD15) are bone marrow-derived immature DCs that accumulate in tumor, suppress immune cells by production of enzyme arginase 1, superoxide and nitric oxide. Tumors themselves produce IL-10, vascular endothelial growth factor (VEGF), GM-CSF, TNF-α, IL-1, IL-6 that blocks DC maturation. Thus, the tumor not only manages to escape the immune cells but also creates a microenvironment to promote progression.(36) The immunosuppression is battled by various treatments such as via cytokines, checkpoint inhibitor against adoptive cell transfers and therapeutic cancer vaccines.(37)

### 1.9 Immune escape

There are several reasons responsible for immune escape of tumors. Some of the reasons could be due to reduced immunogenicity, resistance to immune mediated cytotoxicity, destabilization of immune response, escape through both immunosuppression and alteration of tumor microenvironment.(38),(39) Thus, the older concept that immune system has integrated ability to recognize only non-self is not

enough for immune response. The immunosuppressive tumor microenvironment has initiated newer concepts to balance between immune-stimulating and tumor inhibitory mechanisms. Strategies are being developed to harness the power of immunity against cancer. Therapeutic tools are necessary to halt the tumor progression through effective identification of non-self-antigens. This research work targets to provide a tool to stimulate the immune system to antigenic message and manipulate tolerance and productive immunity.(40)

### 1.10 Dendritic cells: The best-known antigen presenting cells

DCs are the key antigen presenting cells that transfer information to the cells of adaptive immune response.(41) DCs are heterogeneous in origin, morphology, phenotype and function. DCs play a crucial role in inducing immune response against all types of antigens.(42) They are unique among all antigen presenting cells. Table 1.1 mentions the speciality of different APCs.

**Table 1.1: Speciality of different APCs (43)**

| Properties | Dendritic cells | Macrophages | B cells |
|---|---|---|---|
| **Antigen uptake activity** | • Phagocytosis, macropinocytosis, receptor-mediated endocytosis | • Phagocytosis, receptor-mediated endocytosis | • Receptor-mediated endocytosis via immunoglobulin |
| **MHCII expression** | • Constitutive, high level of expression, inducible | • Low level expression, inducible | • Constitutive expression, inducible |
| **Antigen presenting activity** | • Activation of naive T cells | • Activation of naive B cells by recruiting CD4+ T cells | • Recruitment of helper T cells for antibody production |

### 1.11 DC activation process

Upon pathogen encounter DCs engage their PRRs to alert the immune system that a pathogen has breached the immune barrier. In response, the chemokine receptors allow them to migrate from peripheral site of infection to secondary lymphoid organs. Thus, biochemical signals within the tissue microenvironment educates immature DCs to down regulate tissue homing and upregulate chemokine receptor which in turn promotes DCs to lymph node. During this migration, they undergo the process of 'maturation'. Mature DCs initiate DC receptors to pick up the danger signal to present the antigens. The danger signal increases the surface density of MHCII, gathers costimulatory molecules and release cytokines for further immune response. They are the only cells that can prime naive T cells.(43), (44) Activation or tolerization of DCs are determined by the antigen microenvironment. When the foreign or self-antigen are not dangerous the tolerance is expected as the DCs will not mature and no signal will be delivered further.(45)

### 1.12 DC subtypes

DCs are classified in different ways. (46), (47), (48) Figure 1.2 represents the classification of DCs.(49)

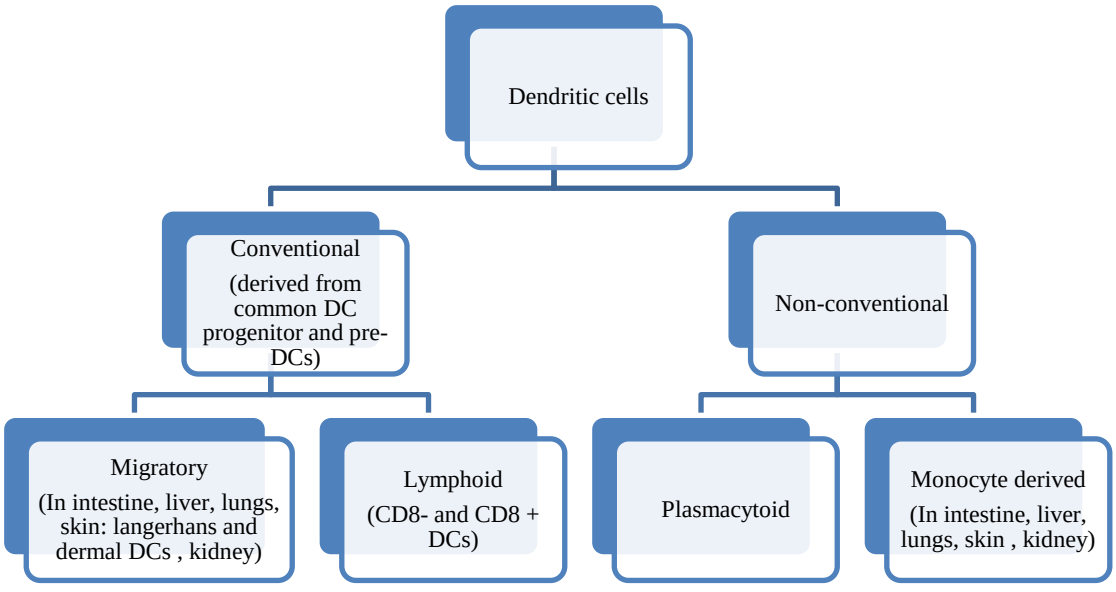


**Figure 1.2: Classification of DCs (49)**

### 1.13 Functions of DC

DCs play a major role in initiating tolerance, memory and T cell differentiation. In the vicinity of DC and T cells, the following signals are required to initiate immune response.(45) DCs are 1,000 times more potent than other APCs in activating resting T cells.(50)

Signal 1: Response of CD4 and CD8 T cells to antigen displayed on MHCI and MHCII molecules

Signal 2: Expression of accessory molecules is required for division and differentiation of T cells

Signal 3: Secretion of cytokines

These three stimulations are necessary for T cell activation.(51)

### 1.14 DC Receptors

Antigens have special structured proteins or carbohydrates known as pathogen associated molecular pattern (PAMPs). Uptake of these antigens occurs by phagocytosis, pinocytosis, macropinocytosis and/or receptor mediated uptake. The process of phagocytosis is triggered by recognition of foreign particles through the recruitment of receptors. Among these, macroendocytosis or receptor mediated uptake are the most efficient ones. Scavenger receptors, PRRs, Fc receptors (CD64 and CD32), complement receptors and viral receptors are the DC surface receptors. The important PRRs on DCs are TLRs, mannose receptors and C-type lectin receptors.(52)

Presently, 15 mammalian TLRs have been discovered. Among them, 10 of the TLRs are present in humans.(53) Some TLRs subset agonists have been employed in clinical trials, whereas some are already in market.(54) The mannose receptor is a C-type lectin that can perform phagocytosis, antigen presentation and processing.(55) Compared to TLRs and mannose receptors, CD205 C-type lectin receptor is the most recent one to be explored.(56)

### 1.15 CD205, a C-type lectin receptor

CD205 receptor is expressed by lymphoid, interstitial, epidermal Langerhans DCs and thymic epithelial cells.(52) This receptor is overexpressed when DCs are mature. CD205 receptor binds primarily with

carbohydrates.(57) This receptor contains an N-terminal domain, a fibronectin domain and multiple carbohydrate recognition domains (CRDs). The number of these CRDs are ten for this receptor.(58) This receptor is an excellent antigen-targeting receptor for monoclonal antibodies to efficiently bind target DCs *in-vivo*.(59) It has been found that, targeting CD205 with anti-CD205 monoclonal antibody enhanced antigen presentation by DCs to T cells (CD4+ and CD8+).(60) Besides, the receptors can both present and cross-present antigens on MHC molecules. This receptor delivers antigens to late endosomes, which then display fragments of antigens on MHCII molecules.(61), (62)

Thus, it is critical to design a delivery system capable to reach and target CD205 receptors *in-vivo*.(63). This potentiates the structural modification of NPs with a complementary ligand to play a significant role in NP delivery to the target site.(64)

**1.16 Cancer Immunotherapy**

Immunotherapy uses the immune system for boosting the cancer patient's immune response. This will improve its ability to recognize tumor. The aim of immunotherapy is to modulate immune response.(65) Presently, there are several treatment options for cancer; but combination approach is the best selected method for cancer patients.(66) For example, radiotherapy might be successful when chemotherapy is coupled with it. Chemotherapy can be more beneficial when coupled with immunotherapy. Nowadays, targeted therapy with monoclonal antibody is a significant treatment option to interact with immune system.(67) Tumor blood vessels are different from normal blood vessels due to their proliferating nature. Increasing the dose of drug may not eliminate the tumor load due to genetic plasticity of tumor cells. This can be the reason for development of resistance against chemotherapeutic drug. Nevertheless, combined chemo-immunotherapy can be advantageous for cancer treatment.(68), (69) Combination therapy enhances vaccine efficacy by several mechanisms. Chemotherapeutic agents act by 'immunogenic tumor cell death'. Prostvac vaccine with chemotherapeutic Docetaxel for patients with prostate cancer is an example of combination therapy.(70)

### 1.17 Types of cancer immunotherapy

The uptake of tumor cells and presentation of their antigens to T cells is a complex criterion. DCs need help to effectively present the antigens to T cells. The process of cancer immunotherapy can be divided in different ways. Generally, it can be divided as specific and non-specific immunotherapy (Figure 1.3).(71)

#### A. Non-specific immunotherapy

Non-specific immunotherapy modulates the immune system generally, without targeting tumor associated antigens (TAAs). It can be further subdivided as:

- **Active immunotherapy:** This induces the generation of immune effector mechanisms. It educates the immune system to recognize tumor cells and induces immune memory.(71)
- **Passive immunotherapy:** It is obtained by supplying readymade immune effectors so that the immune system can consume the effector molecules. This type of immunotherapy is obtained by general stimulants of the immune system the 'immunomodulators' through various mechanisms such as induction of stimulatory cytokines, activation of T cells and APCs. (71), (72)

#### B. Specific immunotherapy

Specific immunotherapy targets one or several TAAs. It can be further subdivided into two groups:

- **Passive immunotherapy:** This is performed by supplying tumor specific monoclonal antibodies. For example, treating breast cancer overexpressing HER-2 antigen.(73), (74) Though the antibodies are either humanized or chimeric, side effects occur due to residual immunogenicity causing serum sickness or hypersensitivity reactions.(75) Similarly, T cells can be adoptively transferred to cancer patients through passive transfer of tumor-reactive T cells into the host that results in the destruction of established tumors.(76)
- **Active immunotherapy (therapeutic vaccine)**

  The goal of therapeutic vaccine is to generate an active immune response against an existing cancer. The vaccine can lead to clonal expansion of cytotoxic T cells that recognize cancer cells

and induce cell death. However, the optimal vaccine should provide both humoral and cellular immunity.(77) Among all the approaches, DC based vaccination strategy has showed encouraging results.(78) However, linear dose-response might not be observed in immunotherapy due to other factors. It depends on number of factors such as route of administration, dose, dosage regimen, adjuvant and immunological status. Moreover, the heterogeneous nature of antigen should be explored, especially in the later stage of the disease. Targeting multiple antigenic epitope should be considered for an effective anti-cancer therapy.(79)

Nevertheless, identification of the important parameters for clinical effectiveness of a vaccine warrants research. In case of prostate cancer, it has been found that mature monocyte DCs are superior to their immature state. In addition, DCs should be able to produce IL-12p70 cytokine. The expansion of newer vaccines is influenced towards Th1 immune response with potential of CTL activity.(80)

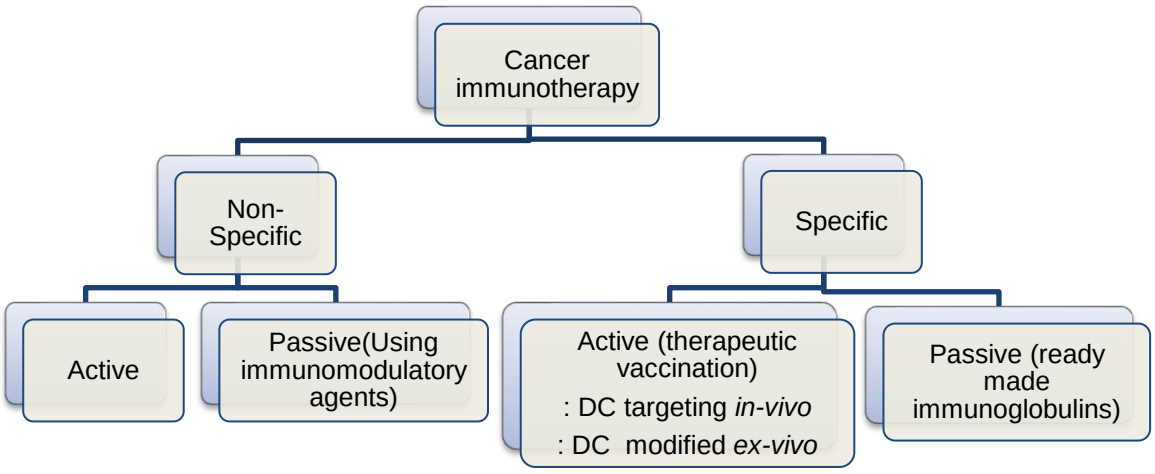


**Figure 1.3: Schematic representation of immunotherapeutic approaches(71)**

DC based therapeutic vaccines can be subdivided as:(81)

- *Ex-vivo* modification of DCs
- *In-vivo* manipulation of DCs

- ***Ex-vivo* modifications of DCs**

In this case, DCs are loaded with antigen; the maturation of DCs are confirmed and then the newly generated complete DC vaccine is injected to the patient. The injected vaccine triggers the immune system which in turn recognizes the cancer cells efficiently and to attack them back. Each vaccine manufactured is unique, customized for individual patient, which is very expensive.(71) However, the obtained immune response and the clinical response were different, which could be partially due to the immunosuppressive environment present in the later stage of the disease.(82)

Sipuleucel-T(Dendreon Corp.) is the first US Food and Drug administration (FDA) approved DC vaccine against prostate cancer. Prostvac is another *ex-vivo* DC vaccine which is pox virus based vaccine targeting prostate specific antigen to treat men with metastatic castration resistant prostate cancer. Choice of antigen is an vital factor for this type of vaccine. Non-mutated self-antigens are preferred over muted ones as it has broader application on the vaccine. However, mutated antigens could provide personalized treatment to avoid this shortcoming.(83)

- ***In-vivo modifications of DC***

The disadvantages of *ex-vivo* DC vaccine seek an alternative to obtain immediate T cell activation. This could be achieved by administration of tumor antigen-adjuvant-ligand conjugated vaccine system. In the absence of adjuvant, antigen-specific tolerance is developed. This type of vaccine is "cell-free vaccine" that targets the endogenous DCs. The *in-vivo* polarization of DCs delivers the antigens selectively to DCs.(82) This *in-vivo* vaccination strategy is simple, inexpensive and labor saving compared to *ex-vivo* DC vaccines.(64)

The *in-vivo* vaccination protocols are aimed to initiate CD8+ T cell differentiation regulated by CD4 T cells. As a result proliferation of tumor antigen specific T cells will occur with long term memory CD8+ T cells.(84) This is the driving strategy of our work to introduce an antibody-NP adjuvant to target DC receptor for effective DC based *in-vivo* immunotherapy.

### 1.18 Mechanism of *in-vivo* delivered DC vaccine

*In-vivo* delivered DC vaccines are manipulated in *ex-vivo* laboratory setup. This *in-vivo* generated vaccine represents an economic option as it requires less labor than *ex-vivo* generated DCs. Tumor expressed well characterized antigens could be delivered so that they are presented on MHC molecules. Strategies that show both CD4 and CD8 effect can provide protective anti-tumor effect. Also, endogenous DCs can be targeted via specific targeting molecules.(85, 86) These cancer vaccines should be capable of epitope distribution, preferentially by eliminating tumor cells that expresses a specific epitope. Therefore, we will get antigen-specific response where the number and the quality of tumor-specific cytotoxic T cells will increase.(87) This produces antigen specific CTLs which will kill the tumor cells.(88)

#### 1.18.1 Components of therapeutic cancer vaccine

The components of cancer vaccine include tumor-specific antigens, carrier or delivery systems and adjuvants. A vaccine should have effective shelf-life, proper delivery device and packaging. Nevertheless, an ideal vaccine is always beyond the choice of adjuvant and immune potentiator.(89)

#### 1.18.2 Selection of tumor antigen

Cancer vaccine contains antigens of varied composition, identity and source. For example, recombinant proteins, synthetic peptides, carbohydrates, extracted tumor derived proteins, monoclonal antibodies can be used as antigen.(90) Antigens should be expressed on tumor cells only because mutated proteins cannot be expressed by MHC molecules. The mutated region is sometimes masked by modification. So, proteins expressed on tumor cells are less possibly expressed by normal cells and good tumor target.(91) Previously it was found that there are two types of antigen classes such as: tumor-specific antigens, which are present only on tumor cells and not on any other cell and tumor-associated antigens, which are present on some tumor cells and some normal cells. However, there are several types of antigens discovered till date.(92)

In immunotherapy, the APCs are modulated so that they can stimulate T cells in an effective manner. Manipulation of this response can be significantly achieved by delivering antigen using a NP system.(93) Studies showed when anti-CD205 Ab ligand is conjugated with ovalbumin, the receptor mediated antigen presentation via MHCI and MHCII increased 1000 and 300 times, respectively. This CD205 receptor targeted antigen conjugate provided immunity upon obtaining maturation stimulation for DCs. Therefore, non-targeted antigens are less effective to activate immune response.(94)

### 1.18.3 Adjuvants and their role in vaccine formulation

Adjuvant is a vital component of ideal vaccine system. Adjuvants should be effective to produce antigen specific immune response, immunological memory, safety profile and stability profile. Modern vaccines are unable to obtain optimum immune response. This justifies the necessity of adjuvants that can produce both cell-based and humoral immune response.(95) Moreover, the need for antigen and the frequency of vaccination decreases when adjuvant is present in the formulation. All the advantages of adjuvants can help immuno-compromised patients.(96) Among all the adjuvants, toll-like receptor (TLRs) agonists have gained attention as it can be displayed on DCs. A ligand can bind with TLRs to help DC maturation, antigen processing and presentation. Different clinical trials are running with use of TLR ligands.(97) When peptide is used as an antigen in NP delivery system, they form complex with MHCI molecules in endoplasmic reticulum and transported to cell surface receptor to be recognized by T cells.(98) However, clinical response with peptide alone has shown low success. This justifies the co-delivery of adjuvant and antigen through NPs.(99)

## 1.19 NPs as delivery system: importance of particle size, shape, charge and surface chemistry

Several delivery systems are used as platforms to be used as vaccine delivery carrier. Liposomes, emulsions, immunostimulatory complexes, polymeric NPs are now widely used. Polyester based particles started in late 70s. In 1976, polyacrylamide nanostructures were first used to obtain immune response. Among the polyesters, PLGA is well known for their numerous properties. Detailed discussion will be in

the next section.(100) The term ‘NP’ is used for diverse range of nanosized particle that includes particle upto 1 µm.(101)

There are several aspects of research on NPs to be kept in mind when formulating a delivery system such as drug loading capacity, site specific targeting, and biological fate of the drug and carrier, toxicity and storage stability. For instance, liposomes might face chemical and physical stability problems solid-lipid NPs might have low drug payload and stability problems, incomplete removal of residual organic solvents and polymer cytotoxicity occurs with some polymer based NPs, protein based particles might face long term storage, aggregation problem in aqueous solution, cationic micelles have toxicity issues, carbon nanotubes are non-biodegradable, dendrimers have toxicity issues; and metallic NPs are unable to load drugs.(102) Biodegradable, biocompatible polymers like PLGA has been approved for use in human beings. These can load high amount of antigen to slowly release from the formulation. In this way the polymer protects the antigen from degradation.(103)

Advances in understanding the properties of NPs such as size, shape and surface properties for biological interactions, are creating new opportunities for their therapeutic applications. Particle size is an important factor for effective NP design. However, 10-100 nm is the best fitted particles for cancer therapy. But internalization of particles is extended up to 5 µm depending upon the type of formulation. Different studies have found that lower particle size (~100 nm) is internalized quickly than 5 µm size particles.(104)

Surface charge also effects particle internalization. Positively charged particles can exhibit perinuclear localization and shorter stay in circulation. Particles with lower surface charge have longer blood circulation time.(104), (105) Both surface property and particle size determines the composition of protein corona attracted towards NPs. Presence of this corona influences particle clearance my mononuclear phagocytic system (MPS). Surface functionalization is the possible mechanism to avoid corona proteins and immunoglobins.(106)

Surface modification of particles can be done by attaching targeting ligands such as transferrin, antibodies, small peptides, aptamer, and folic acid. Particles with ligand can be internalized by phagocytosis, pinocytosis or other mechanisms. Surface manipulation will increase the circulation time of particles and secondly allow selective interaction with cancer cells.(104) Particle shape also plays key role in cellular internalization.(107)

### 1.19.1 PLGA NPs in drug delivery: Structure and composition

PLGA NPs, the well known in its class, approved by United States FDA to be used for various diseases. It is currently under intense development for applications in cancer imaging, vaccines, targeted therapy and tissue engineering.(108)

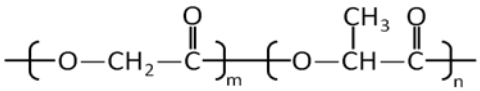

**Figure 1.4: Poly lactide co-glycolide (PLGA) structure (109)**

PLGA is a synthesized by ring-opening copolymerization of two different monomers, glycolic acid and lactic acid (Figure 1.4). During polymerization, monomeric units (of glycolic or lactic acid) are linked together in PLGA by ester linkages yielding a linear, amorphous aliphatic polyester product. The most widely used glycolic and lactic ratio of 50:50 with variety of end groups and viscosities. PLGA is preferred over its monomers as it can be dissolved by wide range of solvents.(109) PLGA NPs can be prepared by various methods. The popular methods are emulsification, solvent evaporation method, nanoprecipitation, polymerization, coacervation, ionic gelation and salting out.(110) Depending on the mode of preparation, NPs might possess different properties and characteristics for optimum delivery of therapeutic agent. Among all the processes, W/O/W or single O/W emulsification-solvent evaporation method are used. PLGA NPs typically range from 10 to 1000 nm in diameter, with the therapeutic agent either entrapped into or adsorbed or chemically coupled onto the polymer matrix.(111) It undergoes hydrolysis in the body to produce biodegradable metabolite monomers, lactic acid and glycolic acid

(Figure 1.5). Therefore, the whole process leaves non-toxic residues after metabolism. This biological degradation occurs at very slow rate, without affecting normal cell function.(112)

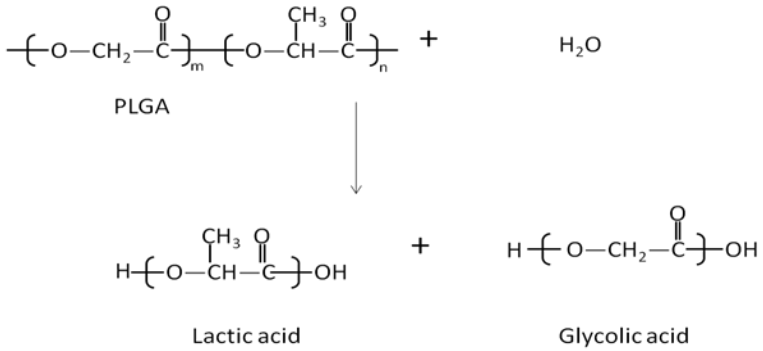


**Figure 1.5: Hydrolysis of PLGA polymer (112)**

### 1.19.2 PLGA NPs as a vaccine delivery system for immunotherapy

Particulate delivery system is considered as recent development in field of immunotherapy.(113) An antigen, an adjuvant and a delivery system is required to formulate NP based ideal cancer vaccine. This cargo system is able to deliver antigen to the APC to manipulate their response.(114) Surface modified NPs will render a hydrophilic layer that is capable to escape reticulo-endothelial system to reach receptors on target APCs (DCs).(115) Table 1.2 summarizes some examples of PLGA based vaccine delivery system.

**Table 1.2: PLGA based vaccine delivery systems and their biological effects**

| **Nanoparticle system** | **Antigen** | **Adjuvant** | **Results** | **Reference#** |
|---|---|---|---|---|
| PLGA NP | OVA | TLR9 agonist/ CpG | • Increased secretion of IFNγ, indicating Th1 based response<br>• No significant difference between OVA-CpG and PLGA-OVA-CpG groups for anti-tumor and cytotoxic T cell response. But, the | (116) |

| | | | | |
|---|---|---|---|---|
| | | | tumor was below 50mm$^2$ after day 17 | |
| PLGA micro-particles | OVA | CpG | • PLGA helped to increase IgG and IFNγ secretion. A Th1 biased humoral response was obtained<br>• No clear benefit of CpG and OVA in microparticles were found | (117) |
| PLGA NP | OVA and MUC1 | MPLA | • The vaccine system increased antigen specific Th1 polarized response<br>• MUC1-pLGA-MPLA combination showed MUC1 specific T cell response and breakdown of self-MUC1 tolerance | (118) |
| PLGA | MUC1 and tetanus toxoid (TT) | CpG and MPLA | • The T cell proliferation observed in the presence of PLGA-MUC1-MPLA was higher than MUC1 and empty NPs<br>• Same data trend was found for TT-PLGA-CpG system. T cell proliferation was significantly higher than soluble OVA pulsed DCs | (119) |
| PLGA micro-spheres | OVA | CpG | • Triggered clonal expansion of primary and secondary antigen specific CD4 and CD8 cells<br>• Out of 5 mouse 4 showed complete tumor regression, one showed retarded tumor growth | (120) |
| PLGA NP | OVA | poly(I:C) or | • Enhanced MHC I restricted antigen | (121) |

| | | | | |
|---|---|---|---|---|
| | | CpG | presentation but not the MHC II restricted, presentation of exogenous antigen<br>• NP with OVA-CpG induced effective proliferation of CD4 and CD8 T cells | |
| PLGA NP | OVA | MPLA or TLR7 | • 10 µg of antigen plus PLGA (MPLA+TLR7) yielded a much greater response than that induced by 50 µg of antigen alone. Thus, 5-fold less dose was required<br>• The antigen-adjuvant combination created memory B cells as well as plasma cell response | (122) |
| PLGA NP | Melanoma antigen recognized by T-cells-1 (MART), gp100, OVA, SIINFEKL and mouse six transmembran e epithelial antigens of the prostate (m STEAP) | Incomplete Freund's adjuvant (IFA) | • PLGA NPs encapsulating a three-peptide (MART-1, gp100:154–162 and gp100: 209–217) generated significantly more robust cytotoxic activity than those encapsulating a two-peptide (MART-1 and gp100:154–162)<br>• The peptide dose encapsulated in PLGA NPs was 63 times less than that emulsified in incomplete Freund's adjuvant<br>• Tumor size in the mice immunized with PLGA-mSTEAP NPs was smaller than tumors in the mice immunized with mSTEAP+ IFA | (123) |
| PLGA NP | Melanoma | MPLA | • Mouse treated with PLGA-TRP2-MPLA had | (114) |

| | | | | |
|---|---|---|---|---|
| | antigen, tyrosinase-related protein 2 | | 60-65-fold high CD8+T cell count<br>• Controlled tumor growth (85%) was observed when treated with the NP system<br>• Increased all cytokines such as IFNγ, TNFα, IL-2, IL-12, IL-6 and decreased production of VEGF | |
| PLGA NP | Tetanus toxoid (TT) | CpG | • Induction of both Th 1 and Th2 immune responses with potent Th1 response | (124) |
| PLGA NP or microparticle | Murine cytomegalovirus epitope pp89 | EP67 | • Sufficient secretion of IFNγ, TNFα and IL-2<br>• Varying the diameter of particles affected the CD8 memory T cell response | (125) |

There are several studies performed with PLGA-antigen combination without using adjuvant. Due to their limitations in adequate immune response incorporation of an adjuvant in formulations in necessary. (126), (127), (128)

### 1.19.3 Drawbacks of NP based vaccine delivery systems

NP based vaccine shows failure to achieve efficacy in clinical trials due to improper relation between maximum tolerated dose and tumor response rate, drug exposure and its efficacy/toxicity and prolong time to achieve immunotherapeutic response.(129) When delivering therapeutic agent through active targeting strategy, the target recognition needs to be highly specific with the scope of accommodating the ligand with greater binding capacity.(130) Difficulties arise when the reproducibility of the manufacturing parameters could not be ensured. In addition, the physicochemical properties of NPs needs to be correlated with their biodistribution and targeting property.(131)

This scenario can be changed by choice of formulation to prepare vaccine, being critical in patient selection, being aware of patients' previous medical history, applying novel technologies to standardize treatment and selection of strong adjuvant in the vaccine.(132) For instance, PLGA based vaccines require the use of organic solvents, sonication and high speed agitation. Proteins/epitopes are susceptible to these experimental conditions. However, strict formulation parameters should be maintained along with use of protein stabilizers (sugars, polysaccharides) for commercial scale-up preparation.(133) Toxicity issues and accumulation of NPs within cells can hinder effective vaccine delivery. To overcome this biodegradable polymeric NPs can be used.(134) To achieve success from therapeutic vaccination, treatment in the last stage of tumor should be avoided. In addition, survival rate will be improved when delivered with suitable combination of antigen-adjuvant in formulation.(135)

### 1.19.4 Surface functionalization of PLGA NPs

To spare the destroying of normal cells over cancer cells requires highly efficient anti-cancer therapeutics to efficiently deliver the drug load to the tumor site. The most commonly used method is employing molecules or ligands that specifically recognize and interact with cancer cells. These molecules include antibodies, growth factors, cytokines, protein or other agents.(136)

NPs should be surface functionalized for the following reasons: (137), (138)

- Non-modified NPs are easily recognized by phagocytic system rich organs and tissues like blood, liver, spleen, lung and bone-marrow.
- Hydrophobic surface of NPs can easily adsorb plasma proteins to the surface. Increasing hydrophilicity of NP surface is a commonly used strategy to avoid this problem.
- Surface functionalization can prolong the circulation time of NPs *in-vivo* until they reach the target site.
- In case of cancer targeting, abnormal tumor structure can hinder localization of NPs to the tumor by enhanced permeability and retention. This can inhibit effective drug delivery.

The theory behind it is to deliver ligand-targeted therapeutics that bind with antigen or receptors that are either uniquely expressed or overexpressed on target cells compared to normal tissues. This allows the specific and targeted delivery of drugs to cancer cells.(139),(140)

#### 1.19.4.1 Functionalization of NP surface with antibody

Antibodies should be linked to the NPs properly, as wrong binding to NPs without specificity may impair the activity of antibody.(141) Antibodies can be linked to NPs by two ways:

**1. Covalent attachment of antibodies to NPs**

There are several approaches through which monoclonal or polyclonal antibodies are covalently linked to the prepared NPs using cross-linkers.

i) Via carbodiimide chemistry: Carboxylic group of NPs and amine group of the antibody combines to form amide bond.(142) 1-Ethyl-3-(3-dimethylaminopropyl) carbodiimide (EDC) couples' carboxylic acid groups of PLGA with the amino group of antibodies. N-hydroxysuccinimide (NHS) is often included in EDC coupling protocols.(143)

ii) Via maleimide: The maleimide group reacts with thiol groups resulting in cross linking that is more selective and precise. Combining thiol groups with amine groups of biomolecules through a maleimide can be achieved when there is no free thiols present in the antibody.(144)

**2. Adsorption of antibodies to NPs**

Besides covalent attachment, antibodies could also be adsorbed to the NP surface. Ligands are coated on NP surface by non-covalent attachment. Hydrophobic PLGA polymers and hydrophobic part of the antibody molecule facilitated this hydrophobic interaction. MAb-decorated NPs could enter the target cells exclusively, while the unmodified NPs were non-selective.(141)

### 1.19.4.2 The use of spacer molecules for attaching the targeting ligands

Thamake *et al* (145) reported non-covalent incorporation of a homobifunctional spacer. The spacer, bis-sulfosuccinimidyl suberate (BS3) was incorporated onto PLGA NPs for effective attachment of antibody to NP surface. BS3 enables formation of amide linkage between the carboxylic group of BS3 and the amine group from the ligand following the hydrolysis and exposure of the carboxylic group of the spacer. The covalent bond between the antibody and BS3 enhances the NPs cellular uptake. (125)

Heterobifunctional crosslinkers have different chemical groups at both ends. For example, an amine-reactive N-hydroxysuccinimide ester (NHS ester) at one end and a sulfhydryl-reactive group on the other end. Doxorubicin containing amine group ($-NH_2$) could be covalently bound with spacer forming thio-ether bond to mAb. The length of different spacer groups were selected in order not to create steric hindrance between Doxorubicin and the mAb.(146)

## 1.20 Methods used in this specific research

### I. Covalent conjugation of antibodies to the NPs surface

Two methods of covalent conjugation were utilized in this research to attach antibody and NP. One was through carbodiimide chemistry; other was using a spacer to attach antibody and NP. For adsorption, antibody was attached with the NPs following controlled procedure.

A. Conjugation method 1: Carbodiimide chemistry
B. Conjugation method 2: Using spacer for covalent conjugation

### II. Physical adsorption of antibodies to the NPs surface (non-covalent)

An alternative means to conjugate ligands to NPs is the use of non-covalent techniques. This simple method, the ligand is added to the mixture of NPs during the attachment of the antibody to the NP.(145)

**1.21 References**


1. Spitzer MH, Gherardini PF, Fragiadakis GK, Bhattacharya N, Yuan RT, Hotson AN, et al. IMMUNOLOGY. An interactive reference framework for modeling a dynamic immune system. Science. 2015 Jul 10;349(6244):1259425. PubMed PMID: 26160952. Pubmed Central PMCID: 4537647.

2. de Visser KE, Eichten A, Coussens LM. Paradoxical roles of the immune system during cancer development. Nature reviews Cancer. 2006 Jan;6(1):24-37. PubMed PMID: 16397525.

3. Janeway CA, Jr., Medzhitov R. Innate immune recognition. Annual review of immunology. 2002;20:197-216. PubMed PMID: 11861602.

4. Paul WE. Bridging innate and adaptive immunity. Cell. 2011 Dec 09;147(6):1212-5. PubMed PMID: 22153065.

5. Chaplin DD. Overview of the immune response. The Journal of allergy and clinical immunology. 2010 Feb;125(2 Suppl 2):S3-23. PubMed PMID: 20176265. Pubmed Central PMCID: 2923430.

6. Iwasaki A, Medzhitov R. Regulation of adaptive immunity by the innate immune system. Science. 2010 Jan 15;327(5963):291-5. PubMed PMID: 20075244. Pubmed Central PMCID: 3645875.

7. Delves PJ, Roitt IM. The immune system. Second of two parts. The New England journal of medicine. 2000 Jul 13;343(2):108-17. PubMed PMID: 10891520.

8. Parkin J, Cohen B. An overview of the immune system. Lancet. 2001 Jun 2;357(9270):1777-89. PubMed PMID: 11403834.

9. Goldman AS, Prabhakar BS. Immunology Overview. In: Baron S, editor. Medical Microbiology. 4th ed. Galveston (TX).1996.

10. Rosa DS, Ribeiro SP, Cunha-Neto E. CD4+ T cell epitope discovery and rational vaccine design. Arch Immunol Ther Exp (Warsz). 2010 Apr;58(2):121-30. PubMed PMID: 20155490.

11. Kemeny DM, Noble A, Holmes BJ, Diaz-Sanchez D. Immune regulation: a new role for the CD8+ T cell. Immunol Today. 1994 Mar;15(3):107-10. PubMed PMID: 8172642.

12. Zhu J, Paul WE. CD4 T cells: fates, functions, and faults. Blood. 2008 Sep 1;112(5):1557-69. PubMed PMID: 18725574. Pubmed Central PMCID: 2518872.

13. Mosmann TR, Sad S. The expanding universe of T-cell subsets: Th1, Th2 and more. Immunol Today. 1996 Mar;17(3):138-46. PubMed PMID: 8820272.

14. Coquerelle C, Moser M. DC subsets in positive and negative regulation of immunity. Immunological reviews. 2010 Mar;234(1):317-34. PubMed PMID: 20193028.

15. Schoenberger SP, Toes RE, van der Voort EI, Offringa R, Melief CJ. T-cell help for cytotoxic T lymphocytes is mediated by CD40-CD40L interactions. Nature. 1998 Jun 4;393(6684):480-3. PubMed PMID: 9624005.

16. Gasteiger G, Ataide M, Kastenmuller W. Lymph node - an organ for T-cell activation and pathogen defense. Immunological reviews. 2016 May;271(1):200-20. PubMed PMID: 27088916.

17. Pennock ND, White JT, Cross EW, Cheney EE, Tamburini BA, Kedl RM. T cell responses: naive to memory and everything in between. Advances in physiology education. 2013 Dec;37(4):273-83. PubMed PMID: 24292902. Pubmed Central PMCID: 4089090.

18. Elgueta R, Benson MJ, de Vries VC, Wasiuk A, Guo Y, Noelle RJ. Molecular mechanism and function of CD40/CD40L engagement in the immune system. Immunological reviews. 2009 May;229(1):152-72. PubMed PMID: 19426221. Pubmed Central PMCID: 3826168.

19. Medzhitov R, Janeway CA, Jr. Innate immunity: impact on the adaptive immune response. Curr Opin Immunol. 1997 Feb;9(1):4-9. PubMed PMID: 9039775.

20. Janeway CJ, Travers P, M. W. Principles of innate and adaptive immunity. 5th ed. Immunobiology:The Immune System in Health and Disease.: New York: Garland Science; 2001.

21. Benencia F, Sprague L, McGinty J, Pate M, Muccioli M. Dendritic cells the tumor microenvironment and the challenges for an effective antitumor vaccination. Journal of biomedicine & biotechnology. 2012;2012:425476. PubMed PMID: 22505809. Pubmed Central PMCID: 3312387.

22. Hoebe K, Janssen E, Beutler B. The interface between innate and adaptive immunity. Nature immunology. 2004 Oct;5(10):971-4. PubMed PMID: 15454919.

23. Schwartz RH. A cell culture model for T lymphocyte clonal anergy. Science. 1990 Jun 15;248(4961):1349-56. PubMed PMID: 2113314.

24. Shedlock DJ, Shen H. Requirement for CD4 T cell help in generating functional CD8 T cell memory. Science. 2003 Apr 11;300(5617):337-9. PubMed PMID: WOS:000182135400059. English.

25. Schwartz JC, Zhang X, Fedorov AA, Nathenson SG, Almo SC. Structural basis for co-stimulation by the human CTLA-4/B7-2 complex. Nature. 2001 Mar 29;410(6828):604-8. PubMed PMID: 11279501.

26. Rodriguez-Fernandez JL, Riol-Blanco L, Delgado-Martin C. What is an immunological synapse? Microbes Infect. 2010 Jun;12(6):438-45. PubMed PMID: 20227515.

27. Acuto O, Michel F. CD28-mediated co-stimulation: a quantitative support for TCR signalling. Nat Rev Immunol. 2003 Dec;3(12):939-51. PubMed PMID: 14647476.

28. Block KI, Boyd DB, Gonzalez N, Vojdani A. Point-counterpoint: the immune system in cancer. Integr Cancer Ther. 2002 Sep;1(3):294-316. PubMed PMID: 14667287.

29. Suckow MA. Cancer vaccines: harnessing the potential of anti-tumor immunity. Vet J. 2013 Oct;198(1):28-33. PubMed PMID: 23850019.

30. Dunn GP, Bruce AT, Ikeda H, Old LJ, Schreiber RD. Cancer immunoediting: from immunosurveillance to tumor escape. Nature immunology. 2002 Nov;3(11):991-8. PubMed PMID: 12407406.

31. Diaz-Cano SJ. Tumor heterogeneity: mechanisms and bases for a reliable application of molecular marker design. International journal of molecular sciences. 2012;13(2):1951-2011. PubMed PMID: 22408433. Pubmed Central PMCID: 3292002.

32. Hanahan D, Weinberg RA. Hallmarks of cancer: the next generation. Cell. 2011 Mar 4;144(5):646-74. PubMed PMID: 21376230.

33. Morris E, Hart D, Gao L, Tsallios A, Xue SA, Stauss H. Generation of tumor-specific T-cell therapies. Blood Rev. 2006 Mar;20(2):61-9. PubMed PMID: 15978709.

34. Soloski MJ. Recognition of tumor cells by the innate immune system. Curr Opin Immunol. 2001 Apr;13(2):154-62. PubMed PMID: 11228407.

35. Bhardwaj N. Harnessing the immune system to treat cancer. J Clin Invest. 2007 May;117(5):1130-6. PubMed PMID: 17476342. Pubmed Central PMCID: 1857237.

36. Whiteside TL. The tumor microenvironment and its role in promoting tumor growth. Oncogene. 2008 Oct 6;27(45):5904-12. PubMed PMID: 18836471. Pubmed Central PMCID: 3689267.

37. Temizoz B, Kuroda E, Ishii KJ. Vaccine adjuvants as potential cancer immunotherapeutics. International immunology. 2016 Mar 22. PubMed PMID: 27006304.

38. Prestwich RJ, Errington F, Hatfield P, Merrick AE, Ilett EJ, Selby PJ, et al. The immune system--is it relevant to cancer development, progression and treatment? Clin Oncol (R Coll Radiol). 2008 Mar;20(2):101-12. PubMed PMID: 18037277.

39. Spranger S. Mechanisms of tumor escape in the context of the T-cell-inflamed and the non-T-cell-inflamed tumor microenvironment. International immunology. 2016 Mar 17. PubMed PMID: 26989092.

40. Zigler M, Shir A, Levitzki A. Targeted cancer immunotherapy. Current opinion in pharmacology. 2013 Aug;13(4):504-10. PubMed PMID: 23648271.

41. Banchereau J, Briere F, Caux C, Davoust J, Lebecque S, Liu YJ, et al. Immunobiology of dendritic cells. Annual review of immunology. 2000;18:767-811. PubMed PMID: 10837075.

42. Kim R, Emi M, Tanabe K, Arihiro K. Potential functional role of plasmacytoid dendritic cells in cancer immunity. Immunology. 2007 Jun;121(2):149-57. PubMed PMID: 17371541. Pubmed Central PMCID: 2265944.

43. Diebold SS. Activation of dendritic cells by toll-like receptors and C-type lectins. Handb Exp Pharmacol. 2009 (188):3-30. PubMed PMID: 19031019.

44. Alvarez D, Vollmann EH, von Andrian UH. Mechanisms and consequences of dendritic cell migration. Immunity. 2008 Sep 19;29(3):325-42. PubMed PMID: 18799141. Pubmed Central PMCID: 2818978.

45. Lipscomb MF, Masten BJ. Dendritic cells: immune regulators in health and disease. Physiol Rev. 2002 Jan;82(1):97-130. PubMed PMID: 11773610.

46. Breckpot K BA, Aerts JL, Thielemans K. Dendritic cells: Subtypes, life cycle, activation, biological functions and their exploitation in cancer immunotherapy. Nova Science Publishers Inc. 2010:1-42

47. Fehres CM, Garcia-Vallejo JJ, Unger WW, van Kooyk Y. Skin-resident antigen-presenting cells: instruction manual for vaccine development. Frontiers in immunology. 2013;4:157. PubMed PMID: 23801994. Pubmed Central PMCID: 3687254.

48. Klechevsky E, Banchereau J. Human dendritic cells subsets as targets and vectors for therapy. Ann N Y Acad Sci. 2013 May;1284:24-30. PubMed PMID: 23651190.

49. Kushwah R, Hu J. Complexity of dendritic cell subsets and their function in the host immune system. Immunology. 2011 Aug;133(4):409-19. PubMed PMID: 21627652. Pubmed Central PMCID: 3143352.

50. Pozzi LM, Maciaszek JW, Rock KL. Both Dendritic Cells and Macrophages Can Stimulate Naive CD8 T Cells In Vivo to Proliferate, Develop Effector Function, and Differentiate into Memory Cells. The Journal of Immunology. 2005;175::2071-81.

51. Corthay A. A three-cell model for activation of naive T helper cells. Scandinavian journal of immunology. 2006 Aug;64(2):93-6. PubMed PMID: 16867153.

52. Clark GJ, Angel N, Kato M, Lopez JA, MacDonald K, Vuckovic S, et al. The role of dendritic cells in the innate immune system. Microbes Infect. 2000 Mar;2(3):257-72. PubMed PMID: 10758402.

53. Schreibelt G, Tel J, Sliepen KH, Benitez-Ribas D, Figdor CG, Adema GJ, et al. Toll-like receptor expression and function in human dendritic cell subsets: implications for dendritic cell-based anti-cancer immunotherapy. Cancer immunology, immunotherapy : CII. 2010 Oct;59(10):1573-82. PubMed PMID: 20204387.

54. Liu K. Dendritic cell, toll-like receptor, and the immune system. J Cancer Mol 2006 13 December 2006;2(6):213-5.

55. Gazi U, Martinez-Pomares L. Influence of the mannose receptor in host immune responses. Immunobiology. 2009 Jul;214(7):554-61. PubMed PMID: 19162368.

56. Ebner S, Ehammer Z, Holzmann S, Schwingshackl P, Forstner M, Stoitzner P, et al. Expression of C-type lectin receptors by subsets of dendritic cells in human skin. International immunology. 2004 Jun;16(6):877-87. PubMed PMID: 15113774.

57. Apostolopoulos V, Thalhammer T, Tzakos AG, Stojanovska L. Targeting antigens to dendritic cell receptors for vaccine development. J Drug Deliv. 2013;2013:869718. PubMed PMID: 24228179. Pubmed Central PMCID: 3817681.

58. Llorca O. Extended and bent conformations of the mannose receptor family. Cell Mol Life Sci. 2008 May;65(9):1302-10. PubMed PMID: 18193159.

59. Bonifaz LC, Bonnyay DP, Charalambous A, Darguste DI, Fujii S, Soares H, et al. In vivo targeting of antigens to maturing dendritic cells via the DEC-205 receptor improves T cell vaccination. The Journal of experimental medicine. 2004 Mar 15;199(6):815-24. PubMed PMID: 15024047. Pubmed Central PMCID: 2212731.

60. Geijtenbeek TB, Gringhuis SI. Signalling through C-type lectin receptors: shaping immune responses. Nat Rev Immunol. 2009 Jul;9(7):465-79. PubMed PMID: 19521399.

61. Shrimpton RE, Butler M, Morel AS, Eren E, Hue SS, Ritter MA. CD205 (DEC-205): a recognition receptor for apoptotic and necrotic self. Mol Immunol. 2009 Mar;46(6):1229-39. PubMed PMID: 19135256. Pubmed Central PMCID: 2680960.

62. Gurer C, Strowig T, Brilot F, Pack M, Trumpfheller C, Arrey F, et al. Targeting the nuclear antigen 1 of Epstein-Barr virus to the human endocytic receptor DEC-205 stimulates protective T-cell responses. Blood. 2008 Aug 15;112(4):1231-9. PubMed PMID: 18519810. Pubmed Central PMCID: 2515117.

63. Wang B, Zaidi N, He LZ, Zhang L, Kuroiwa JM, Keler T, et al. Targeting of the non-mutated tumor antigen HER2/neu to mature dendritic cells induces an integrated immune response that protects

against breast cancer in mice. Breast cancer research : BCR. 2012;14(2):R39. PubMed PMID: 22397502. Pubmed Central PMCID: 3446373.

64. Xu H, Cao X. Dendritic cell vaccines in cancer immunotherapy: from biology to translational medicine. Frontiers of medicine. 2011 Dec;5(4):323-32. PubMed PMID: 22198743.

65. Finn OJ. Immuno-oncology: understanding the function and dysfunction of the immune system in cancer. Annals of oncology : official journal of the European Society for Medical Oncology. 2012 Sep;23 Suppl 8:viii6-9. PubMed PMID: 22918931. Pubmed Central PMCID: 4085883.

66. Characiejus D, Hodzic J, Jacobs JJ. "First do no harm" and the importance of prediction in oncology. EPMA J. 2010 Sep;1(3):369-75. PubMed PMID: 21151487. Pubmed Central PMCID: 2987560.

67. Farkona S, Diamandis EP, Blasutig IM. Cancer immunotherapy: the beginning of the end of cancer? BMC medicine. 2016 May 05;14:73. PubMed PMID: 27151159. Pubmed Central PMCID: 4858828.

68. Roy A, Singh MS, Upadhyay P, Bhaskar S. Combined chemo-immunotherapy as a prospective strategy to combat cancer: a nanoparticle based approach. Molecular pharmaceutics. 2010 Oct 4;7(5):1778-88. PubMed PMID: 20822093.

69. Alexis F, Rhee JW, Richie JP, Radovic-Moreno AF, Langer R, Farokhzad OC. New frontiers in nanotechnology for cancer treatment. Urologic oncology. 2008 Jan-Feb;26(1):74-85. PubMed PMID: 18190835.

70. Schlom J. Therapeutic cancer vaccines: current status and moving forward. J Natl Cancer Inst. 2012 Apr 18;104(8):599-613. PubMed PMID: 22395641. Pubmed Central PMCID: 3328421.

71. Strioga MM, Felzmann T, Powell DJ, Jr., Ostapenko V, Dobrovolskiene NT, Matuskova M, et al. Therapeutic dendritic cell-based cancer vaccines: the state of the art. Crit Rev Immunol. 2013;33(6):489-547. PubMed PMID: 24266347.

72. Thotathil Z, Jameson MB. Early experience with novel immunomodulators for cancer treatment. Expert Opin Investig Drugs. 2007 Sep;16(9):1391-403. PubMed PMID: 17714025.

73. Mellman I, Coukos G, Dranoff G. Cancer immunotherapy comes of age. Nature. 2011 Dec 22;480(7378):480-9. PubMed PMID: 22193102.

74. Singer J, Jensen-Jarolim E. IgE-based immunotherapy of cancer: challenges and chances. Allergy. 2013 Oct 14. PubMed PMID: 24117861.

75. Jensen-Jarolim E, Singer J. Cancer vaccines inducing antibody production: more pros than cons. Expert review of vaccines. 2011 Sep;10(9):1281-9. PubMed PMID: 21919618.

76. Rosenberg SA, Restifo NP, Yang JC, Morgan RA, Dudley ME. Adoptive cell transfer: a clinical path to effective cancer immunotherapy. Nature reviews Cancer. 2008 Apr;8(4):299-308. PubMed PMID: 18354418. Pubmed Central PMCID: 2553205.

77. Serda RE. Particle platforms for cancer immunotherapy. Int J Nanomedicine. 2013;8:1683-96. PubMed PMID: 23761969. Pubmed Central PMCID: 3674015.

78. Hanlon DJ, Aldo PB, Devine L, Alvero AB, Engberg AK, Edelson R, et al. Enhanced stimulation of anti-ovarian cancer CD8(+) T cells by dendritic cells loaded with nanoparticle encapsulated tumor antigen. Am J Reprod Immunol. 2011 Jun;65(6):597-609. PubMed PMID: 21241402. Pubmed Central PMCID: 3082607.

79. Ahmed MS, Bae YS. Dendritic cell-based therapeutic cancer vaccines: past, present and future. Clin Exp Vaccine Res. 2014 Jul;3(2):113-6. PubMed PMID: 25003083. Pubmed Central PMCID: 4083062.

80. Anguille S, Smits EL, Lion E, van Tendeloo VF, Berneman ZN. Clinical use of dendritic cells for cancer therapy. Lancet Oncol. 2014 Jun;15(7):e257-67. PubMed PMID: 24872109.

81. Parmiani G, Cimminiello C, Maccalli C. Increasing immunogenicity of cancer vaccines to improve their clinical outcome. Expert review of vaccines. 2013 Oct;12(10):1111-3. PubMed PMID: 24124873.

82. Palucka K, Banchereau J. Dendritic-cell-based therapeutic cancer vaccines. Immunity. 2013 Jul 25;39(1):38-48. PubMed PMID: 23890062. Pubmed Central PMCID: 3788678.

83. Palucka K, Banchereau J. Cancer immunotherapy via dendritic cells. Nature reviews Cancer. 2012 Apr;12(4):265-77. PubMed PMID: 22437871. Pubmed Central PMCID: 3433802.

84. Demento S, Steenblock ER, Fahmy TM. Biomimetic approaches to modulating the T cell immune response with nano- and micro- particles. Conf Proc IEEE Eng Med Biol Soc. 2009;2009:1161-6. PubMed PMID: 19963488.

85. Gallois A, Bhardwaj N. Dendritic cell-targeted approaches to modulate immune dysfunction in the tumor microenvironment. Frontiers in immunology. 2013;4:436. PubMed PMID: 24339825. Pubmed Central PMCID: 3857536.

86. Datta J, Terhune JH, Lowenfeld L, Cintolo JA, Xu S, Roses RE, et al. Optimizing dendritic cell-based approaches for cancer immunotherapy. The Yale journal of biology and medicine. 2014 Dec;87(4):491-518. PubMed PMID: 25506283. Pubmed Central PMCID: 4257036.

87. Baxevanis CN, Papamichail M, Perez SA. Therapeutic cancer vaccines: a long and winding road to success. Expert review of vaccines. 2014 Jan;13(1):131-44. PubMed PMID: 24224539.

88. Franks HA, Wang Q, Patel PM. New anticancer immunotherapies. Anticancer Res. 2012 Jul;32(7):2439-53. PubMed PMID: 22753700.

89. Amorij JP, Kersten GF, Saluja V, Tonnis WF, Hinrichs WL, Slutter B, et al. Towards tailored vaccine delivery: needs, challenges and perspectives. Journal of controlled release : official journal of the Controlled Release Society. 2012 Jul 20;161(2):363-76. PubMed PMID: 22245687.

90. de Souza AP, Bonorino C. The immune system: endogenous anticancer mechanism. Frontiers in bioscience. 2012 Jun 01;4:2354-64. PubMed PMID: 22652642.

91. Sheng WY, Huang L. Cancer immunotherapy and nanomedicine. Pharmaceutical research. 2011 Feb;28(2):200-14. PubMed PMID: 20821040.

92. Barnas JL, Simpson-Abelson MR, Yokota SJ, Kelleher RJ, Bankert RB. T cells and stromal fibroblasts in human tumor microenvironments represent potential therapeutic targets. Cancer microenvironment : official journal of the International Cancer Microenvironment Society. 2010 Mar 31;3(1):29-47. PubMed PMID: 21209773. Pubmed Central PMCID: 2990491.

93. Stephan MT, Stephan SB, Bak P, Chen J, Irvine DJ. Synapse-directed delivery of immunomodulators using T-cell-conjugated nanoparticles. Biomaterials. 2012 Aug;33(23):5776-87. PubMed PMID: 22594972. Pubmed Central PMCID: 3395588.

94. Bonifaz L, Bonnyay D, Mahnke K, Rivera M, Nussenzweig MC, Steinman RM. Efficient targeting of protein antigen to the dendritic cell receptor DEC-205 in the steady state leads to antigen presentation on major histocompatibility complex class I products and peripheral CD8+ T cell tolerance. The Journal of experimental medicine. 2002 Dec 16;196(12):1627-38. PubMed PMID: 12486105. Pubmed Central PMCID: 2196060.

95. Heegaard PM, Dedieu L, Johnson N, Le Potier MF, Mockey M, Mutinelli F, et al. Adjuvants and delivery systems in veterinary vaccinology: current state and future developments. Arch Virol. 2011 Feb;156(2):183-202. PubMed PMID: 21170730.

96. Vogel FR. Improving vaccine performance with adjuvants. Clin Infect Dis. 2000 Jun;30 Suppl 3:S266-70. PubMed PMID: 10875797.

97. Mantia-Smaldone GM, Chu CS. A review of dendritic cell therapy for cancer: progress and challenges. BioDrugs. 2013 Oct;27(5):453-68. PubMed PMID: 23592406.

98. Weidanz JA, Hawkins O, Verma B, Hildebrand WH. TCR-like biomolecules target peptide/MHC Class I complexes on the surface of infected and cancerous cells. International reviews of immunology. 2011 Oct-Dec;30(5-6):328-40. PubMed PMID: 22053972. Pubmed Central PMCID: 3405915.

99. Boraschi D, Italiani P. From Antigen Delivery System to Adjuvanticy: The Board Application of Nanoparticles in Vaccinology. Vaccines. 2015 Nov 05;3(4):930-9. PubMed PMID: 26556378. Pubmed Central PMCID: 4693225.

100. Correia-Pinto JF, Csaba N, Alonso MJ. Vaccine delivery carriers: insights and future perspectives. International journal of pharmaceutics. 2013 Jan 2;440(1):27-38. PubMed PMID: 22561794.

101. Thorley AJ, Tetley TD. New perspectives in nanomedicine. Pharmacol Ther. 2013 Nov;140(2):176-85. PubMed PMID: 23811125.

102. Mishra D, Hubenak JR, Mathur AB. Nanoparticle systems as tools to improve drug delivery and therapeutic efficacy. Journal of biomedical materials research Part A. 2013 Dec;101(12):3646-60. PubMed PMID: 23878102.

103. Peek LJ, Middaugh CR, Berkland C. Nanotechnology in vaccine delivery. Advanced drug delivery reviews. 2008 May 22;60(8):915-28. PubMed PMID: 18325628.

104. Wang J, Byrne JD, Napier ME, DeSimone JM. More effective nanomedicines through particle design. Small. 2011 Jul 18;7(14):1919-31. PubMed PMID: 21695781. Pubmed Central PMCID: 3136586.

105. Koua L, Suna J, Y. Z, Hea Z. The endocytosis and intracellular fate of nanomedicines: Implication for rational design Asian Journal of Pharmaceutical Sciences. 2013;8(1):1-10.

106. Pearson RM, Juettner VV, Hong S. Biomolecular corona on nanoparticles: a survey of recent literature and its implications in targeted drug delivery. Frontiers in chemistry. 2014;2:108. PubMed PMID: 25506050. Pubmed Central PMCID: 4245918.

107. Moon JJ, Huang B, Irvine DJ. Engineering nano- and microparticles to tune immunity. Advanced materials. 2012 Jul 24;24(28):3724-46. PubMed PMID: 22641380. Pubmed Central PMCID: 3786137.

108. Lu JM, Wang X, Marin-Muller C, Wang H, Lin PH, Yao Q, et al. Current advances in research and clinical applications of PLGA-based nanotechnology. Expert Rev Mol Diagn. 2009 May;9(4):325-41. PubMed PMID: 19435455. Pubmed Central PMCID: 2701163.

109. Parveen S, Sahoo SK. Polymeric nanoparticles for cancer therapy. Journal of drug targeting. 2008 Feb;16(2):108-23. PubMed PMID: 18274932.

110. Grabnar PA, Kristl J. The manufacturing techniques of drug-loaded polymeric nanoparticles from preformed polymers. J Microencapsul. 2011;28(4):323-35. PubMed PMID: 21545323.

111. Mundargi RC, Babu VR, Rangaswamy V, Patel P, Aminabhavi TM. Nano/micro technologies for delivering macromolecular therapeutics using poly(D,L-lactide-co-glycolide) and its derivatives. Journal of controlled release : official journal of the Controlled Release Society. 2008 Feb 11;125(3):193-209. PubMed PMID: 18083265.

112. Makadia HK, Siegel SJ. Poly Lactic-co-Glycolic Acid (PLGA) as Biodegradable Controlled Drug Delivery Carrier. Polymers. 2011 Sep 01;3(3):1377-97. PubMed PMID: 22577513. Pubmed Central PMCID: 3347861.

113. De Souza Reboucas J, Esparza I, Ferrer M, Sanz ML, Irache JM, Gamazo C. Nanoparticulate adjuvants and delivery systems for allergen immunotherapy. Journal of biomedicine & biotechnology. 2012;2012:474605. PubMed PMID: 22496608. Pubmed Central PMCID: 3303624.

114. Hamdy S, Molavi O, Ma Z, Haddadi A, Alshamsan A, Gobti Z, et al. Co-delivery of cancer-associated antigen and Toll-like receptor 4 ligand in PLGA nanoparticles induces potent CD8+ T cell-mediated anti-tumor immunity. Vaccine. 2008 Sep 15;26(39):5046-57. PubMed PMID: 18680779.

115. Danhier F, Ansorena E, Silva JM, Coco R, Le Breton A, Preat V. PLGA-based nanoparticles: an overview of biomedical applications. Journal of controlled release : official journal of the Controlled Release Society. 2012 Jul 20;161(2):505-22. PubMed PMID: 22353619.

116. Nikitczuk KP, Schloss RS, Yarmush ML, Lattime EC. PLGA-polymer encapsulating tumor antigen and CpG DNA administered into the tumor microenvironment elicits a systemic antigen-specific IFN-gamma response and enhances survival. J Cancer Ther. 2013 Jan 1;4(1):280-90. PubMed PMID: 23741626. Pubmed Central PMCID: 3670804.

117. San Roman B, Irache JM, Gomez S, Tsapis N, Gamazo C, Espuelas MS. Co-encapsulation of an antigen and CpG oligonucleotides into PLGA microparticles by TROMS technology. European journal of pharmaceutics and biopharmaceutics : official journal of Arbeitsgemeinschaft fur Pharmazeutische Verfahrenstechnik eV. 2008 Sep;70(1):98-108. PubMed PMID: 18501572.

118. Elamanchili P, Lutsiak CM, Hamdy S, Diwan M, Samuel J. "Pathogen-mimicking" nanoparticles for vaccine delivery to dendritic cells. Journal of immunotherapy. 2007 May-Jun;30(4):378-95. PubMed PMID: 17457213.

119. Diwan M, Elamanchili P, Lane H, Gainer A, Samuel J. Biodegradable nanoparticle mediated antigen delivery to human cord blood derived dendritic cells for induction of primary T cell responses. Journal of drug targeting. 2003;11(8-10):495-507. PubMed PMID: 15203918.

120. Heit A, Schmitz F, Haas T, Busch DH, Wagner H. Antigen co-encapsulated with adjuvants efficiently drive protective T cell immunity. Eur J Immunol. 2007 Aug;37(8):2063-74. PubMed PMID: 17628858.

121. Lee YR, Lee YH, Im SA, Yang IH, Ahn GW, Kim K, et al. Biodegradable nanoparticles containing TLR3 or TLR9 agonists together with antigen enhance MHC-restricted presentation of the antigen. Arch Pharm Res. 2010 Nov;33(11):1859-66. PubMed PMID: 21116790.

122. Kasturi SP, Skountzou I, Albrecht RA, Koutsonanos D, Hua T, Nakaya HI, et al. Programming the magnitude and persistence of antibody responses with innate immunity. Nature. 2011 Feb 24;470(7335):543-7. PubMed PMID: 21350488. Pubmed Central PMCID: 3057367.

123. Ma W, Chen M, Kaushal S, McElroy M, Zhang Y, Ozkan C, et al. PLGA nanoparticle-mediated delivery of tumor antigenic peptides elicits effective immune responses. Int J Nanomedicine. 2012;7:1475-87. PubMed PMID: 22619507. Pubmed Central PMCID: 3356185.

124. Diwan M, Tafaghodi M, Samuel J. Enhancement of immune responses by co-delivery of a CpG oligodeoxynucleotide and tetanus toxoid in biodegradable nanospheres. Journal of controlled release : official journal of the Controlled Release Society. 2002 Dec 13;85(1-3):247-62. PubMed PMID: 12480329.

125. Karuturi BVK, Tallapaka SB, Yeapuri P, Curran SM, Sanderson SD, Vetro JA. Encapsulation of an EP67-Conjugated CTL Peptide Vaccine in Nanoscale Biodegradable Particles Increases the Efficacy of Respiratory Immunization and Affects the Magnitude and Memory Subsets of Vaccine-Generated Mucosal and Systemic CD8+ T Cells in a Diameter-Dependent Manner. Molecular pharmaceutics. 2017 May 01;14(5):1469-81. PubMed PMID: 28319404.

126. Silva AL, Rosalia RA, Sazak A, Carstens MG, Ossendorp F, Oostendorp J, et al. Optimization of encapsulation of a synthetic long peptide in PLGA nanoparticles: low-burst release is crucial for efficient CD8(+) T cell activation. European journal of pharmaceutics and biopharmaceutics : official journal of Arbeitsgemeinschaft fur Pharmazeutische Verfahrenstechnik eV. 2013 Apr;83(3):338-45. PubMed PMID: 23201055.

127. Schlosser E, Mueller M, Fischer S, Basta S, Busch DH, Gander B, et al. TLR ligands and antigen need to be coencapsulated into the same biodegradable microsphere for the generation of potent cytotoxic T lymphocyte responses. Vaccine. 2008 Mar 20;26(13):1626-37. PubMed PMID: 18295941.

128. Ebrahimian M, Hashemi M, Maleki M, Abnous K, Hashemitabar G, Ramezani M, et al. Induction of a balanced Th1/Th2 immune responses by co-delivery of PLGA/ovalbumin nanospheres and CpG ODNs/PEI-SWCNT nanoparticles as TLR9 agonist in BALB/c mice. International journal of pharmaceutics. 2016 Dec 30;515(1-2):708-20. PubMed PMID: 27989827.

129. Lesterhuis WJ, Haanen JB, Punt CJ. Cancer immunotherapy--revisited. Nature reviews Drug discovery. 2011 Aug;10(8):591-600. PubMed PMID: 21804596.

130. Lin YS, Lee MY, Yang CH, Huang KS. Active targeted drug delivery for microbes using nano-carriers. Current topics in medicinal chemistry. 2015;15(15):1525-31. PubMed PMID: 25877093. Pubmed Central PMCID: 4997950.

131. Zhao L, Seth A, Wibowo N, Zhao CX, Mitter N, Yu C, et al. Nanoparticle vaccines. 2014;32 (3):327–37. PubMed PMID: 24295808.

132. Dalgleish AG. Therapeutic cancer vaccines: why so few randomised phase III studies reflect the initial optimism of phase II studies. Vaccine. 2011 Nov 3;29(47):8501-5. PubMed PMID: 21933695.

133. Krishnamachari Y, Geary SM, Lemke CD, Salem AK. Nanoparticle delivery systems in cancer vaccines. Pharmaceutical research. 2011 Feb;28(2):215-36. PubMed PMID: 20721603. Pubmed Central PMCID: 3559243.

134. Gregory AE, Titball R, Williamson D. Vaccine delivery using nanoparticles. Frontiers in cellular and infection microbiology. 2013;3:13. PubMed PMID: 23532930. Pubmed Central PMCID: 3607064.

135. D'Elios MM, Del Prete G, Amedei A. New frontiers in cell-based immunotherapy of cancer. Expert opinion on therapeutic patents. 2009 May;19(5):623-41. PubMed PMID: 19441938.

136. Sinha R, Kim GJ, Nie S, Shin DM. Nanotechnology in cancer therapeutics: bioconjugated nanoparticles for drug delivery. Mol Cancer Ther. 2006 Aug;5(8):1909-17. PubMed PMID: 16928810.

137. Bertrand N, Wu J, Xu X, Kamaly N, Farokhzad OC. Cancer nanotechnology: the impact of passive and active targeting in the era of modern cancer biology. Advanced drug delivery reviews. 2014 Feb;66:2-25. PubMed PMID: 24270007. Pubmed Central PMCID: 4219254.

138. Gunaseelan S, Gunaseelan K, Deshmukh M, Zhang X, Sinko PJ. Surface modifications of nanocarriers for effective intracellular delivery of anti-HIV drugs. Advanced drug delivery reviews. 2010 Mar 18;62(4-5):518-31. PubMed PMID: 19941919. Pubmed Central PMCID: 2841563.

139. Scott AM, Wolchok JD, Old LJ. Antibody therapy of cancer. Nature reviews Cancer. 2012 Mar 22;12(4):278-87. PubMed PMID: 22437872.

140. Blanco E, Hsiao A, Mann AP, Landry MG, Meric-Bernstam F, Ferrari M. Nanomedicine in cancer therapy: innovative trends and prospects. Cancer science. 2011 Jul;102(7):1247-52. PubMed PMID: 21447010.

141. Kocbek P, Obermajer N, Cegnar M, Kos J, Kristl J. Targeting cancer cells using PLGA nanoparticles surface modified with monoclonal antibody. Journal of controlled release : official journal of the Controlled Release Society. 2007 Jul 16;120(1-2):18-26. PubMed PMID: 17509712.

142. Byrne JD, Betancourt T, Brannon-Peppas L. Active targeting schemes for nanoparticle systems in cancer therapeutics. Advanced drug delivery reviews. 2008 Dec 14;60(15):1615-26. PubMed PMID: 18840489.

143. Ikeda J, Sun YL, An KN, Amadio PC, Zhao C. Application of carbodiimide derivatized synovial fluid to enhance extrasynovial tendon gliding ability. The Journal of hand surgery. 2011 Mar;36(3):456-63. PubMed PMID: 21371626. Pubmed Central PMCID: 3625936.

144. Zhang F, Lees E, Amin F, Rivera Gil P, Yang F, Mulvaney P, et al. Polymer-coated nanoparticles: a universal tool for biolabelling experiments. Small. 2011 Nov 18;7(22):3113-27. PubMed PMID: 21928301.

145. Thamake SI, Raut SL, Ranjan AP, Gryczynski Z, Vishwanatha JK. Surface functionalization of PLGA nanoparticles by non-covalent insertion of a homo-bifunctional spacer for active targeting in cancer therapy. Nanotechnology. 2011 Jan 21;22(3):035101. PubMed PMID: 21149963.

146. Lau A, Berube G, Ford CH. Conjugation of doxorubicin to monoclonal anti-carcinoembryonic antigen antibody via novel thiol-directed cross-linking reagents. Bioorganic & medicinal chemistry. 1995 Oct;3(10):1299-304. PubMed PMID: 8564395.

# CHAPTER 2

## 2. Purpose and hypothesis of the project

### 2.1 Main goal

The main goal of this project was to develop an understanding of a detailed relationship between NP structure and activity; and address the key questions regarding the fundamental requirements of nanoparticle structure and chemistry to selectively target specific markers on cells/tissues. To achieve this, various formulations of NPs was developed and optimized. The developed system will be established as a model delivery system for immunotherapeutic purpose.

### 2.2 Hypothesis

The hypothesis of this study can be divided as:

- ✓ Hypothesis 1: Poly-lactide co-glycolic acid (PLGA) NP formulation can be structurally modified with anti-CD205 antibody ligand.
- ✓ Hypothesis 2: PLGA NPs can selectively target dendritic cells (DCs) by enhancing the recognition and DC uptake.
- ✓ Hypothesis 3: PLGA NPs can provide effective immunotherapeutic response in DC and mice model.

### 2.3 Objectives

The purpose of this study was to develop a structurally modified PLGA NP formulation. Here, four groups of PLGA (two types of end group: COOH and ester and each offering two viscosities) were assessed and utilized to develop the suitable formulation for *in-vivo* model. Surface modification of PLGA NPs with antibody against CD205 receptor will accomplish our goal to targeting DCs by

enhancing the recognition and DC uptake. The encapsulation of Ovalbumin (model antigen) and adjuvant (MPLA) in the formulations will stimulate the immune system both *in-vitro* and *in-vivo*. Therefore, the targeted PLGA NPs loaded with antigen-adjuvant can be used as a model therapeutic system for immunotherapeutic purpose in future. The objectives can be divided as follows:

1. Development of suitable emulsification solvent evaporation technique for preparation of PLGA NPs and selection of solvent and cryoprotectant to stabilize the formulations
2. Development of structurally modified NP delivery system with anti CD205 antibody through: a) physical adsorption of antibody onto ester- and COOH-terminated PLGA NPs, b) covalent attachment of antibody to ester- and COOH-terminated PLGA NPs
3. Characterization of antibody modified PLGA NPs in terms of their size, polydispersity index, zeta potential, safety profile, antibody quantification and surface characteristics in comparison with unmodified PLGA NP
4. Selection of a suitable fluorescent dye to assess the uptake of NPs in the DCs. And further development and characterization of coumarin-6 loaded NPs
5. Assessment of the targeting efficiency of coumarin-6 loaded PLGA NPs modified with anti CD205 antibody by DC uptake studies and compare it with unmodified PLGA NPs to establish a relationship between the structure and targeting
6. Development of OVA and/or MPLA loaded PLGA NPs and characterize in terms of particle size, zeta potential, polydispersity index, safety profile, OVA quantification, release of antigen OVA and assessment of structural integrity of OVA
7. Evaluation of OVA and/or MPLA loaded NPs (plain and antibody modified) on enhancing DC stimulatory immune response *in-vitro* through DC maturation study and cytokine estimation. A dose-response relationship will be estimated for *in-vivo* experiments
8. Evaluation of OVA and/or MPLA loaded modified PLGA NPs (plain and antibody modified) on enhancing DC stimulatory immune responses in wild-type (balb/c) and transgenic (OT1) mice model

through proliferation study, IgG secretion and cytokine release and stabilizing the dose-response relationship

# CHAPTER 3

**Note:**

**This paper has been published in International Journal of Nanomedicine.**

**2015 Dec 10; 10:7371-84. doi: 10.2147/IJN.S90866.**

**(https://www.dovepress.com/investigation-and-optimization-of-formulation-parameters-on-preparatio-peer-reviewed-article-IJN)**



## 3. Investigation and optimization of formulation parameters on preparation of targeted anti-CD205 tailored PLGA nanoparticles

Sheikh Tasnim Jahan and Azita Haddadi[1]

Division of Pharmacy, College of Pharmacy and Nutrition, University of Saskatchewan, Saskatoon, SK S7N 5E5, Canada

[1] Corresponding Author: Azita Haddadi, 3D01.01, D Wing Health Sciences, 107 Wiggins Road, College of Pharmacy and Nutrition, University of Saskatchewan, Saskatoon SK, S7N 5E5; Phone: (306) 966-6495; Fax: (306) 966-6377; e-mail: azita.haddadi@usask.ca

### 3. 1 Brief introduction to chapter 3

Chapter 3 is based on two different approaches of nanoparticle preparation using emulsification solvent evaporation technique, choice of suitable solvent, cryopreservation of formulations, surface modification of NPs, cytotoxicity profile and surface display of antibody.

Two types of PLGA polymers with different inherent viscosities (i.v.) are being studied:

a. PLGA with carboxyl end group (uncapped) and inherent viscosities of 0.18 and 0.55-0.75 dl/g
b. PLGA with ester end group (capped) and inherent viscosities of 0.15-0.25 and 0.55-0.75 dl/g

NP preparation and antibody attachment scheme are represented in figure 3.1 and 3.2. The parameters evaluated for both NP preparation and antibody attachment are represented in table 3.1 and 3.2.

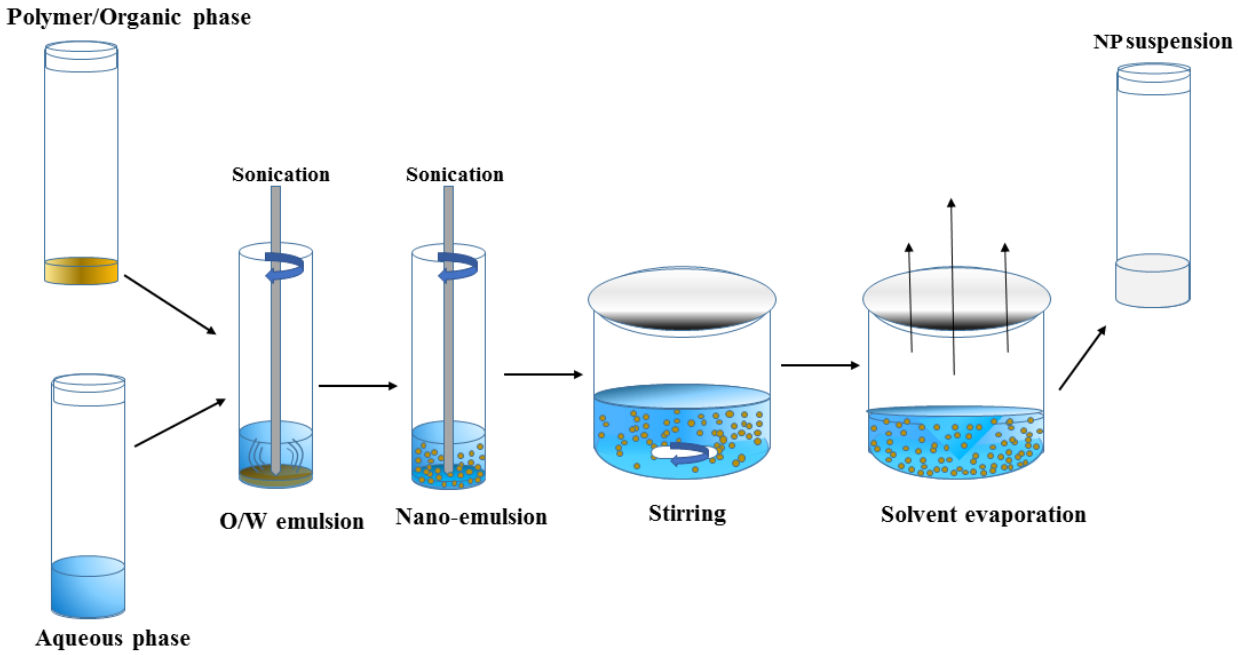


**Figure 3.1: Schematic diagram for emulsification solvent evaporation technique**

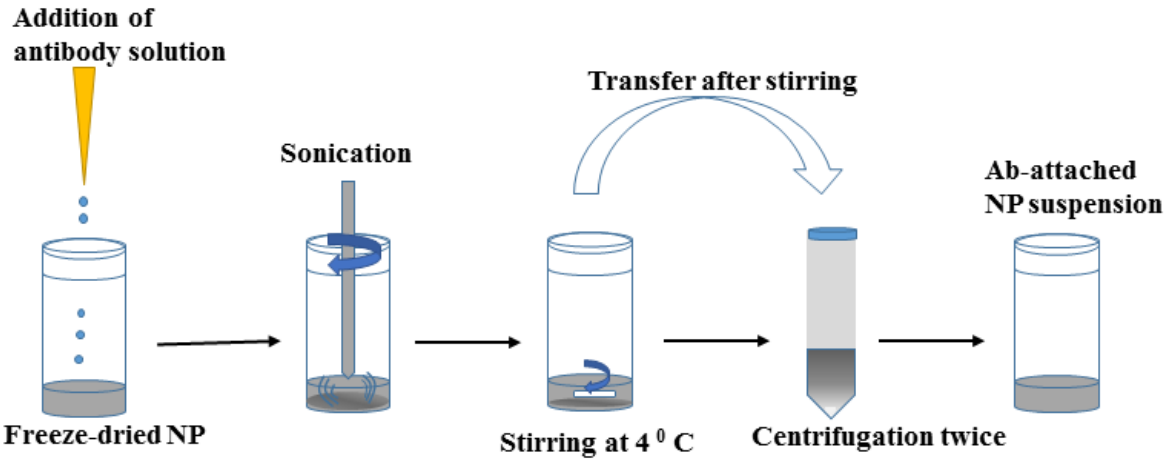


**Figure 3.2: Schematic diagram for Ab-attachment process**

**Table 3.1: Experimental parameters and their levels for NP preparation**

| **Formulation parameters** | **Specific parameter** | **Method 1** | **Method 2** |
|---|---|---|---|
| 1. Polymer | 0.15-0.25 iv PLGA (ester-terminated) | 100 mg | 65 mg |
| | 0.55-0.75 iv PLGA (ester-terminated) | 100 mg | 65 mg |
| | 0.18 iv PLGA (COOH-terminated) | 100 mg | 65 mg |
| | 0.55-0.75 iv PLGA (COOH-terminated) | 100 mg | 65 mg |
| 2. Cross-linker | BS3 | --------- | 1.5 mg (COOH and ester PLGA) |
| 3. Organic solvent | Chloroform | 400 µl | -------- |

| | | | |
|---|---|---|---|
| | Ethyl acetate | --------- | 1 ml |
| 4. Stabilizer | PVA | 5 % | 2.2 % |
| 5. Sonication time | | 1-4 minutes | 2-3 minutes |
| 6. Stirring time | | 2-3 hours | 2-3 hours |
| 7. Centrifugation speed and time (twice) | | 30,000 rpm for 30 mins, 25,000 rpm for 25 mins | 30,000 rpm for 30 mins, 25,000 rpm for 25 mins |
| 8. Freeze-drying | | ≥48 hours | ≥48 hours |

**Table 3.2: Experimental parameters and their levels for antibody attachment**

| **Specific parameters** | **Method 1** | | **Method 2** | |
|---|---|---|---|---|
| | **Adsorption** | **Covalent attachment** | **Adsorption** | **Covalent attachment** |
| **1. Nanoparticles (NP) type** | | | | |
| 0.15-0.25 iv PLGA ester NP | √ | ----- | √ | ----- |
| 0.55-0.75 iv PLGA ester NP | √ | ----- | √ | ----- |
| 0.18 iv PLGA COOH NP | √ | √ | √ | √ |
| 0.55-0.75 iv PLGA COOH NP | √ | √ | √ | √ |
| **2. Cross-linker** | | | | |
| EDC (2mg) | ----- | √ | ----- | ----- |
| NHS (2mg) | ----- | √ | ----- | ----- |
| 4. Sonication time: 30 seconds-1 min | √ | √ | √ | √ |
| 5. Stirring time (4 hours) | √ | √ | √ | √ |
| 6. Centrifugation speed: 14, 000 rpm and time: 25-30 minutes | √ | √ | √ | √ |
| 7. Freeze-drying (≥48 hours) | √ | √ | √ | √ |

**3.2 Abstract**

The purpose of this study was to assess the effect of various formulation parameters on anti-CD205 antibody decorated poly (D, L-lactide co-glycolide) (PLGA) nanoparticles (NPs) in terms of their ability to target dendritic cells (DCs). In brief, emulsification solvent evaporation technique was adapted to design NP formulations using two different viscosity grades (low and high) of both ester and carboxylic acid terminated PLGA. Incorporation of ligand was achieved following physical adsorption or chemical conjugation processes. The physicochemical characterizations of formulations were executed to assess the effects of different solvents (chloroform and ethyl acetate), stabilizer percentage, polymer types, polymer viscosities, ligand-NP bonding types, cross-linkers, and cryoprotectants (sucrose and trehalose). Modification of any of these parameters shows significant improvement of physicochemical properties of NPs. Ethyl acetate was the solvent of choice for the formulations to ensure better emulsion formation. Infrared spectroscopy confirmed the presence of anti-CD205 antibody in the NP formulation. Finally, cytotoxicity assay confirmed the safety profile of the NPs for DCs. Thus, ligand modified structurally concealed PLGA NPs is a promising delivery tool for targeting DCs *in vivo*.

**Keywords:** nanoparticle, anti-CD205, PLGA, dendritic cells

### 3.3 Introduction

Dendritic cells (DCs) are known as the potent antigen presenting cells to induce adaptive immune responses. Manipulating DCs by targeted antigen delivery through various endocytic and secretory pathways is a consequence of delivering site-specific therapeutic delivery system. C-type lectin receptor CD205 (molecular weight of 205 kDa), exclusively expressed on DCs; is a widely studied DC target molecule for induction of immune response. Anti-CD205 monoclonal antibody (mAb) linked delivery system can efficiently deliver its cargo to the processing compartments of DCs in vivo.(1) CD205 receptor possesses a fast internalization speed, where over 80% of surface CD205 are internalized within 90 minutes.(2), (3) The proportion of targeted molecules endocytosed by this receptor in both immature and mature DCs is exceptionally higher compared to other surface receptors. In addition to internalization, antigen presentation on major histocompatibility complex (MHC)-1 and MHC-2, CD205 receptors elicited superior presentation compared to CD11c receptor. Thus, targeting this receptor would be promising in both steady-state and inflammatory conditions.(2), (4) Therefore, CD205 specific antibodies can induce efficient antigen processing and presentation, notably eliciting both T helper1 $CD4^+$ T cell and $CD8^+$ T cell responses. Engagement of anti-CD205 mAb to target CD205 receptors shows high consensus to deliver vaccine utilizing an appropriate delivery system. (5)

Over the past decade, nanoparticles (NPs) have gained increasing attention in the field of drug delivery. Particularly, polyester based NPs offer the advantage of effective delivery of drug to the target site, ensuring therapeutic benefit with minimum side effects. Industry has recently focused on the US Food and Drug Administration (FDA) approved poly (D, L-lactide co-glycolide) (PLGA) based NPs because of their biodegradability, biocompatibility, low toxicity, controlled release, and surface-modification properties.(6), (7) Hence, functionalization of PLGA NPs with ligands such as anti-CD205 antibody presents an opportunity for an innovative antibody-targeted vaccine delivery system. This coupling aims to provide increased payload of drug/antigen, thereby increasing response and reducing the number of doses required. The ligand itself might function in a non-activating manner, which is important for

immunotherapeutic diseases. (8) PLGA polymers are commercially available with different terminal groups, namely, free carboxylic acid (COOH) end groups (uncapped) or esterified terminal groups (capped). The end groups of PLGA can influence drug encapsulation efficiency, degradation, stability, and conjugation of ligands. For example, COOH terminated NPs can result in a slightly acidic environment, that may cause degradation of encapsulated antigen during formulation process or inside endosomal compartment. (9)

The present study focuses on the formulation optimization with anti-CD205 ligand using both capped and uncapped PLGA; each type offered with low and high viscosity grades (Figure 1).(10) Discussions are based on the comparison and evaluation of how different process parameters affect these two subtypes of ester and COOH ended PLGA NPs for in vitro experiment setups. To serve this purpose, standardization of various parameters was executed to obtain NPs with suitable particle size, surface charge, polydispersity index (PDI), surface display, toxicity profile, and structural modification. Therefore, a structure-activity relationship is concluded after analyzing the results. As a consequence, the ultimate goal is to develop a delivery system with suitable formulation strategy that could simulate the in vitro responses in an animal model. Altogether, our results support the potential use of PLGA NPs as therapeutic delivery system to design a cancer vaccine.

### 3.4 Materials and methods

#### 3.4.1 Materials

Ester terminated PLGA (inherent viscosity 0.15–0.25 dL/g and 0.55–0.75 dL/g) and COOH terminated PLGA (inherent viscosity 0.18 dL/g and 0.55–0.75 dL/g) were purchased from LACTEL Absorbable Polymers, Birmingham, AL, USA. Polyvinyl alcohol (PVA), bis(sulfo-succinimidyl) suberate (BS3), alpha minimum essential medium, fetal bovine serum, 3-(4, 5-dimethylthiazol-2-yl)-2, 5-diphenyltetrazolium bromide (MTT) assay kit, and bicinchoninic acid (BCA) assay kit were purchased from Sigma-Aldrich Co., St Louis, MO, USA. Other reagents used were *N*-hydroxysuccinimide esters (sulfo-NHS) and 1-ethyl-3-(-3-dimethylaminopropyl) carbodiimide hydrochloride (EDC) from Thermo

Fisher Scientific, Waltham, MA, USA. Biotin anti-mouse CD205 antibody was purchased from Biolegend (San Diego, CA, USA). JAWSII DC line was obtained from American Type Culture Collection (ATCC), Manassas, VA, USA. GM-CSF was purchased from Thermo Fisher Scientific. Solvents like chloroform and ethyl acetate were of analytical grade.

### 3.4.2 Preparation of NPs by emulsification solvent evaporation method

**Method 1**

PLGA NPs were prepared by the double emulsification solvent evaporation technique as previously reported.(11) Briefly, PLGA was dissolved in chloroform (25% weight/volume [w/v]). Aqueous phase comprised of 5% w/v PVA was added to the oil phase in a drop wise manner and sonicated by probe-sonicator. The resulting primary emulsion was transferred into water to form the secondary emulsion and stirred to evaporate the chloroform. NPs were then collected by centrifugation, washed with distilled water to remove the residual PVA, and resuspended in distilled water. Cryoprotectant was used in the formulations to minimize freeze-drying stress after washing.(12)

**Method 2**

The NPs were prepared following single oil in water emulsification solvent evaporation technique.(13) In brief, PLGA was dissolved in ethyl acetate (6.5% w/v) and transferred into 2.2% of PVA to form the emulsion. The procedure was then followed as mentioned in Method 1 with some minor modifications. To prepare pre-activated NPs for the covalent attachment of ligand, presence of BS3 in the aqueous phase is mandatory. The prepared NPs were lyophilized with cryoprotectants to avoid aggregation. Parameters mentioned in Table 3.3 were considered in the preparation and evaluated for both methods 1 and 2. Discussion will be based on the effect of these parameters on the physicochemical properties of NPs.

### 3.4.3 Antibody coupling to the particle surface

Antibody coupling was carried out through two approaches, physical adsorption and covalent conjugation.

**Physical adsorption of antibody to NPs' surface**

Biotinylated anti-CD205 mAb was added at a certain concentration to previously lyophilized PLGA NPs in phosphate buffered saline (PBS) and stirred for 4 hours in ice. After that, excess PBS was centrifuged and washed out. The NPs were freeze-dried upon re-suspension followed by storage at −20°C. At each washing step, the obtained supernatants were stored to determine the amount of un-conjugated antibody by BCA assay. This is an indirect method to measure the actual amount of antibody attached to the NPs. The control groups for BCA assay were the supernatants obtained from antibody-free NPs of each formulation through the similar conditions maintained in antibody-NP conjugation process.(14)

**Covalent attachment of antibody with NPs**

Two different approaches were followed for covalent attachment where, one was using carbodiimide chemistry with EDC and sulfo-NHS (for method 1); and the other one with the use of BS3 (for method 2). For the first method, EDC/sulfo-NHS solution was added to antibody solution. The resulting suspension was stirred for 4 hours in ice, after which, centrifugation was done twice to remove excess reagents and soluble isourea by-product. Therefore, the amide bonds were formed between the primary amine groups of antibodies with the free carboxylic end groups of PLGA NPs.[14]For the second method, BS3 pre-activated freeze-dried NPs were resuspended in PBS for the covalent attachment of antibody.(13) Upon addition of antibody, the activated NPs underwent the process of conjugation followed by washing twice with PBS of pH 7.2. The covalent amide linkage was formed by replacing lysine groups of the antibody with free carboxylic group of BS3 upon releasing sulfo-NHS groups. The obtained NPs were further freeze-dried followed by storage at −20°C. The reaction schemes for both approaches are shown in Figure 3.3.

**3.4.4 Determination of particle size, zeta potential (ZP), and PDI**

Dynamic light scattering technique was used to measure the particle size, ZP, and PDI using Malvern ZetaSizer, Nano ZS (Malvern Instruments, Malvern, UK).(15) ZP was measured on the basis of

electrophoretic mobility in an electric field.(16) The measurements were performed for both unmodified and modified NPs before and after freeze-drying. Recovery percentage or yield of the preparation technique was calculated from the amount of NPs obtained divided by the total amount of initial PLGA polymer used to prepare NPs (the amount of PVA is negligible).

### 3.4.5 Morphology by scanning electron microscopy (SEM)

Morphology of the NP surface was analyzed by SEM. In brief, PLGA NPs were dispersed in distilled water (0.2% w/v). Appropriate portion of nano-suspension was placed on the carbon tape of the metal stub and allowed to air-dry. The samples were then placed in a sputter coater (S150B; BOC Edwards, Sussex, UK) for 1 minute to produce a gold coating with ~20 nm thickness; and viewed under a scanning electron microscope at voltage of 20–25 kV (Carl Zeiss Evo 60; Carl Zeiss Meditec AG, Jena, Germany).(17)

### 3.4.6 Structural characterization by Fourier transform infrared spectroscopy (FTIR)

FTIR analysis of NPs was recorded on a Bruker IFS 66v/S infrared spectrophotometer (Bruker Optics Inc, Billerica, MA, USA) in the mid-infrared range at the Canadian Light Source (CLS), University of Saskatchewan, Saskatoon, SK, Canada. All samples were mixed with spectroscopic grade potassium bromide and mulled to prepare pellets. The spectra were taken for potassium bromide pellets in the range of 4,000–400 $cm^{-1}$ in absorbance mode.(13), (18) Data analysis was performed with Bruker Opus software. Baseline correction was performed on all raw absorbance spectra.

### 3.4.7 Determination of amount of antibody attached to the NPs

A BCA protein assay was performed to measure the amount of antibody attached per mg of NPs. The antibody was analyzed both directly (on the NP surface) and indirectly (in the supernatant). Briefly, a sample of modified NP was taken and resuspended in water to assess the antibody attached to the surface. Unmodified NPs were used as controls. In indirect method, the collected supernatants during washing steps were stored for BCA assay to quantify the amount of unbound antibody. Ninety-six well plate was

used and the instructions from the BCA assay kit were followed for the quantification. The standard curve was generated by plotting the absorbance versus various concentrations of the standard solution, bovine serum albumin. The standard curve was found to be linear over the range of 0–32 μg/mL. The absorbance was measured at a wavelength of 562 nm in a microplate reader.(19)

### 3.4.8 DC (JAWS II) culture

The DC line obtained from American Type Culture Collection was initiated as recommended. The cell culture was maintained at 37°C and 5% $CO_2$ in complete media for few days to reach the optimum confluency. After that, the cells were stored in cryo-vials containing freezing solution (dimethyl sulfoxide). The complete media is as recommended by ATCC.

### 3.4.9 In vitro cytotoxicity assay

MTT assay was performed to investigate the cytotoxicity of NPs on DC lines using corresponding untreated cells as control. On day 1, the cells were seeded in 96-well plate at a density of 10,000 cells per mL. After overnight incubation, cells were exposed to various formulation treatments. On day 3, 10 μL of MTT solution was added to each well and further incubated for 4 hours. Finally, 100 μL of MTT solvent was added to dissolve the formazan crystals. The absorption intensity of the purple–blue color formed was measured at a wavelength of 570 nm by microplate reader.[15] Cell viability was calculated using the following equation:(20)

$$\text{Percent viability rate} = \frac{\text{Absorbance of treated group} - \text{blank}}{\text{Absorbance of control group without any treatment} - \text{blank}} \times 100 \quad (1)$$

### 3.4.10 Statistics

All data are presented as mean ± standard deviation. The significance of the differences between groups was analyzed by unpaired Student's *t*-test or one-way analysis of variance followed by the Tukey's post hoc test for multiple comparisons. *P*-value of <0.05 was considered as statistically significant. All the

statistical analyses were performed with GraphPad Prism 5.03 software (GraphPad Software, Inc., La Jolla, CA, USA).

## 3.5 Results

### 3.5.1 Effect of polymers' end groups and viscosities

The influence of polymer composition (functional end group and inherent viscosity) on physicochemical properties of NPs was investigated. Particle size is an important parameter that can affect the biopharmaceutical and biodistribution properties of formulations. The smaller particle size will lead to a higher total surface area relating to faster release of its payload.(21) PDI is an index for size distribution where an enhanced PDI value indicates that the particles do not have a uniform distribution.(22)

In method 1, the average particle size and PDI for plain NPs prepared with COOH and ester end groups were found to range from 202 to 237 nm and 231 to 281 nm, respectively as shown in Figure 3.4A. Polymer viscosity (0.15 and 0.55 inherent viscosity) was indicated as a limiting factor for particle size in both COOH and ester terminated NPs. With an increase in polymer viscosity the particle size also increased as shown in Figure 3.4A and B.(23) After statistical evaluation, there was no significant effect observed for the variable end groups of PLGA on plain NPs' particle size, PDI, and ZP (Figure 3.4C) values (Table 3.4 and Figure 3.5). However, the effect of variable end groups and viscosities of the polymer on particle size was found significant for ligand modified NPs (Table 3.4) although these two variables had no effect on their PDI values.

In method 2, both particle size and PDI values were in a fairly desirable range for all NPs before freeze-drying (Figure 3.5A). A proportional relation between polymer viscosity and particle size was observed for plain (Figure 3.4A, B and Figure 3.5A, B) and modified (Table 3.4) NPs. In contrary, no significant correlation could be made between the variable polymer end groups and physicochemical properties.

### 3.5.2 Effect of ligand-NP bonding types

In method 1, low viscosity COOH terminated NP had a significantly higher ($P$<0.05) amount of antibody adsorbed compared to other groups and the particles were in an appropriate size range below 350 nm. The high viscosity COOH terminated NPs had relatively larger size with wide PDI values. In addition, ZP values showed a significant drop toward positive value upon attachment of ligand with NPs as shown in Table 3.4 ($P$<0.05). NPs obtained after covalent attachment of antibody, had the same particle size trend as observed in the adsorbed groups. While larger aggregates were formed with antibody-adsorbed NPs for ester terminated NPs, which was further minimized using cryoprotectant. The original particle size was above the nanometer range, indicating the presence of aggregates (PDI value >0.99).

In method 2, there was a significant decrease in particle size for the covalently modified NPs compared to antibody-adsorbed formulations. But no concrete correlation could be drawn to compare the antibody loading through adsorption and covalent attachment of ligand with NPs. In addition, the inclusion of antibody to NPs shifted the ZP toward positive values, which indirectly confirms the presence of antibody on the NP surface, as summarized in Table 3.4 and Figure 3.5C. This could be ascribed to the amphiphilic properties of antibody or shielding the negative charges on the surface by positively charged antibody.(24), (25) Table 3.4 represents the overall data for particle size, PDI, ZP, and antibody quantification for modified NPs. Furthermore, the SEM photographs confirmed that NPs form spherical shaped particles within the desired size range. SEM images of NPs were taken at a voltage of 20–25 kV at various magnifications as shown in Figure 3.6.

### 3.5.3 Effect of cryoprotectants

The NPs were in a well-dispersed suspension form before freeze-drying; however they formed aggregates upon reconstitution after freeze-drying, which could not be re-dispersed even after sonication. The reason behind this irreversible aggregation could be attributed to freeze-drying stress on the particles rendering a wide range of PDI value before ligand attachment.(26) Use of cryoprotectants could overcome this stress to obtain aggregation-free fine suspension after ligand attachment. However, all the formulations had

significant difference in particle size before and after freeze-drying ($P$<0.05) irrespective of the presence of cryoprotectant.

Notably, the use of trehalose (10%) could not fully minimize the aggregation produced between the prepared NPs following method 1 before ligand attachment compared to sucrose (10%). As a consequence, the rest of the formulations were continued with sucrose (10%). However, 10% sucrose was preferably chosen after comparative optimization based on the different percentages (1%, 5%, and 10%) of sucrose used as cryoprotectant (data not shown). Sucrose was found to be a better cryoprotectant to retain particle size when compared with trehalose used for plain NP formulations prepared following method 1. Thus, the effect of cryoprotectants was partially or not pronounced in formulations under method 1 as represented in Figure 3.4B. The ZP value for plain NPs without cryoprotectants was found to be more negative compared to formulations with sucrose. Even though the presence of sucrose should cause a higher negative charge on particles, the opposite was found.(27)

For method 2, there was significant change in ZP after addition of cryoprotectant ($P$<0.05). Also, the presence of cryoprotectant showed significant difference in particle size for antibody-adsorbed groups ($P$<0.05). However, the change in particle size was not significant when cryoprotectant was used in covalently modified formulations. Table 3.4 demonstrates the effect of sucrose after antibody attachment, where PDI was found to be below or equal to 0.43. Whereas formulations that were freeze-dried without cryoprotectant showed higher PDIs (highest PDI =0.95). There was significant reduction in particle size for all modified NPs after use of cryoprotectant, except the covalently modified formulations of method 2.

### 3.5.4 Effect of cross-linkers

EDC/sulfo-NHS cross-linker was considered to conjugate antibody ligand with prepared NPs following method 1.(28), (29) The presence of cross-linkers could be attributed to larger particles after antibody attachment. In method 2, the BS3 (spacer) pre-activated NP formulations showed fairly considerable physicochemical properties after antibody modification. In both methods, successful attachment of antibody was obtained which was confirmed by BCA assay (Table 3.4).

### 3.5.5 Confirmation of structural modification by FTIR

The peak around 1,750 $cm^{-1}$ is a marked peak that elicits the presence of a carbonyl bond (C=O stretching vibration), which is characteristic of PLGA.(30) An amide stretching is present between 3,310 and 3,250 $cm^{-1}$ in anti-CD205 antibody modified PLGA NP spectra, which corresponds to C=O stretching bond. Theoretically, amide-I vibrations result from C=O stretching vibration near 1,610 $cm^{-1}$ as observed in the spectra for antibody modified NP.(31) Amide-I bond is the most sensitive to prove the structural change in any compound containing proteins. Some contribution in the spectrum from the C=O groups in both BS3 free and BS3 containing NP formulations could also be observed.(32), (33) To confirm the presence of antibody on the NPs, the spectra for only high viscosity COOH ended PLGA NPs and their modification are represented here (Figure 3.7). Spectra for other polymer types and their subtypes are not shown here.

### 3.5.6 Comparison of safety profiles for method 1 and 2

All NP formulations prepared by method 1 (both ester and COOH terminated NPs) retained DC viability (≥80%). The findings indicate that both plain and modified NPs were not toxic to the DCs confirming the safety profile of the NPs as shown in Figures 3.8 and 3.9. Similarly, method 2 based NP formulations demonstrate a viability of >90%.(11) There was no significant difference in viability among different groups (plain and modified) for both methods. However, 0.15E-NP+S showed significant difference ($P$<0.05) compared to other formulations like 0.18C-NP+BS3, 0.55C-NP+BS3, 0.15E-NP+BS3, 0.15E-NP+BS3+S, and 0.55E-NP+BS3+S prepared following method 2.

## 3.6 Discussion

The choice of a suitable NP formulation technique is dependent on the desired physicochemical properties. NP size is an important determinant of the formulation efficacy in vivo. Very large particles (around 1 μm) can cause irritant effects after injection.(34) On the other hand, particles smaller than 5 nm are likely to be cleared by non-phagocytic cells.(35) Alternatively, particles larger than 100 nm have the

chance to be taken up by phagocytic cells (for example, DCs).(34), (36) The formulations prepared by the methods mentioned here, aim to target DC receptors in vivo. Thus the particle size range (309±36 to 544±45 nm) obtained by method 2 could be suitable for DC uptake via subcutaneous delivery.(37), (38) However, toxicity issue is a concern for emulsification solvent evaporation technique. Chlorinated solvents like chloroform and dichloromethane have issues regarding environmental challenges and human use. Considering these issues, ethyl acetate offers a better solubility and safety profile compared to chloroform. As a polar solvent ethyl acetate with a solubility of 8.1 volume/volume in water is comparatively safer.(39) It has lower interfacial tension (1.7 dyne/cm) compared to chloroform (32.8 dyne/cm), which forms more stable emulsions and smaller NPs in PVA solutions.(40) A considerable decrease in particle size was observed when ethyl acetate was used as solvent in method 2. In addition, all the formulations had improved PDI indicating mono-disperse NP suspension. Furthermore, method 2 showed a batch-to-batch reproducibility for all the formulations of interest that will be required for in vivo experiments. The represented SEM images confirmed the formation of spherical NPs within the desired size range (Figure 4). The images confirm the homogenous nature of particles with a uniform and aggregation-free distribution.(41)

There are different emulsion stabilizers available such as PVA, carbopol and polaxamer. Among these, PVA is found to provide homogenous particles with uniform size distribution.(42) It acts on the boundary of aqueous and organic phase to modify the particle size as well as surface charge.(43) PVA is able to maintain the interfacial tension at oil-water interface to obtain small sized particles.(44) In addition, it prevents the aggregation and preserves the hydrophilicity of particles when used above a concentration of 2%.(45) A high concentration of PVA is expected to produce particles with narrow granulometric distribution. Failure to maintain that would lead to the aggregated particles.(46) Between method 1 (5% PVA) and method 2 (2.2% PVA), the difference in particle size could be attributed to not only the difference of PVA concentration but also the effect of solvents. Decrease in PVA concentration from method 1 to method 2 could lead to larger particles. But, PVA concentration of 5% did not play a better

role to reduce particle size due to PVA's optimum packing.(47) In addition, PVA also renders slightly negative charges on the particles.(48)

ZP value is an important parameter that reflects stability of a colloidal suspension.(49) ZP values for COOH terminated NPs were found to be more negative (−25 to −24 mV) compared to ester terminated (−19 to −16 mV) NPs. This could be attributed to the presence of carboxyl group on the COOH terminated NPs. When the viscosity of the polymers increased, ZP value showed slightly more negative charge for uncapped NPs than the capped formulations.(50) When the polymer of higher viscosity is used it increases the concentration of the media resulting in semi-folded particles.(51) Increase in concentration of the organic phase also resulted in viscosity resistance against the net shear stress. Ultimately coalescence of particles occurs to provide increase in NP size.(52), (53) Particles with more positive (above +30 mV) or more negative (below −30 mV) ZP are considered colloidally stable but not pharmaceutically stable.(16), (54) This indicates that ZP beyond this range needs to be kept in solid and dry form rather than colloidal state. Our results show that ZP of antibody modified NPs was about neutral or slightly positive or negative. The prepared NPs were therefore lyophilized for pharmaceutical stability and should be reconstituted immediately before the administration.(16), (55)

Freeze-drying is an essential part in retaining the stability of formulations after preparation. This process could be stressful leading to colloidal preparations having large aggregates, although there are several cryoprotectants available to increase the physical stability of NPs.(56) Cryoprotectants could be water-soluble sugars such as glucose, trehalose, which are added to prevent NPs from aggregating during drying process. Hence, it is advantageous to prepare NPs with addition of cryoprotectants. There are two types of cryoprotectants: intracellular that prevents crystal formation and cell membrane rupture; and extracellular that minimizes hyperosmotic effect during freeze-drying process. Sucrose and trehalose are extracellular cryoprotectants that minimize freeze-drying stress of the formulations.(57) For method 1, antibody modified NPs had higher particle size compared to the plain NPs which was predictable. The PDI value remained fairly high even after using cryoprotectants. No significant differences in the effect of sucrose and trehalose could be identified for these formulations. Addition of cryoprotectant might have formed

hydrogen bond between their hydroxyl group and NP surface resulting in masking of the negative charges of the particles.

It has been reported that presence of stabilizers could also play a major role in NP aggregation in the drying process.(58) The percentage of stabilizer is critical to maintain its influence on both particle size and ZP.(59) In the NP formulations (following method 2), the PVA percentage was 2.2% below the optimum range (2.5%–5%) which necessities the use of cryoprotectant. A minimum of 5% cryoprotectant is necessary to ensure stability of formulations.(60) In another study, aggregation-free PLGA NP suspension was obtained with 1%–2% PVA where 10% of different cryoprotectants (sucrose, trehalose, glucose) were used.(61) Therefore, studies were continued with method 2 formulations using 10% sucrose as cryoprotectant due to its better cryopreservation.

The highest antibody incorporation was obtained with low viscosity ester terminated PLGA NPs (formulations with cryoprotectants for either conjugation method), whereas low viscosity COOH terminated PLGA NPs provided the lowest antibody incorporation (except antibody-adsorbed formulations of method 1). The low viscosity ester terminated PLGA had higher antibody attachment due to higher surface area (smaller size) of NPs. Besides, with the same amount of initial antibody, the COOH terminated PLGA had lower antibody incorporation which could be attributed to the rapid erosion of the polymer.(62) For method 2 based formulations, covalently attached NPs were found to be smaller than physically adsorbed NPs although the antibody attachment between these groups was not significantly different. In addition, ZP did not show any rational correlation between antibody loading and conjugation method for both COOH and ester terminated NPs. It was observed that covalently attached low viscosity COOH and ester terminated polymers resulted in smaller particle size compared to high viscosity polymers, which is expected. Moreover, all the formulations had particle size within desired range for DC uptake.(11), (37) It was found that, the 4 hours stirring time during antibody-NP attachment should be enough to break down the aggregates and to form a fine suspension leaving the surface available for antibody attachment. This is observed from the smaller particle size with acceptable PDI obtained for the low viscosity ester terminated NPs after 4 hours incubation with continuous stirring. However, the

particle size was above the target range with poor PDI values for the high viscosity ester terminated NPs prepared following method 1. On the contrary, ligand modified NP formulations prepared by method 2 showed equally acceptable range for PDI values with the highest of 0.43±0.05 and lowest of 0.22±0.07. The antibody attachment on NP surface was calculated to be in a desired range (2 μg/mg of NP). However, no significant correlation could be made between antibody-NP conjugation methods (adsorption and covalent attachment) and polymers' viscosities. Considering the viability, it was slightly higher with high viscosity grade PLGA for most of the formulations; and conjugation method could not affect DC viability.

The structural modification of BS3 activated formulations was well confirmed by infrared study. In the case of the anti-CD205 conjugated NPs spectrum, presence of N-H stretching of high intensity confirmed the conjugation. Second derivative of all spectra (Figure 5B) clearly shows the presence of an amide bond between BS3 and antibody. This characteristic peak stands out, reflecting the establishment of the antibody conjugation on the NPs.

The results from method 2 were more reproducible and consistent, whereas the formulations prepared by method 1 showed higher deviation from the average in the DC viability tests. Based on the confirmed safety profile of the NP formulations, we can further use them for DC uptake and targeting efficiency study.

### 3.7 Conclusion

In this research, the effects of various processing parameters were investigated. The formulation variables evaluated here could be manipulated to enhance the efficiency of the PLGA NPs. Based on the optimum potential parameters it is concluded that formulations prepared using ethyl acetate as solvent (method 2) are shown to be promising for NP preparation and will be further utilized in our in vitro experiments. Further in vitro investigations such as targeting efficiency, maturation of DCs, cytokine secretion profile, and activation of immune response leading to in vivo studies are being conducted in ongoing studies. Therefore, the structural characterizations reflected in those formulations will direct us to obtain optimum

in vivo effects. This optimization would help other researchers to select the optimal parameters in their study. In conclusion, this systematic investigation could promote the development of PLGA NPs for further application to design a cancer vaccine.

### 3.8 Acknowledgments

This project was supported by funding from Natural Sciences and Engineering Research (NSERC) Discovery Grant and Saskatchewan Health Research Foundation (SHRF) New Investigator Establishment Grant. The authors thank Canadian Light Source (CLS), Saskatoon, Saskatchewan, for providing assistance with infrared spectroscopy and SEM.

### 3.9 Disclosure

The authors report no conflicts of interest in this work.

### 3.10 TABLES

**Table 3.3** Variable parameters considered to prepare the NPs

| | |
|---|---|
| Polymer end group | ▪ Carboxylic acid terminated<br>▪ Ester terminated |
| Polymer viscosities | ▪ 0.18 iv COOH<br>▪ 0.55 iv COOH<br>▪ 0.15 iv ester<br>▪ 0.55 iv ester |
| Organic solvents | ▪ Chloroform<br>▪ Ethyl acetate |
| Cross-linkers | ▪ EDC-NHS<br>▪ BS3 |
| PVA | ▪ 5 %<br>▪ 2.2 % |
| Cryoprotectants | ▪ Sucrose (10%)<br>▪ Trehalose (10 %) |

**Table 3.4** Particle size, PDI, and ZP, and antibody loading for anti-CD205 modified NPs (n=4)

**Notes:** C = COOH ended PLGA; E = ester ended PLGA; S = sucrose (10%). Data are presented as mean ± standard deviation.

| | Formulation | Method-1 | | | | Method-2 | | | |
|---|---|---|---|---|---|---|---|---|---|
| | | Size ± SD (nm) | PDI± SD | ZP± SD (mV) | Ab* loading (µg/mg of NP) | size ± SD (nm) | PDI ± SD | ZP± SD (mV) | Ab loading (µg/mg of NP) |
| Adsorption | **0.18C-NP** | 336±19 | 0.28±0.04 | -12.9±0.6 | 3.62±0.43 | 556±41 | 0.29±0.04 | -1.9±0.3 | 2.73±0.17 |
| | **0.18C-NP+S** | 567±36 | 0.47±0.06 | -2.5±0.2 | 2.64±0.21 | 311±15 | 0.32±0.04 | -2.9±0.2 | 2.11±0.67 |
| | **0.55C-NP** | 978±424 | 0.69±0.12 | -9.1±0.6 | 2.42±0.86 | 1266±193 | 0.63±0.04 | -3.4±0.2 | 2.62±0.67 |
| | **0.55C-NP+S** | 733±52 | 0.58±0.26 | -1.2±0.1 | 1.90±0.31 | 399±143 | 0.31±0.07 | -0.4±0.1 | 2.44±0.27 |
| | **0.15E-NP** | 5270±965 | 0.79±0.25 | 0.3±0.3 | 1.91±0.09 | 3681±453 | 0.75±0.01 | 0.1±0.1 | 2.41±0.30 |
| | **0.15E-NP+S** | 468±14 | 0.69±0.02 | -2.3±0.7 | 3.45±0.38 | 417±51 | 0.43±0.05 | 0.2±0.1 | 3.18±0.48 |
| | **0.55E-NP** | 5507±927 | 1.00±0.00 | -1.9±0.2 | 2.82±0.83 | 1999±404 | 0.95±0.05 | -0.4±0.3 | 2.54±0.33 |
| | **0.55E-** | 1946±41 | 0.97±0.0 | 0.7±0.4 | 2.94±0.46 | 544±45 | 0.39±0.07 | -1.9±0.2 | 2.31±0.57 |

| | | | | | | | | | |
|---|---|---|---|---|---|---|---|---|---|
| | **NP+S** | | 4 | | | | | | |
| **Covalent** | **0.18C-NP** | 426±6 | 0.41±0.02 | -2.5±0.7 | 2.51±0.22 | 349±24 | 0.34±0.04 | -9.4±0.4 | 2.70±0.61 |
| | **0.18C-NP+S** | 774±8 | 0.57±0.01 | 2.6±0.1 | 2.25±0.01 | 421±12 | 0.37±0.05 | 2.1±0.4 | 2.16±0.43 |
| | **0.55C-NP** | 1033±20 | 0.73±0.07 | -1.6±0.5 | 3.53±0.47 | 346±15 | 0.41±0.02 | -2.6±0.3 | 2.13±1.02 |
| | **0.55C-NP+S** | 828±10 | 0.66±0.03 | -2.2±0.1 | 3.22±0.08 | 461±10 | 0.27±0.09 | 1.7±0.5 | 2.31±0.63 |
| | **0.15E-NP** | NA* | NA | NA | NA | 305±156 | 0.65±0.08 | -1.1±0.2 | 1.96±0.16 |
| | **0.15E-NP+S** | NA | NA | NA | NA | 309±36 | 0.22±0.07 | 1.5±0.1 | 2.79±0.24 |
| | **0.55E-NP** | NA | NA | NA | NA | 327±22 | 0.38±0.05 | -4.1±0.2 | 2.62±0.35 |
| | **0.55E-NP+S** | NA | NA | NA | NA | 314±31 | 0.32±0.02 | 2.2±0.5 | 2.71±0.32 |

**Abbreviations:** NP, nanoparticle; PDI, polydispersity index; ZP, zeta potential; SD, standard deviation; NA, not applicable; Ab, anti-CD205 antibody; COOH, carboxylic acid; PLGA, poly(D, L-lactide co-glycolide).

**Abbreviations:** NPs, nanoparticles; PVA, polyvinyl alcohol; iv, inherent viscosity; EDC-NHS, carbodiimide hydrochloride-*N*-hydroxysuccinimide; BS3, bis(sulfo-succinimidyl) suberate.

### 3.11 FIGURES

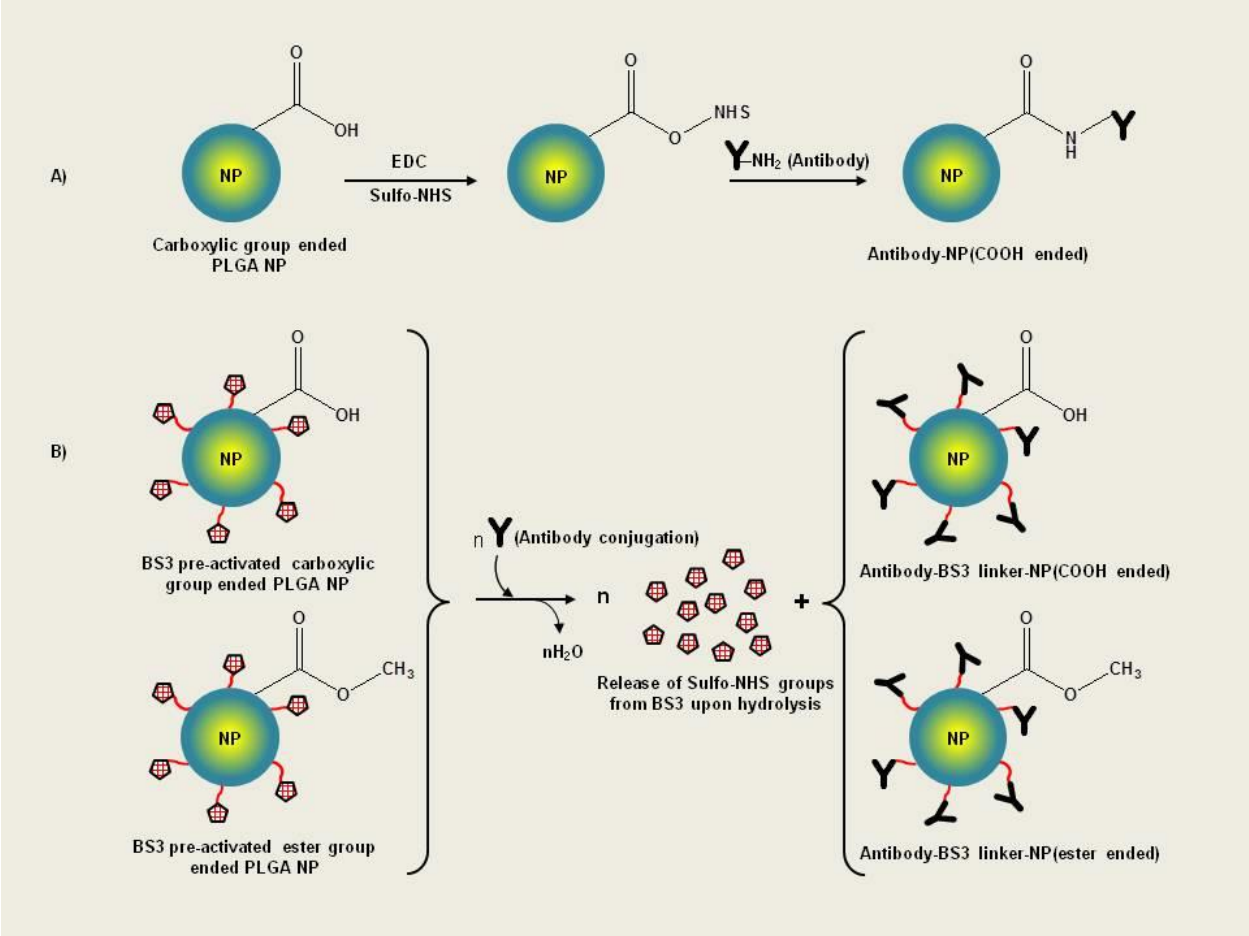


**Figure 3.3** Reaction schemes to prepare targeted PLGA NP.

**Notes:** (**A**) Carbodiimide method, where EDC/sulfo-NHS was used as the cross-linker. COOH terminated PLGA reacts with EDC/sulfo-NHS to form NHS-ester that reacts with antibody to obtain a stable amide bond. (**B**) Using BS3 spacer, where covalent amide bond is formed between ligand and BS3 molecules embedded on pre-activated NPs' surface. This method is applicable for both ester and COOH terminated PLGA NPs.

**Abbreviations:** PLGA, poly (D, L-lactide co-glycolide); NP, nanoparticle; EDC, carbodiimide hydrochloride; NHS, *N*-hydroxysuccinimide; COOH, carboxylic acid; BS3, bis(sulfo-succinimidyl) suberate.

A

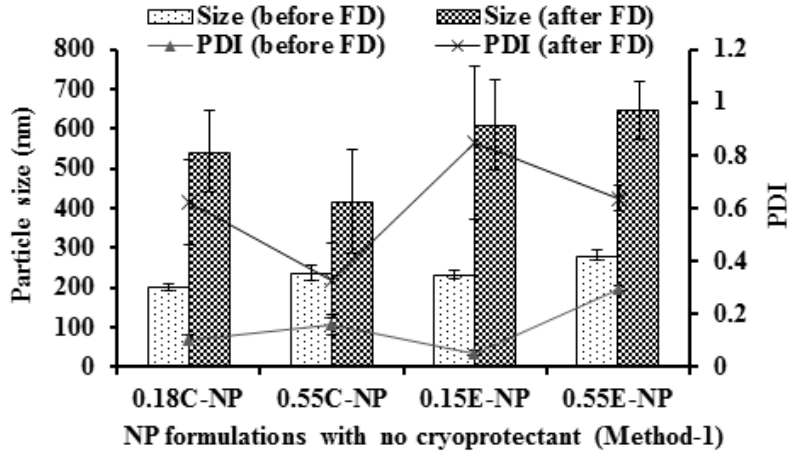


NP formulations with no cryoprotectant (Method-1)

B

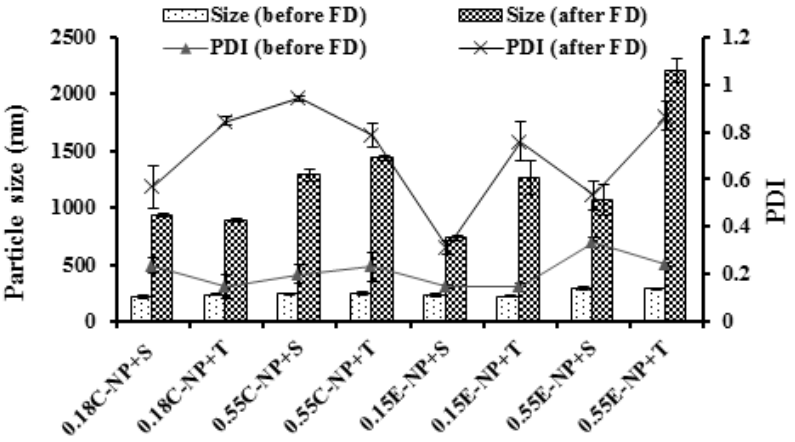


NP formulations with cryoprotectant (Method-1)

C

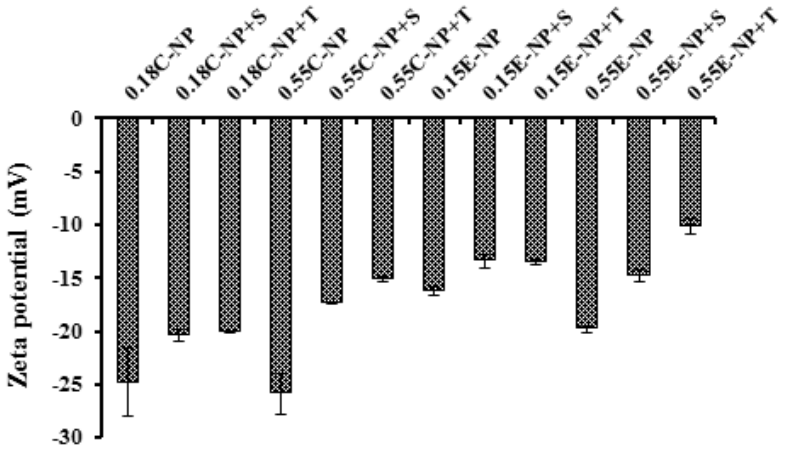


Plain NP formulations with and without cryoprotectant (Method-1)

**Figure 3.4** Particle size, PDI, and ZP of NPs prepared with different PLGA polymer end groups and viscosities following method 1.

**Notes:** The bar diagram and line plots represent particle size and PDI value, respectively. (**A**) Represents the NP formulations prepared without cryoprotectant. (**B**) Represents the same formulations preserved with two different cryoprotectants namely sucrose and trehalose. (**C**) Represents the comparative ZP of all NP formulations with or without cryoprotectant. The level of significance was set to $P<0.05$ (one-way ANOVA followed by Tukey's multiple comparison test method). Each bar and line represents mean ± SD (n=12). C = COOH ended PLGA; E = ester ended PLGA, S = sucrose (10%); T = trehalose (10%).

**Abbreviations:** PDI, polydispersity index; ZP, zeta potential; NP, nanoparticle; PLGA, poly(D, L-lactide co-glycolide); ANOVA, analysis of variance; SD, standard deviation; COOH, carboxylic acid; FD, freeze-drying.

A

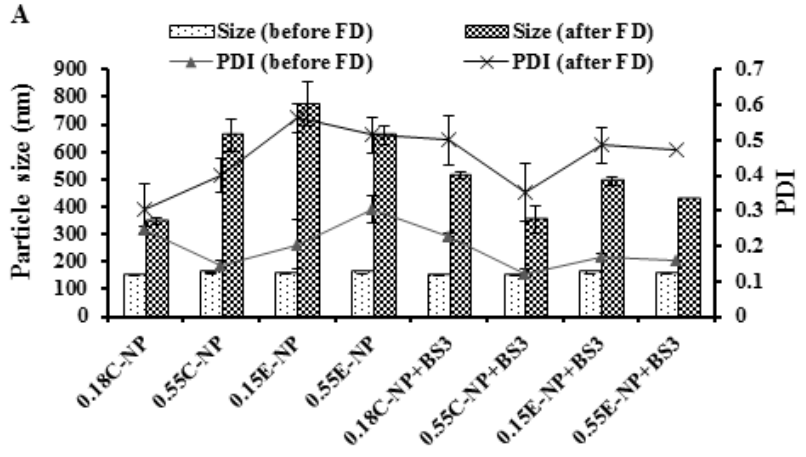


NP formulations with no cryoprotectant (Method-2)

B

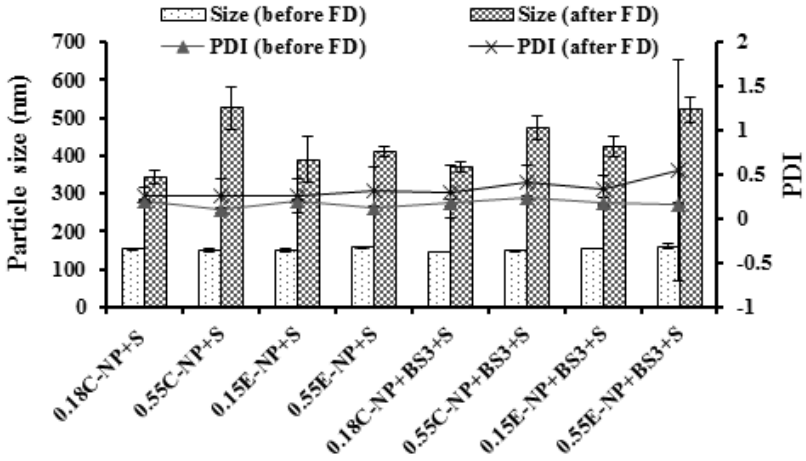


NP formulations with cryoprotectant (Method-2)

C

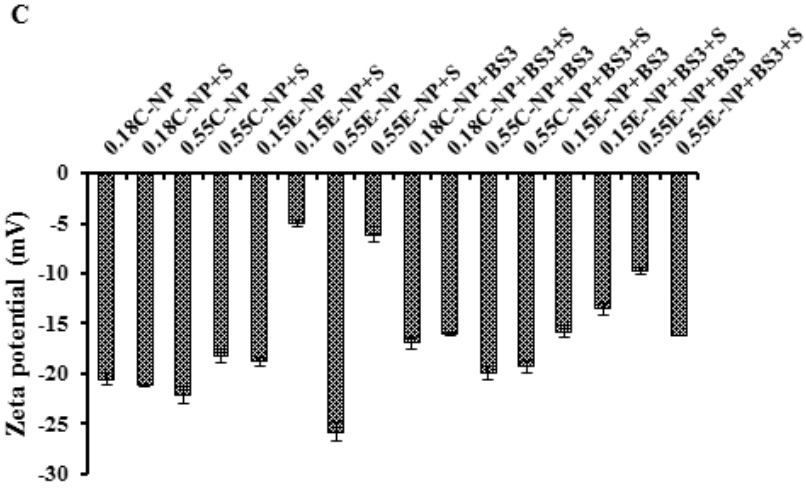


Plain NP formulations with and without cryoprotectant (Method-2)

**Figure 3.5** Particle size, PDI, and ZP of NPs prepared with different PLGA polymer end groups and viscosities following method 2.

**Notes:** The bar diagram and line plots represent particle size and PDI value, respectively. (**A**) Represents all the NP formulations with or without BS3 prepared without cryoprotectant. (**B**) Represents the same formulations preserved with sucrose (10%) as cryoprotectant. (**C**) Represents the comparative ZP of all NP formulations with or without cryoprotectant. The level of significance was set to $P<0.05$ (one-way ANOVA followed by Tukey's multiple comparison test method). Each bar and line represents mean ± SD (n=12). C = COOH ended PLGA; E = ester ended PLGA; S = sucrose (10%).

**Abbreviations:** PDI, polydispersity index; ZP, zeta potential; NP, nanoparticle; PLGA, poly(D, L-lactide co-glycolide); ANOVA, analysis of variance; SD, standard deviation; COOH, carboxylic acid; FD, freeze-drying; BS3, bis(sulfo-succinimidyl) suberate.

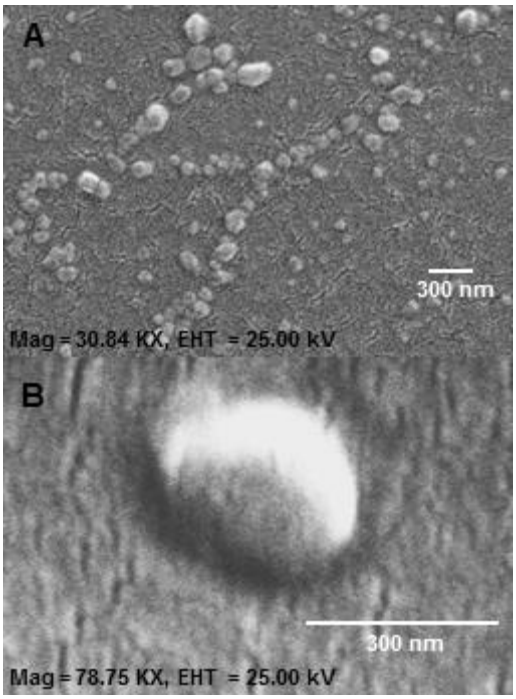


**Figure 3.6** SEM images.

**Notes:** SEM images of NPs (**A**) 0.15 iv ester terminated PLGA NPs at magnification of 30.84 KX at EHT (extra high tension) 25 kV; (**B**) antibody modified 0.15 iv ester terminated PLGA NPs at

magnification of 78.75 KX at EHT 25 kV.

**Abbreviations:** SEM, scanning electron microscopy; NPs, nanoparticles; PLGA, poly(D, L-lactide co-glycolide); iv, inherent viscosity; Mag, magnification.

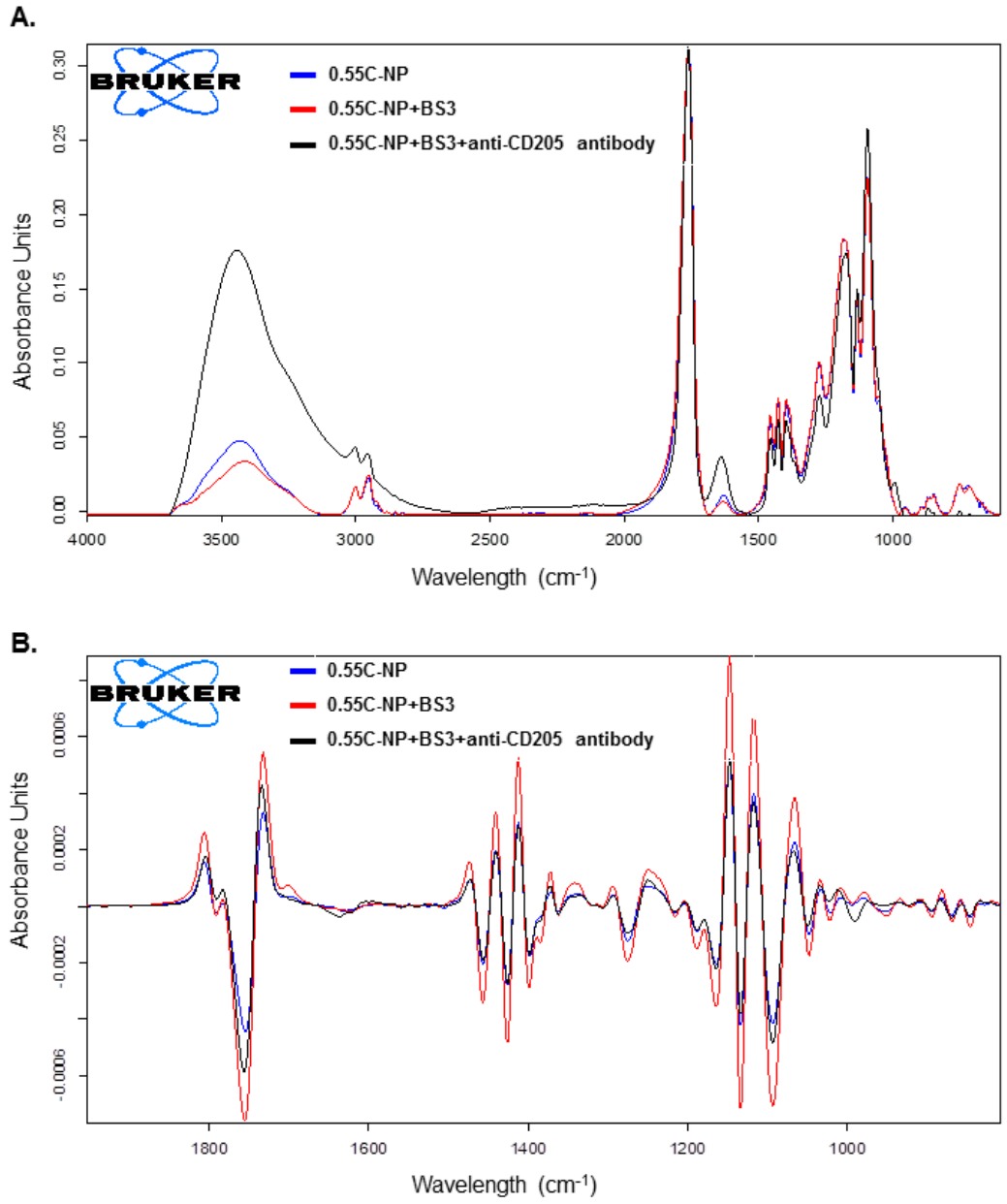


**Figure 3.7** Infrared spectrum of NPs.

**Notes:** Primary (**A**) and secondary derivative (**B**) of IR spectrum for 0.55C-NP (0.55 iv COOH terminated plain PLGA NPs) (blue), 0.55C-NP+BS3 (BS3 containing 0.55 iv COOH terminated PLGA NPs) (red), and 0.55C-NP+BS3+anti-CD205 antibody (BS3 containing 0.55 iv COOH terminated Ab modified PLGA NPs) (black). Data are represented in absorbance unit versus wavelength ($cm^{-1}$).

**Abbreviations:** IR, infrared; NP, nanoparticle; COOH, carboxylic acid; PLGA, poly(D, L-lactide co-glycolide); BS3, bis(sulfo-succinimidyl) suberate; iv, inherent viscosity; Ab, anti-CD205 antibody.

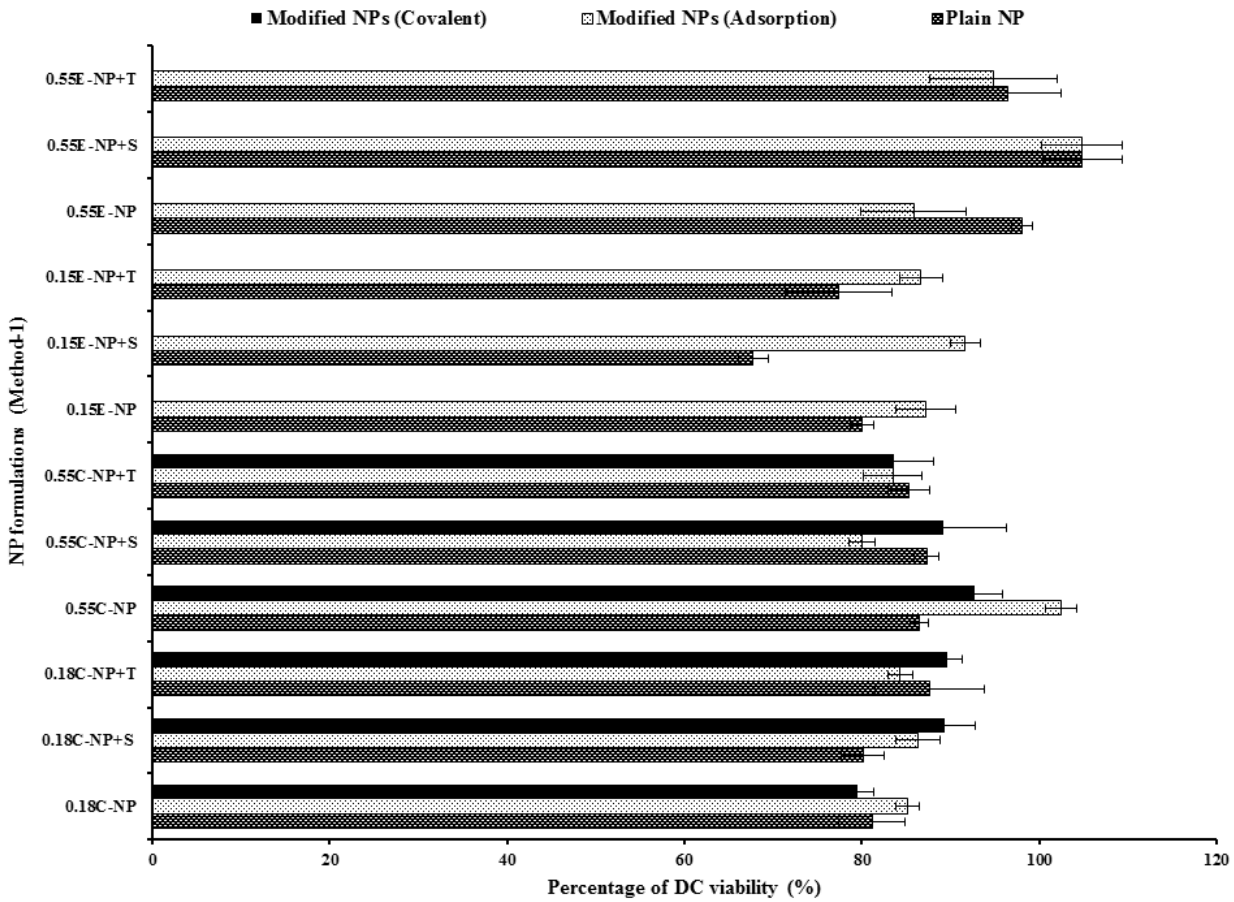


**Figure 3.8** DC viability (MTT assay) after 24 hours of exposure to plain and antibody modified NPs (method 1).

**Notes:** The treated NP concentration was 1 mg/mL for cell density of 10,000. Result was calculated

based on the absorbance of treated cells in comparison with untreated cells, where blank values were subtracted from each group (n=3). C = COOH ended PLGA, E = ester ended PLGA, S = sucrose (10%), and T = trehalose (10%).

**Abbreviations:** DC, dendritic cell; MTT, 3-(4, 5-dimethylthiazol-2-yl)-2, 5-diphenyltetrazolium bromide; NPs, nanoparticles; COOH, carboxylic acid; PLGA, poly(D, L-lactide co-glycolide).

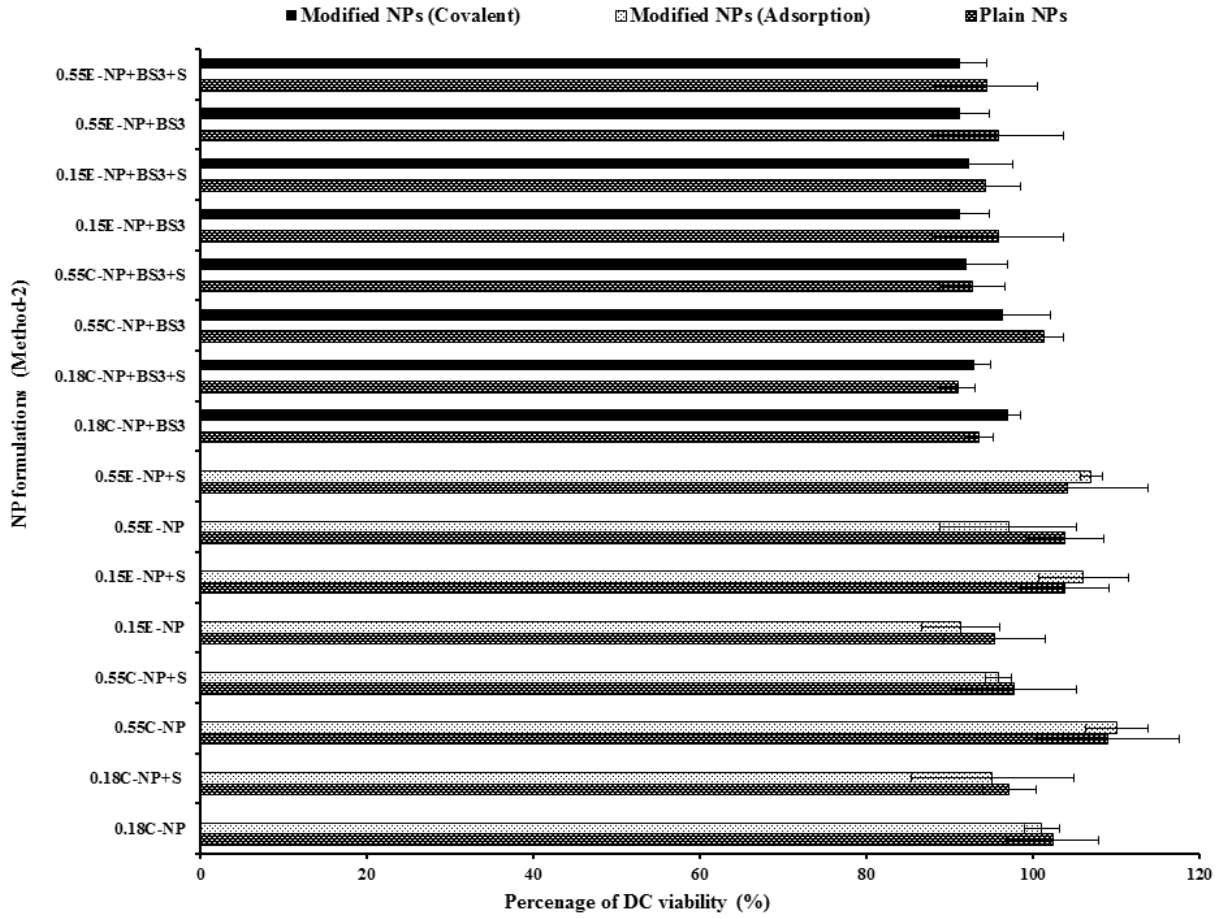


**Figure 3.9** DC viability (MTT assay) after 24 hours of exposure to plain and modified NPs (method 2).

**Notes:** The treated NP concentration was 1 mg/mL for cell density of 10,000. Result was calculated based on the absorbance of treated cells in comparison with untreated cells, where blank values were subtracted from each group (n=3). C = COOH ended PLGA, E = ester ended PLGA, and S = sucrose

(10%).

**Abbreviations:** DC, dendritic cell; MTT, 3-(4, 5-dimethylthiazol-2-yl)-2, 5-diphenyltetrazolium bromide; NPs, nanoparticles; COOH, carboxylic acid; PLGA, poly (D, L-lactide co-glycolide).

### 3.12 References


1. Bandyopadhyay A, Fine RL, Demento S, Bockenstedt LK, Fahmy TM. The impact of nanoparticle ligand density on dendritic-cell targeted vaccines. *Biomaterials.* Apr 2011;32(11):3094-3105.

2. Reuter A, Panozza SE, Macri C, et al. Criteria for dendritic cell receptor selection for efficient antibody-targeted vaccination. *Journal of immunology.* Mar 15 2015;194(6):2696-2705.

3. Butler M, Morel AS, Jordan WJ, et al. Altered expression and endocytic function of CD205 in human dendritic cells, and detection of a CD205-DCL-1 fusion protein upon dendritic cell maturation. *Immunology.* Mar 2007;120(3):362-371.

4. Platzer B, Stout M, Fiebiger E. Antigen cross-presentation of immune complexes. *Frontiers in immunology.* 2014;5:140.

5. Barbuto S, Idoyaga J, Vila-Perello M, et al. Induction of innate and adaptive immunity by delivery of poly dA:dT to dendritic cells. *Nature chemical biology.* Apr 2013;9(4):250-256.

6. Cooper DL, Harirforoosh S. Design and optimization of PLGA-based diclofenac loaded nanoparticles. *PloS one.* 2014;9(1):e87326.

7. Danhier F, Ansorena E, Silva JM, Coco R, Le Breton A, Preat V. PLGA-based nanoparticles: an overview of biomedical applications. *Journal of controlled release : official journal of the Controlled Release Society.* Jul 20 2012;161(2):505-522.

8. Lewis JS, Zaveri TD, Crooks CP, 2nd, Keselowsky BG. Microparticle surface modifications targeting dendritic cells for non-activating applications. *Biomaterials.* Oct 2012;33(29):7221-7232.

9. Haddadi A, Hamdy S, Ghotbi Z, Samuel J, Lavasanifar A. Immunoadjuvant activity of the nanoparticles' surface modified with mannan. *Nanotechnology.* Sep 5 2014;25(35):355101.

10. Sah H, Thoma LA, Desu HR, Sah E, Wood GC. Concepts and practices used to develop functional PLGA-based nanoparticulate systems. *International journal of nanomedicine.* 2013;8:747-765.

11. Ghotbi Z, Haddadi A, Hamdy S, Hung RW, Samuel J, Lavasanifar A. Active targeting of dendritic cells with mannan-decorated PLGA nanoparticles. *Journal of drug targeting.* May 2011;19(4):281-292.

12. Keum CG, Noh YW, Baek JS, et al. Practical preparation procedures for docetaxel-loaded nanoparticles using polylactic acid-co-glycolic acid. *International journal of nanomedicine.* 2011;6:2225-2234.

13. Thamake SI, Raut SL, Ranjan AP, Gryczynski Z, Vishwanatha JK. Surface functionalization of PLGA nanoparticles by non-covalent insertion of a homo-bifunctional spacer for active targeting in cancer therapy. *Nanotechnology.* Jan 21 2011;22(3):035101.

14. Kocbek P, Obermajer N, Cegnar M, Kos J, Kristl J. Targeting cancer cells using PLGA nanoparticles surface modified with monoclonal antibody. *Journal of controlled release : official journal of the Controlled Release Society.* Jul 16 2007;120(1-2):18-26.

15. Zou W, Liu C, Chen Z, Zhang N. Studies on bioadhesive PLGA nanoparticles: A promising gene delivery system for efficient gene therapy to lung cancer. *International journal of pharmaceutics.* Mar 31 2009;370(1-2):187-195.

16. Mukherjee B, Santra K, Pattnaik G, Ghosh S. Preparation, characterization and in-vitro evaluation of sustained release protein-loaded nanoparticles based on biodegradable polymers. *International journal of nanomedicine.* 2008;3(4):487-496.

17. Al-Nemrawi NK, Dave RH. Formulation and characterization of acetaminophen nanoparticles in orally disintegrating films. *Drug delivery.* Jul 11 2014:1-10.

18. Kaur R, Chitanda JM, Michel D, et al. Lysine-functionalized nanodiamonds: synthesis, physiochemical characterization, and nucleic acid binding studies. *International journal of nanomedicine.* 2012;7:3851-3866.

19. Valencia PM, Hanewich-Hollatz MH, Gao W, et al. Effects of ligands with different water solubilities on self-assembly and properties of targeted nanoparticles. *Biomaterials.* Sep

2011;32(26):6226-6233.

20. Li F, Sun J, Zhu H, Wen X, Lin C, Shi D. Preparation and characterization novel polymer-coated magnetic nanoparticles as carriers for doxorubicin. *Colloids Surf B Biointerfaces.* Nov 1 2011;88(1):58-62.

21. Dillen K, Vandervoort J, Van den Mooter G, Verheyden L, Ludwig A. Factorial design, physicochemical characterisation and activity of ciprofloxacin-PLGA nanoparticles. *International journal of pharmaceutics.* May 4 2004;275(1-2):171-187.

22. Tsai YM, Chien CF, Lin LC, Tsai TH. Curcumin and its nano-formulation: the kinetics of tissue distribution and blood-brain barrier penetration. *International journal of pharmaceutics.* Sep 15 2011;416(1):331-338.

23. Mundargi RC, Babu VR, Rangaswamy V, Patel P, Aminabhavi TM. Nano/micro technologies for delivering macromolecular therapeutics using poly(D,L-lactide-co-glycolide) and its derivatives. *Journal of controlled release : official journal of the Controlled Release Society.* Feb 11 2008;125(3):193-209.

24. Copp JA, Fang RH, Luk BT, et al. Clearance of pathological antibodies using biomimetic nanoparticles. *Proceedings of the National Academy of Sciences of the United States of America.* Sep 16 2014;111(37):13481-13486.

25. Sperling RA, Parak WJ. Surface modification, functionalization and bioconjugation of colloidal inorganic nanoparticles. *Philosophical transactions. Series A, Mathematical, physical, and engineering sciences.* Mar 28 2010;368(1915):1333-1383.

26. Hermans K, Van den Plas D, Everaert A, Weyenberg W, Ludwig A. Full factorial design, physicochemical characterisation and biological assessment of cyclosporine A loaded cationic nanoparticles. *Eur J Pharm Biopharm.* Sep 2012;82(1):27-35.

27. Fonte P, Soares S, Costa A, et al. Effect of cryoprotectants on the porosity and stability of insulin-loaded PLGA nanoparticles after freeze-drying. *Biomatter*. Oct-Dec 2012;2(4):329-339.

28. Ikeda J, Sun YL, An KN, Amadio PC, Zhao C. Application of carbodiimide derivatized synovial fluid to enhance extrasynovial tendon gliding ability. *J Hand Surg Am.* Mar 2011;36(3):456-463.

29. Byrne JD, Betancourt T, Brannon-Peppas L. Active targeting schemes for nanoparticle systems in cancer therapeutics. *Advanced drug delivery reviews.* Dec 14 2008;60(15):1615-1626.

30. Sampath M, Lakra R, Korrapati P, Sengottuvelan B. Curcumin loaded poly (lactic-co-glycolic) acid nanofiber for the treatment of carcinoma. *Colloids Surf B Biointerfaces.* May 1 2014;117:128-134.

31. Kountz SL. The effect of bioscience and technological momentum on the surgical treatment of chronic illness. *Surgery.* Jun 1975;77(6):735-740.

32. Barth A. Infrared spectroscopy of proteins. *Biochimica et biophysica acta.* Sep 2007;1767(9):1073-1101.

33. Glassford SE, Byrne B, Kazarian SG. Recent applications of ATR FTIR spectroscopy and imaging to proteins. *Biochimica et biophysica acta.* Dec 2013;1834(12):2849-2858.

34. Cohen-Sela E, Chorny M, Koroukhov N, Danenberg HD, Golomb G. A new double emulsion solvent diffusion technique for encapsulating hydrophilic molecules in PLGA nanoparticles. *Journal of controlled release : official journal of the Controlled Release Society.* Jan 19 2009;133(2):90-95.

35. Choi HS, Liu W, Misra P, et al. Renal clearance of quantum dots. *Nature biotechnology.* Oct 2007;25(10):1165-1170.

36. Kettiger H, Schipanski A, Wick P, Huwyler J. Engineered nanomaterial uptake and tissue distribution: from cell to organism. *International journal of nanomedicine.* 2013;8:3255-3269.

37. Hamdy S, Haddadi A, Shayeganpour A, Samuel J, Lavasanifar A. Activation of antigen-specific T cell-responses by mannan-decorated PLGA nanoparticles. *Pharmaceutical research.* Sep 2011;28(9):2288-2301.

38. Gutierro I, Hernandez RM, Igartua M, Gascon AR, Pedraz JL. Size dependent immune response after subcutaneous, oral and intranasal administration of BSA loaded nanospheres. *Vaccine.*

Nov 22 2002;21(1-2):67-77.

39. Soppimath KS, Aminabhavi TM. Ethyl acetate as a dispersing solvent in the production of poly(DL-lactide-co-glycolide) microspheres: effect of process parameters and polymer type. *Journal of microencapsulation.* May-Jun 2002;19(3):281-292.

40. Sahana DK, Mittal G, Bhardwaj V, Kumar MN. PLGA nanoparticles for oral delivery of hydrophobic drugs: influence of organic solvent on nanoparticle formation and release behavior in vitro and in vivo using estradiol as a model drug. *Journal of pharmaceutical sciences.* Apr 2008;97(4):1530-1542.

41. Jose S, Sowmya S, Cinu TA, Aleykutty NA, Thomas S, Souto EB. Surface modified PLGA nanoparticles for brain targeting of Bacoside-A. *European journal of pharmaceutical sciences : official journal of the European Federation for Pharmaceutical Sciences.* Oct 15 2014;63:29-35.

42. Yoncheva K, Vandervoort J, Ludwig A. Influence of process parameters of high-pressure emulsification method on the properties of pilocarpine-loaded nanoparticles. *Journal of microencapsulation.* Jul-Aug 2003;20(4):449-458.

43. Vandervoort J, Ludwig A. Biocompatible stabilizers in the preparation of PLGA nanoparticles: a factorial design study. *International journal of pharmaceutics.* May 15 2002;238(1-2):77-92.

44. Wang H, Jia Y, Hu W, Jiang H, Zhang J, Zhang L. Effect of preparation conditions on the size and encapsulation properties of mPEG-PLGA nanoparticles simultaneously loaded with vincristine sulfate and curcumin. *Pharm Dev Technol.* May-Jun 2013;18(3):694-700.

45. Mobarak DH, Salah S, Elkheshen SA. Formulation of ciprofloxacin hydrochloride loaded biodegradable nanoparticles: optimization of technique and process variables. *Pharm Dev Technol.* Nov 2014;19(7):891-900.

46. Makadia HK, Siegel SJ. Poly Lactic-co-Glycolic Acid (PLGA) as Biodegradable Controlled Drug Delivery Carrier. *Polymers (Basel).* Sep 1 2011;3(3):1377-1397.

47. Sanad RA, Abdel Malak NS, El-Bayoomy TS, Badawi AA. Preparation and characterization of

oxybenzone-loaded solid lipid nanoparticles (SLNs) with enhanced safety and sunscreening efficacy: SPF and UVA-PF. *Drug discoveries & therapeutics.* Dec 2010;4(6):472-483.

48. Vandervoort J, Yoncheva K, Ludwig A. Influence of the homogenisation procedure on the physicochemical properties of PLGA nanoparticles. *Chemical & pharmaceutical bulletin.* Nov 2004;52(11):1273-1279.

49. Nabi-Meibodi M, Vatanara A, Najafabadi AR, et al. The effective encapsulation of a hydrophobic lipid-insoluble drug in solid lipid nanoparticles using a modified double emulsion solvent evaporation method. *Colloids Surf B Biointerfaces.* Dec 1 2013;112:408-414.

50. Gomez-Gaete C, Bustos GL, Godoy RR, et al. Successful factorial design for the optimization of methylprednisolone encapsulation in biodegradable nanoparticles. *Drug development and industrial pharmacy.* Feb 2013;39(2):310-320.

51. Premaletha K, Licy CD, Jose S, Saraladevi A, Shirwaikar A, Shirwaikar A. Formulation, characterization and optimization of hepatitis B surface antigen (HBsAg)-loaded chitosan microspheres for oral delivery. *Pharm Dev Technol.* Mar-Apr 2012;17(2):251-258.

52. Awotwe-Otoo D, Zidan AS, Rahman Z, Habib MJ. Evaluation of anticancer drug-loaded nanoparticle characteristics by nondestructive methodologies. *AAPS PharmSciTech.* Jun 2012;13(2):611-622.

53. Li X, Xu Y, Chen G, Wei P, Ping Q. PLGA nanoparticles for the oral delivery of 5-Fluorouracil using high pressure homogenization-emulsification as the preparation method and in vitro/in vivo studies. *Drug development and industrial pharmacy.* Jan 2008;34(1):107-115.

54. Westesen K. Novel lipid-based colloidal dispersions as potential drug administration systems – expectations and reality. *Colloid Polym Sci.* 2000/07/01 2000;278(7):608-618.

55. Pinto Reis C, Neufeld RJ, Ribeiro AJ, Veiga F. Nanoencapsulation I. Methods for preparation of drug-loaded polymeric nanoparticles. *Nanomedicine: Nanotechnology, Biology and Medicine.* 3// 2006;2(1):8-21.

56. Rizkalla N, Range C, Lacasse FX, Hildgen P. Effect of various formulation parameters on the properties of polymeric nanoparticles prepared by multiple emulsion method. *Journal of microencapsulation.* Feb 2006;23(1):39-57.

57. Janz Fde L, Debes Ade A, Cavaglieri Rde C, et al. Evaluation of distinct freezing methods and cryoprotectants for human amniotic fluid stem cells cryopreservation. *J Biomed Biotechnol.* 2012;2012:649353.

58. Zhang X, Guan J, Ni R, Li LC, Mao S. Preparation and solidification of redispersible nanosuspensions. *Journal of pharmaceutical sciences.* Jul 2014;103(7):2166-2176.

59. Mura S, Hillaireau H, Nicolas J, et al. Influence of surface charge on the potential toxicity of PLGA nanoparticles towards Calu-3 cells. *International journal of nanomedicine.* 2011;6:2591-2605.

60. Abdelwahed W, Degobert G, Stainmesse S, Fessi H. Freeze-drying of nanoparticles: formulation, process and storage considerations. *Advanced drug delivery reviews.* Dec 30 2006;58(15):1688-1713.

61. Jeong YI, Shim YH, Kim C, Lim GT, Choi KC, Yoon C. Effect of cryoprotectants on the reconstitution of surfactant-free nanoparticles of poly(DL-lactide-co-glycolide). *Journal of microencapsulation.* Sep 2005;22(6):593-601.

62. Lam XM, Duenas ET, Daugherty AL, Levin N, Cleland JL. Sustained release of recombinant human insulin-like growth factor-I for treatment of diabetes. *Journal of controlled release : official journal of the Controlled Release Society.* Jul 3 2000;67(2-3):281-292.

# CHAPTER 4

## 4. Design and immunological evaluation of anti-CD205 tailored PLGA based nanoparticulate cancer vaccine

Sheikh Tasnim Jahan, Sams M. A. Sadat, and Azita Haddadi[2]

Division of Pharmacy, College of Pharmacy and Nutrition, University of Saskatchewan, Saskatoon, SK S7N 5E5, Canada

[2] Corresponding Author: Azita Haddadi
3D01.01, D Wing Health Sciences, 107 Wiggins Road, College of Pharmacy and Nutrition, University of Saskatchewan, Saskatoon SK, S7N 5E5; Phone: (306) 966-6495; Fax: (306) 966-6377; e-mail: azita.haddadi@usask.ca

## 4.1 Brief introduction to chapter 4

The main goal of the present study is to establish the development of OVA and/or MPLA loaded NPs targeted with antibody, their physicochemical characterization, DC uptake study, safety profile of OVA NPs on DCs, release pattern of OVA, DC maturation study and cytokine secretion profiles.

The rationale behind these experiments is to achieve robust immune response from dual combination of MPLA-OVA loaded targeted NPs. It is more likely that MPLA-OVA combination in NPs can simultaneously induce T helper (Th) cells and cytotoxic T lymphocytes (CTL). However, it is necessary to deliver this antigen-adjuvant combination within a carrier system to avoid degradation and early release of antigenic material. In addition, the carrier will demonstrate a controlled release of therapeutics for a prolonged period of time to subsequently overcome the administration of booster doses. Moreover, the surface decorated carrier will deliver the antigen-adjuvant cargo to the target cell (professional antigen presenting DC) to obtain enhanced immune response.

The method to formulate nanoparticles was double-emulsification solvent evaporation technique. Dynamic light scattering was used to gauge particle size, polydispersity index and zeta potential. MTS [3-(4, 5-dimethylthiazol-2-yl)-5-(3-carboxymethoxyphenyl)-2-(4-sulfophenyl)-2H-tetrazolium] assay was performed to determine the viability of DCs. Circular dichroism was used to confirm the structural integrity of particles. Bicinchoninic acid assay (BCA) was performed to quantify the OVA after loading and release study. Flow cytometry was used for evaluation of DC maturation markers (CD40, CD86 and MHCII). Enzyme linked immunosorbent assay (ELISA) was used to quantify the cytokines.

**4.2 Abstract**

The aim of this research was to develop a targeted antigen-adjuvant assembled delivery system that will enable dendritic cells (DCs) to efficiently mature to recognize antigens released from tumor cells. In brief, model antigen, ovalbumin (OVA) and monophosphoryl lipid A (MPLA) adjuvant were encapsulated within the nanoparticle (NP) by double emulsification solvent evaporation method. Targeted NPs were obtained through ligand incorporation via physical adsorption or chemical conjugation process. Intracellular uptake of the NPs was assessed using Coumarin-6 dye. Evaluation of physicochemical characterization of NPs was performed based on the polymer end groups, their viscosities and ligand-NP bonding type. Remarkably, the developed delivery system had suitable physicochemical properties such as particle size, surface charge, OVA encapsulation efficiency, bi-phasic OVA release pattern, and safety profile. The ligand modified formulations had higher targeting efficiency than the non-tailored NPs. This was also evidenced when the targeted formulations expressed comparatively higher fold increase in surface activation markers such as CD40, CD86, and MHCII molecules. The maturation of DCs was further confirmed through secretion of extracellular cytokines compared to control cells in the DC microenvironment. In conclusion, the DC stimulatory response was integrated to develop a relationship between the NP structure and desired immune response. Therefore, the present study narrates comparative evaluation of some selected parameters to choose the suitable formulation for *in-vivo* cancer immunotherapy**.**

**Keywords:** Nanoparticle, Ovalbumin, MPLA, anti-CD205, PLGA, dendritic cells

## 4.3 Introduction

Cancer is the most detrimental disease in first world nations as well as developing countries. The goal of cancer therapy is to eradicate tumor cells without effecting normal healthy cells.(1) Moreover, therapeutic approaches are smartly chosen based on their selective targeting of malignant cells. Nowadays, novel treatment option like immunotherapy has excelled with favorable outcomes and limited side-effects. It is well-accepted complementary intervention for patients with weakened immune system resulted from long-term cancer treatments. It has the potential to augment the therapeutic response with synergistic efficacy when combined other treatment modalities.(2) The immunotherapeutic approach can appear as an ideal treatment option due to its unique mechanism of action.(3)

A cancer patient receives immunotherapy through therapeutic vaccine that induces antigen specific T cells, tumor relevant chemokine receptors but avoids interaction with suppressor cells and their expansion.(4) This type of vaccine aims in clonal expansion of cytotoxic T cells that identifies cancer cells and kills them by sequential events of perforin and granzyme release, thereby activating the caspase cascade and finally leading to apoptosis.(5), (6) In contrary, clinical trials were found to be ineffective initially. Failure in clinical trials is due to lack of optimal immune stimulation (either for mature DC or suppressive DC), inadequate antigen loading, incorrect route of administration and dose, prior analysis of DC transcriptosome.(7), (8) Therefore, to fight the limitation of the immune system to detect cancer inspired the researchers to manipulate DCs with target specific tools.

The *in-vivo* therapeutic vaccination involves the targeted delivery of antigen to DCs which will fuse tumor antigen to antibody (Ab) specific for a DC receptor. This strategy is cost-effective and less laborious compared to *ex-vivo* DC vaccines.(9) For example, when anti-CD205 Ab is conjugated with OVA, the receptor mediated antigen presentation increases significantly for major histocompatibility complex (MHC) class I and MHC class II (MHCII). The target CD205 receptor could continually delete peripheral T cells at steady state to establish tolerance and solely provide immunity when DCs are matured.(10) Whereas, in case of *ex-vivo* vaccination, when DCs are injected, problems such as failure to reach lymph node, insufficient amount of injected DCs, and disorder of immuno-function due to

immunosuppressive environment occur. The molecules in that environment (CTLA-4, PD-1, CD200, IL-10, TGF-β) are capable to inhibit the T cell function by formation of regulatory T (Tregs) cells.(11)

Nanoparticle based delivery systems are popular carrier for delivery of antigenic material to antigen presenting cells (APCs).(12) To become an ideal delivery system, the combination with antigen and adjuvant is very important. This cargo system will be able to deliver specific antigen to the APCs to manipulate their response.(13), (14) The present study aims to deliver surface modified NP to obtain immunological responses as mentioned in Figure 4.1. Surface modified NPs possess a hydrophilic layer that tends to escape reticuloendothelial system to reach receptors on target APCs, specifically the DCs.(15)

Immunostimulatory particulate delivery systems with biodegradable polymers have gained popularity due to their size, controlled release properties, and biocompatibility with tissues. Poly-lactic-co-glycolide (PLGA) based delivery system has become an interesting strategy for antigen based cancer immunotherapy.(16) Biodegradable PLGA is approved by the US FDA and European Medicine Agency (EMA) for use in humans.(17) The encapsulation of protein antigen in the PLGA particle protects the protein from degradation *in-vivo*. The antigen loaded particles release antigen in a controlled manner to prolong the availability of antigen *in-vivo*. However, the extended release of antigen as well as induction of innate and adaptive immune response are concerns.(18), (19)

For this study, we have chosen anti-CD205 monoclonal Ab to target CD205 receptor on DC because it is the extensively studied receptor for antigen delivery.(20) The formulations were designed using capped and uncapped PLGA; both offering low and high viscosity grades. Results are discussed based on a relative evaluation of the physicochemical properties, *in-vitro* studies and immunological responses. The purpose of this study is to assess the desired formulations that would be safe to deliver *in-vivo* to release its content in a controlled release manner to obtain necessary immunotherapeutic response.

## 4.4 Materials and methods

### 4.4.1 Materials

MPLA (molecular weight 1763.469 Da) was obtained from Avanti Polar Lipids Inc. (Alabama, USA). Ester terminated PLGA 50:50 (inherent viscosity or iv 0.15-0.25 dl/g and 0.55-0.75 dl/g) and COOH terminated PLGA 50:50 (iv 0.18 dl/g and 0.55-0.75 dl/g) were purchased from Lactel, Absorbable Polymers (Birmingham, AL, USA). Polyvinyl alcohol (PVA), bis (sulfo-succinimidyl) suberate (BS3), ovalbumin from chicken egg white (grade V), Coumarin-6, alpha minimum essential medium, fetal bovine serum (FBS) and bicinchoninic acid (BCA) assay kit was purchased from Sigma-Aldrich Co. (St Louis, MO, USA). Cell titre non-radioactive cell proliferation assay MTS [3-(4, 5-dimethylthiazol-2-yl)-5-(3- carboxymethoxyphenyl)-2-(4-sulfophenyl)-2H-tetrazolium was purchased from Promega (Madison, WI, USA). Biotin anti-mouse CD205 monoclonal Ab (MAb) was purchased from Biolegend (San Diego, CA, USA). JAWSII dendritic cell line was obtained from American Type Culture Collection (ATCC), Manassas, VA, USA. Granulocyte-macrophage colony stimulating factor (GM-CSF) and slow fade gold Antifade mountant with DAPI (4′,6-diamidino-2-phenylindole) were purchased from Thermo Fischer Scientific, Waltham, MA, USA. Anti-mouse CD16/CD32 MAb (Fc blocker), CD40, CD86, MHCII Abs, and their respective isotype controls were purchased from BD Biosciences (San Jose, CA, USA). Murine IFNγ, IL12p70, IL-6, and TNF-α ELISA kits were purchased from eBioscience (San Diego, CA, USA). All other reagents such as ethyl acetate, methanol, sodium hydroxide (NaOH), sodium dodecyl sulfate (SDS) were of analytical grade.

### 4.4.2 Preparation, surface modification and quantification of coumarin-6 loaded NPs

PLGA NPs were prepared using the oil/water (O/W) emulsification solvent evaporation technique as mentioned elsewhere.(21) Briefly, 6.5% (w/v) PLGA was dissolved in ethyl acetate solvent. Subsequently, 100 µg of coumarin-6 was added to this organic phase. The organic phase was transferred in drops into the aqueous phase comprised of 2.2 % polyvinyl alcohol (PVA). To obtain pre-activated NPs, BS3 was present in the aqueous PVA solution. The resulting primary emulsion was stirred, washed and resuspended in water. Cryoprotectant (10% sucrose) was added to obtain aggregation free lyophilized

NPs.(22) The freeze-dried NPs were surface modified with anti-CD205 Ab via adsorption and covalently attachment process as mentioned previously.(23) Briefly, 20 mg of NPs was taken and dispersed in phosphate buffer solution, PBS (pH 7.2) followed by stirring ($4^0$C, 4 hours) and washing of unattached anti-CD205 Ab. The amount of Ab was quantified by BCA assay.(24)

Amount of coumarin-6 was quantified using fluorimetry using microplate reader with an excitation wavelength at 430 nm and an emission wavelength at 485 nm. First, coumarin-6 loaded NPs were dispersed in methanol for 24 hours.(25) The supernatant was collected after washing the NPs twice by centrifugation. A standard curve of coumarin-6 was prepared in the concentration ranged from 0.78-100 µg/ml.(22) The encapsulation efficiency and loading of coumarin-6 was calculated based on the following equations: (26)

$$Coumarin-6\ loading = \frac{Amount\ of\ laoded\ coumarin-6\ (\mu g)}{Amount\ of\ polymer\ (mg)}$$

$$Encapsulation\ efficiency\ (\%) = \frac{Amount\ of\ loaded\ coumarin-6\ \ (mg)}{Amount\ of\ coumarin-6\ added\ (mg)} \times 100$$

**4.4.3 Surface modification and quantification of OVA loaded NPs**

OVA loaded NPs were prepared by water/oil/water double emulsification solvent evaporation method as mentioned elsewhere.(27) In brief, 10 mg OVA of was dissolved in100 µl PBS and transferred to PLGA-ethyl acetate solution. 200 µg of MPLA dissolved in 1:4 methanol-chloroform mixture was added to the PLGA mixture for the formulations with MPLA. The sonicated primary emulsion was added to 2.2% of PVA to form a secondary emulsion. Once the organic solvent was evaporated; suspension was washed twice, freeze-dried, and stored at -$20^0$C. All the formulations were cryopreserved with 10% sucrose solution.(14)

Surface modification of OVA loaded NPs was obtained using physical adsorption and covalent attachment method as mentioned in the previous section. The amount of OVA in NPs was quantified using BCA assay.(28) Briefly, 5 mg of NPs were re-dispersed in 3ml of 0.05M NaOH containing 1% of SDS. The suspension was incubated overnight in an orbital shaker. Next day, the supernatant was

collected after centrifugation. Samples were placed in a 96-well plate (Corning Costar, USA) and absorbance was measured at 565 nm using a microplate reader. The result was compared with a standard curve prepared by OVA in the concentration range of 15.6 µg/ml to 1000 µg/ml. (29), (30)

**4.4.4 Cell viability assay**

DCs were seeded at a density of 10,000 cells per well in 96-well plates with complete media containing alpha minimum essential medium (MEM) media, 20% FBS, 5 ng/ml of GM-CSF, and 1% penicillin-streptomycin-amphotericin B cocktail.(31) For the assay, MTS [3-(4, 5-dimethylthiazol-2-yl)-5-(3-carboxymethoxyphenyl)-2-(4-sulfophenyl)-2H-tetrazolium] reagent was used per manufacturer's directions. Briefly, NP suspension was diluted in complete medium and 20 µl of each dilution containing 1 mg/ml OVA was added in triplicate wells. The samples were incubated for 72 hours. After that, 10 µl of MTS reagent was added to each well and the plate was incubated again for 2 hours at $37^0$C. The absorbance was measured at 490 nm with a microplate reader.(32)

**4.4.5 OVA release study**

*In-vitro* release studies of OVA from PLGA NPs were carried out by incubating specific amount of NPs in 2 ml of PBS at $37^0$C with agitation. At predetermined times (for 20 days), the suspension was centrifuged. OVA containing supernatants were collected and stored at $-20^0$C. Later, the protein present in samples were determined by BCA assay kit and read with a microplate reader at 565 nm.(33)

**4.4.6 DC uptake study**

DCs were treated with different formulations of coumarin-6 loaded NPs. DCs were harvested after 24 hours of incubation with the formulations. The cells were washed with ice-cold FACS buffer to remove non-internalized NPs. About 2 x $10^5$ cells were incubated with anti-mouse Fc blocker for 15 minutes. The suspension was then washed with FACS buffer. Test groups were surface modified NPs and non-modified NPs. Untreated cells were used as negative control. Fold-increase in DC uptake was calculated dividing the mean fluorescence intensity (MFI) of coumarin-6 positive cells (test groups) by untreated cells. All samples were acquired on BD FACS Calibur machine and analyzed using Kaluza flow

software.(27) For analysis by flow cytometry, a total of 10,000 gated events were used. The detector was adjusted in a way so that the negative population appears in the first logarithmic decade.

**4.4.7 Intracellular localization of NPs analyzed by confocal laser scanning microscopy (CLSM)**

About 5 x $10^6$ DCs were seeded in a six-well plate. After stabilization for 2 hours, the DCs were treated with coumarin-6 loaded NPs. After overnight incubation, the cells were washed with PBS and fixed with 4% paraformaldehyde solution for 20 minutes. The cell nuclei were then counterstained for 20 minutes with DAPI (1 mg/ml). The cells were examined under fluorescence microscopy (IX71-F22FL/PH, OLYMPUS). Finally, the uptake was visualized in a glass bottom petridish with a confocal laser scanning microscope (LSM 510 Meta, Carl Zeiss, Germany).(34)

**4.4.8 Characterization of surface phenotype by flow cytometry**

Different NP formulations were incubated overnight with about 5 x $10^5$ DCs in six-well plates. After overnight incubation, about 2 x $10^5$ of DCs were collected. Then, cells were washed thoroughly and incubated with Fc blocker to block any non-specific binding. Next, the cells were stained with phycoerythrin (PE) conjugated specific Abs for CD40, anti-CD86 or MHCII for 30 minutes at $4^0$C. The isotype standard for each maturation marker was also used to measure background fluorescence intensity.(35) Lipopolysaccharide (LPS) 1µg/ml was used as positive control. And an unstimulated cell was used as negative control. NP-DC samples were acquired on FACS Calibur machine and analyzed using Cell Quest Pro software.

**4.4.9 Detection of cytokine secretion**

The supernatants from the DC culture was stored at -20°C for analysis of the level of IL-12, IL-6, IFNγ and TNF-α using commercially available enzyme-linked immunosorbent assay (ELISA) kits. The samples were then placed in 96-well microplate using a microplate reader at 450 nm (background 570 nm) according to manufacturer's directions.(35) The minimum detection levels of the cytokines were 15, 4, 15, and 15 pg/ml for IL-12, IL-6, IFNγ, and TNF-α, respectively.

### 4.4.10 Statistical analysis

The data are given as mean ± SD and statistical significance was determined by Student's t-test. Values of $p < 0.05$ were considered statistically significant unless specifically mentioned. Data were analyzed using GraphPad Prism 5.03 software (GraphPad Software, Inc., La Jolla, CA, USA).

## 4.5 Results

### 4.5.1 Characterization of coumarin-6 loaded plain and Ab modified NPs

Table 4.1 summarizes the NP size, polydispersity index (PDI), zeta potential (ZP), encapsulation efficiency (EE), and coumarin-6 loading (per mg of NPs). The particle size of plain NPs ranged from 121±5 to 162±5 nm. All the formulations were cryopreserved with 10% sucrose. Following Ab attachment (both adsorbed and covalent), the particle size was 201±10 to 562±5 nm. The increase in polymer viscosity increased both particle size and PDI although they were not significantly different. The EE of coumarin-6 ranged from 73.91±2.87 to 88.13±2.01% for plain NPs and 64.13±2.98 to 73.75±0.99% for Ab modified formulations. The presence of BS3 did not show any effect on the formulations. Moreover, particle size showed significant relationship with PDI, ZP, EE, and loading of coumarin-6 (***$p<0.05$). The formulations (plain and modified) had ZP value of -8.91±0.26 to -1.93±0.18 mV. No significant relation within groups was observed as performed by statistical software.

### 4.5.2 DC uptake study

A quantitative uptake of coumarin-6 loaded NPs by DCs is represented in Figure 4.2A and Figure 4.2B. Treatment of DCs with Ab modified NPs allowed higher uptake of particles compared to non-modified NPs as found in other studies.(27) As shown in Figure 4.2A (a - h), compared to untreated cells (control), a clear significant shift for MFI towards right for coumarin-6 loaded NPs was observed in all the histograms. Moreover, highest shift was visible when Ab was present in the formulation.

The bar diagrams in Figure 4.2B represents the comparative fold increase in MFI for all the treatment groups. For example, there was a significant increase in MFI for the Ab adsorbed COOH (0.18 iv) terminated NPs compared to the plain unmodified formulations (***$p<0.05$). For these two groups, the fold increase in MFI was 30 [Plain NP] and 89 [NP-AD] compared to control (***$p<0.05$). Similarly,

covalently attached 0.18 iv COOH terminated NPs [NP-COV] showed significantly higher fold increase in MFI (77) compared to that (18) of plain unmodified formulations [Plain-BS-NP] (***$p<0.05$). However, covalently attached formulation of this PLGA NPs [NP-COV] had lower MFI than its Ab adsorbed [NP-AD] formulations (**$p<0.05$). A similar trend was observed for the high viscosity COOH terminated PLGA NPs and fold increase in MFI for [Plain NP], [NP-AD], [Plain-BS-NP], and [NP-COV] was 60, 121, 57, and 110, respectively. In addition, when comparing between two viscosity grades, the high viscosity formulations showed significantly higher fold increase in MFI compared to the low viscosity COOH terminated formulations (***$p<0.05$).

For ester terminated NPs, there was significant difference for fold increase in MFI for the plain and Ab modified formulations (***$p<0.05$). The BS3 containing 0.15 iv ester formulations had comparatively higher fold increase in MFI when compared with the formulations without BS3 (***$p<0.05$). The fold increase in MFI for [Plain NP], [NP-AD], [Plain-BS-NP], and [NP-COV] of low viscosity ester terminated PLGA NPs was 27, 45, 67, and 129, respectively. When comparing between the [Plain NP] and [NP-AD] formulations of high viscosity ester PLGA, [NP-AD] formulations showed 179 times higher fold increase in MFI (***$p<0.05$). Similar result was observed for Ab adsorbed ester ended NPs of the two viscosity grades. When both viscosities of ester terminated NPs were compared, the high viscosity [NP-COV] formulations did not necessarily show higher fold increase in MFI as observed for its low viscosity grade. Among the low viscosity PLGA NP formulations, 0.15E-COV had the highest targeting efficiency as represented in Figure 4.2B.

Figure 4.2C represents the intracellular localization of coumarin-6 loaded NPs (green color) that was further confirmed by CLSM. The images show that anti-CD205 Ab modified NPs had comparatively higher uptake of NPs by DCs than unmodified NPs.

### 4.5.3 Characterization of OVA/OVA-MPLA loaded plain and Ab modified NPs

Table 4.2 represents the NP size, PDI, ZP, EE, and loading (per mg of NPs) of OVA. The size of OVA, OVA-MPLA, Ab-OVA, Ab-OVA-MPLA loaded PLGA NPs were within 171 ± 3 nm, 159 ± 4 nm, 379 ± 2 nm, and 501 ± 9 nm, respectively. The ZP for all Ab free OVA and OVA-MPLA NPs ranged from -

27.1 ± 0.77 mV to -18.42 ± 0.03 mV. The integration of Ab reduced the overall negative surface charge of NPs. For the Ab modified formulations, the zeta values ranged from 1.31 ± 0.17 mV to 4.54 ± 0.21 mV. Good reproducibility in size and ZP was observed between different batches of NPs. The PDI, ZP, EE, and OVA loading had significant relationship with particle size (***$p<0.05$). The OVA EE for the OVA/OVA-MPLA NPs and Ab modified OVA/OVA-MPLA NPs were within 59.15 ± 1.56% and 42.56 ± 2.56%, respectively. There was no significant difference within groups as analyzed by statistical software.

**4.5.4 OVA release study**

The *in-vitro* release study for OVA loaded NPs demonstrated a substantial effect on release percentage depending on polymer's molecular weight and type. After 12 hours, the cumulative release of OVA from low and high viscosity COOH terminated NP was 39.88% and 30.87%, respectively (Figure 4.3A). Similarly (post 12 hour), OVA release for the low and high viscosity ester terminated NP was 31.49% and 26%, respectively (Figure 4.3A). The release following 12 hours was significantly higher than the initial (1st hour) release (*$p<0.05$). After day 7, the release of OVA from both COOH and ester terminated NPs was increased cumulatively (Figure 4.3B) (*$p<0.05$). About 2 weeks were required to release about 50% of the OVA from the high viscosity PLGA NPs (COOH > ester; *$p>0.05$). Whereas, low viscosity PLGA NPs were found to release 50% of OVA within 24 hours (COOH ended) and 7 days (ester ended). However, all OVA loaded PLGA NPs exhibited biphasic behavior over 20 days of release study as represented in Figure 4.3.(36)

**4.5.5 Cell viability assay**

The viability percentage was 79 to 93% with OVA concentration of 0.5 mg/ml.(37) Plain NPs (without OVA) had 90-100% viability as mentioned previously.(21) Soluble OVA showed reasonable toxicity to DCs (79.34%). No significant reduction of viability was observed when MPLA was present in the formulations as represented in Figure 4.4.

### 4.5.6 The effect of surface modification with anti-CD205 Ab on DC maturation

The groups were untreated DCs (negative control), DCs treated with LPS 1µg/ml (positive control), and DCs treated with OVA and OVA-MPLA NPs (test groups). Figure 4.5 and Figure 4.6 represents the comparative expressions of maturation markers (CD40, CD86, and MHCII). For all treatment groups, DCs were incubated with variable amounts of NPs containing constant amount of loaded OVA. It is evident that, the presence of anti-CD205 Ab in formulations increases MFI and percentage of positive cells compared to untreated DCs (**$p<0.05$).(28) As represented in Figure 4.5A, Ab adsorbed low viscosity COOH terminated NPs showed higher expression of all three markers (*$p<0.05$). As a result, the Ab adsorbed OVA-MPLA low viscosity COOH terminated NPs showed higher upregulation of all the markers (CD40 MFI: 68.80, CD86 MFI: 132.75, and MHCII MFI: 279.03) compared to its covalently Ab attached groups (CD40 MFI: 58.51, CD86 MFI: 78.64, and MHCII MFI: 131.48) (Figure 4.5A). Considering the comparative fold increase in MFI for the same PLGA type, the Ab modified high viscosity COOH terminated OVA/MPLA loaded NPs followed similar trend as its low viscosity grade. The highest maturation of DCs were obtained with 0.18C-OVMP-AD NPs that showed 5, 7, and 9 fold increase in MFI for expression of CD40, CD86, and MHCII molecules compared to the unstimulated cells, respectively (Figure 4.6A). Following similar trend as low viscosity, Ab adsorbed formulations of high viscosity COOH terminated NPs showed higher expression of all three markers (Figure 4.5B and Figure 4.6B).

For ester terminated NPs, 0.15E-OVMP-COV NPs showed superior expression of activation markers than the 0.15E-OVMP-AD NPs. Simultaneously, the percentage of CD40+ cells and MFI was higher for the 0.15 iv ester terminated OVA/MPLA modified NPs (Figure 4.5C). For example, 0.15E-OVMP-COV NPs expressed 4, 5, and 7 fold increase in MFI than the 0.15E-OVMP-AD NPs (Figure 6C). Between the two viscosities of ester terminated PLGA NPs, a similar trend as the COOH terminated OVA/MPLA formulations were observed. Figure 4.5D and Figure 4.6D represents the histogram and bar diagrams for the 0.55 iv ester terminated PLGA NPs.

Presence of MPLA in all these formulations showed significant change in MFI and percentage of positive cells compared to untreated cells (*$p<0.05$). It is worth mentioning that, both high viscosity PLGAs NPs showed lower expression of three markers in comparison to its low viscosity subtype. When comparing the effect of PLGA viscosity on maturation, the low viscosity formulations showed comparatively higher shift in MFI.

### 4.5.7 Cytokine secretion profile

In parallel to the phenotypic up-regulation of co-stimulatory molecules, mature DCs also secreted immunological playmakers such as IL-12, IL-6, IFNγ, and TNF-α upon exposure to free OVA, OVA-MPLA, Ab-AD, Ab-COV NP groups.(38) Figure 4.7 shows the secretion of cytokines in the DC supernatants upon stimulation with titrated amount of NPs. There was consistently high secretion of cytokines by the anti-CD205 Ab modified OVA-MPLA NPs within similar groups (Figure 4.7A – 4.7H). Highest amount of IL-12 (2165.22 ± 215 pg/ml) was secreted after DC stimulation with 0.18C-OVMP-COV NPs. Highest amount of IL-6 (1343.23 ± 87 pg/ml), and IFNγ (2691.45 ± 70 pg/ml) was detected in the supernatants of 0.18C-OVMP-AD NPs. This was significantly high compared to the minimal secretion of the cytokines by free OVA treated DCs (***$p<0.05$). TNF-α concentration was significantly highest with the 0.55C-OVMP-COV NPs (2434.35 ± pg/ml) when compared with free OVA (***$p<0.05$).

## 4.6 Discussion

Coumarin-6 is widely used in uptake studies due to its biocompatibility, low leaking rate, and high fluorescence activity.(39) In this study, coumarin-6 loaded NPs had suitable physicochemical properties to perform *in-vitro* cellular uptake. All these formulations had acceptable particle size range (121±5 nm to 562±5 nm) (Table 4.1). Particle size has a proportional relationship with the NP uptake.(34) Particles of 100-200 nm are usually internalized by receptor mediated endocytosis. Larger particle (>500 nm) are taken up by phagocytosis process.(40) This justifies the higher uptake of Ab-modified larger particles that occurred by combination of mechanisms. The large surface area of these particles is beneficial for higher loading of anti-CD205 Ab by adsorption mechanism.(3) Consequently, anti-CD205 Ab coated NPs had greater affinity for DCs than other blood opsonins.(41) This distinct surface modification escapes body's

natural defense systems with improved circulation time and higher chance to reach the target cells.(42) Bar diagrams in Figure 4.2B represents the comparative change in MFI when coumarin-6 is present in the formulations. There was a substantial increase in MFI for the high viscosity COOH terminated PLGA NPs because these formulations encapsulated more coumarin-6 compared to low viscosity PLGA formulations (Figure 4.2). On contrary, BS3 embedded low viscosity ester terminated NPs showed higher uptake compared to the high viscosity ester formulations. This could be attributed to PLGA erosion and exposure of entrapped Abs in low viscosity ester terminated NPs.(43) Relatively lower uptake in high viscosity ester formulations (with BS3), could be due to less embedment of BS3 available to link with anti-CD205 Ab (Figure 4.2B). Moreover, masking of BS3 with the hydrophobic PLGA chain could also contribute to lower uptake of high viscosity ester formulations.(23) Lower encapsulation of coumarin-6 was also observed in the BS3 containing NPs, which justifies the lower MFI. Accordingly, the targeting efficiency of 0.55E-AD NPs was the highest (179 times versus 30) when compared with its unmodified NPs.

Physicochemical properties of NPs are also important to correlate with desired immune response. Table 4.2 represents the cationic charged NPs after Ab conjugation with desired size range (323 ± 3 nm to 501 ± 9 nm). For subcutaneous vaccine delivery, particle size ranged from 200-500 nm is immunogenic.(44) Furthermore, positively charged particles are favorable for vaccination and ZP values close to zero were likely to result in aggregation.(45) Formulations, that possess ZP value greater than +30mV and less than -30mV are considered colloidally stable. Beyond this range, cryopreservation is required to maintain stability during shelf-life of the vaccine.(46) In the present study, 10% sucrose was suitable as that resulted in aggregation free slightly positive freeze-dried NPs. However, the particle size and ZP are not the sole determinant of immune response *in vivo*.(44) For the ester terminated NPs, the highest encapsulation efficiency of OVA was with 0.55E-BS-OVMP-NPs (59.15 ± 1.56 %) although there was no significant difference between groups. In case of COOH terminated NPs, the highest OVA was loaded in 0.55C-BS-OVMP-NP (55.42 ± 0.21 µg/mg of NPs). The ionic interactions between the amine groups of OVA and the COOH groups of PLGA are responsible for the overall encapsulation efficiency.(33)

PLGA is one of the most popular biodegradable polymers for drug delivery systems.(15) The viscosity increase will result in prolonged degradation rate of the polymer.(42) PLGA follows biphasic release behavior, where its content is released from the surface to the medium in the initial phase due to its solubility and water penetration into the polymer matrix (Figure 4.3A). In the second phase, progressive drug release occurred throughout the time frame by diffusion and erosion of the polymer (Figure 4.3B). The presence of COOH terminated group results in autocatalysis of the PLGA degradation process.(43). The similar pattern of PLGA degradation could have occurred in this study. From the OVA release study, it could be confirmed that, the release of a protein from a polymeric matrix in an aqueous media slows down due to polymer gelation. This change in polymer suspension is favorable for sustain release of protein from the NPs *in-vivo*.(47) In addition, MTS assay shows that incorporating OVA in the formulations did not show any significant effects on DC viability over 72 hours in the culture media (Figure 4.4).(48)

To confirm the maturation of DCs, the expression of maturation markers (CD40, CD86, and MHCII) and a cytokine cocktail (IL-12, IL-6, IFNγ, and TNF-α) was investigated to compare various formulations (Figure 4.5, Figure 4.6, and Figure 4.7).(49) The maturation of DCs was induced by the OVA and OVA-MPLA formulations rather than soluble OVA. Within 24 hours period, about 30% of OVA was released from all types of PLGA NPs. The expression of stimulatory and costimulatory molecules during 24 hours was due to release of OVA in the DC microenvironment. This is a good indication that the formulations would release sufficient amount of OVA while subcutaneous injection to mice model over the three weeks period of vaccination. The DC maturation was further triggered by MPLA that increased the expression of all three markers, preferably in the Ab tailored NPs.(50) MPLA is able to induce antigen-specific immune response without affecting the systems in the body (cardiovascular, reproductive and respiratory). It can boost both cell-mediated and humoral immunity when incorporated in vaccine formulations.(33) The superiority of the Ab-AD groups over the Ab-COV was also obvious in the formulations (with exception with 0.15 iv ester terminated NP formulations). This could be attributed to

fast release of the loosely bound surface linked OVA from the OVA-AD groups in the DC media. Although, Ab-adsorbed OVA-MPLA formulations showed better maturation of DCs, both Ab-AD and Ab-COV formulations should be administered in mouse model to conclude about their efficacy post vaccination.

DCs are stimulated by secreting cytokines after well recognition of certain patterns of pathogens. Secretion of the cytokines indicates the signal required for activation of T cells.(51) The immuno-stimulatory effect of formulations was evaluated by the levels of various cytokines. The findings of this study reveal that Ab modified NPs consistently showed higher cytokine secretion compared to unmodified NPs. Moreover, co-delivery of OVA-MPLA resulted in significant secretion of T helper 1 (Th1) type cytokines including IL-12, IL-6, IFNγ, and TNF-α. It is known that, IL-12 influences T cell differentiation, which is further regulated by IL-6. IL-6 is a potent regulator of DC maturation *in-vivo*.(52) In addition, IL-12 also induces the percentages of IFNγ producing cells. Therefore, the release of these cytokines can efficiently convert immature DCs into T cell stimulatory mature DCs.(53) The cytokine cocktail present in the DC supernatant shows a Th1 biased immune response. These results are consistent with earlier studies where MPLA was able to mature DCs with expression of markers as well as secretion of cytokines. (35) (38)

**4.7 Conclusion**

In this study, we have developed anti-CD205 targeted NPs for subcutaneous delivery of therapeutic vaccines. The PLGA NPs were produced by emulsification solvent-evaporation method with suitable physicochemical properties. The low viscosity ester terminated NPs had the smallest size and suitable ZP among all the formulations. Compared with the Ab-free NPs, the functionalized PLGA NPs showed higher ability to recognize the CD205 receptors on DCs. The targeting efficiency of the antibody adsorbed high viscosity ester terminated NPs was the highest. Among all the formulations, the ligand attached low viscosity COOH terminated NPs could mature the DCs most with about 50 % of OVA released in 24 hours. In addition, ligand attached low viscosity COOH terminated NPs was also able to stimulate DCs to secret rational amount of cytokines. This respective formulation can be chosen to

conduct in-*vivo* vaccination experiments due to its ability to maintain all other desired physicochemical properties. Taken together, all results support our hypothesis that anti-CD205 Ab modified NPs are effective in terms of *in-vitro* DC stimulation with either type of polymers depending on the aim of treatment. However, researchers could also design the *in-vivo* experiments by choosing any of the PLGA types mentioned in this study. In future, we aim to subcutaneously inject the formulations containing OVA-MPLA (non-targeted and targeted) to develop the dose-response relationship in animal model. Therefore, this model vaccine delivery system could be adapted to design a therapeutic cancer vaccine to harness patient's immune responses.

### 4.8 Acknowledgments

This project was supported by research grants from Natural Sciences and Engineering Research (NSERC) and Saskatchewan Health Research Foundation (SHRF). The authors thank College of Pharmacy and Nutrition, University of Saskatchewan for providing assistance with flow cytometer. The authors also thank department of Biology, University of Saskatchewan for providing help with confocal microscopy.

### 4.9 Conflict of interest

The author(s) disclose that this article content has no conflict of interest.

### 4.10 TABLES

**Table 4.1.** Particle size, PDI, ZP, EE of coumarin-6 (%) and coumarin-6 loading (μg/mg) of COOH and ester terminated NPs before and after Ab attachment (n=3).

| Formulation | Size ± SD (nm) | PDI ± SD | ZP ± SD (mV) | EE of Coumarin-6 ± SD (%) | Coumarin-6 loading ± SD (μg/mg) |
|---|---|---|---|---|---|
| 0.18C-NP | 132 ± 7 | 0.12 ± 0.03 | -8.01 ± 0.52 | 73.91 ± 2.87 | 16.78 ± 0.71 |
| 0.55C-NP | 141 ± 7 | 0.23 ± 0.09 | -7.01 ± 0.74 | 75.37 ± 3.12 | 22.26 ± 2.20 |
| 0.15E-NP | 129 ± 4 | 0.24 ± 0.05 | -6.02 ± 0.34 | 81.63 ± 0.32 | 23.18 ± 1.90 |
| 0.55E-NP | 137 ± 3 | 0.26 ± 0.03 | -5.87 ± 0.54 | 83.13 ± 0.67 | 24.20 ± 3.60 |
| 0.18C-BS-NP | 121 ± 5 | 0.26 ± 0.03 | -7.23 ± 0.11 | 81.90 ± 2.38 | 11.59 ± 0.99 |
| 0.55C-BS-NP | 143 ± 6 | 0.32 ± 0.03 | -8.32 ± 0.19 | 83.83 ± 4.02 | 15.91 ± 0.12 |
| 0.15E-BS-NP | 144 ± 3 | 0.25 ± 0.04 | -6.32 ± 0.11 | 79.18 ± 1.98 | 21.78 ± 0.34 |
| 0.55E-BS-NP | 162 ± 5 | 0.26 ± 0.06 | -7.91 ± 0.26 | 88.13 ± 2.01 | 25.80 ± 1.21 |
| Ab-0.18C-NP | 263 ± 7 | 0.30 ± 0.03 | -2.22 ± 0.01 | 67.13±1.19 | 8.01±0.78 |
| Ab-0.55C-NP | 340 ± 4 | 0.36 ± 0.05 | -1.93 ± 0.18 | 73.75 ± 0.99 | 10.14 ± 0.19 |
| Ab-0.15E-NP | 276 ± 6 | 0.32 ± 0.07 | -2.54 ± 0.21 | 70.15 ± 1.25 | 11.26 ± 0.54 |
| Ab-0.55E-NP | 402 ± 9 | 0.33 ± 0.02 | -2.34 ± 0.12 | 71.23 ± 0.91 | 12.68 ± 0.44 |
| Ab-0.18C-BS-NP | 201 ± 10 | 0.36 ± 0.04 | -7.42 ± 0.21 | 70.25 ± 1.46 | 10.77 ± 1.84 |
| Ab-0.55C-BS-NP | 443 ± 6 | 0.42 ± 0.03 | -6.27 ± 0.22 | 72.79 ± 3.24 | 12.86 ± 0.54 |
| Ab-0.15E-BS-NP | 474 ± 3 | 0.35 ± 0.04 | -5.31 ± 0.14 | 64.13 ± 2.98 | 9.75 ± 0.62 |
| Ab-0.55E-BS-NP | 562 ± 5 | 0.46 ± 0.06 | -5.11 ± 0.68 | 69.83 ± 2.57 | 15.82 ± 0.27 |

**Formulation keys:** SD=Standard deviation, ZP=Zeta potential, EE= Encapsulation efficiency, NP=Nanoparticle, Ab=Antibody, BS=BS3, C = COOH, E = Ester.

**Table 4.2.** Particle size, PDI, ZP, EE of OVA (%) and OVA loading (μg/mg) of COOH and ester terminated NPs before and after Ab attachment (n=3).

| Formulation | Size ± SD (nm) | PDI ± SD | ZP ± SD (mV) | EE of OVA ± SD (%) | OVA loading ± SD (μg/mg) |
|---|---|---|---|---|---|
| 0.18C-OV-NP | 150 ± 5 | 0.22 ± 0.89 | -22.55 ± 0.32 | 45.68 ± 1.01 | 63.21 ± 2.11 |
| 0.55C-OV-NP | 156 ± 2 | 0.21 ± 0.11 | -24.76 ± 0.42 | 46.21 ± 3.11 | 62.56 ± 3.60 |
| 0.15E-OV-NP | 170 ± 6 | 0.32 ± 0.03 | -20.11 ± 0.32 | 41.86 ± 0.98 | 67.18 ± 3.50 |
| 0.55E-OV-NP | 171 ± 3 | 0.31 ± 0.06 | -19.11 ± 0.87 | 42.13 ± 2.54 | 70.33 ± 2.80 |
| 0.18C-OVMP-NP | 141 ± 2 | 0.26 ± 0.01 | -19.01 ± 0.56 | 39.01 ± 1.35 | 53.11 ± 1.44 |
| 0.55C-OVMP-NP | 145 ± 5 | 0.32 ± 0.03 | -26.21 ± 0.25 | 45.73 ± 2.91 | 59.27 ± 1.21 |
| 0.15E-OVMP-NP | 151 ± 3 | 0.36 ± 0.06 | -19.16 ± 0.15 | 41.45 ± 1.46 | 57.16 ± 2.98 |
| 0.55E-OVMP-NP | 152 ± 6 | 0.21 ± 0.07 | -20.01 ± 0.61 | 52.62 ± 5.22 | 62.64 ± 1.64 |
| 0.18C-BS-OV-NP | 141 ± 6 | 0.45 ± 0.91 | -27.1 ± 0.77 | 38.03 ± 2.38 | 65.42 ± 2.90 |
| 0.55C-BS-OV-NP | 143 ± 2 | 0.31 ± 0.04 | -24.02 ± 0.07 | 40.55 ± 1.25 | 65.91 ± 0.52 |
| 0.15E-BS-OV-NP | 144 ± 9 | 0.21 ± 0.07 | -21.03 ± 0.55 | 51.12 ± 0.74 | 62.09 ± 0.24 |
| 0.55E-BS-OV-NP | 163 ± 8 | 0.31 ± 0.09 | -19.1 ± 0.48 | 48.13 ± 0.91 | 68.48 ± 2.27 |
| 0.18C-BS -OVMP-NP | 156 ± 7 | 0.24 ± 1.20 | -25.11 ± 0.44 | 49.10 ± 0.43 | 51.65 ± 0.56 |
| 0.5C-BS -OVMP-NP | 159 ± 4 | 0.21 ± 0.98 | -24.11 ± 0.35 | 55.42 ± 0.21 | 54.11 ± 4.15 |
| 0.15E-BS -OVMP-NP | 144 ± 9 | 0.23 ± 0.34 | -18.42 ± 0.03 | 56.11 ± 0.55 | 49.01 ± 1.33 |
| 0.55E-BS -OVMP-NP | 151 ± 2 | 0.36 ± 0.14 | -19.45 ± 0.56 | 59.15 ± 1.56 | 51.35 ± 0.46 |

| | | | | | |
|---|---|---|---|---|---|
| Ab-0.18C-OV-NP | 323 ± 3 | 0.31 ± 0.09 | 1.31 ± 0.17 | 31.13 ± 1.10 | 39.91 ± 1.21 |
| Ab-0.55C-OV-NP | 330 ± 1 | 0.36 ± 0.02 | 2.95 ± 0.18 | 33.75 ± 0.91 | 40.14 ± 0.19 |
| Ab-0.15E-OV-NP | 376 ± 5 | 0.30 ± 0.17 | 4.54 ± 0.21 | 30.15 ± 1.01 | 32.57 ± 0.74 |
| Ab-0.55E-OV-NP | 379 ± 2 | 0.30 ± 0.03 | 3.32 ± 0.43 | 30.23 ± 2.90 | 49.58 ± 0.47 |
| Ab-0.18C-OVMP-NP | 413 ± 6 | 0.31 ± 0.9 | 3.13 ± 0.11 | 39..04 ± 1.25 | 42.15 ± 1.52 |
| Ab-0.55C-OVMP-NP | 461 ± 3 | 0.31 ± 0.05 | 2.91 ± 0.34 | 35.53 ± 2.21 | 44.11 ± 1.46 |
| Ab-0.15E-OVMP-NP | 421 ± 1 | 0.28 ± 0.41 | 2.97 ± 0.34 | 35.21 ± 1.15 | 39.16 ± 2.21 |
| Ab-0.55E-OVMP-NP | 486 ± 4 | 0.34 ± 0.25 | 4.25 ± 0.52 | 42.56 ± 2.56 | 40.15 ± 3.11 |
| Ab-0.18C-BS-OV-NP | 401 ± 1 | 0.21 ± 0.31 | 1.92 ± 0.01 | 41.46 ± 0.61 | 39.01 ± 0.56 |
| Ab-0.55C-BS-OV-NP | 501 ± 9 | 0.23 ± 0.21 | 1.45 ± 0.15 | 40.42 ± 0.36 | 40.15 ± 0.62 |
| Ab-0.15E-BS-OV-NP | 337 ± 5 | 0.31 ± 0.52 | 1.67 ± 0.01 | 40.46 ± 0.11 | 37.90 ± 0.42 |
| Ab-0.55E-BS-OV-NP | 487 ± 3 | 0.21 ± 0.62 | 3.51 ± 0.03 | 45.24 ± 0.09 | 42.15 ± 0.55 |
| Ab-0.18C-BS-OVMP-NP | 380 ± 1 | 0.31 ± 0.09 | 1.42 ± 0.04 | 29.01 ± 2.01 | 40.15 ± 0.91 |
| Ab-0.55C-BS-OVMP-NP | 419 ± 4 | 0.29 ± 0.05 | 1.99 ± 0.13 | 34.11 ± 0.23 | 42.43 ± 0.55 |
| Ab-0.15E-BS-OVMP-NP | 324 ± 3 | 0.31 ± 0.04 | 3.22 ± 0.11 | 36.21 ± 0.93 | 40.11 ± 0.21 |
| Ab-0.55E-BS-OVMP-NP | 407 ± 9 | 0.39 ± 0.06 | 1.87 ± 0.02 | 39.01 ± 0.14 | 41.45 ± 0.91 |

**Formulation keys:** SD=Standard deviation, ZP=Zeta potential, PDI=Polydispersity index, EE= Encapsulation efficiency, NP=Nanoparticle, Ab=Antibody, BS=BS3, C = COOH, E = Ester, OV=Ovalbumin, MP=Monophosphoryl lipid A.

## 4.11 FIGURES

**Figure 4.1.** Graphical representation of NPs uptake by the immature DC and subsequent activation as well as maturation of DC followed by various cytokine production, antigen presentation, and expression of co-stimulatory markers.

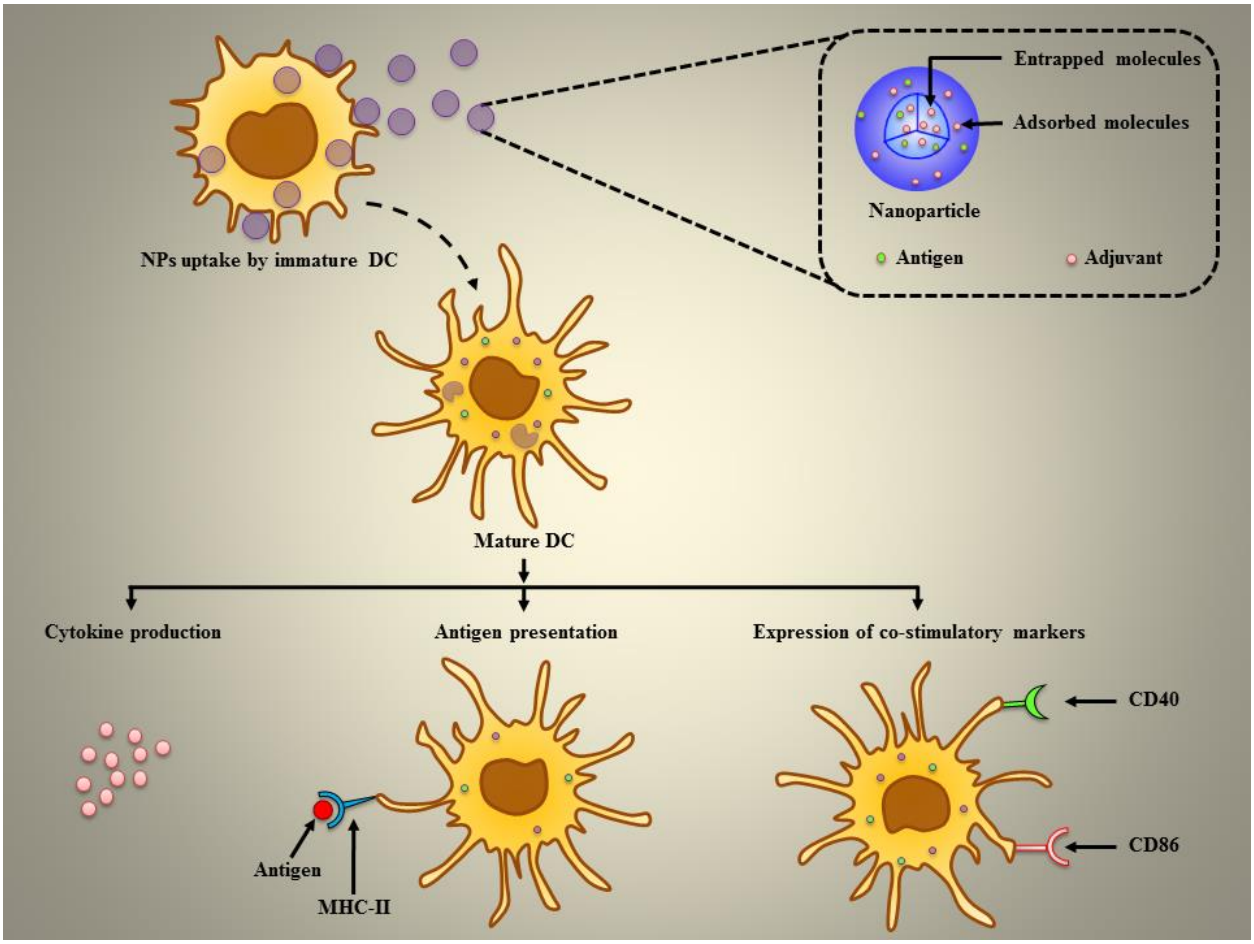

**Figure 4.2:** Maturation study with OVA loaded NPs. A) The effect of antibody decorated PLGA NPs on DC uptake assessed by flow cytometry. Column (a-d): Overlay of the histograms of untreated cells (red), cells treated with plain NPs (green), and cells treated with Ab-modified NPs (purple) for 0.18 iv COOH and 0.55 iv COOH groups with and without BS3. Column (e-h): Overlay of the histograms representing DC uptake of 0.15 iv ester and 0.55 iv ester terminated NPs being formulated with and without BS3. Histograms are representative of three individual experiments. B) The bar diagram showing comparative fold increase in MFI of plain NPs and DCs treated with Ab-modified formulations for 0.18 iv COOH, 0.55 iv COOH, 0.15 iv ester, and 0.55 iv ester terminated NPs respectively. MFI for different NPs has been compared considering untreated cells (coumarin-6 only) as 1. All the studies were done in triplicates ($p<0.05$). Formulation key: C = COOH, E = Ester, BS = BS3, AD = Adsorption, COV = Covalent. C) Representative overlapped CLSM images for coumarin-6 loaded NPs (0.18 iv COOH only) in DCs. Blue color represents the DAPI stained nuclei which are encompassed by green fluorescence for the groups treated with coumarin-6 loaded NPs.

A)

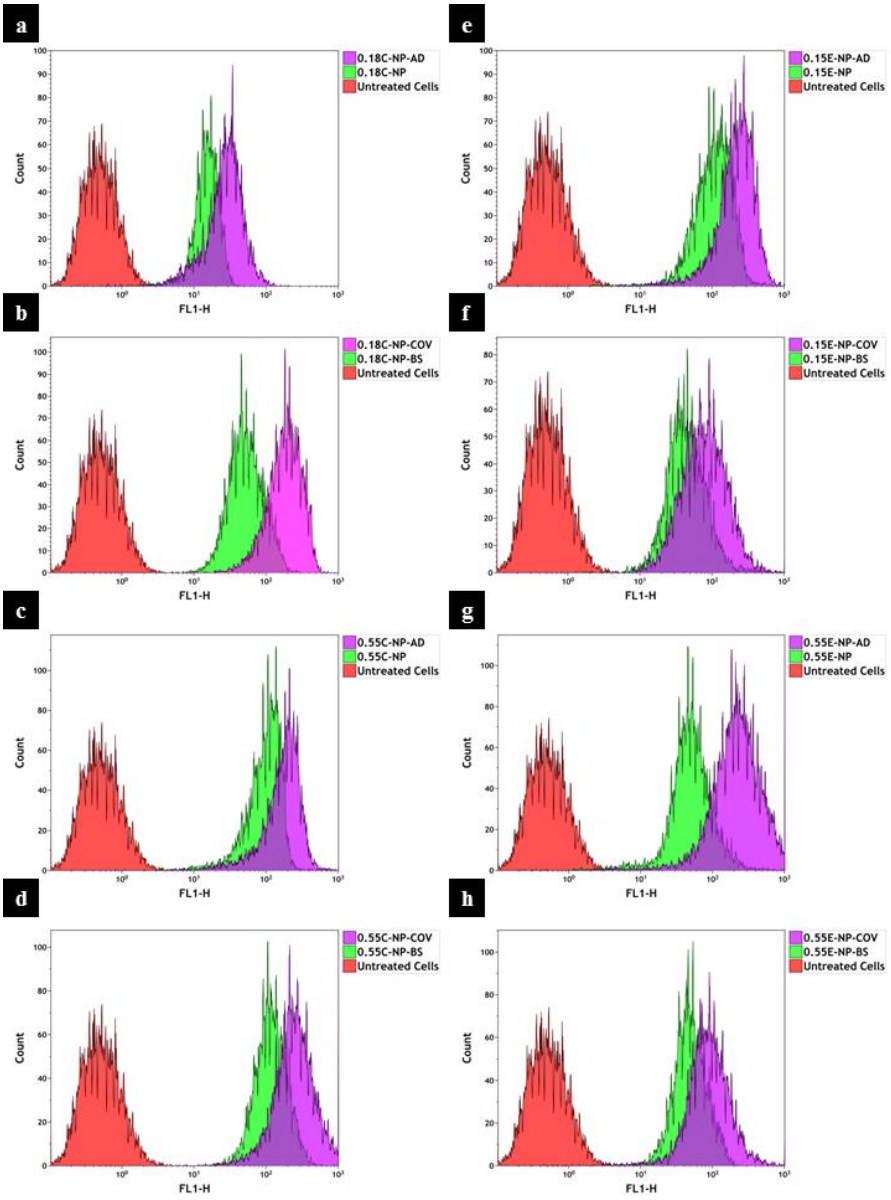
a
0.18C-NP-AD
0.18C-NP
Untreated Cells
Count
FL1-H
b
0.18C-NP-COV
0.18C-NP-BS
Untreated Cells
Count
FL1-H
c
0.55C-NP-AD
0.55C-NP
Untreated Cells
Count
FL1-H
d
0.55C-NP-COV
0.55C-NP-BS
Untreated Cells
Count
FL1-H
e
0.15E-NP-AD
0.15E-NP
Untreated Cells
Count
FL1-H
f
0.15E-NP-COV
0.15E-NP-BS
Untreated Cells
Count
FL1-H
g
0.55E-NP-AD
0.55E-NP
Untreated Cells
Count
FL1-H
h
0.55E-NP-COV
0.55E-NP-BS
Untreated Cells
Count
FL1-H

B)

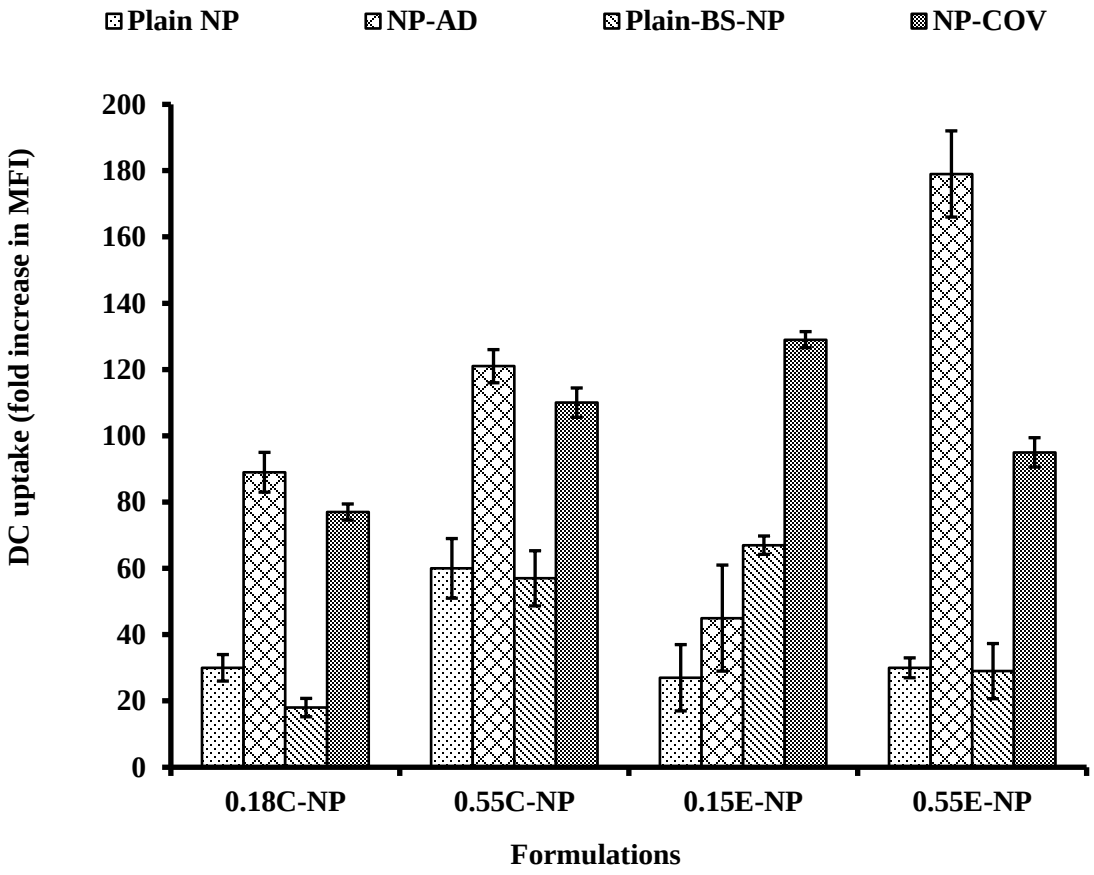
Plain NP
NP-AD
Plain-BS-NP
NP-COV
DC uptake (fold increase in MFI)
200
180
160
140
120
100
80
60
40
20
0
0.18C-NP
0.55C-NP
0.15E-NP
0.55E-NP
Formulations

C)

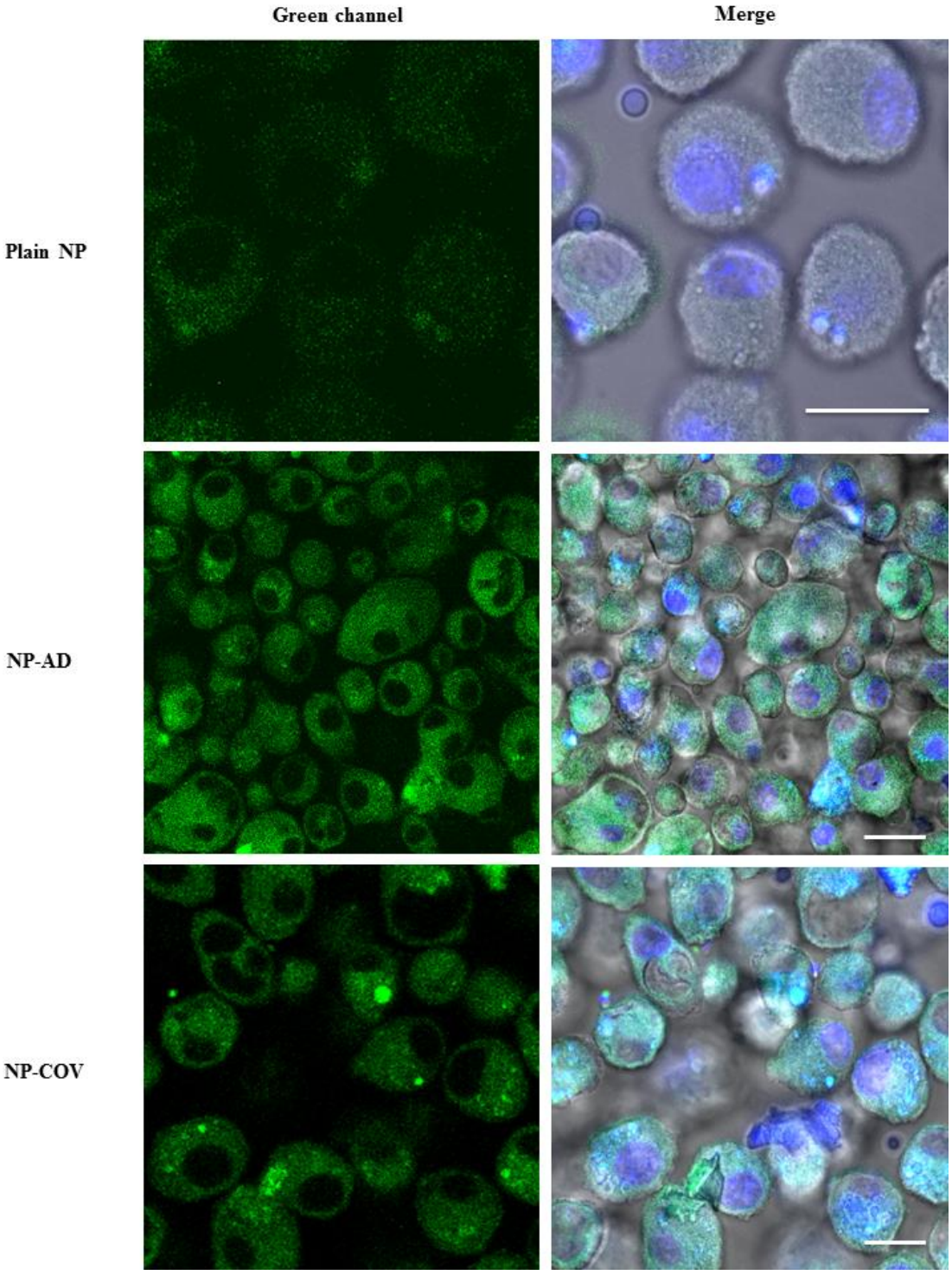

**Figure 4.3.** Cumulative percentage release of OVA from different PLGA graded NPs over time period of 20 days. The line diagram represents the release profile of 0.18 iv COOH terminated, 0.55 iv COOH terminated, 0.15 iv ester terminated, and 0.55 iv ester terminated PLGA-OVA NPs in a PBS (pH 7.4) at 37˚C. Diagrams A and B represent the initial burst release and sustained release of OVA, respectively. Here, n = 3, d = day, hr = hour.

A)

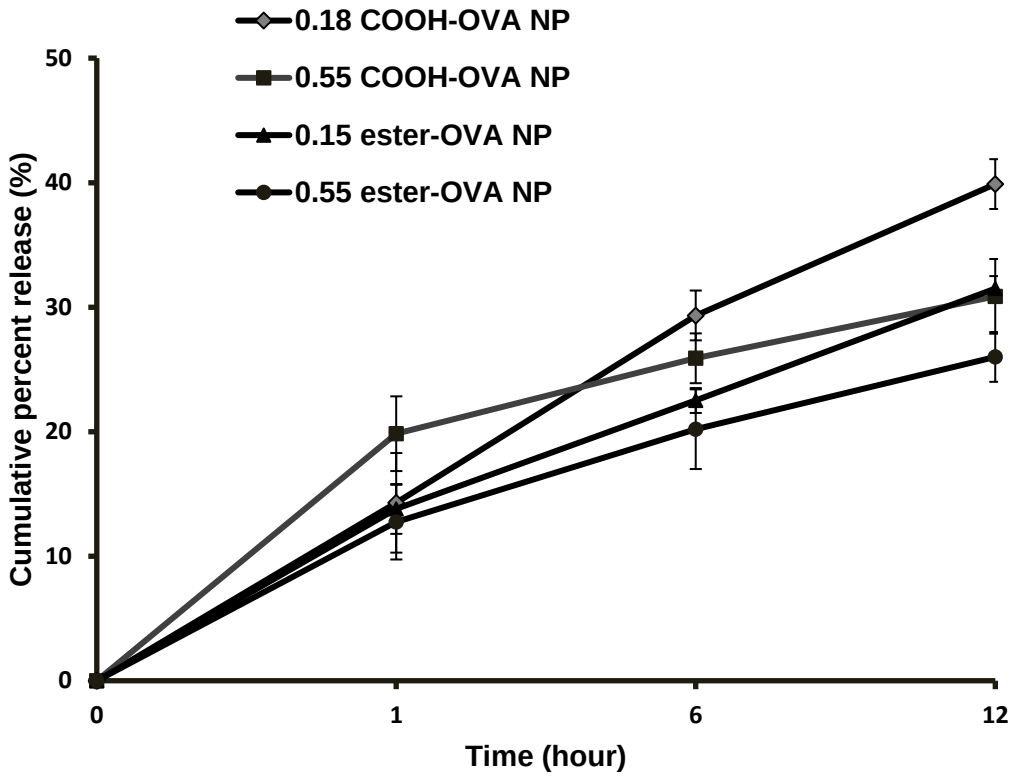

B)

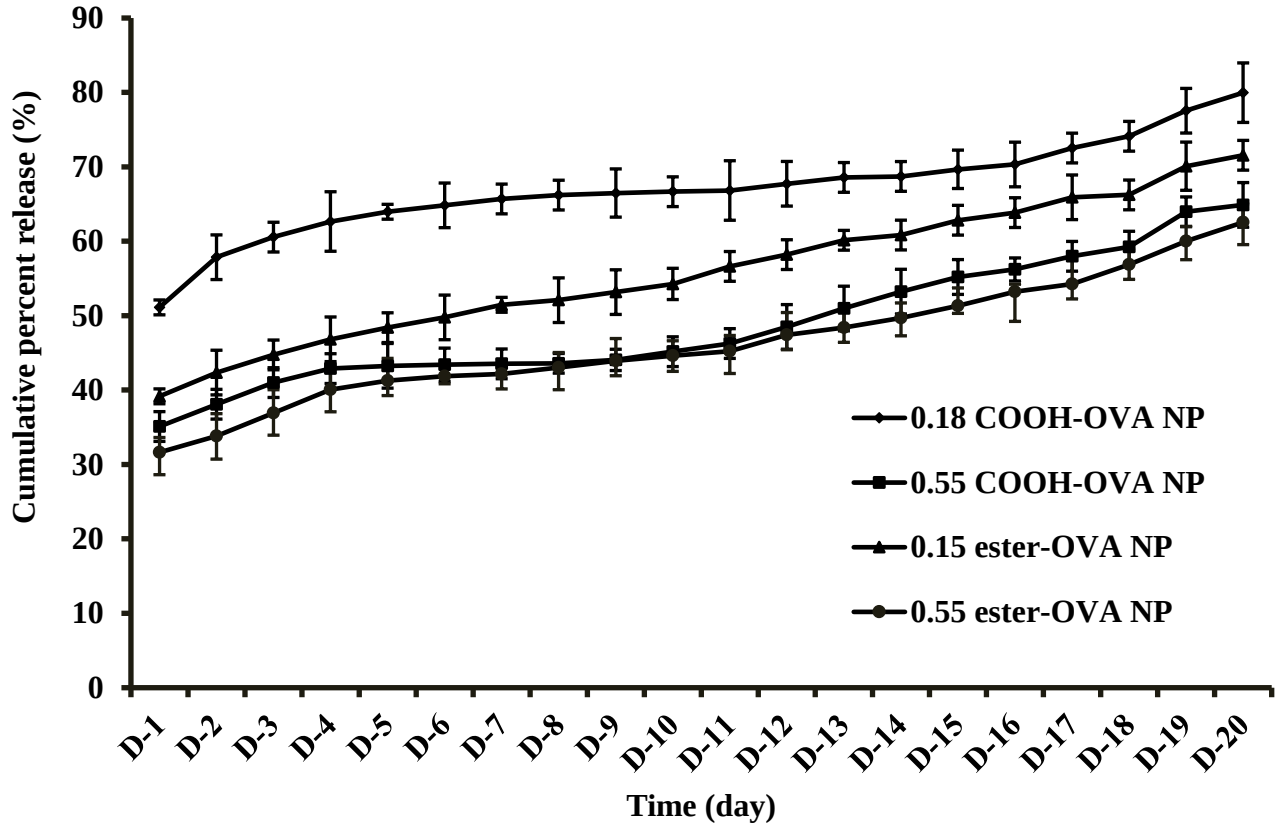
Cumulative percent release (%)
90
80
70
60
50
40
30
20
10
0
D-1
D-2
D-3
D-4
D-5
D-6
D-7
D-8
D-9
D-10
D-11
D-12
D-13
D-14
D-15
D-16
D-17
D-18
D-19
D-20
Time (day)
0.18 COOH-OVA NP
0.55 COOH-OVA NP
0.15 ester-OVA NP
0.55 ester-OVA NP

**Figure 4.4.** Cell viability (MTS assay) of DCs treated for 72 hours with OVA containing PLGA NP formulations (n = 3). The treated NP concentration was 1 mg/ml for cell density of 10,000.

Formulation keys: C = COOH ended PLGA, E = Ester ended PLGA, OV = OVA, MP = MPLA, AD = adsorption, COV = covalent.

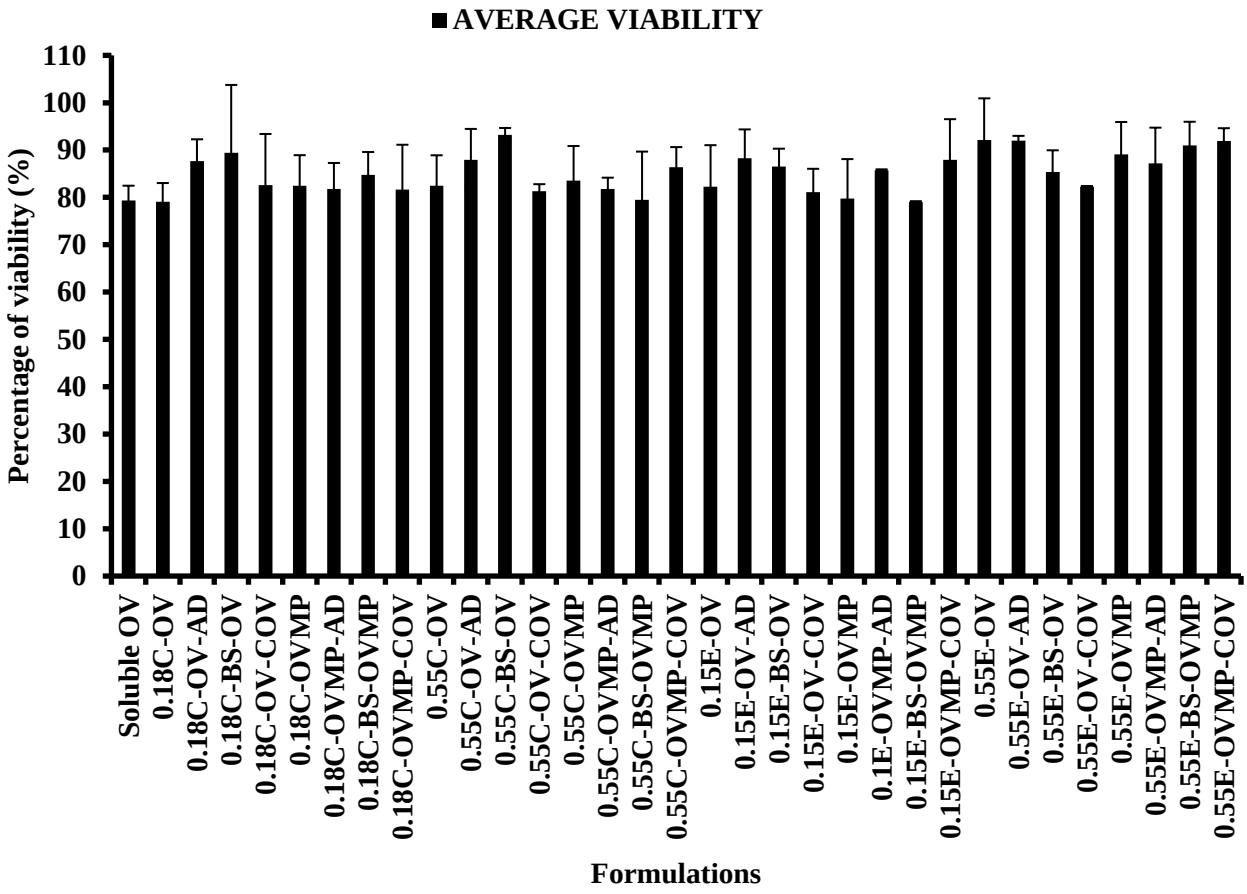

**Figure 4.5**. Effect of CD205 antibody modified PLGA NPs on the up-regulation of CD40, CD86, and MHCII molecule upon DC maturation. Untreated DC was used as negative control. LPS treated DCs were positive control. After 24 hours incubation, non-adherent cells were harvested, stained with the antibodies and analyzed by flow cytometry as described in the methods section. Expression of maturation markers by 0.18 iv COOH (A), 0.55 COOH (B), 0.15 ester (C), and 0.55 ester (D) terminated PLGA NPs. The top and bottom numeric values on the histograms represent percentages of positive cells and MFI for CD40, CD86, and MHCII markers. Representative histograms from one of three individual experiments are shown here.

Formulation keys: NP=Nanoparticle, AD=Adsorption, COV=Covalent binding, C = COOH, E=Ester, OV=Ovalbumin, MP=Monophosphoryl lipid A.

**A) 0.18 COOH**

**CD40**

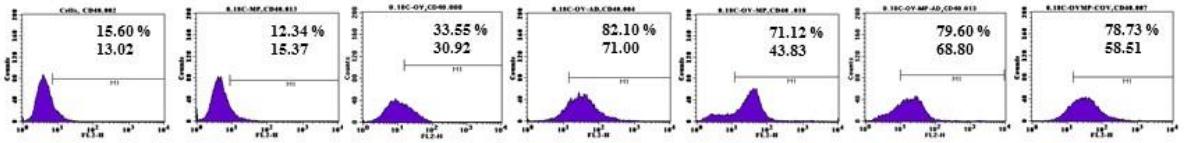


**CD86**

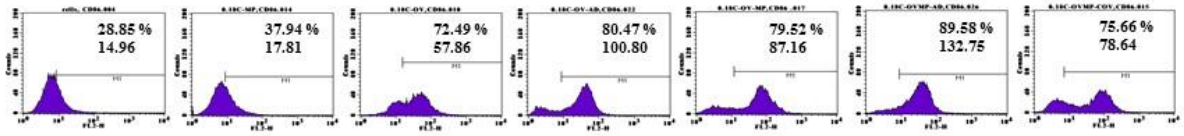


**MHCII**

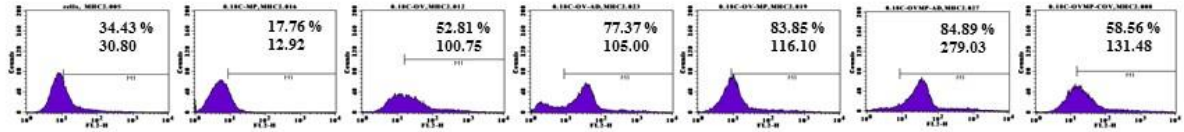


**B) 0.55 COOH**

**CD40**

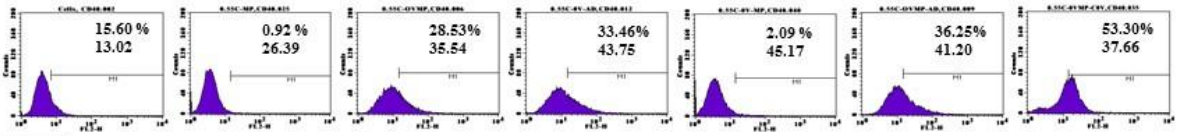


**CD86**

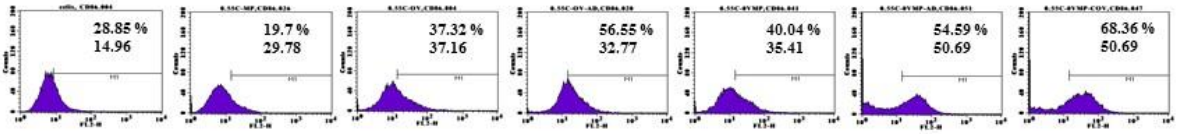


**MHCII**

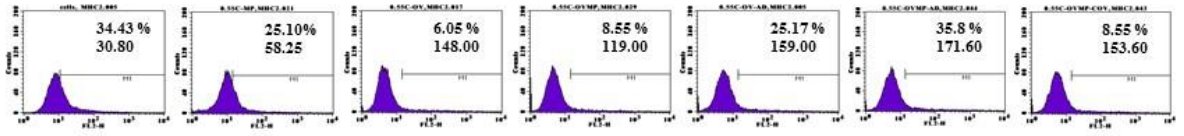

C) 0.15 Ester

CD40

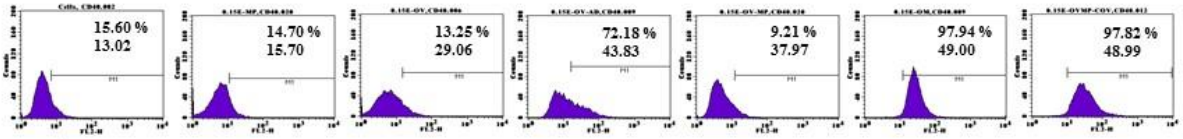


CD86

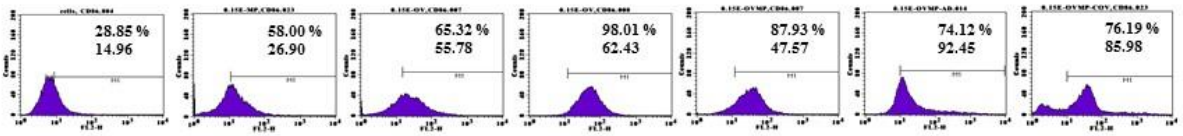


MHCII

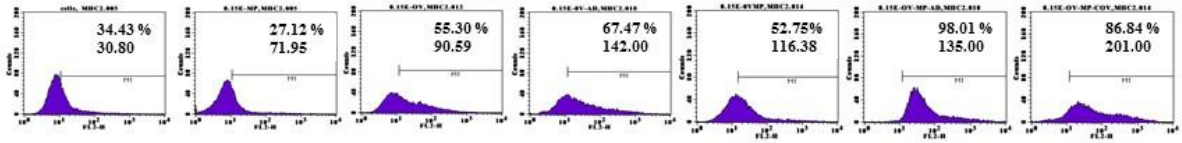


D) 0.55 Ester

CD40

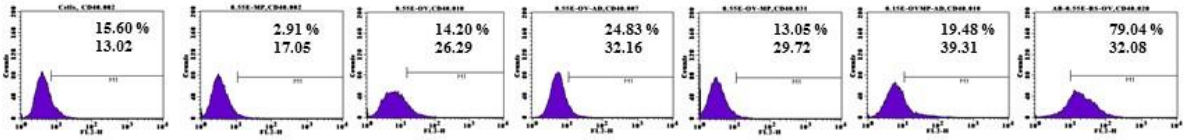


CD86

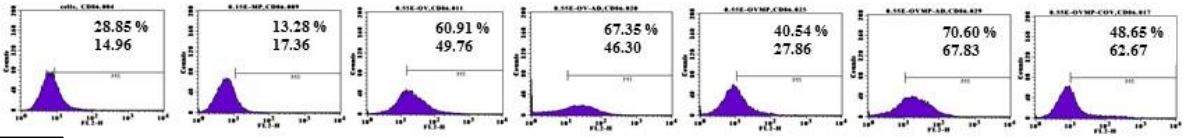


MHCII

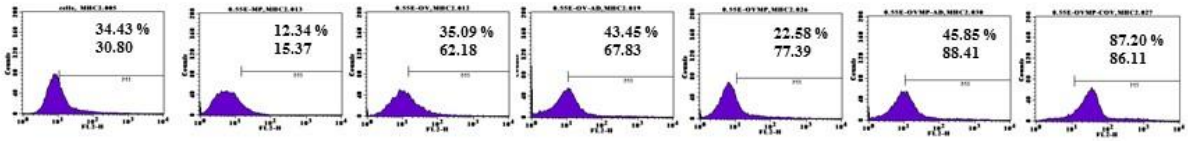

**Figure 4.6.** Bar diagrams representing the fold increase in MFI for DC maturation markers after treatment with 0.18 iv COOH (A), 0.55 COOH (B), 0.15 ester (C), and 0.55 ester (D) terminated PLGA NPs. Results are representative of at least three experiments.

Formulation keys: NP=Nanoparticle, AD=Adsorption, COV=Covalent binding, C = COOH, E=Ester, OV=Ovalbumin, MP=Monophosphoryl lipid A.

A)

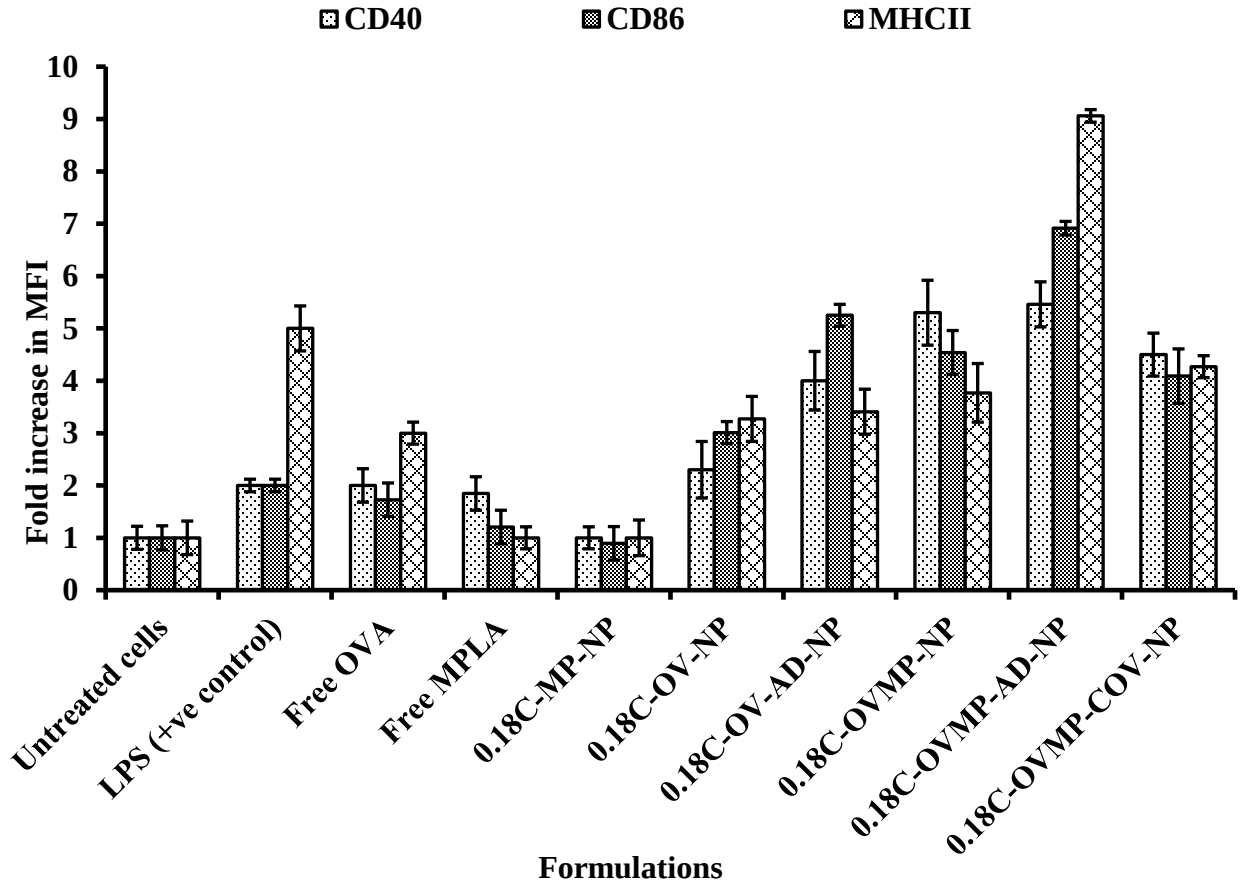

B)

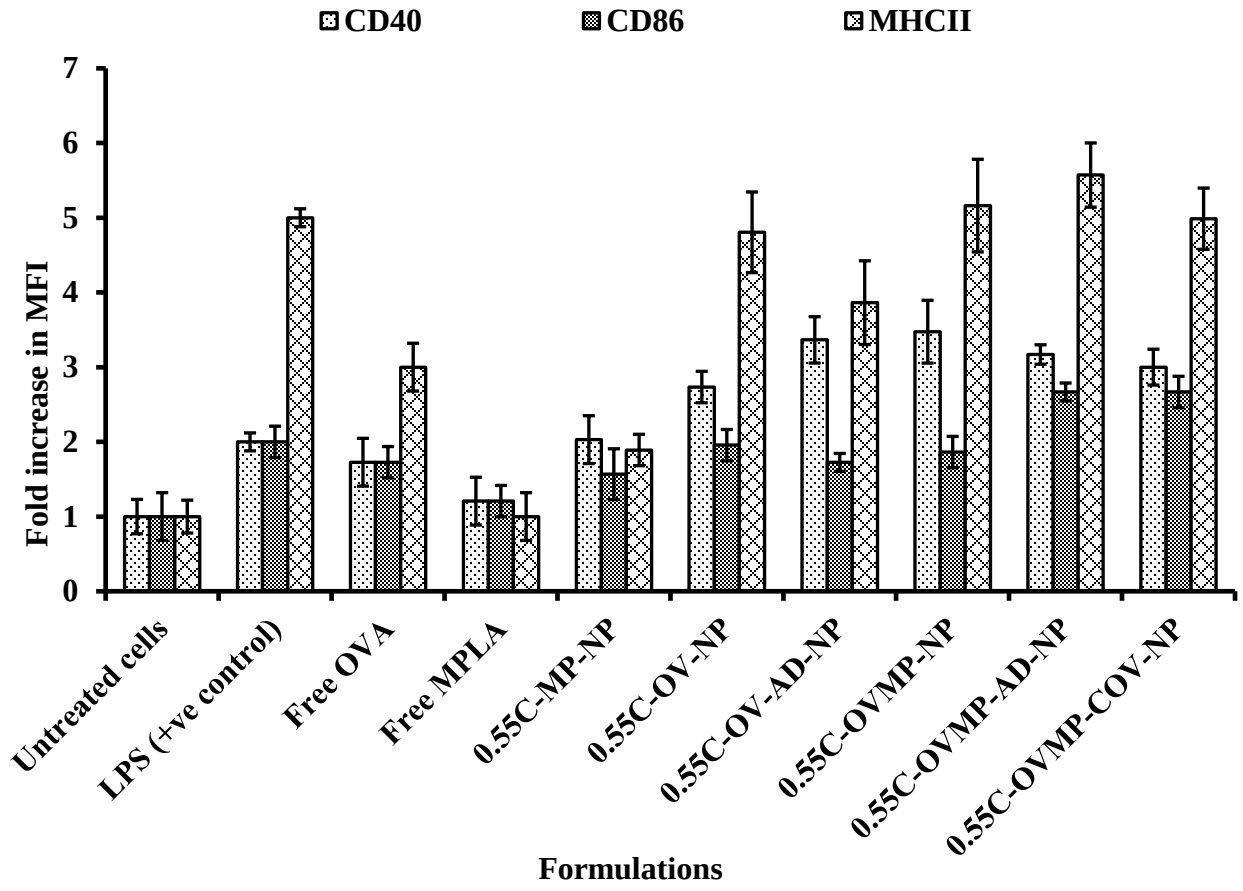
CD40
CD86
MHCII
Fold increase in MFI
0
1
2
3
4
5
6
7
Untreated cells
LPS (+ve control)
Free OVA
Free MPLA
0.55C-MP-NP
0.55C-OV-NP
0.55C-OV-AD-NP
0.55C-OVMP-NP
0.55C-OVMP-AD-NP
0.55C-OVMP-COV-NP
Formulations

C)

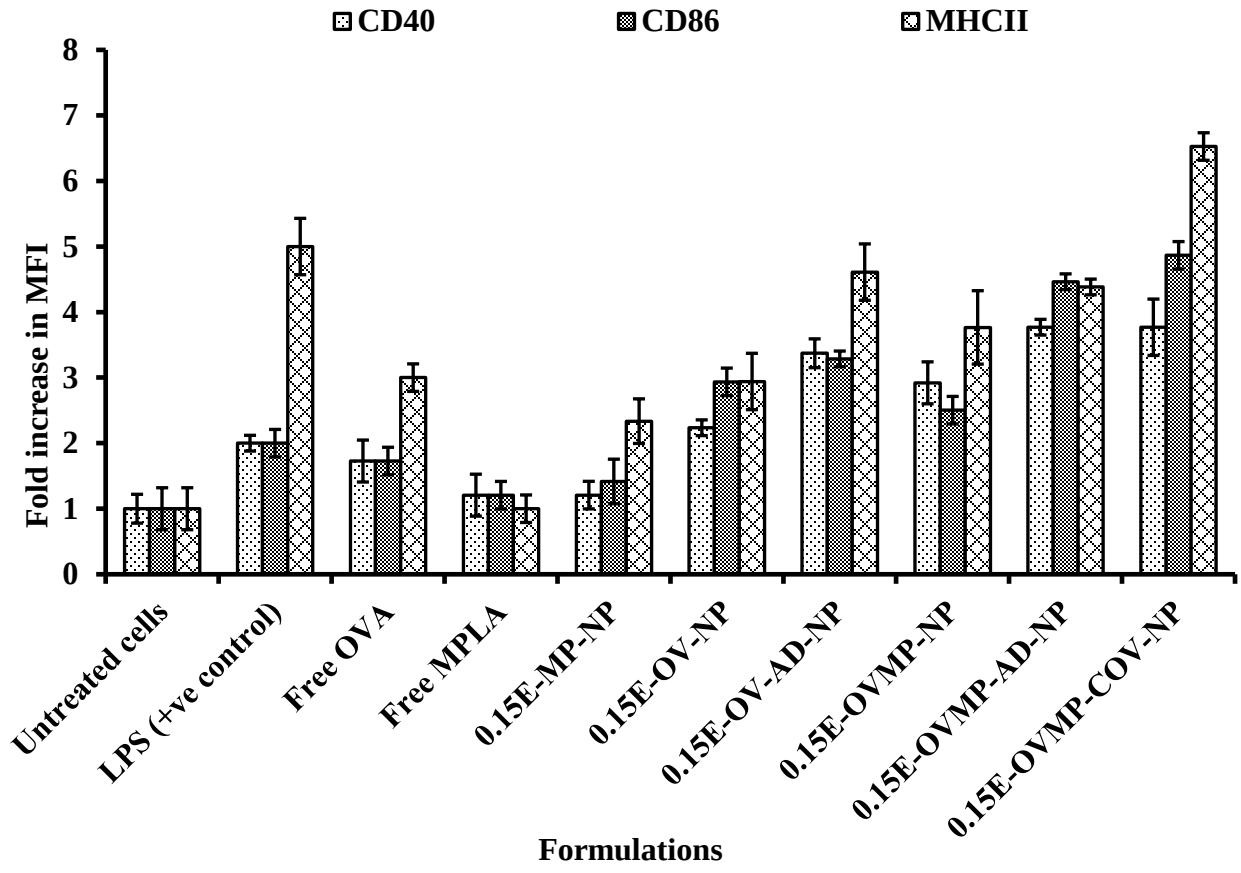
CD40
CD86
MHCII
Fold increase in MFI
0
1
2
3
4
5
6
7
8
Untreated cells
LPS (+ve control)
Free OVA
Free MPLA
0.15E-MP-NP
0.15E-OV-NP
0.15E-OV-AD-NP
0.15E-OVMP-NP
0.15E-OVMP-AD-NP
0.15E-OVMP-COV-NP
Formulations

D)

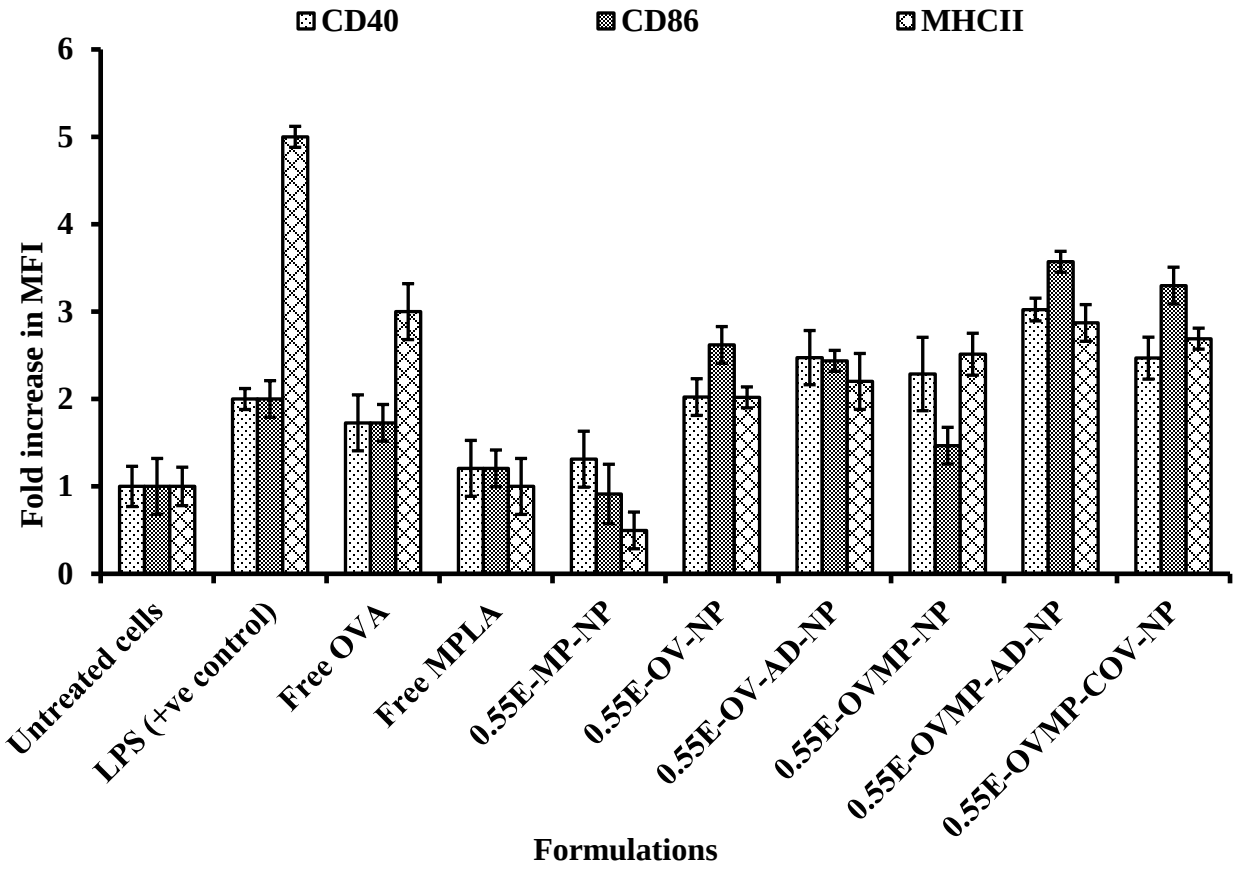
CD40
CD86
MHCII
Fold increase in MFI
0
1
2
3
4
5
6
Untreated cells
LPS (+ve control)
Free OVA
Free MPLA
0.55E-MP-NP
0.55E-OV-NP
0.55E-OV-AD-NP
0.55E-OVMP-NP
0.55E-OVMP-AD-NP
0.55E-OVMP-COV-NP
Formulations

**Figure 4.7.** Effect of OVA/OVA-MPLA NPs for cytokines secretion from mature DCs. Untreated DC was used as negative control. LPS treated DCs were positive control. After 24 hours incubation, DC culture supernatants were analyzed for IFNγ (A, B), IL-12, (C, D), IL-6 (E, F), and TNF-α (G, H) secretion. This figure is representative for 0.18 iv COOH, 0.55 iv COOH, 0.15 ester, and 0.55 ester terminated plain and anti-CD205 tailored NPs (n=3) ($p<0.05$).

Formulation keys: NP=Nanoparticle, AD=Adsorption, COV=Covalent binding, C = COOH, E=Ester, OV=Ovalbumin, MP=Monophosphoryl lipid A, LPS=Lipopolysaccharide.

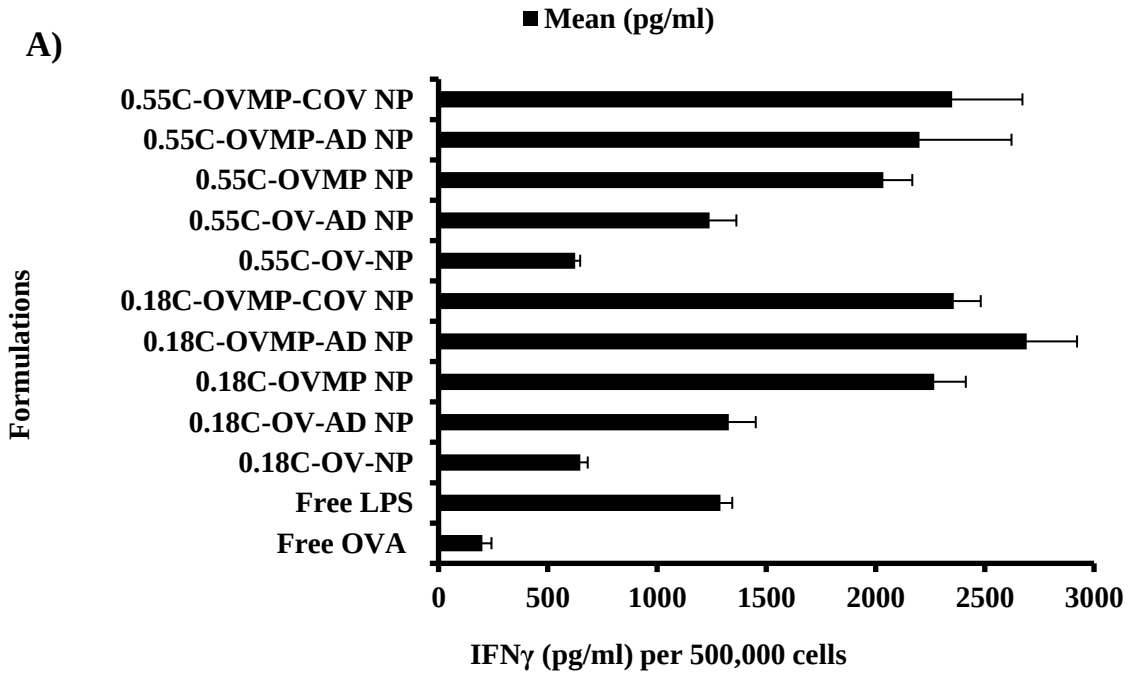

**B)**

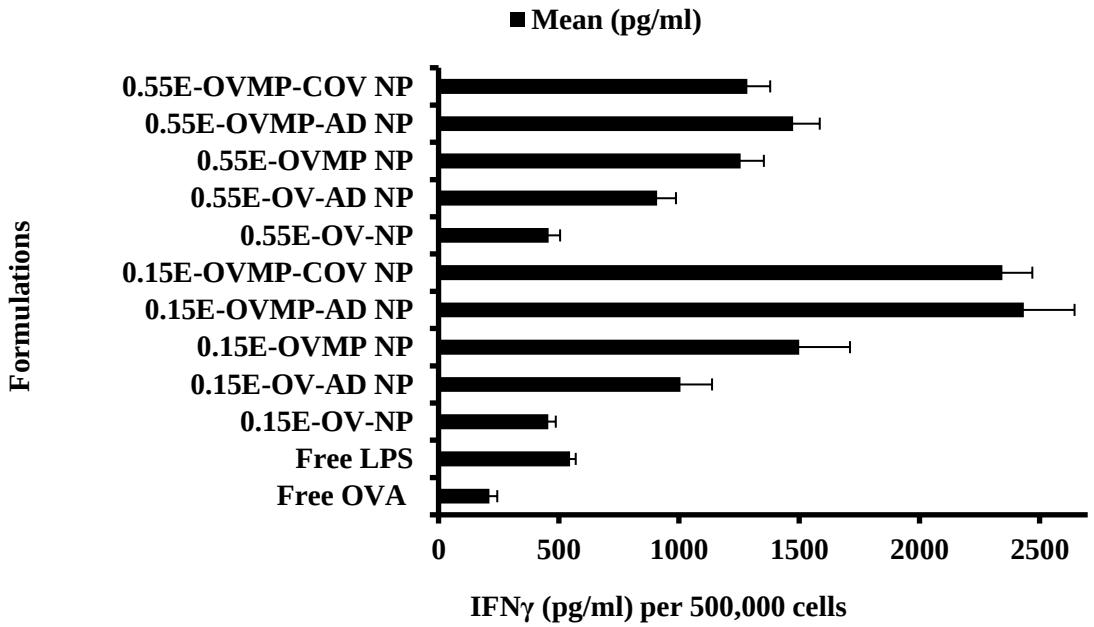
Mean (pg/ml)
Formulations
0.55E-OVMP-COV NP
0.55E-OVMP-AD NP
0.55E-OVMP NP
0.55E-OV-AD NP
0.55E-OV-NP
0.15E-OVMP-COV NP
0.15E-OVMP-AD NP
0.15E-OVMP NP
0.15E-OV-AD NP
0.15E-OV-NP
Free LPS
Free OVA
0
500
1000
1500
2000
2500
IFNγ (pg/ml) per 500,000 cells

**C)**

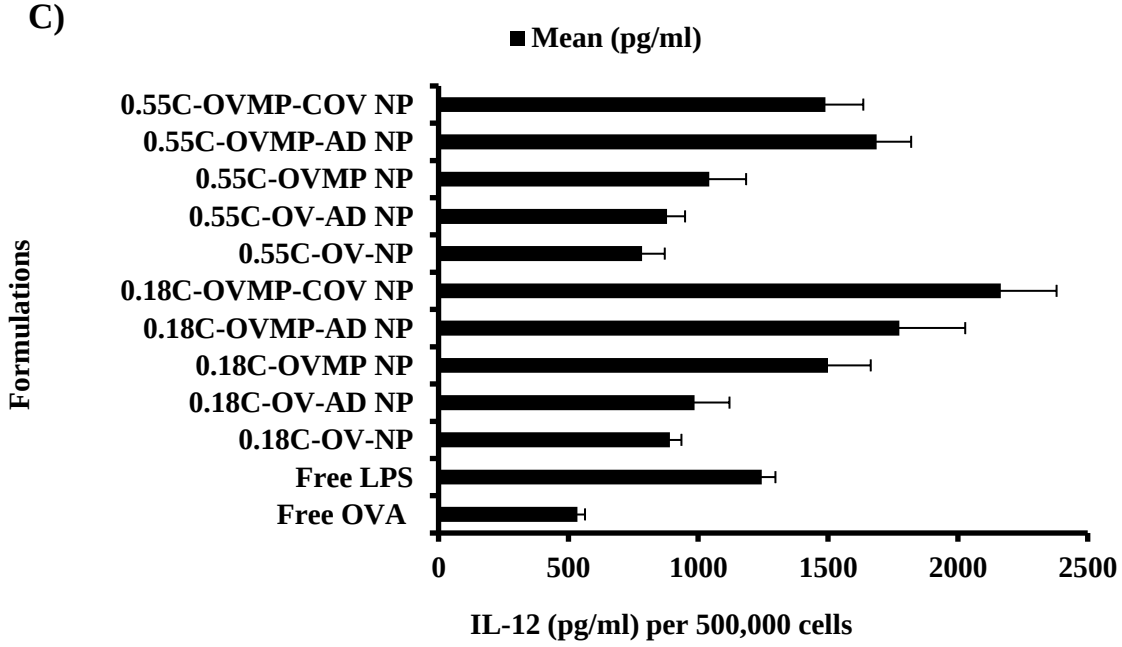
Mean (pg/ml)
Formulations
0.55C-OVMP-COV NP
0.55C-OVMP-AD NP
0.55C-OVMP NP
0.55C-OV-AD NP
0.55C-OV-NP
0.18C-OVMP-COV NP
0.18C-OVMP-AD NP
0.18C-OVMP NP
0.18C-OV-AD NP
0.18C-OV-NP
Free LPS
Free OVA
0
500
1000
1500
2000
2500
IL-12 (pg/ml) per 500,000 cells

**D)**

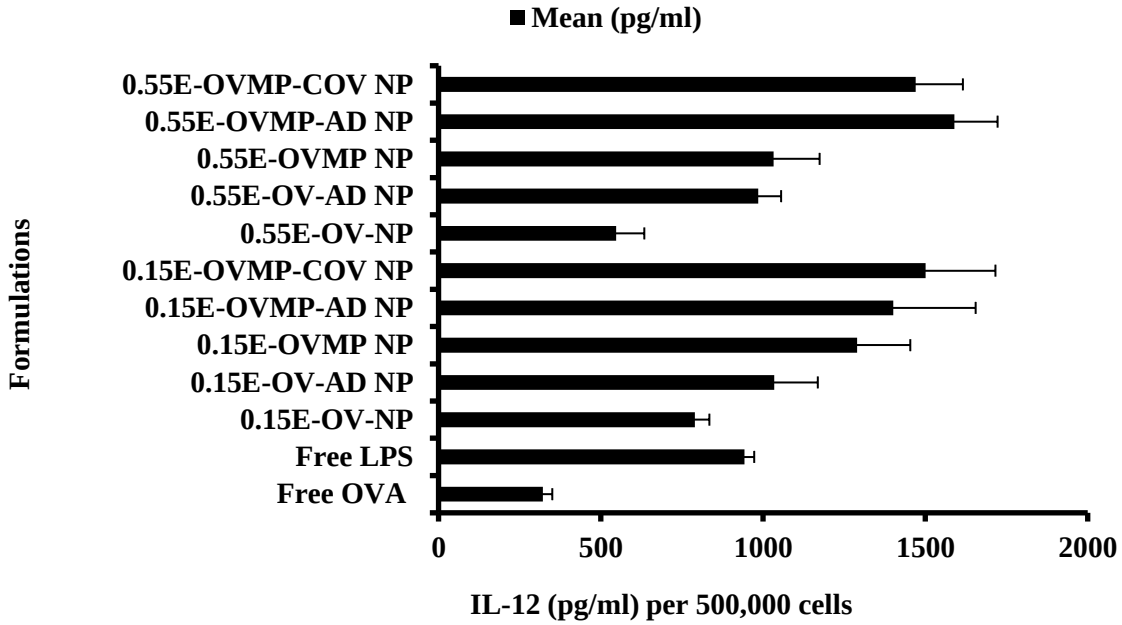
Mean (pg/ml)
0.55E-OVMP-COV NP
0.55E-OVMP-AD NP
0.55E-OVMP NP
0.55E-OV-AD NP
0.55E-OV-NP
0.15E-OVMP-COV NP
0.15E-OVMP-AD NP
0.15E-OVMP NP
0.15E-OV-AD NP
0.15E-OV-NP
Free LPS
Free OVA
Formulations
0
500
1000
1500
2000
IL-12 (pg/ml) per 500,000 cells

**E)**

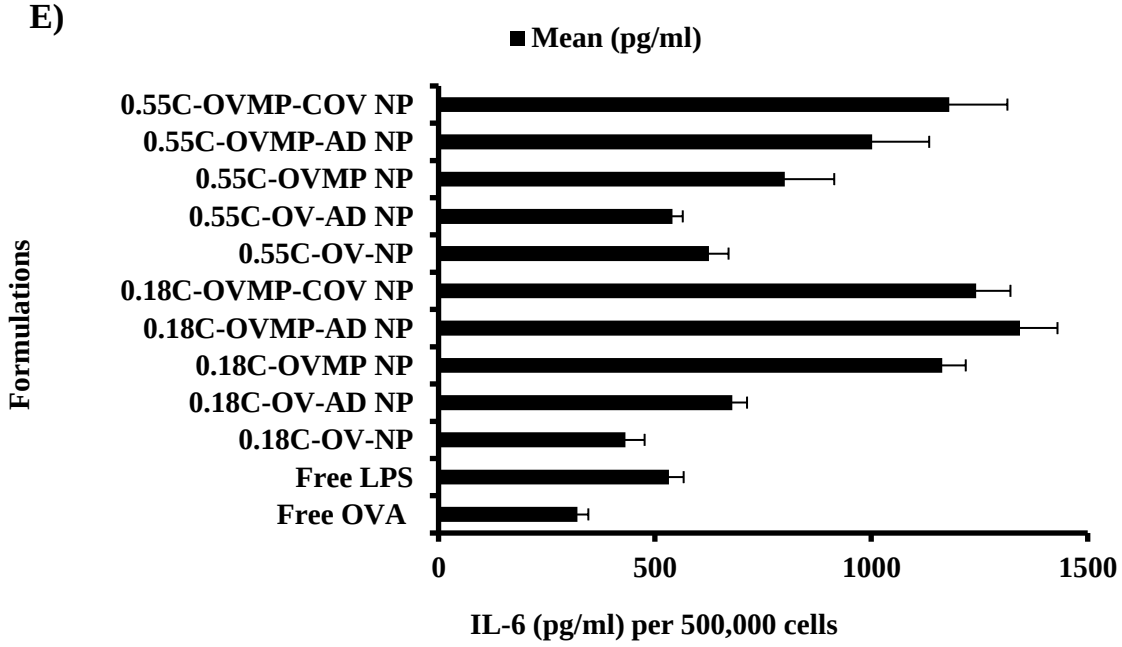
Mean (pg/ml)
0.55C-OVMP-COV NP
0.55C-OVMP-AD NP
0.55C-OVMP NP
0.55C-OV-AD NP
0.55C-OV-NP
0.18C-OVMP-COV NP
0.18C-OVMP-AD NP
0.18C-OVMP NP
0.18C-OV-AD NP
0.18C-OV-NP
Free LPS
Free OVA
Formulations
0
500
1000
1500
IL-6 (pg/ml) per 500,000 cells

F)

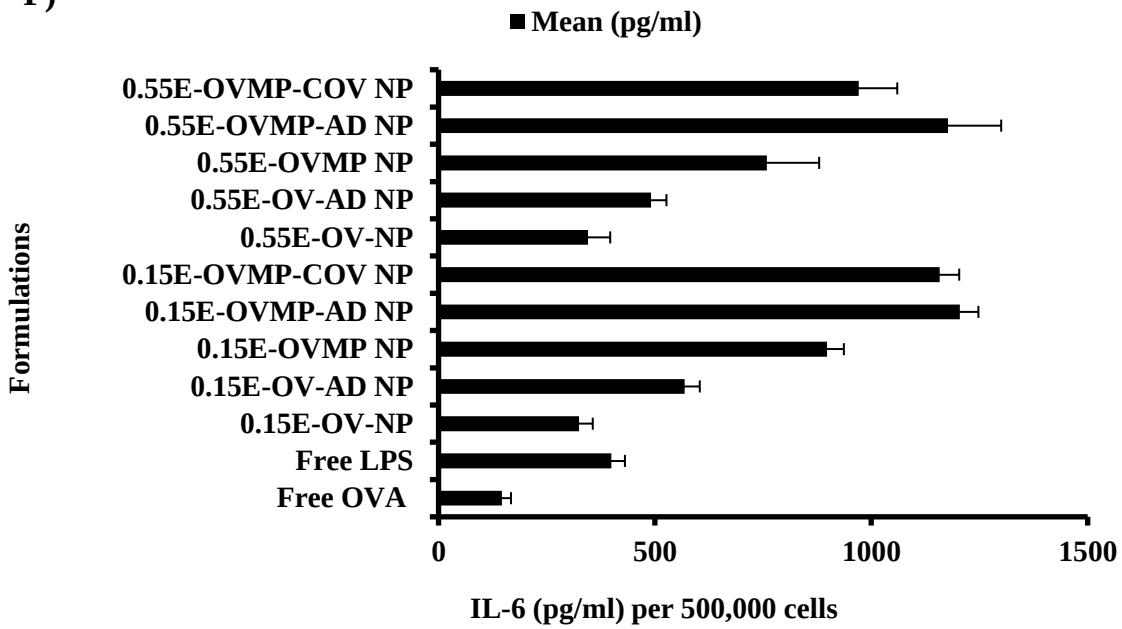
Mean (pg/ml)
0.55E-OVMP-COV NP
0.55E-OVMP-AD NP
0.55E-OVMP NP
0.55E-OV-AD NP
0.55E-OV-NP
0.15E-OVMP-COV NP
0.15E-OVMP-AD NP
0.15E-OVMP NP
0.15E-OV-AD NP
0.15E-OV-NP
Free LPS
Free OVA
Formulations
0
500
1000
1500
IL-6 (pg/ml) per 500,000 cells

G)

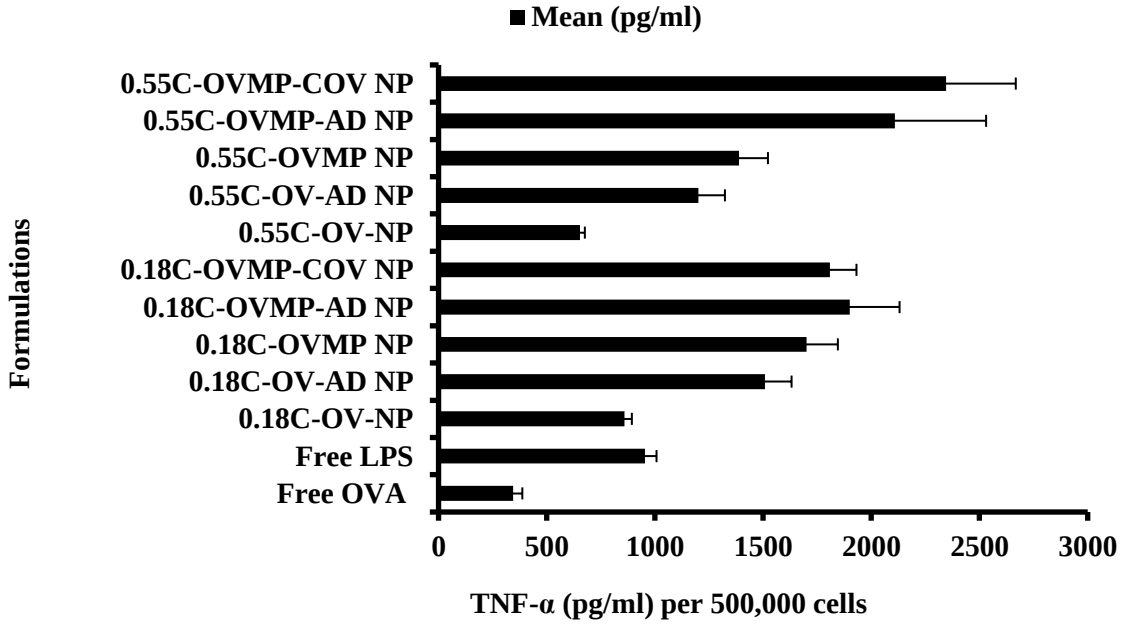
Mean (pg/ml)
0.55C-OVMP-COV NP
0.55C-OVMP-AD NP
0.55C-OVMP NP
0.55C-OV-AD NP
0.55C-OV-NP
0.18C-OVMP-COV NP
0.18C-OVMP-AD NP
0.18C-OVMP NP
0.18C-OV-AD NP
0.18C-OV-NP
Free LPS
Free OVA
Formulations
0
500
1000
1500
2000
2500
3000
TNF-α (pg/ml) per 500,000 cells

**H)**

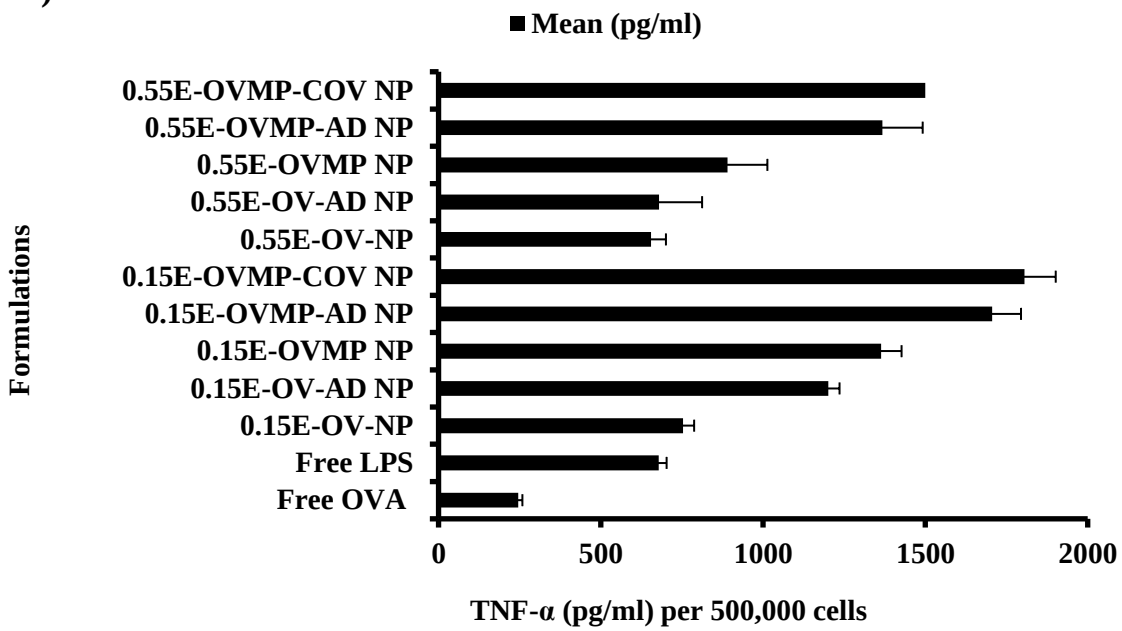
Mean (pg/ml)
Formulations
0.55E-OVMP-COV NP
0.55E-OVMP-AD NP
0.55E-OVMP NP
0.55E-OV-AD NP
0.55E-OV-NP
0.15E-OVMP-COV NP
0.15E-OVMP-AD NP
0.15E-OVMP NP
0.15E-OV-AD NP
0.15E-OV-NP
Free LPS
Free OVA
0
500
1000
1500
2000
TNF-α (pg/ml) per 500,000 cells

## 4.12 References


1. Sloan FA, Gelband H. Cancer Causes and Risk Factors and the Elements of Cancer Control. Institute of Medicine (US) Committee on Cancer Control in Low- and Middle-Income Countries: Washington (DC): National Academies Press (US); 2007.

2. Roy A, Singh MS, Upadhyay P, Bhaskar S. Nanoparticle mediated co-delivery of paclitaxel and a TLR-4 agonist results in tumor regression and enhanced immune response in the tumor microenvironment of a mouse model. International journal of pharmaceutics. 2013 Mar 10;445(1-2):171-80. PubMed PMID: 23376226.

3. Hamdy S, Haddadi A, Hung RW, Lavasanifar A. Targeting dendritic cells with nano-particulate PLGA cancer vaccine formulations. Advanced drug delivery reviews. 2011 Sep 10;63(10-11):943-55. PubMed PMID: 21679733.

4. Kalinski P, Edington H, Zeh HJ, Okada H, Butterfield LH, Kirkwood JM, et al. Dendritic cells in cancer immunotherapy: vaccines or autologous transplants? Immunol Res. 2011 Aug;50(2-3):235-47. PubMed PMID: 21717071. Pubmed Central PMCID: 3695396.

5. Sanchez-Ruiz Y, Valitutti S, Dupre L. Stepwise maturation of lytic granules during differentiation and activation of human CD8+ T lymphocytes. PloS one. 2011;6(11):e27057. PubMed PMID: 22073254. Pubmed Central PMCID: 3208563.

6. Whiteside TL. Immune responses to malignancies. The Journal of allergy and clinical immunology. 2010 Feb;125(2 Suppl 2):S272-83. PubMed PMID: 20061007. Pubmed Central PMCID: 3721350.

7. D HY, Appel S. Current status and future perspectives of dendritic cell-based cancer immunotherapy. Scandinavian journal of immunology. 2013 Aug;78(2):167-71. PubMed PMID: 23672402.

8. Butterfield LH. Dendritic cells in cancer immunotherapy clinical trials: are we making progress? Frontiers in immunology. 2013 Dec 13;4:454. PubMed PMID: 24379816. Pubmed Central PMCID: 3861778.

9. Xu H, Cao X. Dendritic cell vaccines in cancer immunotherapy: from biology to translational medicine. Frontiers of medicine. 2011 Dec;5(4):323-32. PubMed PMID: 22198743.

10. Bonifaz L, Bonnyay D, Mahnke K, Rivera M, Nussenzweig MC, Steinman RM. Efficient targeting of protein antigen to the dendritic cell receptor DEC-205 in the steady state leads to antigen presentation on major histocompatibility complex class I products and peripheral CD8+ T cell tolerance. The Journal of experimental medicine. 2002 Dec 16;196(12):1627-38. PubMed PMID: 12486105. Pubmed Central PMCID: 2196060.

11. Yanofsky VR, Mitsui H, Felsen D, Carucci JA. Understanding dendritic cells and their role in cutaneous carcinoma and cancer immunotherapy. Clin Dev Immunol. 2013;2013:624123. PubMed PMID: 23606870. Pubmed Central PMCID: 3625554.

12. De Souza Reboucas J, Esparza I, Ferrer M, Sanz ML, Irache JM, Gamazo C. Nanoparticulate adjuvants and delivery systems for allergen immunotherapy. Journal of biomedicine & biotechnology. 2012;2012:474605. PubMed PMID: 22496608. Pubmed Central PMCID: 3303624.

13. Demento S, Steenblock ER, Fahmy TM. Biomimetic approaches to modulating the T cell immune response with nano- and micro- particles. Conf Proc IEEE Eng Med Biol Soc. 2009;2009:1161-6. PubMed PMID: 19963488.

14. Hamdy S, Molavi O, Ma Z, Haddadi A, Alshamsan A, Gobti Z, et al. Co-delivery of cancer-associated antigen and Toll-like receptor 4 ligand in PLGA nanoparticles induces potent CD8+ T cell-mediated anti-tumor immunity. Vaccine. 2008 Sep 15;26(39):5046-57. PubMed PMID: 18680779.

15. Danhier F, Ansorena E, Silva JM, Coco R, Le Breton A, Preat V. PLGA-based nanoparticles: an overview of biomedical applications. Journal of controlled release : official journal of the Controlled Release Society. 2012 Jul 20;161(2):505-22. PubMed PMID: 22353619.

16. Silva AL, Rosalia RA, Sazak A, Carstens MG, Ossendorp F, Oostendorp J, et al. Optimization of encapsulation of a synthetic long peptide in PLGA nanoparticles: low-burst release is crucial for efficient CD8(+) T cell activation. European journal of pharmaceutics and biopharmaceutics : official journal of Arbeitsgemeinschaft fur Pharmazeutische Verfahrenstechnik eV. 2013 Apr;83(3):338-45. PubMed PMID: 23201055.

17. Han FY, Thurecht KJ, Whittaker AK, Smith MT. Bioerodable PLGA-Based Microparticles for Producing Sustained-Release Drug Formulations and Strategies for Improving Drug Loading. Frontiers in pharmacology. 2016;7:185. PubMed PMID: 27445821. Pubmed Central PMCID: 4923250.

18. Rice-Ficht AC, Arenas-Gamboa AM, Kahl-McDonagh MM, Ficht TA. Polymeric particles in vaccine delivery. Current opinion in microbiology. 2010 Feb;13(1):106-12. PubMed PMID: 20079678.

19. Diwan M, Elamanchili P, Lane H, Gainer A, Samuel J. Biodegradable nanoparticle mediated antigen delivery to human cord blood derived dendritic cells for induction of primary T cell responses. Journal of drug targeting. 2003;11(8-10):495-507. PubMed PMID: 15203918.

20. Raghuwanshi D, Mishra V, Suresh MR, Kaur K. A simple approach for enhanced immune response using engineered dendritic cell targeted nanoparticles. Vaccine. 2012 Nov 26;30(50):7292-9. PubMed PMID: 23022399.

21. Jahan ST, Haddadi A. Investigation and optimization of formulation parameters on preparation of targeted anti-CD205 tailored PLGA nanoparticles. Int J Nanomedicine. 2015;10:7371-84. PubMed PMID: 26677326. Pubmed Central PMCID: 4677653.

22. Corrigan OI, Li X. Quantifying drug release from PLGA nanoparticulates. European journal of pharmaceutical sciences : official journal of the European Federation for Pharmaceutical Sciences. 2009 Jun 28;37(3-4):477-85. PubMed PMID: 19379812.

23. Thamake SI, Raut SL, Ranjan AP, Gryczynski Z, Vishwanatha JK. Surface functionalization of PLGA nanoparticles by non-covalent insertion of a homo-bifunctional spacer for active targeting in cancer therapy. Nanotechnology. 2011 Jan 21;22(3):035101. PubMed PMID: 21149963.

24. Kocbek P, Obermajer N, Cegnar M, Kos J, Kristl J. Targeting cancer cells using PLGA nanoparticles surface modified with monoclonal antibody. Journal of controlled release : official journal of the Controlled Release Society. 2007 Jul 16;120(1-2):18-26. PubMed PMID: 17509712.

25. Yu ZG, Wang Q, Li K, Li YQ, Gao XX. Determination and pharmacokinetics of 6,7-dimethoxycoumarin in rat plasma after intragastric administration of different decoctions of yinchenhao tang. Journal of chromatographic science. 2007 Sep;45(8):544-8. PubMed PMID: 18019567.

26. Haddadi A, Elamanchili P, Lavasanifar A, Das S, Shapiro J, Samuel J. Delivery of rapamycin by PLGA nanoparticles enhances its suppressive activity on dendritic cells. Journal of biomedical materials research Part A. 2008 Mar 15;84(4):885-98. PubMed PMID: 17647224.

27. Hamdy S, Haddadi A, Shayeganpour A, Samuel J, Lavasanifar A. Activation of antigen-specific T cell-responses by mannan-decorated PLGA nanoparticles. Pharmaceutical research. 2011 Sep;28(9):2288-301. PubMed PMID: 21560020.

28. Bandyopadhyay A, Fine RL, Demento S, Bockenstedt LK, Fahmy TM. The impact of nanoparticle ligand density on dendritic-cell targeted vaccines. Biomaterials. 2011 Apr;32(11):3094-105. PubMed PMID: 21262534. Pubmed Central PMCID: 4570971.

29. Chen H, Gao J, Lu Y, Kou G, Zhang H, Fan L, et al. Preparation and characterization of PE38KDEL-loaded anti-HER2 nanoparticles for targeted cancer therapy. Journal of controlled release : official journal of the Controlled Release Society. 2008 Jun 24;128(3):209-16. PubMed PMID: 18450313.

30. Hamdy S, Elamanchili P, Alshamsan A, Molavi O, Satou T, Samuel J. Enhanced antigen-specific primary CD4+ and CD8+ responses by codelivery of ovalbumin and toll-like receptor ligand monophosphoryl lipid A in poly(D,L-lactic-co-glycolic acid) nanoparticles. Journal of biomedical materials research Part A. 2007 Jun 01;81(3):652-62. PubMed PMID: 17187395.

31. Ghotbi Z, Haddadi A, Hamdy S, Hung RW, Samuel J, Lavasanifar A. Active targeting of dendritic cells with mannan-decorated PLGA nanoparticles. Journal of drug targeting. 2011 May;19(4):281-92. PubMed PMID: 20590403.

32. Heo MB, Lim YT. Programmed nanoparticles for combined immunomodulation, antigen presentation and tracking of immunotherapeutic cells. Biomaterials. 2014 Jan;35(1):590-600. PubMed PMID: 24125775.

33. Sarti F, Perera G, Hintzen F, Kotti K, Karageorgiou V, Kammona O, et al. In vivo evidence of oral vaccination with PLGA nanoparticles containing the immunostimulant monophosphoryl lipid A. Biomaterials. 2011 Jun;32(16):4052-7. PubMed PMID: 21377204.

34. Zhu L, Chen L, Cao QR, Chen D, Cui J. Preparation and evaluation of mannose receptor mediated macrophage targeting delivery system. Journal of controlled release : official journal of the Controlled Release Society. 2011 Nov 30;152 Suppl 1:e190-1. PubMed PMID: 22195844.

35. Haddadi A, Hamdy S, Ghotbi Z, Samuel J, Lavasanifar A. Immunoadjuvant activity of the nanoparticles' surface modified with mannan. Nanotechnology. 2014 Sep 05;25(35):355101. PubMed PMID: 25119543.

36. Solbrig CM, Saucier-Sawyer JK, Cody V, Saltzman WM, Hanlon DJ. Polymer nanoparticles for immunotherapy from encapsulated tumor-associated antigens and whole tumor cells. Molecular pharmaceutics. 2007 Jan-Feb;4(1):47-57. PubMed PMID: 17217312.

37. Heo MB, Cho MY, Lim YT. Polymer nanoparticles for enhanced immune response: combined delivery of tumor antigen and small interference RNA for immunosuppressive gene to dendritic cells. Acta biomaterialia. 2014 May;10(5):2169-76. PubMed PMID: 24394635.

38. Hamdy S, Haddadi A, Somayaji V, Ruan D, Samuel J. Pharmaceutical analysis of synthetic lipid A-based vaccine adjuvants in poly (D,L-lactic-co-glycolic acid) nanoparticle formulations. Journal of pharmaceutical and biomedical analysis. 2007 Aug 15;44(4):914-23. PubMed PMID: 17590559.

39. Bao X, Gao M, Xu H, Liu KX, Zhang CH, Jiang N, et al. A novel oleanolic acid-loaded PLGA-TPGS nanoparticle for liver cancer treatment. Drug development and industrial pharmacy. 2015;41(7):1193-203. PubMed PMID: 25026246.

40. Win KY, Feng SS. Effects of particle size and surface coating on cellular uptake of polymeric nanoparticles for oral delivery of anticancer drugs. Biomaterials. 2005 May;26(15):2713-22. PubMed PMID: 15585275.

41. Cruz LJ, Tacken PJ, Fokkink R, Figdor CG. The influence of PEG chain length and targeting moiety on antibody-mediated delivery of nanoparticle vaccines to human dendritic cells. Biomaterials. 2011 Oct;32(28):6791-803. PubMed PMID: 21724247.

42. Dinarvand R, Sepehri N, Manoochehri S, Rouhani H, Atyabi F. Polylactide-co-glycolide nanoparticles for controlled delivery of anticancer agents. Int J Nanomedicine. 2011;6:877-95. PubMed PMID: 21720501. Pubmed Central PMCID: 3124394.

43. Makadia HK, Siegel SJ. Poly Lactic-co-Glycolic Acid (PLGA) as Biodegradable Controlled Drug Delivery Carrier. Polymers. 2011 Sep 01;3(3):1377-97. PubMed PMID: 22577513. Pubmed Central PMCID: 3347861.

44. Slutter B, Bal S, Keijzer C, Mallants R, Hagenaars N, Que I, et al. Nasal vaccination with N-trimethyl chitosan and PLGA based nanoparticles: nanoparticle characteristics determine quality and strength of the antibody response in mice against the encapsulated antigen. Vaccine. 2010 Aug 31;28(38):6282-91. PubMed PMID: 20638455.

45. Kumar A, Wonganan P, Sandoval MA, Li X, Zhu S, Cui Z. Microneedle-mediated transcutaneous immunization with plasmid DNA coated on cationic PLGA nanoparticles. Journal of controlled release : official journal of the Controlled Release Society. 2012 Oct 28;163(2):230-9. PubMed PMID: 22921518. Pubmed Central PMCID: 3478475.

46. Mukherjee B, Santra K, Pattnaik G, Ghosh S. Preparation, characterization and in-vitro evaluation of sustained release protein-loaded nanoparticles based on biodegradable polymers. Int J Nanomedicine. 2008;3(4):487-96. PubMed PMID: 19337417. Pubmed Central PMCID: 2636584.

47. Wu F, Jin T. Polymer-based sustained-release dosage forms for protein drugs, challenges, and recent advances. AAPS PharmSciTech. 2008;9(4):1218-29. PubMed PMID: 19085110. Pubmed Central PMCID: 2628253.

48. Alshamsan A, Haddadi A, Hamdy S, Samuel J, El-Kadi AO, Uludag H, et al. STAT3 silencing in dendritic cells by siRNA polyplexes encapsulated in PLGA nanoparticles for the modulation of anticancer immune response. Molecular pharmaceutics. 2010 Oct 04;7(5):1643-54. PubMed PMID: 20804176.

49. Kaka AS, Foster AE, Weiss HL, Rooney CM, Leen AM. Using dendritic cell maturation and IL-12 producing capacity as markers of function: a cautionary tale. Journal of immunotherapy. 2008 May;31(4):359-69. PubMed PMID: 18391760. Pubmed Central PMCID: 2744357.

50. Krishnamachari Y, Geary SM, Lemke CD, Salem AK. Nanoparticle delivery systems in cancer vaccines. Pharmaceutical research. 2011 Feb;28(2):215-36. PubMed PMID: 20721603. Pubmed Central PMCID: 3559243.

51. Langenkamp A, Messi M, Lanzavecchia A, Sallusto F. Kinetics of dendritic cell activation: impact on priming of TH1, TH2 and nonpolarized T cells. Nature immunology. 2000 Oct;1(4):311-6. PubMed PMID: 11017102.

52. Demento SL, Bonafe N, Cui W, Kaech SM, Caplan MJ, Fikrig E, et al. TLR9-targeted biodegradable nanoparticles as immunization vectors protect against West Nile encephalitis. Journal of immunology. 2010 Sep 01;185(5):2989-97. PubMed PMID: 20660705. Pubmed Central PMCID: 3753007.

53. Mahnke K, Schmitt E, Bonifaz L, Enk AH, Jonuleit H. Immature, but not inactive: the tolerogenic function of immature dendritic cells. Immunology and cell biology. 2002 Oct;80(5):477-83. PubMed PMID: 12225384.

# CHAPTER 5

## 5. Potentiating antigen specific immune response by targeted delivery of PLGA based model cancer vaccine

Sheikh Tasnim Jahan, Sams M. A. Sadat, and Azita Haddadi[3]

Division of Pharmacy, College of Pharmacy and Nutrition, University of Saskatchewan, Saskatoon, SK S7N 5E5, Canada

[3] Corresponding Author: Azita Haddadi
3D01.01, D Wing Health Sciences, 107 Wiggins Road, College of Pharmacy and Nutrition, University of Saskatchewan, Saskatoon SK, S7N 5E5; Phone: (306) 966-6495; Fax: (306) 966-6377; e-mail: azita.haddadi@usask.ca

## 5.1 Brief introduction to chapter 5

This chapter is mainly focused on evaluation of immune stimulatory response of the developed model vaccine. The experiments included are assessment of structural integrity of OVA for 20 days, vaccination of WT balb/c mice, isolation of T cells, *in-vitro* co-culture experiments, flow cytometry experiments to assess T cell proliferation, estimation of cytokines, determination of IgG levels, vaccination of OT1 mice, CTL (CD8) proliferation study and estimation of cytokine secretions.

Formulations were developed by emulsification solvent evaporation method. The polymer that was selected for animal experiments was 0.18iv COOH terminated PLGA. Several formulations were developed and characterized in terms of their particle size, zeta potential, PDI, loading of OVA and EE. Several groups were included in the mice vaccination study. The dose-response relationship was established based on the results obtained from chapter 4. The animal experiments were conducted with OT1 mice to assess their ability to produce CTLs necessary to destroy antigens.

In conclusion, the presence of MPLA is necessary to augment dynamic response to produce CTLs to destroy the cancer antigens and produce memory T cells prevent further relapse. The MPLA-OVA encapsulated targeted PLGA nanoparticles stands out as a promising model delivery system to provide clinical benefits.

## 5.2 Abstract

Targeted delivery of therapeutics has the potential to localize the therapeutic agent to a target tissue with no side-effects. This article aims in developing a model targeted immunotherapeutic approach that will harness effective T cell response. Here, we investigated how ovalbumin (OVA) loaded targeted PLGA nanoparticle (NP) formulation impacted antigen-adjuvant exposure to the immune system. The NPs were prepared by double emulsification solvent evaporation technique. The anti-CD-205 targeted formulations were obtained either through physical adsorption or covalent conjugation method. The structural integrity of OVA was confirmed by circular dichroism spectroscopy. Our results indicated that the combined formulation induced more powerful responses than each single component formulation. Wild type (WT) balb/c mice immunized with the targeted PLGA NPs encapsulated with OVA-MPLA induced antigen-specific IgG antibodies with high avidity, increased secretion of cytokines and generation of memory T cells. OVA specific T cell receptor (TCR) transgenic OT1 mice showed highest production of cytotoxic T cells (CTLs) and increased secretion of cytokines upon immunization with the targeted OVA-MPLA formulations. This enhanced response might be attributed to OVA depot effect at the subcutaneous site of injection and effective induction of dendritic cells (DCs) activation and helper T (Th) cell differentiation in the lymph nodes. Therefore, the PLGA based vaccine delivery system would have significant implications for rational vaccine design.

**Keywords:** Nanoparticle, Ovalbumin, MPLA, vaccine, anti-CD205, PLGA

## 5.3 Introduction

The idea of using patient's immune system has advanced in clinical field only in the last decade. These recent advances highlight the role of immunosuppressive microenvironment in tumor progression. This active immunotherapy depend on patient's immune system to recognize and destroy intended target.(1) The ability to show an immune response upon reinfection is the foundation of vaccination. The immune response is mediated by antigen specific memory T cells that can generate faster than naïve T cells.(2)

The evolution of DC-based vaccine is promising in terms of restoring the capability of DCs to recognize non-self antigens. Since now, Provenge (Dendreon Corp.) is the FDA approved only cancer vaccine in market.(3) However, intricacies are not limited to DC subset, tumor antigens, antigen loading and route of administration. The *ex-vivo* generated DC vaccines have some pitfalls which guides towards *in-vivo* manipulated vaccines. Though, there is question regarding the targeting specificity and efficiency of these strategies, there are several advantages that approves the logistics of vaccine preparation for future.(4)

Nowadays, targeted cancer vaccine utilizing an unique antigen shared by various cancer can be a strategy to elicit maximum coverage.(5) The strategy to load DCs with antigens and adjuvants using particulate delivery system is gaining tremendous popularity due to several advantages. It maintains the controlled arrival of antigen-adjuvant to the antigen presenting cells (APCs) to be presented on the major histocompatibility complex (MHC) molecules. Lastly, the extensive groundwork essential for tailor-made vaccine can be minimized using cost-effective, large scale production of *in-vivo* vaccines for large number of patients.(6)

Adjuvant is a key component of ideal particulate vaccines. Modern vaccines can produce optimum immune response in presence of adjuvant through their combined diversity.(7) Among all the adjuvants, TLRs agonists have gained attention as it can be displayed on DCs. In addition, a ligand binding to this receptor can efficiently facilitate antigen processing, presentation as well as DC maturation.(8) Among the TLR agonists, MPLA have gained popularity due to its less toxicity than lipopolysaccharide (LPS). MPLA, a modified synthetic derivative of LPS has been shown to promote T helper (Th) cell-1 influenced antigen specific response and used in therapeutic vaccines for several types of diseases.

Codelivery of OVA and MPLA will trigger the TLR pathway to generate mature DCs for inducing primary T cell response. The induction of T cell responses is an important aim of vaccination.(9)

FDA approved poly (D, L-lactic-co-glycolic-acid) (PLGA) are tested delivery vehicles that can increase the immunogenicity of the incorporated vaccine antigens/adjuvants.(10) The present research highlights the use of OVA-MPLA loaded in PLGA NPs used as a delivery system.(11) The formulations were modified using CD-205 targeting ligand for the CD-205 receptors on DCs. This active targeting strategy can induce higher humoral and cellular immune responses. The activation of T cells by PLGA NPs is represented in figure 5.1. Consistent with other studies, these targeted NPs were able to produce strong immune responses upon immunization to mice model.(12), (13) In particular, the CD8+ T cell activation will be monitored. Activated CD8+T cells can kill the malignant cells and acquire long-lasting memory preventing relapses.(14)

The purpose of this research was to investigate the use of PLGA NPs as a vaccine delivery system to codeliver antigen along with MPLA for induction of potent T cell responses. The physicochemical properties will be linked with the biological effects to formulate the cancer vaccine.(15) First, physicochemical properties of 0.18 i.v. (or iv) COOH terminated PLGA NPs will be discussed. Based on previous *in-vitro* experiments on various types of PLGA viscosities (low and high) and end groups (ester/COOH), the most optimized delivery vehicle was selected. Subsequently, the antigen specific immune response was evaluated in WT balb/c mice. Assessment of T cell proliferation, serum IgG level and cytokine secretion profile was performed following vaccination of WT mice. Finally, immune response of TCR transgenic OT-1 mice derived CD8 T cell upon nano-vaccine delivery system was evaluated. All these experimental approaches allow us to establish a NP-dose response relationship which could be mimicked to explore novel cancer vaccines in future.

## 5.4 Materials and methods

### 5.4.1 Materials

MPLA (molecular weight 1763.469 Da) was purchased from Avanti Polar Lipids Inc. (Alabama, USA). COOH terminated PLGA 50:50 (iv 0.18 dl/g and 0.55-0.75 dl/g) were purchased from Lactel, Absorbable

Polymers (Birmingham, AL, USA). Polyvinyl alcohol (PVA), bis (sulfo-succinimidyl) suberate (BS3), ovalbumin from chicken egg white (grade V), alpha minimum essential medium, fetal bovine serum (FBS) and bicinchoninic acid (BCA) assay kit was purchased from Sigma-Aldrich Co. (St Louis, MO, USA). Biotin anti-mouse CD205 monoclonal Ab (MAb) was purchased from Biolegend (San Diego, CA, USA). JAWSII dendritic cell line was obtained from American Type Culture Collection (ATCC), Manassas, VA, USA. Granulocyte-macrophage colony stimulating factor (GM-CSF) was purchased from Thermo Fischer Scientific (Waltham, MA, USA). CellTrace Carboxyfluorescein succinimidyl ester (CFSE) cell proliferation kit was purchased from molecular probes (Eugene, OR, United States). Anti-mouse CD16/CD32 MAb (Fc blocker), TNF-α ELISA kits and PEcy5 CD3 molecular complex were purchased from BD Biosciences (San Jose, CA, USA). Easysep CD3 and CD8 cell isolation kit was purchased from Stemcell technologies (Vancouver, BC, Canada). Endofit ovalbumin and SIINFEKL peptide was from InvivoGen (San Diego, CA, USA). Keyhole limpet hemocyanin (KLH) was purchased from EMD Millipore (ON, Canada). Murine IFNγ, IL-2 and IL-6 ELISA kits were purchased from eBioscience (San Diego, CA, USA). Reserve-AP Anti-Mouse IgG (H+L) Antibody, Human Serum Adsorbed and Phosphatase labeled was purchased from KPL Inc. (Gaithersburg, MD, USA). All other reagents such as ethyl acetate, methanol, sodium hydroxide (NaOH), sodium dodecyl sulfate (SDS) were of analytical grade.

**5.4.2 Preparation, surface modification and quantification of OVA loaded NPs**

PLGA NPs encapsulated with OVA and/or MPLA were prepared by water/oil/water double emulsification solvent evaporation method as mentioned elsewhere.(16) Briefly, 10 mg OVA of was dissolved in100 µl PBS and added to the polymer-solvent solution. For the formulations with MPLA, 200 µg of MPLA was dissolved in 1:4 methanol-chloroform mixture was added to the polymer-solvent mixture. The resulting mixture was then emulsified in 2.2% of PVA to form a secondary emulsion. The NPs were collected after 2 hours of stirring followed by centrifugation. Finally, the NPs were freeze-dried and stored for further use. (17) Surface modification of NPs was performed through physical adsorption

and covalent binding process as mentioned previously.(18) The amount of OVA in NP formulations was quantified using BCA assay.(19)

### 5.4.3 Assessment of structural integrity of OVA in the NP by circular dichroism (CD)

CD spectra were recorded using Chirascan Plus CD Spectrometer (Applied Photophysics, Leatherhead, Surrey, UK) to assess the structural integrity of OVA in NPs. CD data were collected from 197 to 280 nm at a scan time of 0.5 second per point (total time per sample is 4 minutes) at 20°C using a 1mm quartz cuvette. Data were averaged over 3 scans and expressed as millidegrees. Baseline was corrected for every sample before acquiring data. OVA solution in phosphate buffered saline (PBS) was used as the reference. OVA samples were collected after 20 days of incubation in PBS. The percentage of alpha-helix, anti-parallel and parallel beta sheet, beta-turn and random coil of the secondary structure of OVA was estimated by CDNN software. The recorded CD spectra and the deconvolution results of the samples were compared to those of the standard to evaluate changes in the secondary structure of the OVA samples.(20)

### 5.4.4 Animal experiments

#### 5.4.1.1 Mouse model

WT mice (balb/c) were purchased from the Charles River International (St-onstant, Quebec, Canada). TCR transgenic OT1 mice (background C57bl/6) were purchased from Charles River International (Domain des Oncins, Germain Nuelles, France). All experiments were performed in accordance to the University of Saskatcheewan guidelines for the care and use of laboratory animals (protocol # 20140073). All experiments were performed using 8–16 week old female mice.

#### 5.4.1.2 Isolation and culture of murine bone marrow-derived DCs (BM-DCs)

Primary DC were generated from murine BM-precursors from femur of mice. Briefly, femurs of mice (balb/c for WT and C57BL/6 for OT1) were removed and cleaned from surrounding tissues. For disinfection, intact bones were put in 70 % ethanol for 2 minutes and washed with Hank's balanced salt

solution (HBSS). Later, both ends of the bone was cut with a sterile scissor and the BM was flushed from intact bones with PBS using an syringe. Cells were triturated, filtered (by 40 μm cell strainer) and collected in a 15-ml centrifuge tube. The single-cell suspension was obtained after subsequent washes with DC complete media (RPMI-1640 with L-glutamine and Gentamycin) supplemented with 20 ng/mL of GM-CSF and 10 % heat-inactivated FBS. On day 3, 10 mL of fresh DC media containing 20 ng/mL GM-CSF was added. At day 6, culture media was replaced by fresh media containing 20 ng of GM-CSF. At day 7, BM-DCs were ready for co-culture with T cells. The purity of the DCs were about 85 % based on the expression of CD11c. The viabilty of the cells were about 90-95 % on day 7.(21)

**5.4.1.3 Mouse vaccination experiment**

WT balb/c mice (5 mice/group) were subcutaneously vaccinated in the right flank region with specific amount of NPs. Fourteen days later all mice received similar booster dose of immunization. Seven days after the second immunization, draining lymph nodes and spleens were isolated to perform the co-culture experiment for ELISA and flow cytometry. CD3+T cells were isolated as suggested by the manufacturer. Blood was collected by cardio-puncture after 21 days after priming. Sera isolated by centrifuge were stored at -20$^0$C for analysis. OVA-specific total IgG was measured by ELISA.(22) The animal groups for the experiments were unimmunized mice (collected T cells served as APC), free OVA, free OVMP, OV-NP, OV-MP NP, Ab-modified OVA-NP and Ab-modified OVA-MPLA treated mice for 0.18 COOH terminated NP, respectively.

OT1 mice (4 mice/group) were also vaccinated in the comparable manner. Spleens and lymph nodes were collected and processed as required. CD8+T cells were isolated as described in the manufacturer's protocol. The groups were control group-no treatment, free OVA, free OVMP, OV-BS-NP, OV-AD NP, OV-COV-NP, OVMP-BS NP, OVMP-AD NP and OVMP-COV NP.

#### 5.4.1.4 Preparation of single cell suspension of the mouse splenocytes

T cells were isolated from mice spleen after following several steps. Briefly, mouse was sacrified to collect the spleen in sterile condition. The washed spleen was minced through 70 µm pore size strainer. The collected cell suspension was washed with RPMI, 1% antibiotic, 2% glutamine and 10 % FBS containing complete RPMI media. The red blood cells were lysed with lysis buffer for 5 minutes. After that, the cell suspension washed twice and counted. Isolation of CD3+ and CD8+ positive cells were performed by negative selection method using the Easysep cell isolation kit as per manufacturer's protocol.(23)

#### 5.4.1.5 T cell proliferation assay using CFSE method

The T cells were stained with CFSE to assess the proliferation through dye-dilution. In brief, the T cells were isolated from splenocytes and labeled with CFSE at a concentration of 2.5 µM. The reaction was quenched by adding FBS to the cell suspension. Followed by two washes, the cell count was set to $1X10^6$/ml. 100 µl of T cells (responders) and 100 µl irradiated (700 rad) DCs stimulators were co-cultured in 96-well plates. The number of T cells per well was kept constant ($1X10^5$ T cells); DC:T cell ratio was thus either 1:4 and 1:10. For WT mice, several other ratios (data not shown) were evaluated, although 1:4 ratio showed the best fit. For OT1 mice, results with 1:4 ratio is mentioned in the result section. For each groups, DCs were plated in two different numbers ($25\ X10^3$ and $10\ X10^3$).(24) FOr WT mouse, different DC:T cell co-culture were then pulsed with either 20 µM Ovaendofit (CD3 test protein) and 20 µM of KLH (irrelevant antigen). For OT1 mouse, DC:T coculture was restimulated with 1 µM of $OVA_{257–264}$ epitope (SIINFEKL, CD8 test peptide) or 1 µM of KLH (irrelevant antigen). Five days after co-culture in 96-well plates, the cells were harvested, stained with respective antibody (CD3 or CD8) to determine the CFSE labeled T cell divisions by flow cytometry. Data were further analysed using Flowjo software, version 7.6.5 (Ashland, OR, USA).(25)

#### 5.4.1.6 Determination of total IgG

OVA-specific IgG in the serum were quantitatively determined by enzyme-linked immunosorbent assay (ELISA) as mentioned elsewhere.(26) Briefly, U-bottom 96 well plates were coated with 10 µg/ml of OVA followed by incubation at $4^0$C overnight. The next day, plates were washed with PBST (PBS containing 0.05% of Tween 20) and blocked by incubating with 1 % (m/ v) BSA for 1 hour at $37^0$C. After washing with PBST, 100 µl of appropriate sera dilutions were added to each well and incubated overnight at $4^0$C. Next day, plates were washed and incubated with goat anti-mouse IgG (H+L)-alkaline phosphatase at 100 µl/well for 2 hours at $37^0$C. Thereafter, the plates were washed again with PBST, and 100 µl of PNPP substrate was added to each well and incubated for 20 minutes at room temperature. The optical density was measured at 405nm (background 490nm) by microplate reader linked with UV spectrophotometer (Biotek, VT, USA).

#### 5.4.1.7 Determination of cytokine levels by ELISA

The supernatants from the co-culture was collected and stored at -20°C for analysis of the level of IL-2, IL-6, IFNγ and TNF-α using commercially available enzyme-linked immunosorbent assay (ELISA) kits in a 96-well microplate using a microplate reader at 405 nm (background 490 nm) according to manufacturer's directions.(27) The minimum detection levels of the cytokines were 3, 4, 15, and 15 pg/ml for IL-2, IL-6, IFNγ, and TNF-α, respectively.

#### 5.4.1.8 Statistical analysis

The data are given as mean ± SD and statistical significance was determined by Student's t-test. Values of $p < 0.05$ were considered statistically significant unless specifically mentioned. All data were analyzed using GraphPad Prism 5.03 software (GraphPad Software, Inc., La Jolla, CA, USA). Flow cytometry experiments were analyzed using Flowjo 7.6.5 software.

## 5.5 Results

### 5.5.1 Characterization of NPs

The 0.18 iv PLGA NPs prepared by the double emulsification solvent evaporation technique, had a narrow size distribution as represented in figure 5.2 (A-D). The mean size of plain OV-NP and OVMP-NP was within 141 ± 2 nm and 156 ± 7 nm, respectively. Modified NPs were larger, due to the presence of encapsulated anti-CD-205 antibody. The size for OV-Ab-NP and OVMP-Ab-NPs was within 401 ± 1 nm and 413 ± 6 nm, respectively. The incorporation of Ab in the NPs leads to a reduced surface charge of 3.13 ± 0.11 mV compared to plain NPs with -27.1 ± 0.77 mV. The antigen loading of plain and modified OV-NPs and OVMP-NPs was ranged from 39.01 ± 0.56 to 65.42 ± 2.90 μg/mg of NPs.(27)

### 5.5.2 Confirmation of structural integrity of OVA in NPs

Secondary structural stability was analyzed by CD spectra of 0.18 COOH terminated PLGA NPs as represented in figure 5.3A and 5.3B. Figure 5.3B represents the percentages of α-helix, β-anti-parallel, β-parallel, β-turn and random coil of the secondary structure present in free OVA, OV-NP, OV-COV-NP and OVMP-COV-NP samples. The results demonstrate that the release process within 20 days had no significant effect (p-value > 0.05) on the structural integrity of OVA when compared with the standard solution.

### 5.5.3 *In-vitro* CD3+ T cell proliferation post-vaccination

To examine the effect of NPs on T cell proliferation, CFSE dilution in OVA-specific T cells was analyzed after co-incubation with DCs for four days. Cell division and the percentage of cells having diluted fluorescent intensity was analyzed using Flowjo software as mentioned in figure 5.4A.(28) When restimulated with relevant Ovaendofit protein, 0.18C-OVMP-AD NPs led to a substantially high increase in the number of T cells undergoing division (96 %). In contrast, non-targeted 0.18C-OVMP NPs could induce only 87.5 % of T cell division. We observed only 41.7 % and 38 % of T cell divisions for plain 0.18C-OV NPs and 0.18C-OV-AD NPs, respectively. Besides, T cells obtained from unimmunized mice

showed 0.54 % of proliferated T cells. In contrast, presence of KLH or absence of restimulation showed low percentages of cell divisions. Figure 5.4B (a-c) represents the bar diagrams for 0.18C-OVMP-AD NPs demonstrating the generations of cell divisions in presence of Ovaendofit, KLH and no restimulation.

### 5.5.4 *In-vitro* secretion of cytokines from WT balb/c mice derived CD3 T cells and DCs

Cytokines that are mostly produced by responder T cells in presence of irradiated DCs are IFNγ, IL-2, IL-6 and TNF-α (figure 5.5A-5L).(28) Among seven groups (unimmunized mice, free OVA, free OVMP, 0.18C-OV NP, 0.18C-OV-AD NP, 0.18C-OVMP NP, O.18C-OVMP-AD NP), there was significantly high ($p<0.05$) amount of cytokines secreted by 0.18C-OVMP-AD NPs upon restimulation with OVA-relevant protein when compared with the unimmunized mice group. The amount secreted by this formulation was such as, IFNγ (12943.31 ± 325 pg/ml), IL-2 (1294.22 ± 16.78 pg/ml), IL-6 (1299.66 ± 137.77 pg/ml) and TNF-α (4566.21 ± 341.11 pg/ml). Presence of MPLA in the formulation had significant impact on secretion of all four cytokines.

### 5.5.5 Estimation of total IgG

After 21 days of vaccination, the serum total IgG was observed as mentioned in figure 5.6. Compared to free OVA, all the groups produced significantly high amount of anti-OVA IgG titers ($p<0.05$). There was significant difference in IgG titer among the groups: free OVMP, 0.18C-OV NP, 0.18C-OV-AD NP, 0.18C-OVMP NP, O.18C-OVMP-AD NP. Mice treated with 0.18C-OVMP-AD NP serum had highest OVA-specific IgG antibodies. This confirms that the increase in humoral immune response by this group could be due to presence of both OVA and MPLA in the targeted PLGA NPs.(29)

### 5.5.6 *In-vitro CD8+ T cell proliferation post-vaccination*

Figure 5.7 (A-C) represents the CTL cell proliferation assay from mice in the vaccination study.(30) Compared to unimmunized, free OVA and free OVMP vaccinated mice groups, there is significantly higher percentage of CFSE+CD8+ T cells in the NP groups (plain and modified) ($p<0.05$) (figure 5.7A). In presence of recall peptide SIINFEKL, the CD-205 targeted 0.18C-OVMP-AD NPs showed 98 % of divided CTLs in contrast to 0.18C-OVMP-COV NPs (88.9 %) (figure 5A). This is higher than the non-

targeted formulations (61 %), but there is no significant difference between the AD-NP and COV-NP groups ($p<0.05$). Both of these targted NPs showed antigen specific proliferation of CD8+ T cells, whereas restimulation with KLH showed most of the divisions limited upto generation 2 (figure 5.7B and 5.7C). Similar trend was observed when there was no restimulation.

### 5.5.7 *In-vitro* secretion of cytokines from OT1 mice derived CD8 T cells and DCs

After 5 days of restimulation, cytokines were quantified by ELISA as represented in figure 5.8 (A-L). Upon restimulation with relevant peptide SIINFEKL, 0.18C-OVMP-COV NP induced the highest amount of Th1 cytokine IL-2 (1898.94 ± 111.11 pg/ml) which is significantly different from other groups except 0.18C-OVMP-COV NPs (figure 5.8D) ($p<0.05$). Similar trend was observed for IFNγ and IL-6 secretion by 0.18C-OVMP-AD NPs upon SIINFEKL restimulation ($p<0.05$). Moreover, the highest level of TNF-α was induced by 0.18C-OVMP-AD NPs. There was significant difference in TNF-α secretion between 0.18C-OVMP-COV NP and 0.18C-OVMP-AD NP (3862.19 ± 48.12 pg/ml vs. 2795.19 pg/ml) ($p<0.05$). In contrast, in presence of restimulation with KLH and absence of restimulation, the level of all four cytokine secretions was significantly low ($p<0.05$). The levels of targeted formulation conjugated with TLR ligand was significantly higher than that of non-targeted or targeted formulations ($p<0.05$). (31)

## 5.6 Discussion

In this study, we analyzed the functionality of T cells by immunization with PLGA NP encapsulated with model antigen OVA, immune stimulatory MPLA and targeting moiety (anti-CD205 Ab). This trio-combined PLGA NPs showed enhanced antigen presentation (mentioned in previous paper) by DCs, proliferation of OVA-specific CD8+ T cells and high production of type 1 cytokines. This PLGA based vaccine delivery sytem is promising due to its own properties.(32)

The physicochemical properties of the model vaccine ensured batch to batch reproducibility. The small differences in size between different formulations demonstrated consistency of the method of preparation. The narrow size distribution (PDI: 0.22 ± 0.89 to 0.39 ± 0.06) along with particle size below 500 nm is indicative of immunogenicity of particles. Several sttudies on NPs have relvealed that size factor is not the only reason for the immunogenicity.(33)

A series of CD spectra measurements were performed to examine the secondary structure of OVA in the plain and modified OVA loaded PLGA NP samples. All samples indicate a high content of α-helix structure in proteins found in far-UV region between 208 to 222 nm.(34) The spectrum for Ab-modified groups showed that even after 20 days there was minimal change in the secondary structure of protein. The differences in the height of the spectral valleys are due to differences in concentrations of the OVA formulations. Therefore, the relative proportions of the secondary structures of the OVA in NP samples were comparable to standard (free) OVA. This indirectly confirms the application of OVA-NPs for biological models.(20)

T cells were labelled with CFSE to track its offspring that are divided with half the number of carboxyfluorescein labelled molecules. Each cell division can be then tracked by subsequent decrease in fluorescence by flow cytometry.(35) The proliferation of overall T cells showed OVA specific increase in cell divisions which is pronounced with targeted formulation containing both antigen and adjuvant. In addition, T cells obtained after vaccination of WT mice with targeted PLGA NP loaded with OVA-MPLA when exposed to DCs produced significantly high quantity of cytokines. The effect of restimulation was pronounced in presence of Ovaendo, not KLH, which confirms the antigen specific response *in-vitro*. Besides, the targeted formulation (0.18C-OVMP-AD NP) effectively induced significantly highest level of humoral response compared to other groups. Therefore, subcutaneous application of NP vaccination dose induced proliferation of T cells accompanied by elevated levels of OVA-specific cytokine secretion as well as total IgG antibodies.(36)

It is speculated that the antigen loaded particles possess an inherent capacity to drive CTL proliferation.(37, 38) We immunized OT1 mice twice to induce the activation of endogenous SIINFEKL-specific T cells. Thus, the proliferation of antigen specific T cells was increased post vaccination. Compared with the PBS group, vaccination with targeted OVMP-NPs significantly increased the percentages of OVA specific $CD8^+$ T cells as measured due to the restimulation with $OVA_{257–264}$ (SIINFEKL) in the context of MHCI.(25) There was a trend for increased OVA-specific $CD8^+$ T cell responses in the OVMP-NP group, compared to free OVA and free OVMP. It is expected that OVA alone

in the absence of MPLA, does not elicit adequate T cell activation and formation of cytotoxic T cells as found with OV-NPs. The evaluation of cytokines produced in the co-culture indicated a strong bias towards Th1 phenotype, characterized by high level of IFNγ production in both WT and OT1 mice.(39) Most tumor associated antigens are intracellular proteins, which bind with newly synthesized MHCI molecules and shuttled to the cell surface for recognition by T cells. Thus, to be an effective vaccine, cell mediated immunity, particularly production of CTLs are most important. These CTLs can show cytotoxicity, secrete effector cytokines; such as IFNγ and TNF-α, which can mediate local inflammation.(40) The DC targeting vaccines utilizes this unique ability to stimulate CTLs to response to kill cancerous cells. However, a balance should be maintained between proper maturation signal and activating CTLs with adequate production of IL-2.(41)

The outcomes confirm the validity of all *in-vitro* results as well as the usefulness of PLGA as the vaccine carrier. The overall formulation process is a guideline to reduce the number of components used in traditional vaccines. However, the efficiency of the vaccination depends on effective antigen presentation to T cells. Inclusion of adjuvants together with antigen in the NPs leads to increased stimulation of APCs as it matures to process the antigen for T cell activation.(42) Largely, the vaccination with targeted NPs containing adjuvant enhanced both B and T cell immune responses.(43)

**5.7 Conclusion**

We successfully generated OVA-MPLA loaded PLGA NPs as a new vaccine carrier system and characterized them *in-vitro*. Using WT balb/c and OT1 mice models for antigen-specific T cell activation, we showed that OVA-loaded PLGA-based NPs activated T cell and increases antigen specific T cell proliferation. Furthermore we observed the generation of CD8 T cells *in-vitro* specifically for targeted OVA-MPLA formulations. Covalently modified formulations showed higher percentages of proliferations compared to the Ab-adsorbed formulations. The results attributed that PLGA NPs protected the NPs *in-vivo* and showed both cellular and humoral response. In total, targeted formulations loaded with adjuvant-antigen is a suitable model for future vaccine formulations. Specifically, these NPs may serve as carrier for cancer-derived antigens in order to improve tumor-specific immunity. Further

experiments need to address when disease specific antigens will be incorporated in the PLGA NPs to achieve the success of vaccination in a therapeutic setting. In designing a vaccine, several facts should be taken in consideration to break the chance of irreversible autoimmunity. Nevertheless, the DC immunobiology and formulation parameters that influence the immune response will evolve; it is understandable that particulate based delivery systems will become a reality in future.

### 5.8 Acknowledgments

This project was supported by research grant from Natural Sciences and Engineering Research (NSERC). The authors thank College of and Nutrition, University of Saskatchewan for providing the facility of flow cytometer. The authors wish to thank Mark Boyd for assisting with flow cytometry. The authors also thank Mehran Yarahmadi for helping with animal handling and experiments.

### 5.9 Conflict of interest

The author(s) disclose that this article content has no conflict of interest.

## 5.10 FIGURES

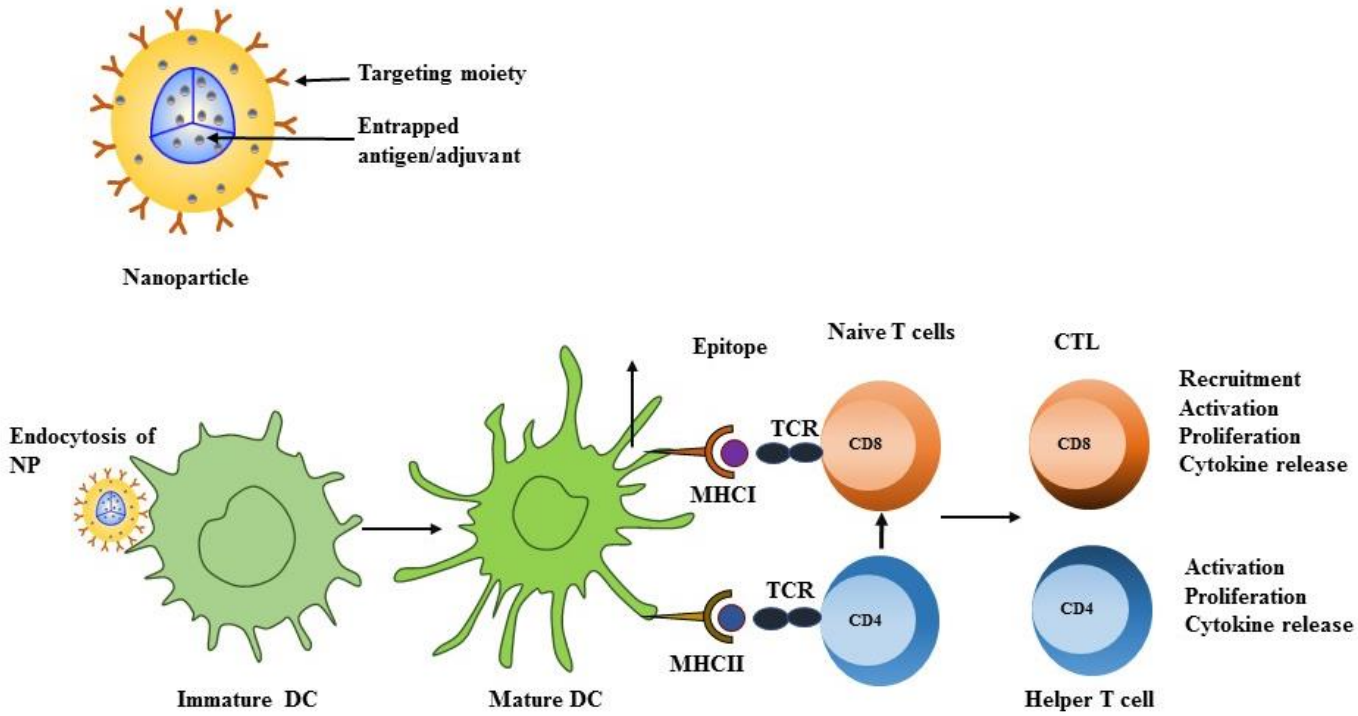


**Figure 5.1.** Activation of T cells by PLGA NP based cancer vaccine.

**Abbreviations:** DC, dendritic cell, PLGA, poly (D, L-lactide co-glycolide), TCR, T cell receptor, MHC, Major histocompatibility complex, CTL, cytotoxic T lymphocyte, NP=Nanoparticle.

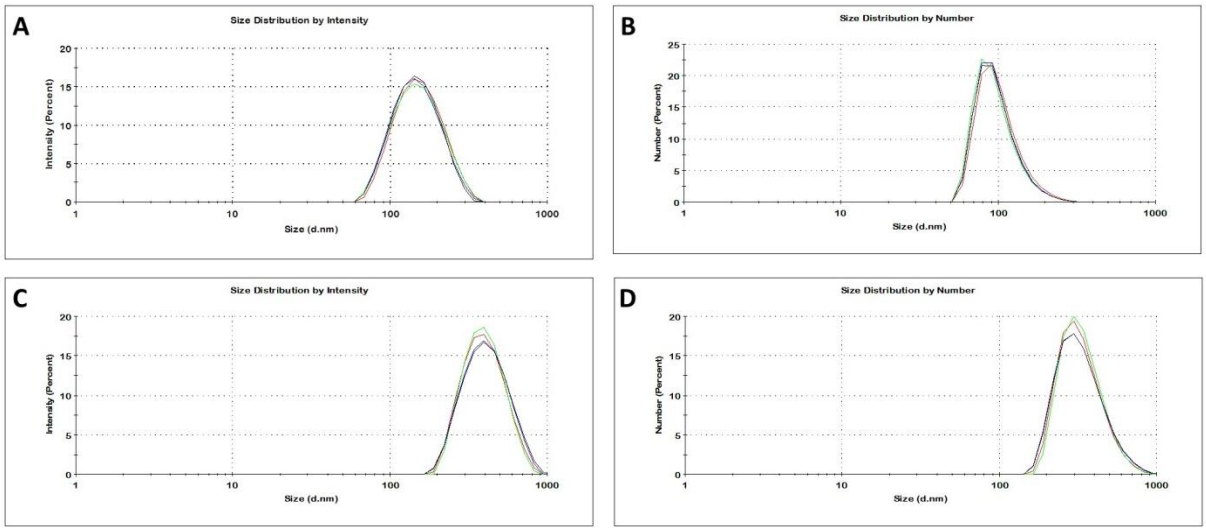


**Figure 5.2**. Representative size distribution curve for particle size. (A) and (B) are size distribution curve by intensity and number, respectively for plain OVMP-NP. (C) and (D) are size distribution curve by intensity and number, respectively for modified (COV)-OVMP-NP.

**Notes**: Particle size is measured by Malvern zetasizer nanoseries by DLS technique. Size is represented as d.nm (d=diameter).

**Abbreviations**: NP=Nanoparticle, AD=Adsorption, COV=Covalent binding, OV=Ovalbumin, MP=Monophosphoryl lipid A.

**A**

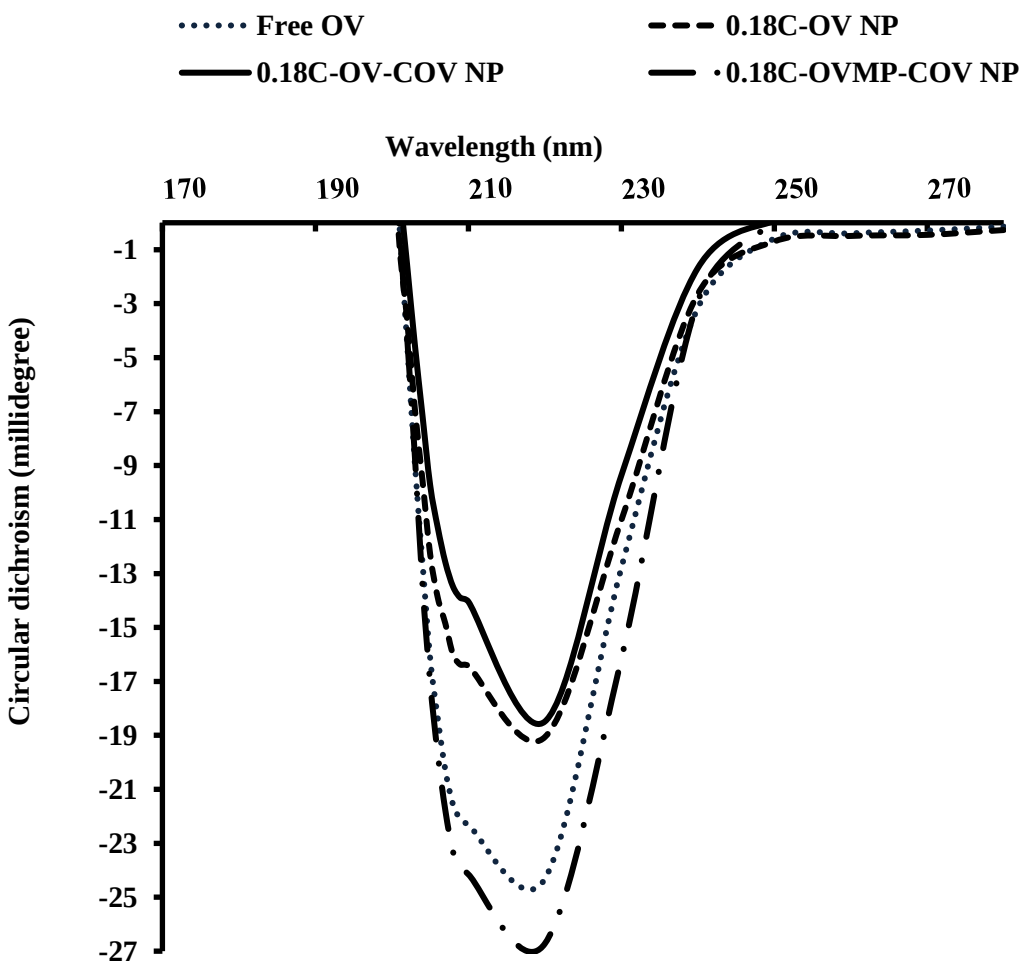
Free OV
0.18C-OV NP
0.18C-OV-COV NP
·0.18C-OVMP-COV NP
Wavelength (nm)
170
190
210
230
250
270
Circular dichroism (millidegree)
-1
-3
-5
-7
-9
-11
-13
-15
-17
-19
-21
-23
-25
-27

**B**

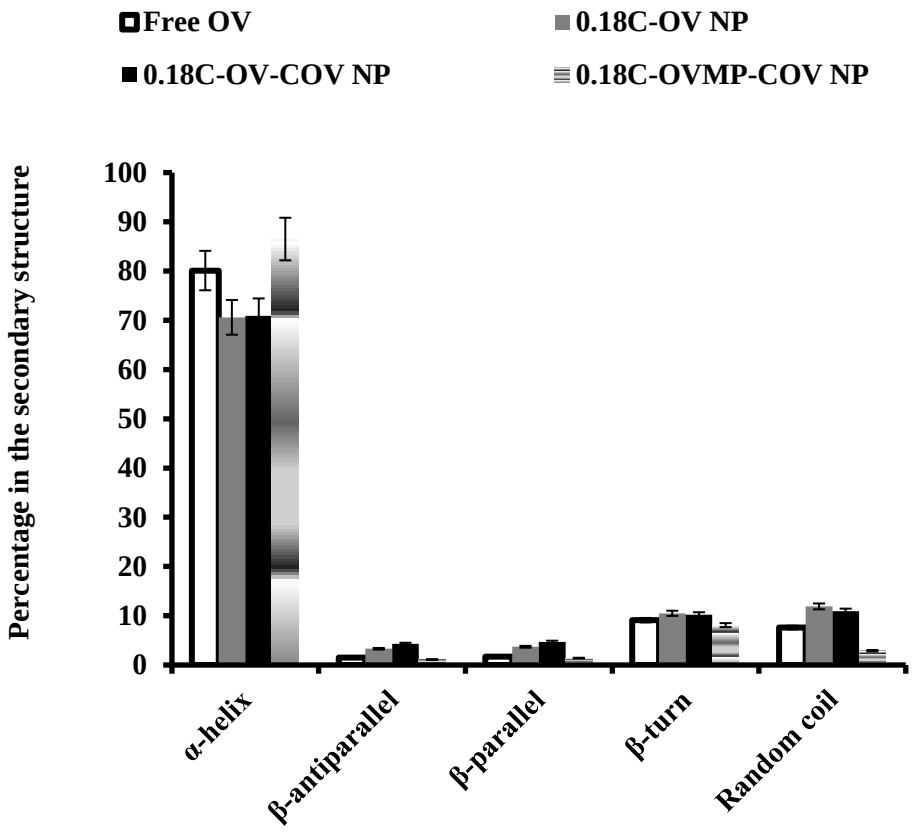


**Figure 5.3**. CD spectra of NPs. A) Representative CD spectra of 0.18 COOH terminated PLGA NPs. B) Percentages of α-helix, β-anti-parallel, β-parallel, β-turn and random coil of the secondary structure for free OVA, 0.18C-OV-NP, 0.18C-OV-COV-NP and 0.18C-OVMP-COV-NP after 20 days in PBS media. (n=3)

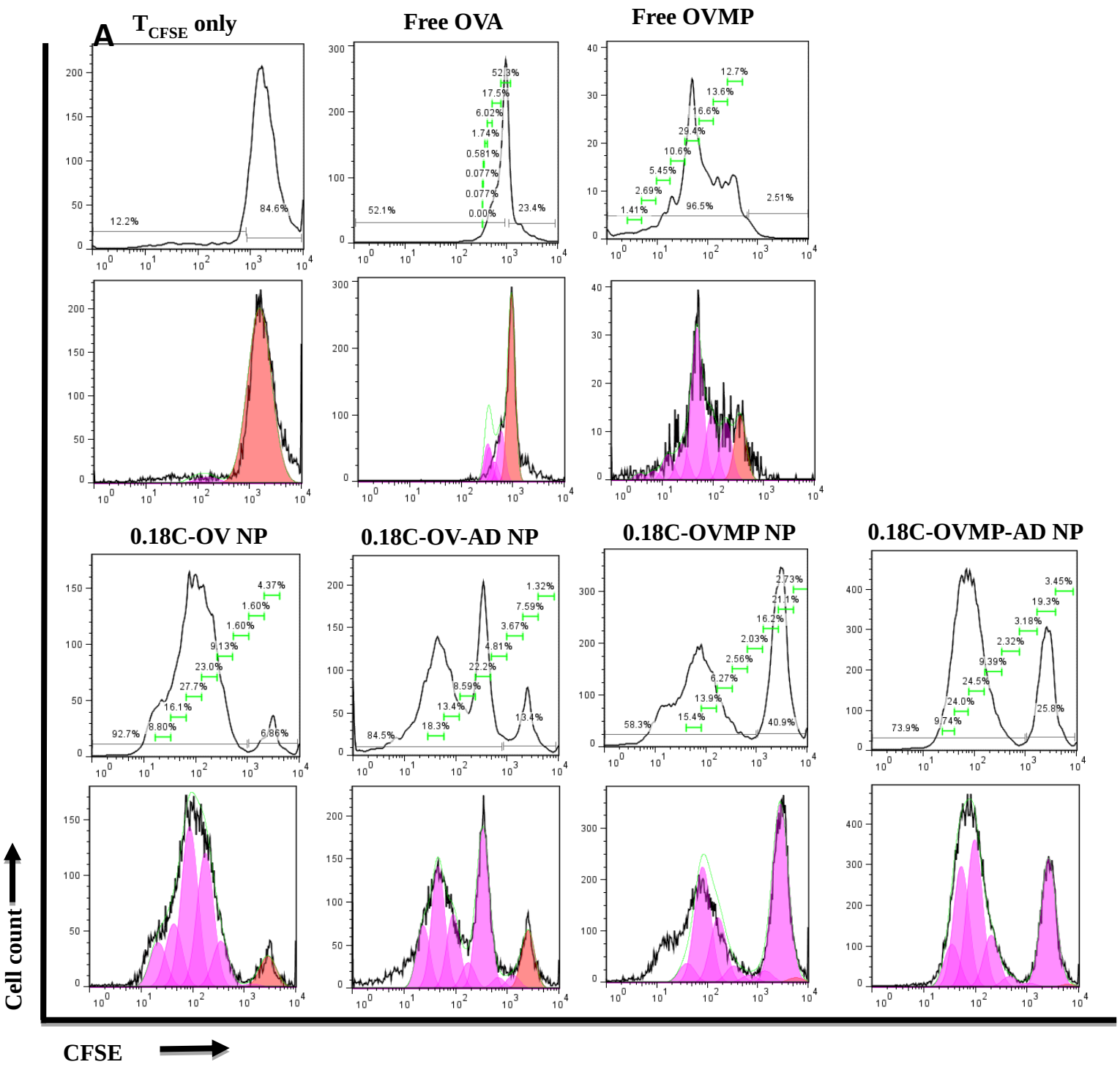
A
T CFSE only
Free OVA
Free OVMP
0.18C-OV NP
0.18C-OV-AD NP
0.18C-OVMP NP
0.18C-OVMP-AD NP
Cell count
CFSE

**B**

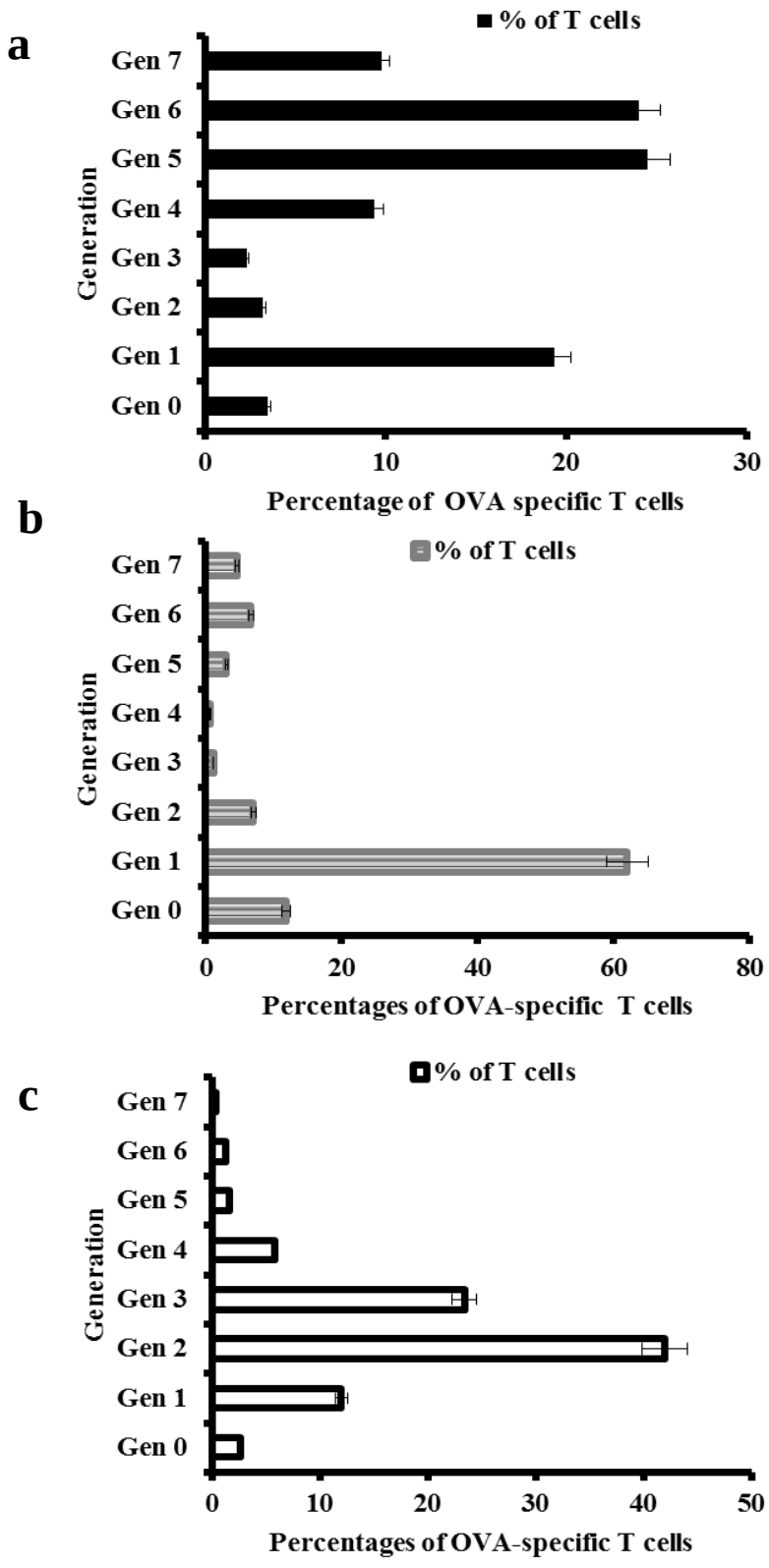
a
% of T cells
Gen 7
Gen 6
Gen 5
Gen 4
Gen 3
Gen 2
Gen 1
Gen 0
Generation
0
10
20
30
Percentage of OVA specific T cells
b
% of T cells
Gen 7
Gen 6
Gen 5
Gen 4
Gen 3
Gen 2
Gen 1
Gen 0
Generation
0
20
40
60
80
Percentages of OVA-specific T cells
c
% of T cells
Gen 7
Gen 6
Gen 5
Gen 4
Gen 3
Gen 2
Gen 1
Gen 0
Generation
0
10
20
30
40
50
Percentages of OVA-specific T cells

**Figure 5.4.** T cell proliferation assay from WT mice in the vaccination study. (A) Data is represented as histograms and Flowjo-analyzed cell-divisions for each group. *In-vitro* CFSE-labelled T cells obtained from a specific mice group was co-cultured with irradiated primary DCs. After four days, the cells were harvested, washed and stained with respective antibodies to determine the number of divisions by flow cytometry. (B) Bar diagram representing the percentages of generations present during cell divisions when restimulated with 20 µM Ovaendofit (a), 20 µM KLH (b) and in presence of no stimulation (c) for 0.18C-OVMP-AD NPs.

**Abbreviations:** NP=Nanoparticle, AD=Adsorption, C=COOH terminated PLGA NP, OV=Ovalbumin, MP=Monophosphoryl lipid A (MPLA).

A

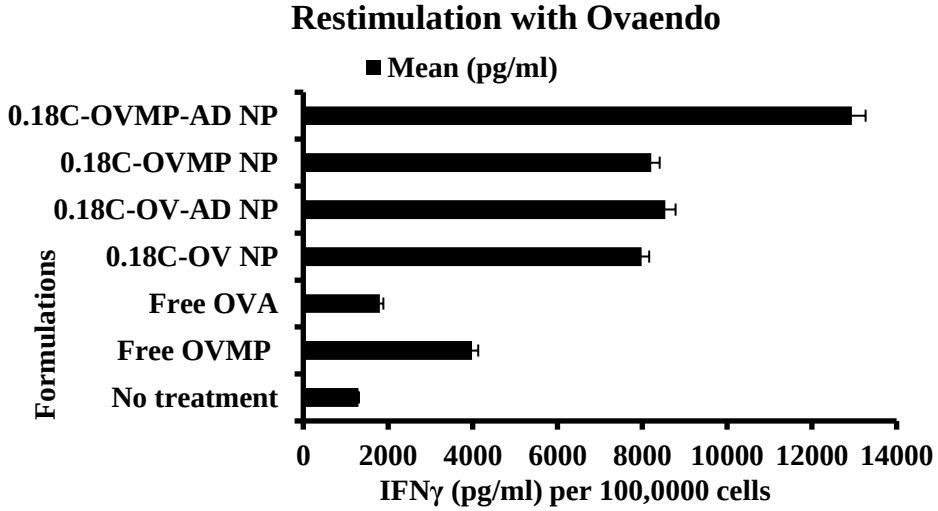
Restimulation with Ovaendo
Mean (pg/ml)
0.18C-OVMP-AD NP
0.18C-OVMP NP
0.18C-OV-AD NP
0.18C-OV NP
Free OVA
Free OVMP
No treatment
Formulations
0 2000 4000 6000 8000 10000 12000 14000
IFNγ (pg/ml) per 100,0000 cells

B

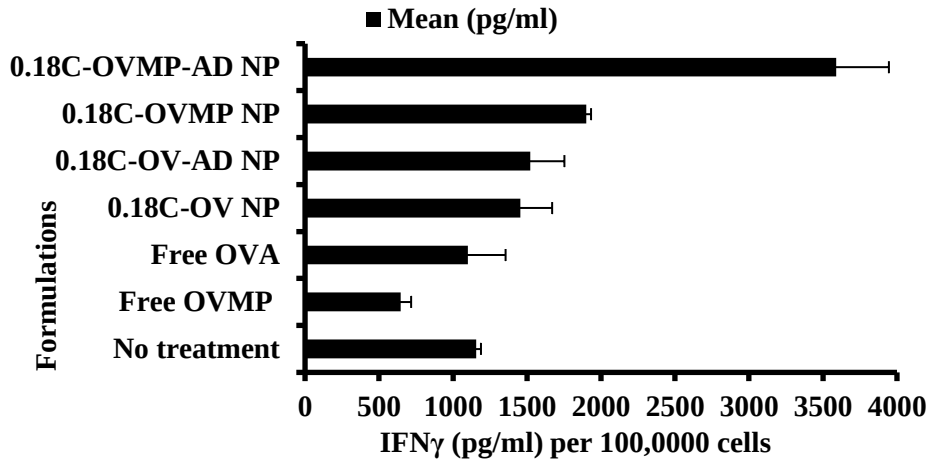
Restimulation with KLH
Mean (pg/ml)
0.18C-OVMP-AD NP
0.18C-OVMP NP
0.18C-OV-AD NP
0.18C-OV NP
Free OVA
Free OVMP
No treatment
Formulations
0 500 1000 1500 2000 2500 3000 3500 4000
IFNγ (pg/ml) per 100,0000 cells

C

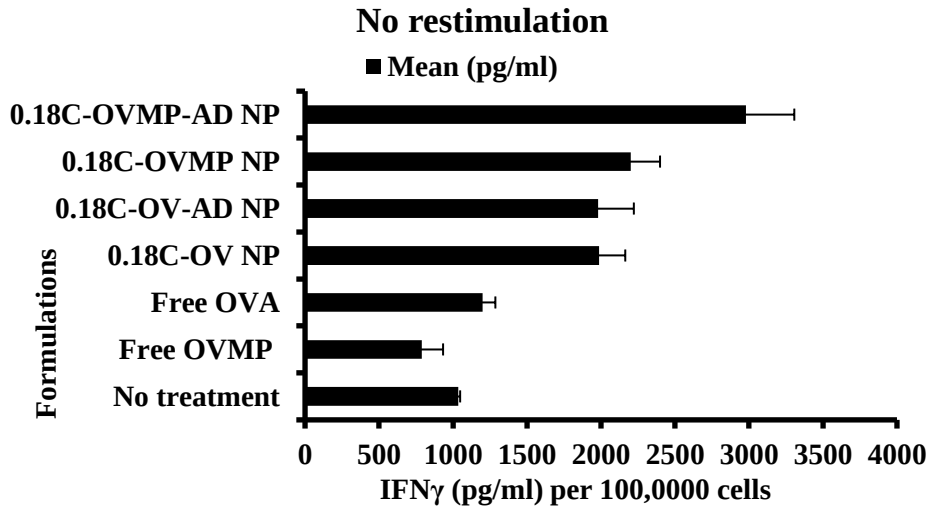
No restimulation
Mean (pg/ml)
0.18C-OVMP-AD NP
0.18C-OVMP NP
0.18C-OV-AD NP
0.18C-OV NP
Free OVA
Free OVMP
No treatment
Formulations
0 500 1000 1500 2000 2500 3000 3500 4000
IFNγ (pg/ml) per 100,0000 cells

D

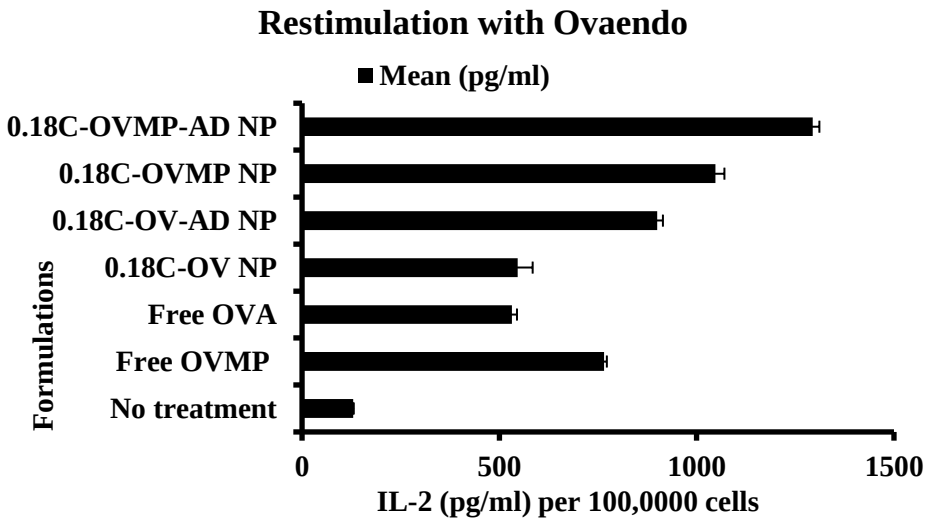
Restimulation with Ovaendo
Mean (pg/ml)
0.18C-OVMP-AD NP
0.18C-OVMP NP
0.18C-OV-AD NP
0.18C-OV NP
Free OVA
Free OVMP
No treatment
Formulations
0
500
1000
1500
IL-2 (pg/ml) per 100,0000 cells

E

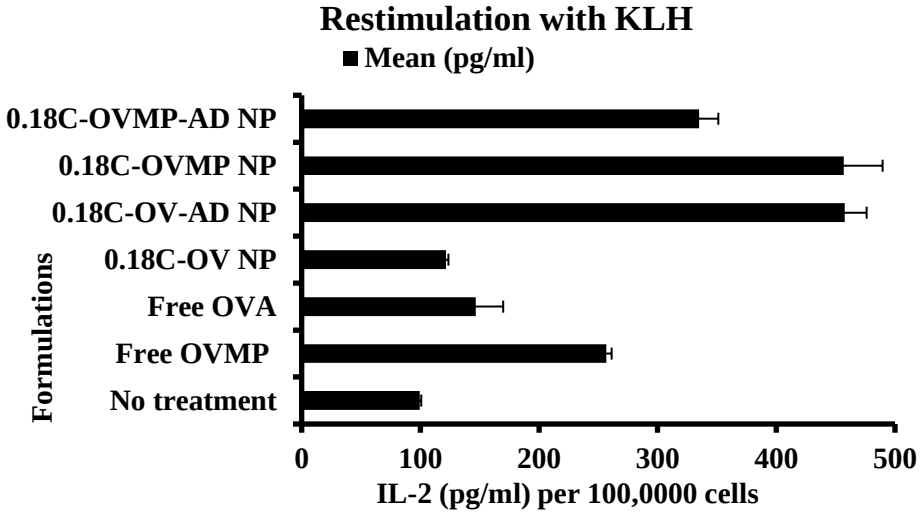
Restimulation with KLH
Mean (pg/ml)
0.18C-OVMP-AD NP
0.18C-OVMP NP
0.18C-OV-AD NP
0.18C-OV NP
Free OVA
Free OVMP
No treatment
Formulations
0
100
200
300
400
500
IL-2 (pg/ml) per 100,0000 cells

F

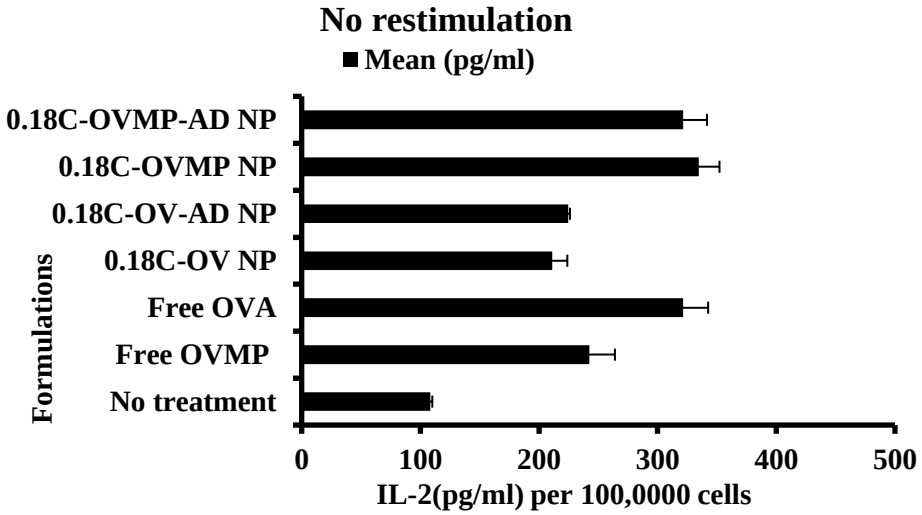
No restimulation
Mean (pg/ml)
0.18C-OVMP-AD NP
0.18C-OVMP NP
0.18C-OV-AD NP
0.18C-OV NP
Free OVA
Free OVMP
No treatment
Formulations
0
100
200
300
400
500
IL-2(pg/ml) per 100,0000 cells

G

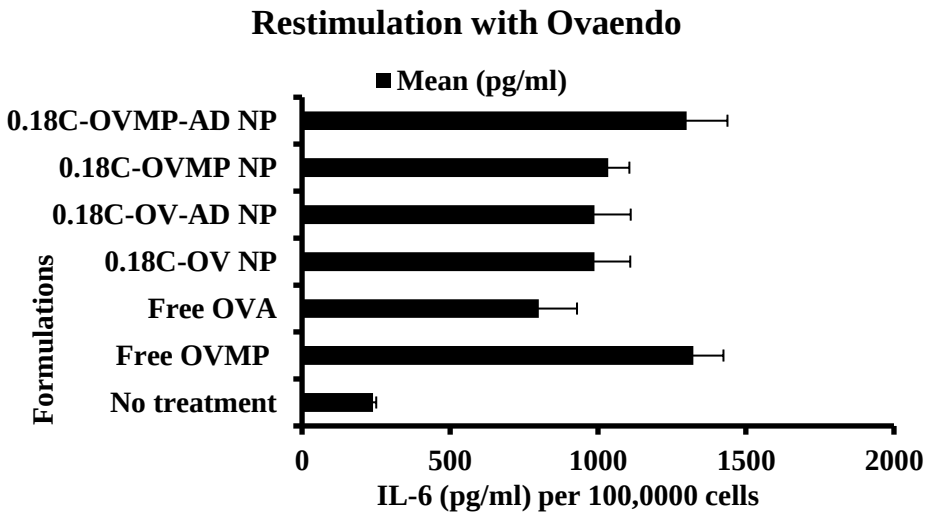
Restimulation with Ovaendo
Mean (pg/ml)
0.18C-OVMP-AD NP
0.18C-OVMP NP
0.18C-OV-AD NP
0.18C-OV NP
Free OVA
Free OVMP
No treatment
Formulations
0
500
1000
1500
2000
IL-6 (pg/ml) per 100,0000 cells

H

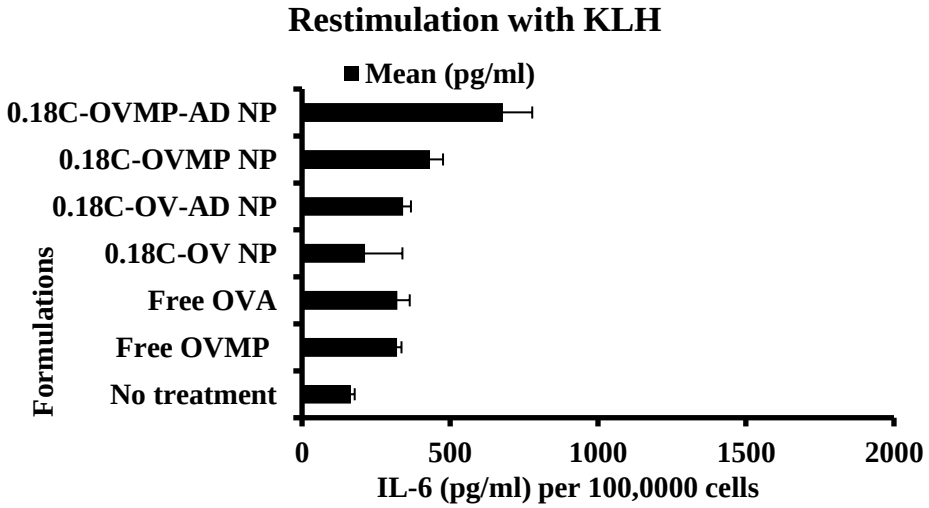
Restimulation with KLH
Mean (pg/ml)
0.18C-OVMP-AD NP
0.18C-OVMP NP
0.18C-OV-AD NP
0.18C-OV NP
Free OVA
Free OVMP
No treatment
Formulations
0
500
1000
1500
2000
IL-6 (pg/ml) per 100,0000 cells

I

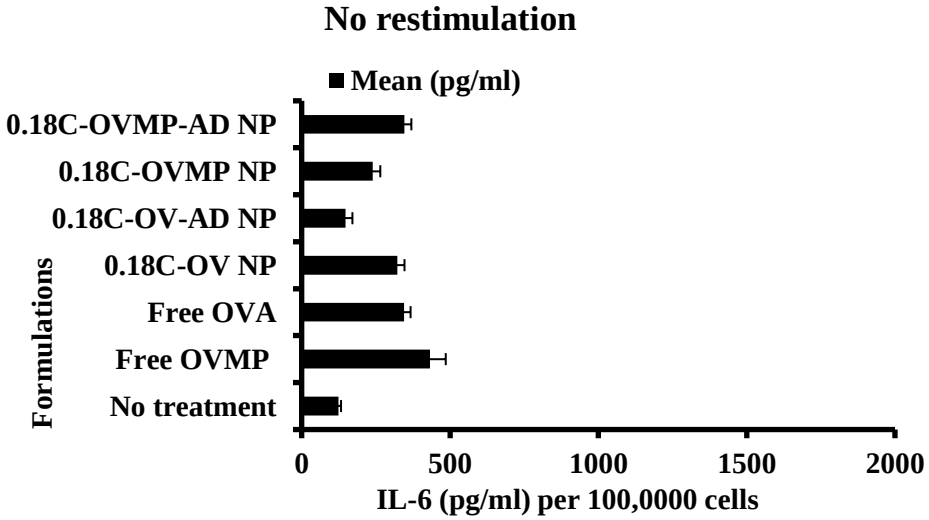
No restimulation
Mean (pg/ml)
0.18C-OVMP-AD NP
0.18C-OVMP NP
0.18C-OV-AD NP
0.18C-OV NP
Free OVA
Free OVMP
No treatment
Formulations
0
500
1000
1500
2000
IL-6 (pg/ml) per 100,0000 cells

J

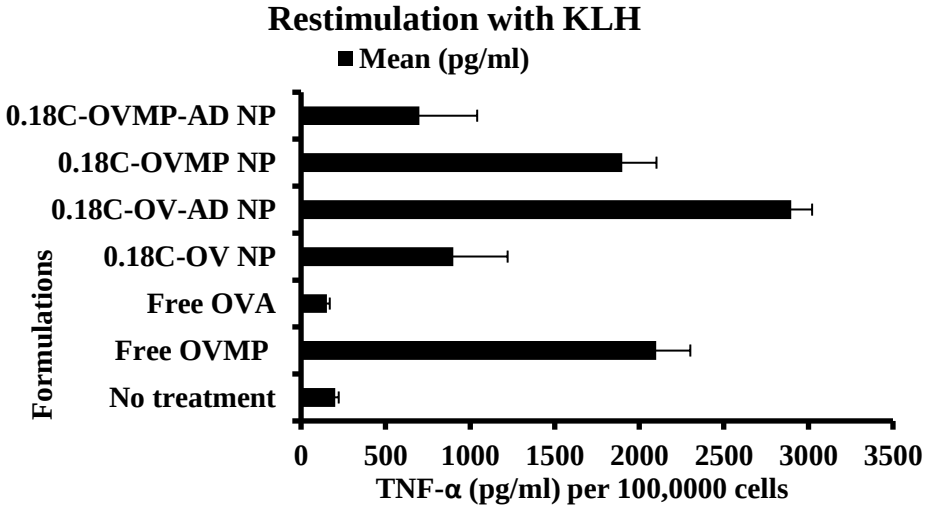
Restimulation with KLH
Mean (pg/ml)
0.18C-OVMP-AD NP
0.18C-OVMP NP
0.18C-OV-AD NP
0.18C-OV NP
Free OVA
Free OVMP
No treatment
Formulations
0
500
1000
1500
2000
2500
3000
3500
TNF-α (pg/ml) per 100,0000 cells

K

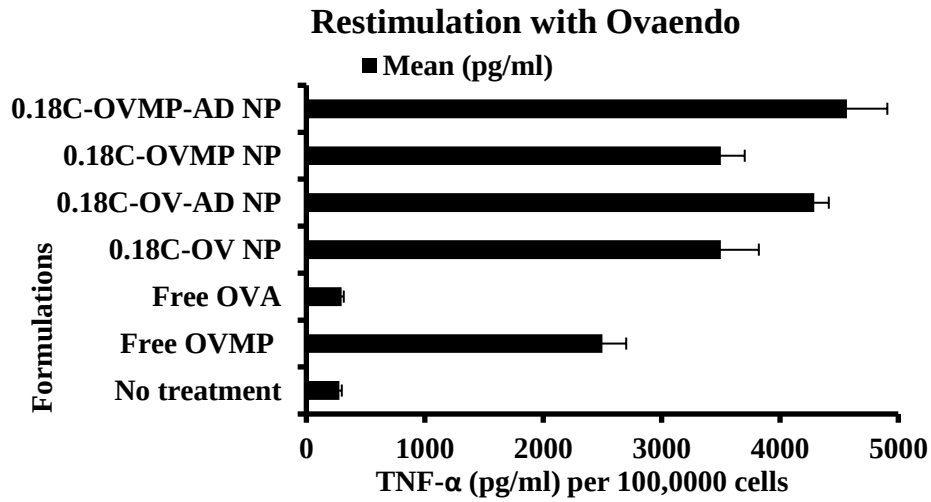
Restimulation with Ovaendo
Mean (pg/ml)
0.18C-OVMP-AD NP
0.18C-OVMP NP
0.18C-OV-AD NP
0.18C-OV NP
Free OVA
Free OVMP
No treatment
Formulations
0
1000
2000
3000
4000
5000
TNF-α (pg/ml) per 100,0000 cells

L

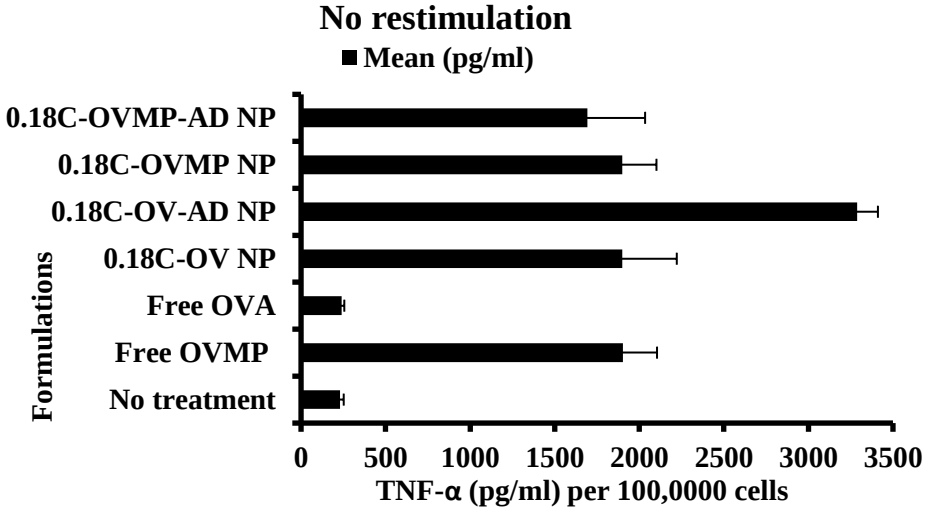
No restimulation
Mean (pg/ml)
0.18C-OVMP-AD NP
0.18C-OVMP NP
0.18C-OV-AD NP
0.18C-OV NP
Free OVA
Free OVMP
No treatment
Formulations
0
500
1000
1500
2000
2500
3000
3500
TNF-α (pg/ml) per 100,0000 cells

**Figure 5.5 (A-L):** Cytokine levels in the supernatants of cultured T cells from WT balb/c mice in the vaccination study. Notes: DCs and CD3+T cells were in a ratio of 1:4, where T cells were 100, 000 cells/well and DCs were 25, 000 cells/well in the co-culture. After four days of incubation, the culture supernatants were analyzed for IFNγ (A, B, C), IL-2, (D, E, F), IL-6 (G, H, I), and TNF-α (J, K, L) secretion. Figure A, D, G and J are cytokine secretion in co-culture after restimulation with 20 µM of Ovaendo relevant protein *in-vitro*. B, E, H and K are cytokine secretion in co-culture after restimulation with 20 µM of KLH irrelevant protein *in-vitro*. Figure C, F, I and L are cytokine secretion in co-culture after no restimulation *in-vitro*. (n=3) ($p<0.05$)

**Abbreviations:** NP=Nanoparticle, AD=Adsorption, C=COOH terminated PLGA NP, OV=Ovalbumin, MP=Monophosphoryl lipid A (MPLA).

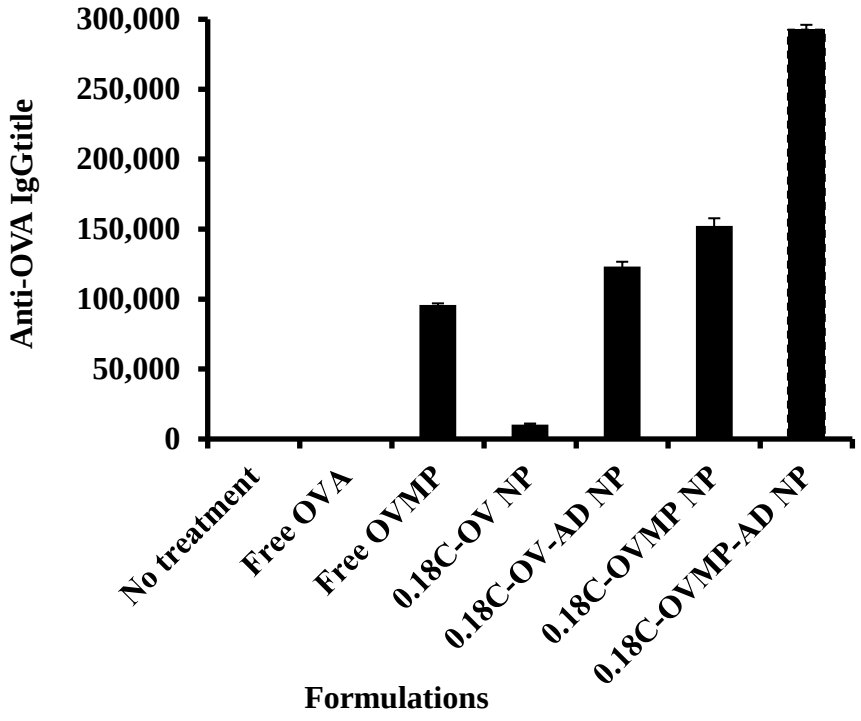


**Figure 5.6.** OVA-specific serum IgG titer estimation SC vaccination of WT balb/c mice. Notes: After SC vaccination, the mice were cardio-punctured to collect blood. Blood was centrifuged to collect the serum from supernatant. Total IgG was measured using ELISA technique. (n=3) ($p<0.05$)

**Abbreviations:** NP=Nanoparticle, AD=Adsorption, C=COOH terminated PLGA NP, OV=Ovalbumin, MP=Monophosphoryl lipid A (MPLA).

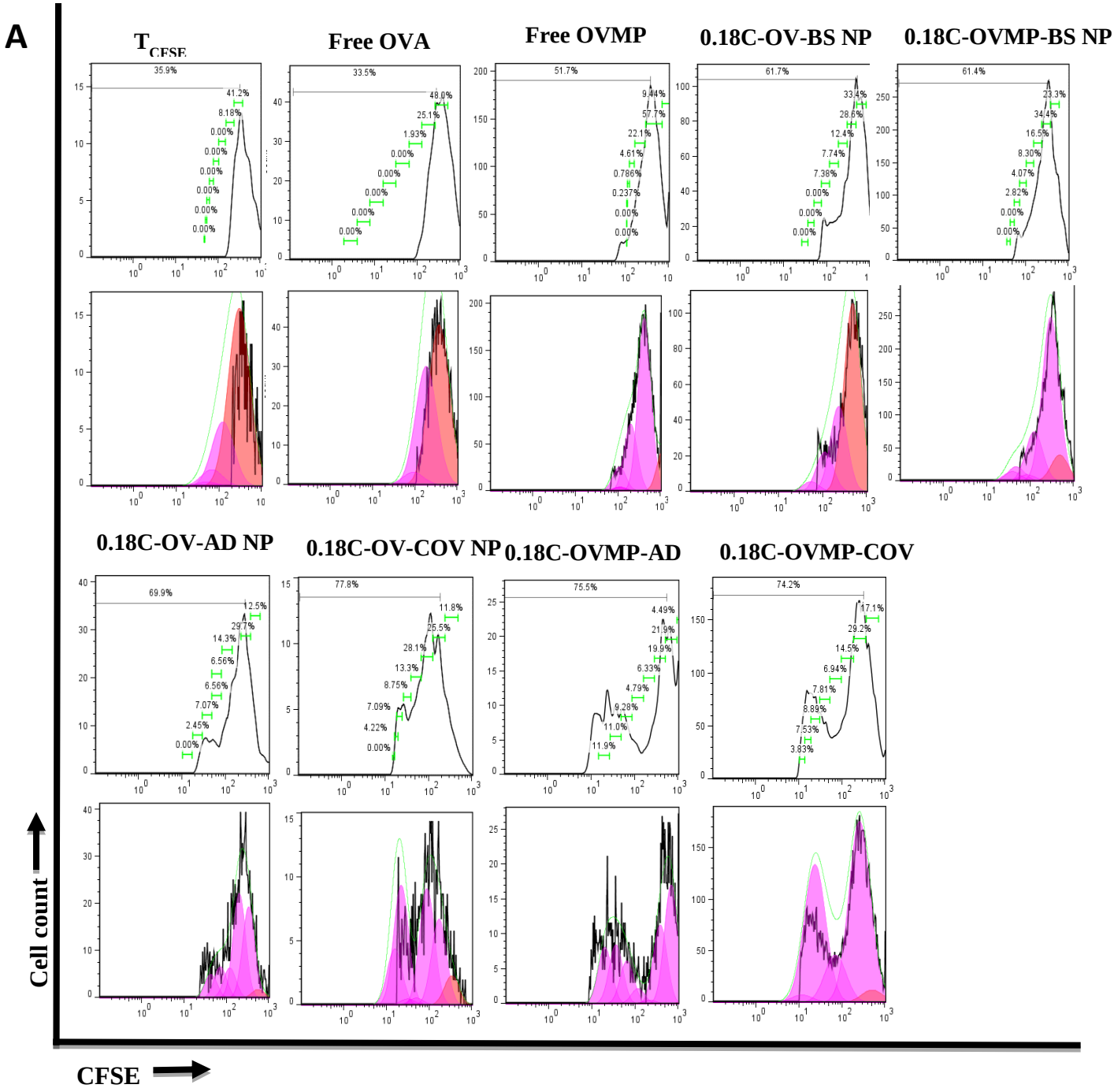
A
$T_{CFSE}$
Free OVA
Free OVMP
0.18C-OV-BS NP
0.18C-OVMP-BS NP
0.18C-OV-AD NP
0.18C-OV-COV NP
0.18C-OVMP-AD
0.18C-OVMP-COV
Cell count
CFSE

**B**

**a**

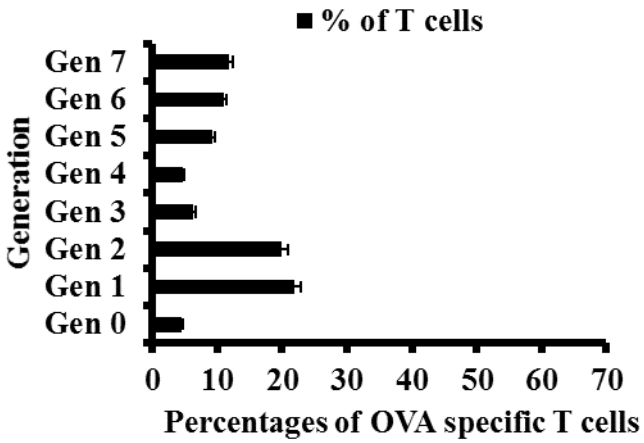
% of T cells
Generation
Gen 7
Gen 6
Gen 5
Gen 4
Gen 3
Gen 2
Gen 1
Gen 0
0 10 20 30 40 50 60 70
Percentages of OVA specific T cells

**b**

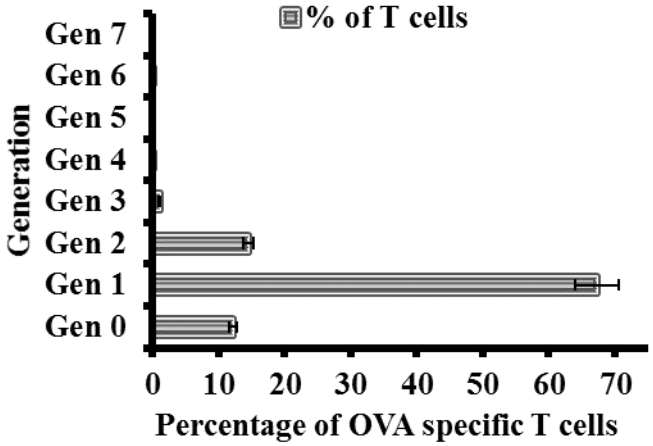
% of T cells
Generation
Gen 7
Gen 6
Gen 5
Gen 4
Gen 3
Gen 2
Gen 1
Gen 0
0 10 20 30 40 50 60 70
Percentage of OVA specific T cells

**c**

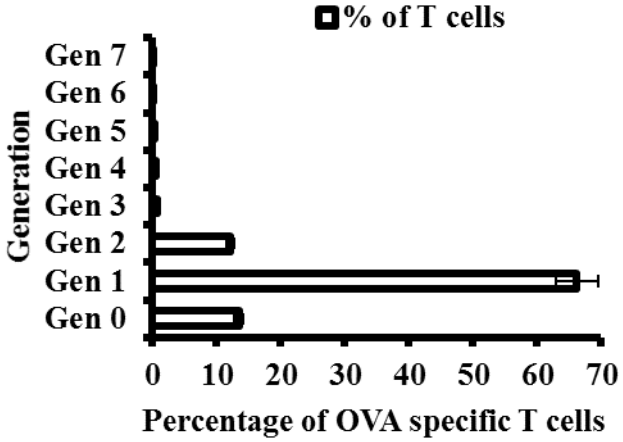
% of T cells
Generation
Gen 7
Gen 6
Gen 5
Gen 4
Gen 3
Gen 2
Gen 1
Gen 0
0 10 20 30 40 50 60 70
Percentage of OVA specific T cells

C

a

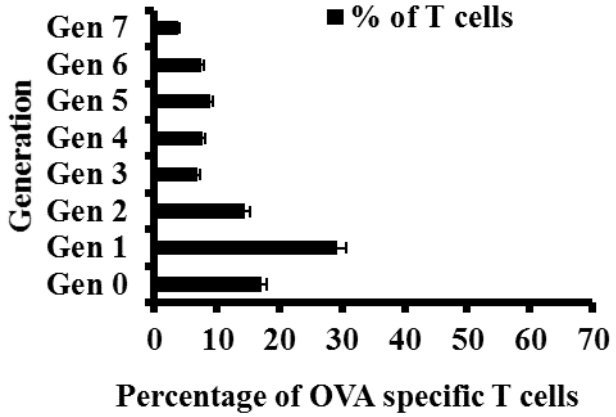
% of T cells
Gen 7
Gen 6
Gen 5
Gen 4
Gen 3
Gen 2
Gen 1
Gen 0
Generation
0 10 20 30 40 50 60 70
Percentage of OVA specific T cells

b

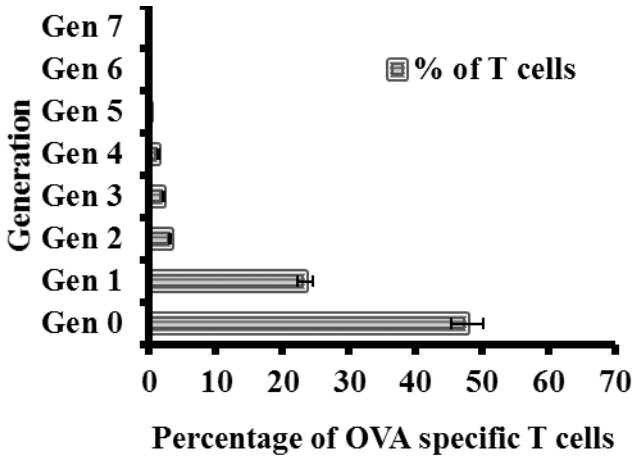
% of T cells
Gen 7
Gen 6
Gen 5
Gen 4
Gen 3
Gen 2
Gen 1
Gen 0
Generation
0 10 20 30 40 50 60 70
Percentage of OVA specific T cells

c

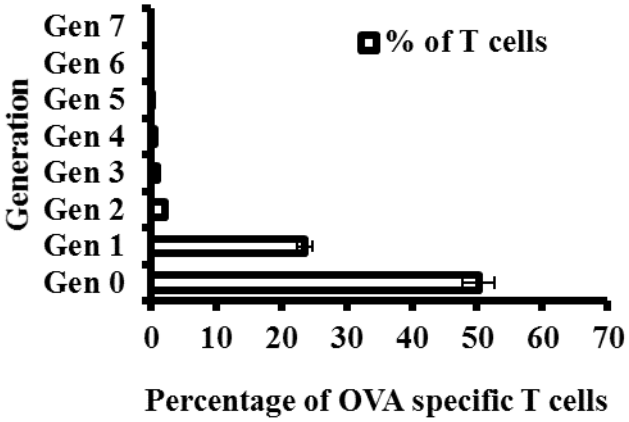
% of T cells
Gen 7
Gen 6
Gen 5
Gen 4
Gen 3
Gen 2
Gen 1
Gen 0
Generation
0 10 20 30 40 50 60 70
Percentage of OVA specific T cells

**Figure 5.7.** T cell proliferation assay from OT1 mice in the vaccination study. (A) Data is represented as histograms and Flowjo-analyzed cell-divisions for each group. *In-vitro* CFSE-labelled T cells obtained from a specific mice group was co-cultured with irradiated primary DCs. After five days, the cells were harvested, washed and stained with respective antibodies to determine the number of divisions by flow cytometry. (B) Bar diagram representing the percentages of generations present during cell divisions when restimulated with 1 µM SIINFEKL (a), 1 µM KLH (b) and in presence of no stimulation (c) for 0.18C-OVMP-AD NPs. (C) Bar diagram representing the percentages of generations present during cell divisions when restimulated with 1 µM SIINFEKL (a), 1 µM KLH (b) and in presence of no stimulation (c) for 0.18C-OVMP-COV NPs.

**Abbreviations:** NP=Nanoparticle, AD=Adsorption, COV=Covalent binding, C=COOH, E=Ester, OV=Ovalbumin, MP=Monophosphoryl lipid A (MPLA).

A

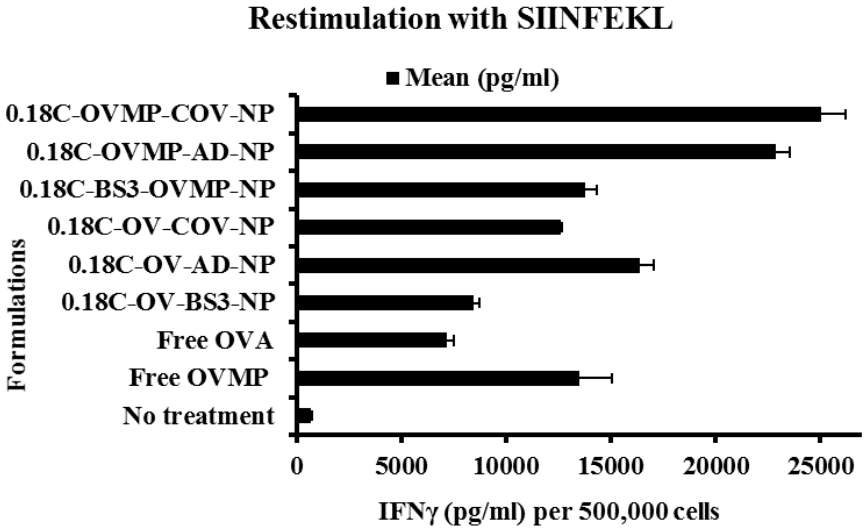
Restimulation with SIINFEKL
Mean (pg/ml)
0.18C-OVMP-COV-NP
0.18C-OVMP-AD-NP
0.18C-BS3-OVMP-NP
0.18C-OV-COV-NP
0.18C-OV-AD-NP
0.18C-OV-BS3-NP
Free OVA
Free OVMP
No treatment
Formulations
0
5000
10000
15000
20000
25000
IFNγ (pg/ml) per 500,000 cells

B

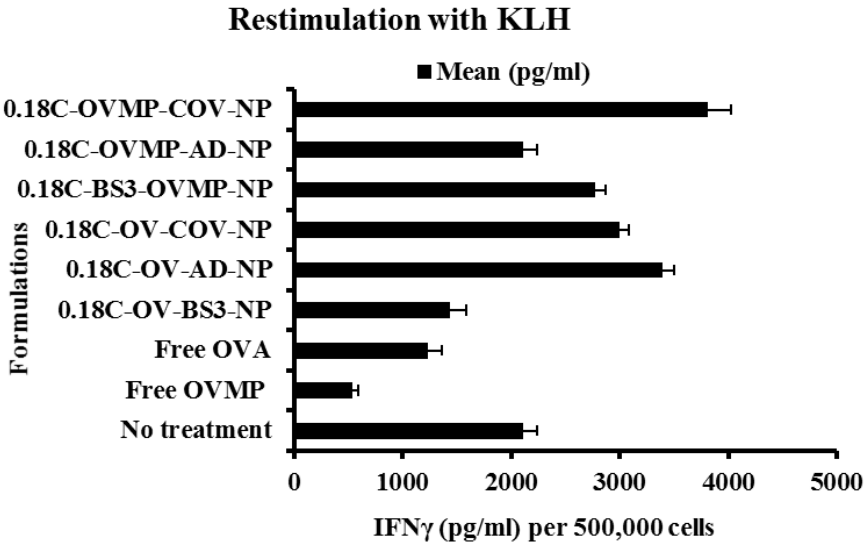
Restimulation with KLH
Mean (pg/ml)
0.18C-OVMP-COV-NP
0.18C-OVMP-AD-NP
0.18C-BS3-OVMP-NP
0.18C-OV-COV-NP
0.18C-OV-AD-NP
0.18C-OV-BS3-NP
Free OVA
Free OVMP
No treatment
Formulations
0
1000
2000
3000
4000
5000
IFNγ (pg/ml) per 500,000 cells

C

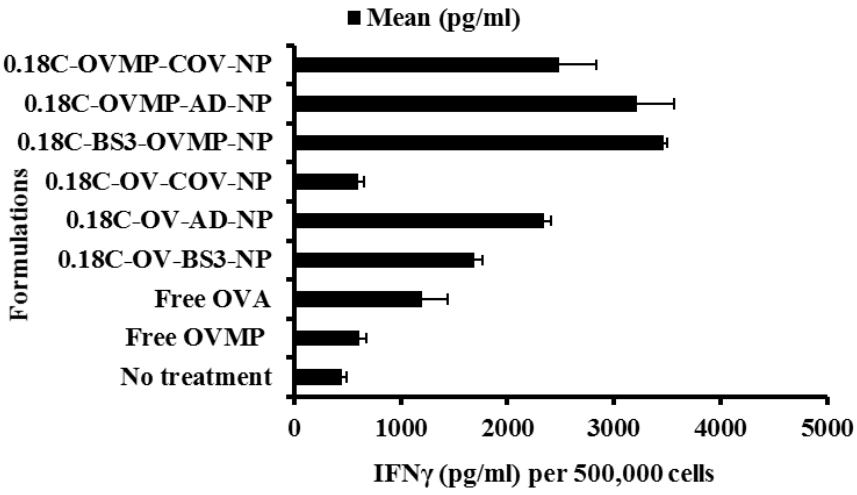
No restimulation
Mean (pg/ml)
0.18C-OVMP-COV-NP
0.18C-OVMP-AD-NP
0.18C-BS3-OVMP-NP
0.18C-OV-COV-NP
0.18C-OV-AD-NP
0.18C-OV-BS3-NP
Free OVA
Free OVMP
No treatment
Formulations
0
1000
2000
3000
4000
5000
IFNγ (pg/ml) per 500,000 cells

D

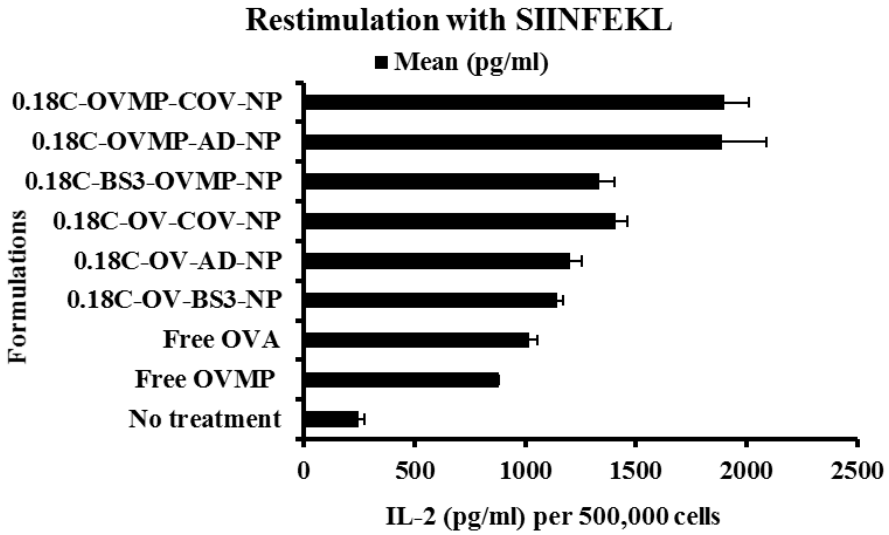
Restimulation with SIINFEKL
Mean (pg/ml)
0.18C-OVMP-COV-NP
0.18C-OVMP-AD-NP
0.18C-BS3-OVMP-NP
0.18C-OV-COV-NP
0.18C-OV-AD-NP
0.18C-OV-BS3-NP
Free OVA
Free OVMP
No treatment
Formulations
0
500
1000
1500
2000
2500
IL-2 (pg/ml) per 500,000 cells

E

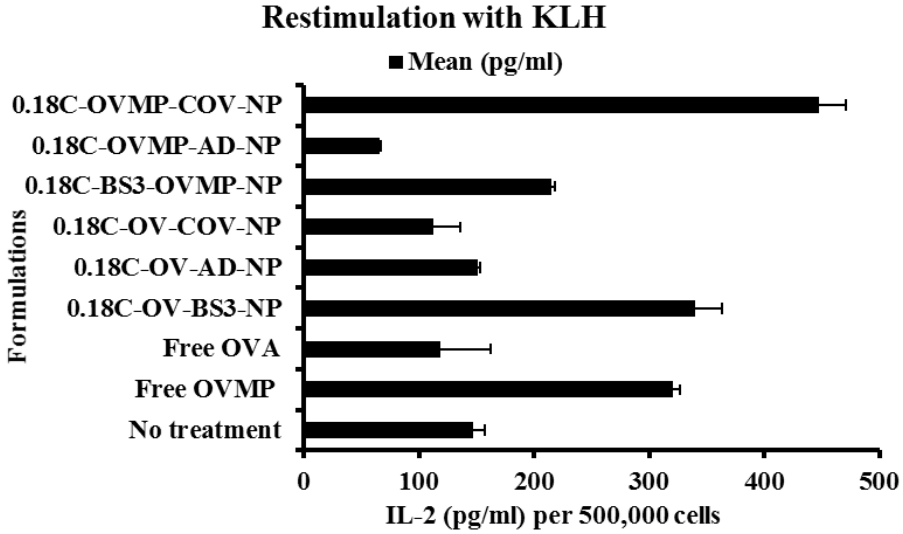
Restimulation with KLH
Mean (pg/ml)
0.18C-OVMP-COV-NP
0.18C-OVMP-AD-NP
0.18C-BS3-OVMP-NP
0.18C-OV-COV-NP
0.18C-OV-AD-NP
0.18C-OV-BS3-NP
Free OVA
Free OVMP
No treatment
Formulations
0
100
200
300
400
500
IL-2 (pg/ml) per 500,000 cells

F

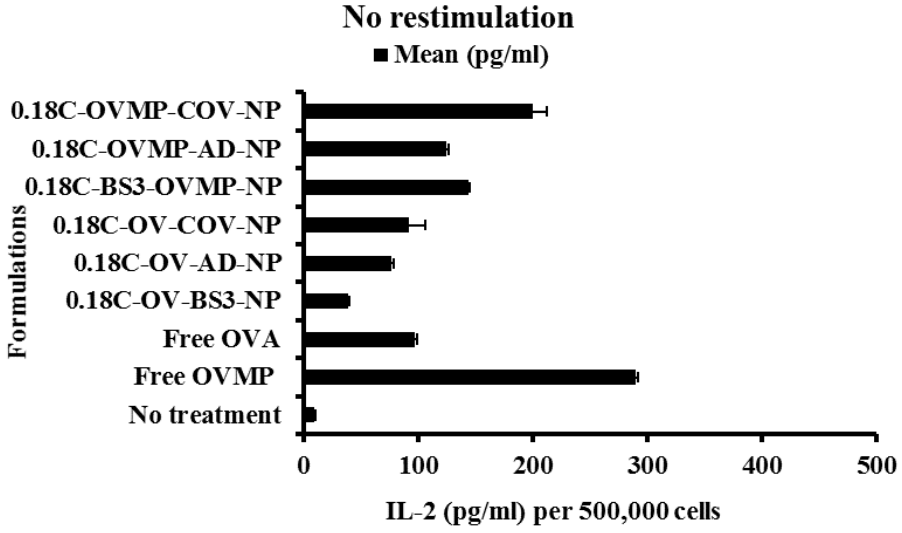
No restimulation
Mean (pg/ml)
0.18C-OVMP-COV-NP
0.18C-OVMP-AD-NP
0.18C-BS3-OVMP-NP
0.18C-OV-COV-NP
0.18C-OV-AD-NP
0.18C-OV-BS3-NP
Free OVA
Free OVMP
No treatment
Formulations
0
100
200
300
400
500
IL-2 (pg/ml) per 500,000 cells

G

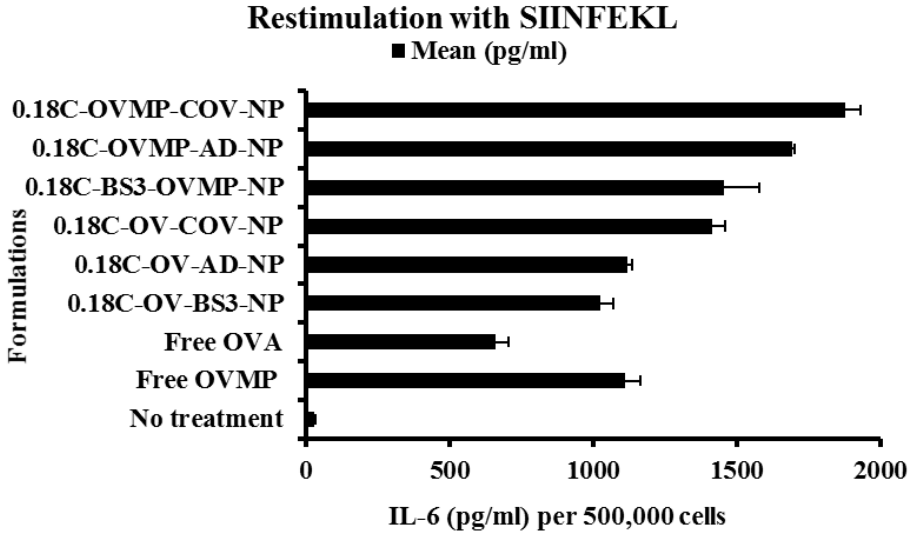
Restimulation with SIINFEKL
Mean (pg/ml)
0.18C-OVMP-COV-NP
0.18C-OVMP-AD-NP
0.18C-BS3-OVMP-NP
0.18C-OV-COV-NP
0.18C-OV-AD-NP
0.18C-OV-BS3-NP
Free OVA
Free OVMP
No treatment
Formulations
0
500
1000
1500
2000
IL-6 (pg/ml) per 500,000 cells

H

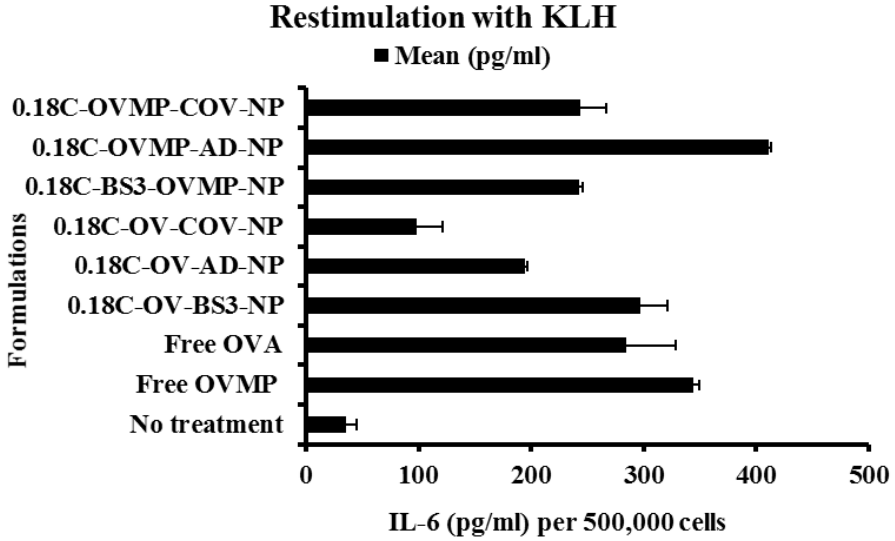
Restimulation with KLH
Mean (pg/ml)
0.18C-OVMP-COV-NP
0.18C-OVMP-AD-NP
0.18C-BS3-OVMP-NP
0.18C-OV-COV-NP
0.18C-OV-AD-NP
0.18C-OV-BS3-NP
Free OVA
Free OVMP
No treatment
Formulations
0
100
200
300
400
500
IL-6 (pg/ml) per 500,000 cells

I

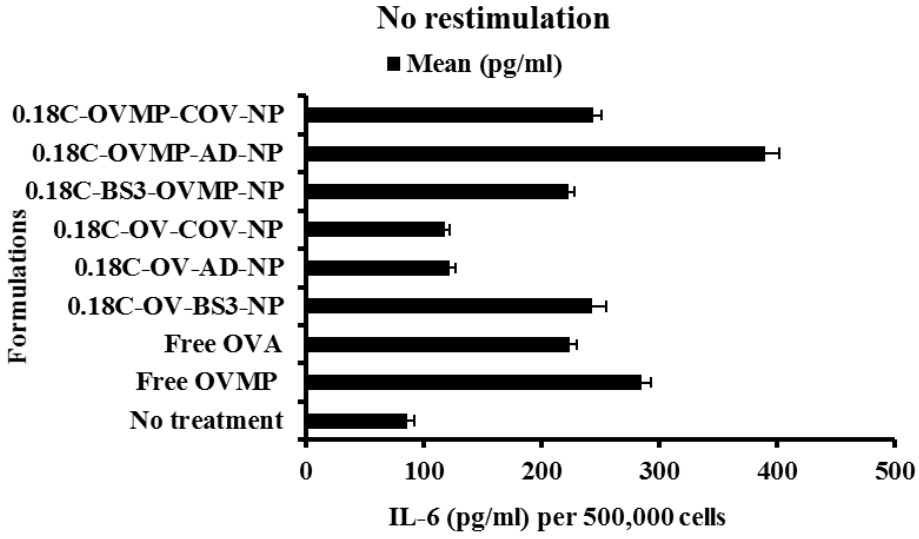
No restimulation
Mean (pg/ml)
0.18C-OVMP-COV-NP
0.18C-OVMP-AD-NP
0.18C-BS3-OVMP-NP
0.18C-OV-COV-NP
0.18C-OV-AD-NP
0.18C-OV-BS3-NP
Free OVA
Free OVMP
No treatment
Formulations
0
100
200
300
400
500
IL-6 (pg/ml) per 500,000 cells

J

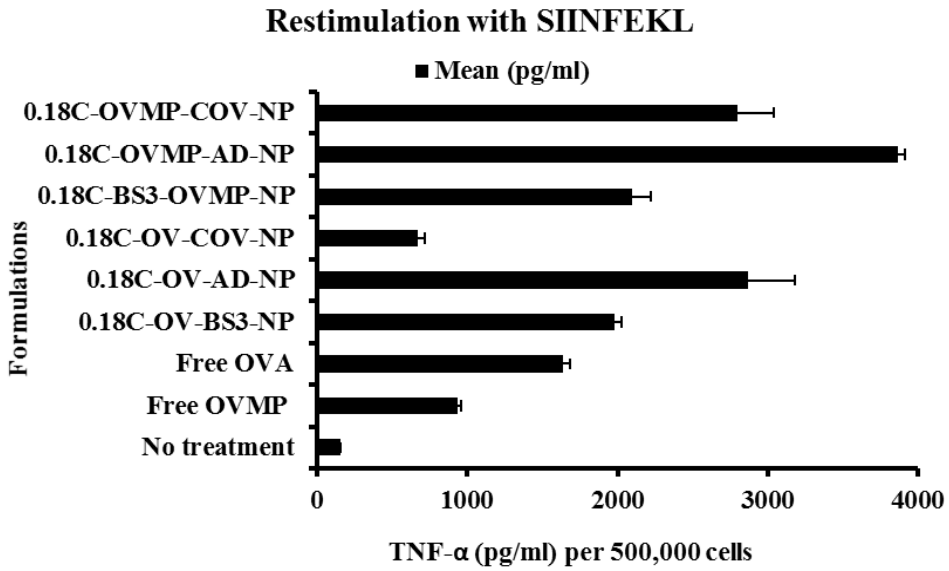
Restimulation with SIINFEKL
Mean (pg/ml)
0.18C-OVMP-COV-NP
0.18C-OVMP-AD-NP
0.18C-BS3-OVMP-NP
0.18C-OV-COV-NP
0.18C-OV-AD-NP
0.18C-OV-BS3-NP
Free OVA
Free OVMP
No treatment
Formulations
0
1000
2000
3000
4000
TNF-α (pg/ml) per 500,000 cells

K

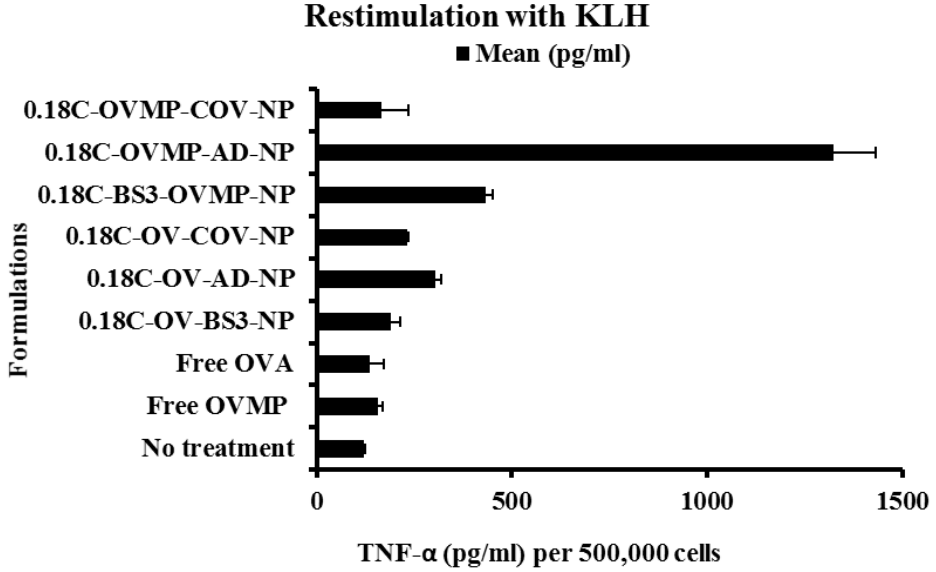
Restimulation with KLH
Mean (pg/ml)
0.18C-OVMP-COV-NP
0.18C-OVMP-AD-NP
0.18C-BS3-OVMP-NP
0.18C-OV-COV-NP
0.18C-OV-AD-NP
0.18C-OV-BS3-NP
Free OVA
Free OVMP
No treatment
Formulations
0
500
1000
1500
TNF-α (pg/ml) per 500,000 cells

L

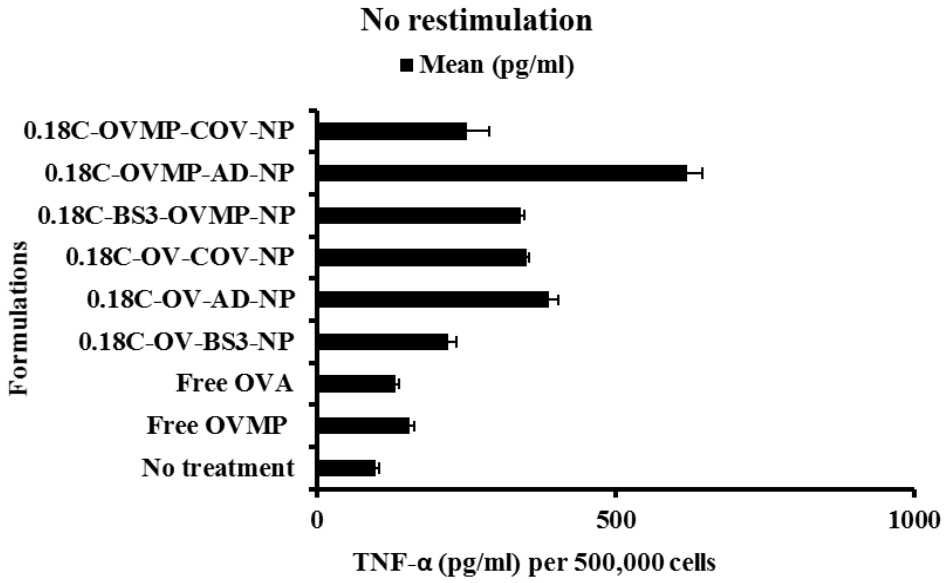
No restimulation
Mean (pg/ml)
0.18C-OVMP-COV-NP
0.18C-OVMP-AD-NP
0.18C-BS3-OVMP-NP
0.18C-OV-COV-NP
0.18C-OV-AD-NP
0.18C-OV-BS3-NP
Free OVA
Free OVMP
No treatment
Formulations
0
500
1000
TNF-α (pg/ml) per 500,000 cells

**Figure 5.8.** Cytokine levels in the supernatants of cultured T cells from OT1 mice in the vaccination study. Notes: DCs and CD8+T cells were in a ratio of 1:4, where T cells were 100, 000 cells/well and DCs were 25, 000 cells/well in the co-culture. After five days of incubation, the culture supernatants were analyzed for IFNγ (A, B, C), IL-2, (D, E, F), IL-6 (G, H, I), and TNF-α (J, K, L) secretion. Figure A, D, G and J are cytokine secretion in co-culture after restimulation with 1 µM of SIINFEKL peptide *in-vitro*. B, E, H and K are cytokine secretion in co-culture after restimulation with 1 µM of KLH (irrelevant protein) *in-vitro*. Figure C, F, I and L are cytokine secretion in co-culture after no restimulation *in-vitro*. (n=3) ($p<0.05$)

**Abbreviations:** NP=Nanoparticle, AD=Adsorption, C=COOH terminated PLGA NP, OV=Ovalbumin, MP=Monophosphoryl lipid A (MPLA).

## 5.11 References


1. Yaddanapudi K, Mitchell RA, Eaton JW. Cancer vaccines: Looking to the future. Oncoimmunology. 2013 Mar 01;2(3):e23403. PubMed PMID: 23802081. Pubmed Central PMCID: 3661166.
2. Shedlock DJ, Shen H. Requirement for CD4 T cell help in generating functional CD8 T cell memory. Science. 2003 Apr 11;300(5617):337-9. PubMed PMID: WOS:000182135400059. English.
3. Snook AE, Waldman SA. Advances in cancer immunotherapy. Discovery medicine. 2013 Feb;15(81):120-5. PubMed PMID: 23449114. Pubmed Central PMCID: 4066887.
4. Hanks BA. Immune evasion pathways and the design of dendritic cell-based cancer vaccines. Discovery medicine. 2016 Feb;21(114):135-42. PubMed PMID: 27011049. Pubmed Central PMCID: 4934601.
5. Voena C, Chiarle R. Advances in cancer immunology and cancer immunotherapy. Discovery medicine. 2016 Feb;21(114):125-33. PubMed PMID: 27011048.
6. Hamdy S, Haddadi A, Hung RW, Lavasanifar A. Targeting dendritic cells with nano-particulate PLGA cancer vaccine formulations. Advanced drug delivery reviews. 2011 Sep 10;63(10-11):943-55. PubMed PMID: 21679733.
7. Vogel FR. Improving vaccine performance with adjuvants. Clin Infect Dis. 2000 Jun;30 Suppl 3:S266-70. PubMed PMID: 10875797.
8. Mantia-Smaldone GM, Chu CS. A review of dendritic cell therapy for cancer: progress and challenges. BioDrugs. 2013 Oct;27(5):453-68. PubMed PMID: 23592406.
9. Hamdy S, Elamanchili P, Alshamsan A, Molavi O, Satou T, Samuel J. Enhanced antigen-specific primary CD4+ and CD8+ responses by codelivery of ovalbumin and toll-like receptor ligand monophosphoryl lipid A in poly(D,L-lactic-co-glycolic acid) nanoparticles. Journal of biomedical materials research Part A. 2007 Jun 01;81(3):652-62. PubMed PMID: 17187395.
10. Haddadi A, Hamdy S, Ghotbi Z, Samuel J, Lavasanifar A. Immunoadjuvant activity of the nanoparticles' surface modified with mannan. Nanotechnology. 2014 Sep 05;25(35):355101. PubMed PMID: 25119543.
11. Kasturi SP, Skountzou I, Albrecht RA, Koutsonanos D, Hua T, Nakaya HI, et al. Programming the magnitude and persistence of antibody responses with innate immunity. Nature. 2011 Feb 24;470(7335):543-7. PubMed PMID: 21350488. Pubmed Central PMCID: 3057367.
12. Cruz LJ, Rosalia RA, Kleinovink JW, Rueda F, Lowik CW, Ossendorp F. Targeting nanoparticles to CD40, DEC-205 or CD11c molecules on dendritic cells for efficient CD8(+) T cell

response: a comparative study. Journal of controlled release : official journal of the Controlled Release Society. 2014 Oct 28;192:209-18. PubMed PMID: 25068703.

13. Saluja SS, Hanlon DJ, Sharp FA, Hong E, Khalil D, Robinson E, et al. Targeting human dendritic cells via DEC-205 using PLGA nanoparticles leads to enhanced cross-presentation of a melanoma-associated antigen. Int J Nanomedicine. 2014;9:5231-46. PubMed PMID: 25419128. Pubmed Central PMCID: 4235494.

14. Silva JM, Zupancic E, Vandermeulen G, Oliveira VG, Salgado A, Videira M, et al. In vivo delivery of peptides and Toll-like receptor ligands by mannose-functionalized polymeric nanoparticles induces prophylactic and therapeutic anti-tumor immune responses in a melanoma model. Journal of controlled release : official journal of the Controlled Release Society. 2015 Jan 28;198:91-103. PubMed PMID: 25483429.

15. Peres C, Matos AI, Conniot J, Sainz V, Zupancic E, Silva JM, et al. Poly(lactic acid)-based particulate systems are promising tools for immune modulation. Acta biomaterialia. 2017 Jan 15;48:41-57. PubMed PMID: 27826003.

16. Schlosser E, Mueller M, Fischer S, Basta S, Busch DH, Gander B, et al. TLR ligands and antigen need to be coencapsulated into the same biodegradable microsphere for the generation of potent cytotoxic T lymphocyte responses. Vaccine. 2008 Mar 20;26(13):1626-37. PubMed PMID: 18295941.

17. Elamanchili P, Lutsiak CM, Hamdy S, Diwan M, Samuel J. "Pathogen-mimicking" nanoparticles for vaccine delivery to dendritic cells. Journal of immunotherapy. 2007 May-Jun;30(4):378-95. PubMed PMID: 17457213.

18. Jahan ST, Haddadi A. Investigation and optimization of formulation parameters on preparation of targeted anti-CD205 tailored PLGA nanoparticles. Int J Nanomedicine. 2015;10:7371-84. PubMed PMID: 26677326. Pubmed Central PMCID: 4677653.

19. Bandyopadhyay A, Fine RL, Demento S, Bockenstedt LK, Fahmy TM. The impact of nanoparticle ligand density on dendritic-cell targeted vaccines. Biomaterials. 2011 Apr;32(11):3094-105. PubMed PMID: 21262534. Pubmed Central PMCID: 4570971.

20. Izadifar M, Kelly ME, Haddadi A, Chen X. Optimization of nanoparticles for cardiovascular tissue engineering. Nanotechnology. 2015 Jun 12;26(23):235301. PubMed PMID: 25987360.

21. Ghotbi Z, Haddadi A, Hamdy S, Hung RW, Samuel J, Lavasanifar A. Active targeting of dendritic cells with mannan-decorated PLGA nanoparticles. Journal of drug targeting. 2011 May;19(4):281-92. PubMed PMID: 20590403.

22. Sarti F, Perera G, Hintzen F, Kotti K, Karageorgiou V, Kammona O, et al. In vivo evidence of oral vaccination with PLGA nanoparticles containing the immunostimulant monophosphoryl lipid A. Biomaterials. 2011 Jun;32(16):4052-7. PubMed PMID: 21377204.

23. Desmet CJ, Ishii KJ. Nucleic acid sensing at the interface between innate and adaptive immunity in vaccination. Nat Rev Immunol. 2012 Jul;12(7):479-91. PubMed PMID: 22728526.

24. Umeshappa CS, Huang H, Xie Y, Wei Y, Mulligan SJ, Deng Y, et al. CD4+ Th-APC with acquired peptide/MHC class I and II complexes stimulate type 1 helper CD4+ and central memory CD8+ T cell responses. Journal of immunology. 2009 Jan 01;182(1):193-206. PubMed PMID: 19109150.

25. Hamdy S, Haddadi A, Shayeganpour A, Samuel J, Lavasanifar A. Activation of antigen-specific T cell-responses by mannan-decorated PLGA nanoparticles. Pharmaceutical research. 2011 Sep;28(9):2288-301. PubMed PMID: 21560020.

26. Zhang W, Wang L, Liu Y, Chen X, Liu Q, Jia J, et al. Immune responses to vaccines involving a combined antigen-nanoparticle mixture and nanoparticle-encapsulated antigen formulation. Biomaterials. 2014 Jul;35(23):6086-97. PubMed PMID: 24780166.

27. Hamdy S, Molavi O, Ma Z, Haddadi A, Alshamsan A, Gobti Z, et al. Co-delivery of cancer-associated antigen and Toll-like receptor 4 ligand in PLGA nanoparticles induces potent CD8+ T cell-mediated anti-tumor immunity. Vaccine. 2008 Sep 15;26(39):5046-57. PubMed PMID: 18680779.

28. Chittasupho C, Shannon L, Siahaan TJ, Vines CM, Berkland C. Nanoparticles targeting dendritic cell surface molecules effectively block T cell conjugation and shift response. ACS nano. 2011 Mar 22;5(3):1693-702. PubMed PMID: 21375342. Pubmed Central PMCID: 4207654.

29. Slutter B, Plapied L, Fievez V, Sande MA, des Rieux A, Schneider YJ, et al. Mechanistic study of the adjuvant effect of biodegradable nanoparticles in mucosal vaccination. Journal of controlled release : official journal of the Controlled Release Society. 2009 Sep 1;138(2):113-21. PubMed PMID: 19445980.

30. Cohen JA, Beaudette TT, Tseng WW, Bachelder EM, Mende I, Engleman EG, et al. T-cell activation by antigen-loaded pH-sensitive hydrogel particles in vivo: the effect of particle size. Bioconjugate chemistry. 2009 Jan;20(1):111-9. PubMed PMID: 19102625. Pubmed Central PMCID: 2640420.

31. Raghuwanshi D, Mishra V, Suresh MR, Kaur K. A simple approach for enhanced immune response using engineered dendritic cell targeted nanoparticles. Vaccine. 2012 Nov 26;30(50):7292-9. PubMed PMID: 23022399.

32. Rosalia RA, Silva AL, Camps M, Allam A, Jiskoot W, van der Burg SH, et al. Efficient ex vivo induction of T cells with potent anti-tumor activity by protein antigen encapsulated in nanoparticles. Cancer immunology, immunotherapy : CII. 2013 Jul;62(7):1161-73. PubMed PMID: 23613147.

33. Slutter B, Bal S, Keijzer C, Mallants R, Hagenaars N, Que I, et al. Nasal vaccination with N-trimethyl chitosan and PLGA based nanoparticles: nanoparticle characteristics determine quality and

strength of the antibody response in mice against the encapsulated antigen. Vaccine. 2010 Aug 31;28(38):6282-91. PubMed PMID: 20638455.

34. Liu Y, Ji F, Liu R. The interaction of bovine serum albumin with doxorubicin-loaded superparamagnetic iron oxide nanoparticles: spectroscope and molecular modelling identification. Nanotoxicology. 2013 Feb;7(1):97-104. PubMed PMID: 22087533.

35. Quah BJ, Parish CR. The use of carboxyfluorescein diacetate succinimidyl ester (CFSE) to monitor lymphocyte proliferation. Journal of visualized experiments : JoVE. 2010 Oct 12(44). PubMed PMID: 20972413. Pubmed Central PMCID: 3185625.

36. Bershteyn A, Hanson MC, Crespo MP, Moon JJ, Li AV, Suh H, et al. Robust IgG responses to nanograms of antigen using a biomimetic lipid-coated particle vaccine. Journal of controlled release : official journal of the Controlled Release Society. 2012 Feb 10;157(3):354-65. PubMed PMID: 21820024. Pubmed Central PMCID: 3811132.

37. Hanlon DJ, Aldo PB, Devine L, Alvero AB, Engberg AK, Edelson R, et al. Enhanced stimulation of anti-ovarian cancer CD8(+) T cells by dendritic cells loaded with nanoparticle encapsulated tumor antigen. Am J Reprod Immunol. 2011 Jun;65(6):597-609. PubMed PMID: 21241402. Pubmed Central PMCID: 3082607.

38. Tacken PJ, Zeelenberg IS, Cruz LJ, van Hout-Kuijer MA, van de Glind G, Fokkink RG, et al. Targeted delivery of TLR ligands to human and mouse dendritic cells strongly enhances adjuvanticity. Blood. 2011 Dec 22;118(26):6836-44. PubMed PMID: 21967977.

39. Petrizzo A, Conte C, Tagliamonte M, Napolitano M, Bifulco K, Carriero V, et al. Functional characterization of biodegradable nanoparticles as antigen delivery system. Journal of experimental & clinical cancer research : CR. 2015 Oct 06;34:114. PubMed PMID: 26444005. Pubmed Central PMCID: 4596393.

40. Silva JM, Videira M, Gaspar R, Preat V, Florindo HF. Immune system targeting by biodegradable nanoparticles for cancer vaccines. Journal of controlled release : official journal of the Controlled Release Society. 2013 Jun 10;168(2):179-99. PubMed PMID: 23524187.

41. Joshi MD, Unger WJ, Storm G, van Kooyk Y, Mastrobattista E. Targeting tumor antigens to dendritic cells using particulate carriers. Journal of controlled release : official journal of the Controlled Release Society. 2012 Jul 10;161(1):25-37. PubMed PMID: 22580109.

42. Rietscher R, Schroder M, Janke J, Czaplewska J, Gottschaldt M, Scherliess R, et al. Antigen delivery via hydrophilic PEG-b-PAGE-b-PLGA nanoparticles boosts vaccination induced T cell immunity. European journal of pharmaceutics and biopharmaceutics : official journal of Arbeitsgemeinschaft fur Pharmazeutische Verfahrenstechnik eV. 2016 May;102:20-31. PubMed PMID: 26940132.

43. Fromen CA, Robbins GR, Shen TW, Kai MP, Ting JP, DeSimone JM. Controlled analysis of nanoparticle charge on mucosal and systemic antibody responses following pulmonary immunization. Proceedings of the National Academy of Sciences of the United States of America. 2015 Jan 13;112(2):488-93. PubMed PMID: 25548169. Pubmed Central PMCID: 4299250.

# Chapter 6

## 6. General discussion, future directions and conclusions

### 6.1. General discussion

Although the discussions specific for Chapters 3-5 have been made, the intent of this chapter is to provide an overall discussion of the thesis work. The overall goal of the project was to understand the relationship between NP structure and activity, and address the key questions. This will in term direct to determine the best featured criteria for a targeted cancer vaccine.

Chapter 3 was about developing the best suitable method to prepare PLGA NPs. Emulsification solvent evaporation method was used to prepare NPs. Several modifications such as change in PVA concentration, switching between solvent types, modification in sonication time and amplitude, modification in centrifugation time and speed were performed based on trial and error method. Two solvents were employed to prepare NPs, from which ethyl acetate was chosen as the best one for further experiments. The next step was to select a suitable cryoprotectant from sucrose and trehalose. Sucrose was most suitable when the reconstitution of the nano-suspension was done. Formulations having cryoprotectant provided aggregation free colloidal dispersion. Several parameters were evaluated to obtain NPs with physicochemical properties. The major challenge of designing PLGA based targeted system was the ability to conjugate the anti-CD-205 Ab to the NPs. The non-covalent adsorption method was a simple process.(1) But the covalent bonding between the ligand and the BS3-NPs necessitate confirming by IR spectroscopy.(2) A proportional relationship between NP size and viscosity was observed for both plain and modified NPs. However, no significant relationship was observed between terminal group of PLGA and physicochemical properties. In addition, no significant correlation could be featured to compare the antibody loading through either of the methods (adsorption and covalent attachment). In conclusion, formulations prepared with ethyl acetate were promising for NP preparation and was further utilized in *ex-vivo* experiments.

Chapter 4 was based on the targeting efficiency assessment and expression of maturation markers on DCs. Formulations were developed with coumarin-6 fluorescent dye to assess the uptake of NPs by DCs. The mechanisms involved here was either phagocytosis or receptor mediated endocytosis.(3) Flow cytometry experiment with fluorescent dye loaded NPs showed that the ligand modified formulations were better uptaken by DCs when compared with the non-modified ones. High viscosity ester and COOH terminated coumarin-6 loaded NPs had higher uptake (AD>COV) which could be attributed due to higher amount of ligand loading on the NPs, though there was no significant difference in ligand loading on NPs. Another reason could be higher level of coumarin-6 loading in high viscosity grades contributed to greater MFI by those NPs. Maturation study of DCs demonstrates that ligand modified OVA-adjuvant loaded NPs performed higher upregulation of maturation markers. Though, the loading of OVA was higher in high viscosity grade polymers (ester or COOH terminated), the expression of markers were comparatively lower compared to low viscosity formulations. This could be attributed to less OVA release from the PLGA network. When evaluating the release pattern of OVA in the media for 20 days, a biphasic pattern was observed. The low viscosity PLGA NPs were found to release 50% of OVA within 24 hours (COOH ended) and 7 days (ester ended). About 14 days were required to release 50 % of OVA from the high viscosity PLGA NPs (both COOH and ester, where COOH>ester). Formulations had suitable physicochemical properties with 79-93% of cell viability after 3 days. In addition, sufficient secretion of T helper cell 1 (Th1) and Th2 cytokines was observed. This confirmed the maturation of DCs. Treatment of DCs with MPLA containing NPs released higher amount of Th1 cytokines (IFN-γ, IL-12, IL-2) than control groups. All the above results justify the successful delivery of targeted NP vaccine system *in-vitro* to assess their targeting efficiency and DC stimulatory immune response.

Chapter 5 describes the potentiating of antigen-specific immune response by targeted NPs during the vaccination study. The formulations developed (chapter 4) were assessed to observe their capability to stimulate T cells *in-vivo*. Three weeks' vaccination regimen was designed where WT mice were vaccinated twice. At the end of three weeks, spleens and lymph nodes were collected to co-culture T cells

with DCs. The co-culture was exposed to recall antigen, irrelevant antigen and no stimulation. It was seen that in presence of recall (relevant) antigen, the T cells had higher proliferation. In addition, sufficient quantity of cytokines was secreted in the DC: T cell microenvironment. All the four polymeric groups (low viscosity ester, high viscosity ester, low viscosity COOH and high viscosity COOH NPs) were evaluated for the T cell proliferation experiment. However, among all low viscosity COOH terminated OVA-PLGA NPs were most promising. The level of IgG secreted by several groups of low viscosity COOH terminated OVA loaded PLGA NPs was also high. The results obtained so far were indicative for further experiments to be carried out in OT1 mice. With 20 times lower dose of recall antigenic peptide SIINFEKL, the proliferation was higher than the WT mice. The proliferation of CD8+ T cells was most prominent when both OVA and MPLA are present in the formulations. The percent of CD8+ T cell proliferation and cytokine secretion by the targeted NPs confirmed the antigen-specific immune responses.

A systematic conclusion was drawn based on the observations. The following results could be concluded:

**A. Effect of polymer viscosity**

- A proportional relation was observed between polymer viscosity and the particle size. This was observed for both ester- and COOH- terminated polymers.
- Zeta potential value did not show any significant relation with polymer viscosity.
- High viscosity grade PLGA NPs showed slightly higher viability percentage. However, there was no significant difference in viability percentage for the OVA loaded NPs ester and COOH terminated NPs.
- A proportional relation between coumarin-6 loading and polymer viscosity of PLGA was observed, but it was not statistically significant.
- With increase in polymer viscosity the DC uptake also increased. Uptake was highest with the high viscosity ester terminated NPs.

- An inversely proportional relation was observed between polymer viscosity and the release of OVA over the specified time.
- With increase in viscosity the OVA loading increased, but it was not significant.
- Low viscosity formulations showed comparatively higher DC maturation than the high viscosity PLGA NPs.
- Low viscosity 0.18C-PLGA NPs showed higher secretion of IL-12, IL-6 and IFN-γ. And, 0.55C-PLGA NPs showed higher secretion of TNF-α in *in-vitro* stimulated DC media.
- Low viscosity COOH terminated NPs showed higher proliferation of CD3+T cells and cytokine secretion *in-vitro* compared to other groups

**B. Effect of polymer type**

- When comparing polymer type, the COOH-terminated polymers (low and high viscosity) provided smaller particles compared to ester-terminated polymers.

  This was not the case for OVA/OVA-MPLA loaded NPs. There was no correlation between particle size and polymer type.
- Zeta potential value did not show significant relationship with the polymer type (ester/COOH), though COOH terminated NPs had slightly higher negative charge.
- There was no significant change in viability percentage of DCs for different type of polymers.
- Coumarin-6 loading was not affected by polymer type.
- OVA loading was not affected by polymer type.
- Ester terminated targeted NPs had the highest uptake compared to targeted COOH terminated NPs.
- COOH terminated OVA loaded NPs showed comparatively higher OVA release than ester terminated NPs.
- DC maturation and polymer type did not show any correlation.
- There was no correlation between cytokine secretion *in-vitro* from stimulated DCs.

- COOH terminated NPs showed comparatively higher proliferation of CD3+ T cells than the ester terminated NPs.

**C. Effect of antibody attachment method**

- Covalently attached low viscosity COOH and ester terminated PLGA NPs resulted in smaller particle size compared to high viscosity polymers. Though the antibody loading between these groups was not significantly different. For the OVA-MPLA NPs same trend was observed. Whereas, for OVA-NPs the Ab-AD groups had smaller size than the Ab-COV groups.
- Zeta potential and antibody loading was not correlated.
- Zeta potential did not show any significant relation with bonding type.
- Bonding type has no significant effect on DC viability.
- Coumarin-6 loading had no significant relationship with bonding type.
- OVA loading had no significant relationship with bonding type.
- DC uptake of NPs increased when they were modified with anti-CD-205 antibody.
- Ab-adsorbed groups showed higher uptake than the covalently attached Ab-NP except 0.15E-NPs.
- Ab-adsorbed groups showed better maturation than the covalently attached Ab-NP.
- Ab-modified groups had higher secretion of cytokines compared to the non-modified groups.
- Ab-modified groups showed higher proliferation of both CD3+ and CD8+ T cells in *in-vitro*.

## 6.2 Future directions

Based on the mentioned outcomes, the objectives of this research were successful. The physicochemical properties of the NPs were suitable for subcutaneous delivery of this model vaccine. Simulation of formulation parameters can be performed by other researchers in future. In future, some extension of this experiment can be continued as follows:

i) Assessment of CD4 and CD8 T cell proliferation in WT mice
ii) Estimation and comparison of Th1 and Th2 CD4 cytokines
iii) Use of TLR4 knockout mice to observe the role of adjuvant in the PLGA carrier-OVA-MPLA tri-combination
iv) Granzyme and perforin expression in OT1 mice can be determined by flow cytometry using anti-human perforin and anti-human granzyme B antibodies
v) Assessment of CD4 effect in OT2 mice
vi) Experiments can be designed to load cancer antigens in the NPs with subsequent vaccination of mice followed by tumor challenge. Tumor growth can be monitored after booster dose of vaccine. Tumor size can be measured several times in a week using a slide caliper. Tumor volume can be estimated according to the formula: Tumor volume=0.5 X length X width$^2$
vii) Intracellular cytokines (IFN$\gamma$, IL-4) can be determined by flow cytometry staining

Therefore, critical factors like particle size, polymer degradability, adjuvant effect needs to be optimized during every step of development of nanocarriers capable of delivering the antigen. In general, it can be said that for effective antigen delivery to the DCs, detailed understanding of the three components (antigen, adjuvant and targeting moiety) of the delivery system is necessary to ensure batch to batch reproducibility.

## 6.3 Conclusion

Overall, a comprehensive evaluation of effect of formulation parameters was performed in this project. PLGA was evaluated in terms of its terminal group and viscosity to select the best suitable formulations to determine the dose-response relationship. Low viscosity COOH terminated PLGA NP was found to produce competitive immune response both *in-vitro* and *in-vivo*. These findings would be insightful when designing a vaccine for a specific type of cancer. In conclusion, the findings confirm that PLGA NPs carrying cancer antigens will be able to produce antigen specific immune responses. This response could be generalized to any type of cancer depending on the antigen loaded in NPs, which could be considered a vaccine for a wide range of cancer types. Yet, the understanding of DC immunobiology and formulation parameters that influences the immune response will evolve; it is obvious that particulate based delivery systems will become a reality in near future.

## 6.4 References

1. Karra N, Nassar T, Ripin AN, Schwob O, Borlak J, Benita S. Antibody conjugated PLGA nanoparticles for targeted delivery of paclitaxel palmitate: efficacy and biofate in a lung cancer mouse model. Small. 2013 Dec 20;9(24):4221-36. PubMed PMID: 23873835.
2. Jahan ST, Haddadi A. Investigation and optimization of formulation parameters on preparation of targeted anti-CD205 tailored PLGA nanoparticles. Int J Nanomedicine. 2015;10:7371-84. PubMed PMID: 26677326. Pubmed Central PMCID: 4677653.
3. Oh N, Park JH. Endocytosis and exocytosis of nanoparticles in mammalian cells. Int J Nanomedicine. 2014;9 Suppl 1:51-63. PubMed PMID: 24872703. Pubmed Central PMCID: 4024976.

# Appendix A

## A.1 Development and characterization of TMRD loaded NPs

TMRD loaded NPs were prepared by double-emulsification solvent evaporation method. TMRD is soluble in PBS and dissolved in the first aqueous phase. Sonication of the primary W/O phase provided a better nano-emulsion formation. Second sonication enhanced mixing the secondary aqueous phase (PVA) with the primary emulsion. The NPs were collected following washing the free PVA, which provided a white to light pink color. The NP preparation scheme is given in figure A.1.

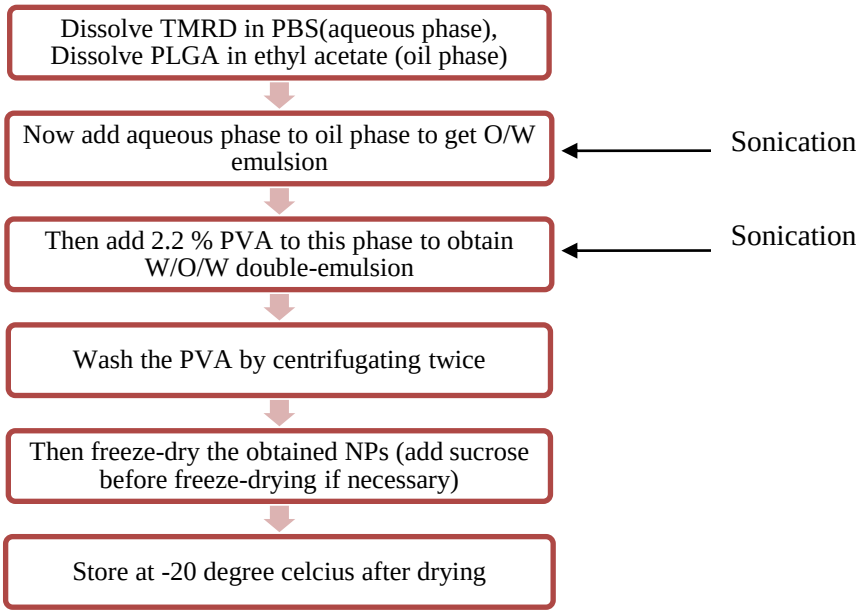


Figure A.1. Preparation scheme of TMRD loaded NPs

Tables A.1 summarize the characterization of TMRD loaded NPs in terms of their particle size, PDI and ZP. Plain NPs were prepared for all the PLGA categories (low and high viscosity) as the control groups. NPs containing cryoprotectants were prepared for only low viscosity (0.18 i.v. COOH and 0.15 i.v. ester) PLGA groups. Particle aggregation after freeze-drying was minimized using sucrose as a cryoprotectant. All the formulations as prepared for coumarin-6 loaded NPs were not formulated due to poor loading of

water-soluble TMRD. Some selected formulations were prepared with numbers of replicates before changing the fluorescent tag for preparing NPs for the uptake studies.

Table A.1: TMRD loaded COOH-terminated NPs prepared using method 2 (n=3)

| **Formulation** | **Recovery %** | **Particle size (nm)** | | **PDI** | | **ZP (mV)** | |
|---|---|---|---|---|---|---|---|
| | | **BFD** | **AFD** | **BFD** | **AFD** | **BFD** | **AFD** |
| 0.18C-NP | 46 % | 132±2 | 208±6 | 0.23±0.01 | 0.20±0.01 | -17.78±0.43 | -3.16±0.20 |
| 0.18C-NP+S | 54 % | 136±7 | 187±9 | 0.27±0.05 | 0.17±0.02 | -10.32±0.52 | -2.72±0.34 |
| 0.55C-NP | 49 % | 149±3 | 894±33 | 0.11±0.02 | 0.65±0.03 | -12.78±0.42 | -0.93±1.49 |
| 0.55C-NP+BS3 | 51 % | 135±1 | 523±3 | 0.23±0.01 | 0.35±0.01 | -5.06±0.32 | -1.42±0.03 |
| 0.15E-NP | 55% | 150±3 | 759±23 | 0.19±0.02 | 0.54±0.05 | -5.66±0.32 | -4.01±0.04 |
| 0.15E-NP+BS3 | 54 % | 163±4 | 432±4 | 0.19±0.01 | 0.43±0.02 | -9.88±0.34 | -5.53±0.29 |
| 0.15E-NP+S | 52% | 167±5 | 322±21 | 0.17±0.01 | 0.23±0.08 | -5.9±0.25 | -3.42±0.04 |
| 0.55E-NP | 56% | 148±3 | 553±6 | 0.14±0.01 | 0.32±0.09 | -10.9±0.43 | -3.48±0.83 |

Notes: Data are represented as mean±SD

Abbreviations: BFD= before freeze-drying, AFD=after freeze-drying, PDI=polydispersity index, C=COOH terminated PLGA, NP= Nanoparticle, ZP= Zeta potential, E=Ester terminated PLGA, S=Sucrose 10 %

**A.2 Characterization of antibody modified TMRD NPs**

Table A.2 contains BCA assay data for antibody modified NPs. COOH terminated and ester terminated NPs showed 3.12±0.23 and 3.31±0.43 μg of antibody per mg of NPs, respectively. These are the primary formulations selected to prepare antibody modified NPs. Antibody loading in the NPs were in reasonable range (2-3 μg/per of NP). The next step was to load TMRD in the NPs and determine the percentage of loading and EE.

Table A.2: Antibody attachment on TMRD loaded NPs prepared using method 2 (n=3)

| **Formulation** | **Particle size (nm)** | **PDI** | **ZP (mV)** | **EE of Ab (%)** | **Ab loading (μg/mg of NP)** |
|---|---|---|---|---|---|
| 0.18C-NP | 476±78 | 0.430±0.06 | -4.02±0.10 | 72.12 % | 2.89±0.87 |
| 0.18C-NP+S | 421±13 | 0.255±0.02 | -2.08±0.16 | 65.29% | 3.12±0.23 |
| 0.55C-NP | 511± 12 | 0.229±0.09 | -3.01±0.11 | 73.23 % | 3.11±0.34 |
| 0.55C-NP+BS3 | 145±1 | 0.157±0 | -2.89±0.24 | 69.92 % | 3.01±0.25 |
| 0.15E-NP | 667±12 | 0.487±0.08 | -5.79±0.21 | 68.45 % | 3.31±0.43 |
| 0.15E-NP+BS3 | 452±11 | 0.279±0.03 | -11.28±0.54 | 70.45 % | 3.16±0.15 |
| 0.15E-NP+S | 324±14 | 0.238±0.07 | -0.60±0.11 | 68.13 % | 2.75±0.47 |
| 0.55E-NP | 529±21 | 1.45±0.06 | -2.90±0.64 | 63.22 % | 2.91±0.45 |

Notes: Data are represented as mean±SD

Abbreviations: S= Sucrose (10%), PDI=polydispersity index, C=COOH terminated PLGA, E=Ester terminated PLGA, NP= Nanoparticle, ZP= Zeta potential, EE= Encapsulation efficiency, Ab=anti-CD205 antibody

### A.3 TMRD loading and encapsulation efficiency

2 mg of TMRD-loaded NPs was dispersed in 5.0 ml of 0.1 M NaOH solution containing 5% (w/v) sodium dodecyl sulphate (SDS). This mixture was stirred for 24 hours in dark at room temperature until a completely clear solution was obtained. The fluorescence intensity was measured at emission wavelength of 582 nm using a fluorescent spectrophotometer with a microplate reader. Analyses were performed by comparing the fluorescence intensity of each sample to a calibration curve obtained from standard solutions of TMRD in 0.1M NaOH containing 5% (w/v) SDS. (1)

Table A.3 represents the loading and encapsulation efficiency of TMRD in plain and antibody-modified NPs. It was observed that only 1.78±0.22 to 3.01±0.29 μg of TMRD was loaded per mg of plain NPs.

Besides, for antibody-modified NPs it was 1.22±0.85 to 2.29±0.87 μg of TMRD loaded per mg of modified NPs. This low amount of TMRD loading was further confirmed by fluorescence microscopy images of NPs. Figure A.2 shows presence of low amount of TMRD in the formulations when observed under fluorescence microscope.

Table A.3: TMRD loading and encapsulation efficiency in NPs (n=3)

| **Without antibody** | | | **With antibody** | |
|---|---|---|---|---|
| **Formulation** | **EE of TMRD (%)** | **TMRD loading (μg/mg of NP)** | **EE of TMRD (%)** | **TMRD loading (μg/mg of NP)** |
| 0.18C-NP | 40.2 % | 2.45±0.21 | 31.22 % | 1.49±0.09 |
| 0.18C-NP+S | 31.23 % | 2.23±0.18 | 28.40 % | 1.22±0.85 |
| 0.55C-NP | 45.72 % | 3.01±0.29 | 30.10 % | 2.29±0.87 |
| 0.55C-NP+BS3 | 21.48% | 1.78±0.22 | 23.56 % | 1.67±0.60 |
| 0.15E-NP | 32.57 % | 2.46±0.69 | 29.21 % | 2.01±0.22 |
| 0.15E-NP+BS3 | 23.11 % | 1.99±0.51 | 33.59 % | 1.56±0.17 |
| 0.15E-NP+S | 33.14 % | 2.23±0.18 | 27.22 % | 1.55±0.42 |
| 0.55E-NP | 25.99 % | 2.32±0.09 | 22.11 % | 1.34±0.04 |

Notes: Data are represented as mean±SD

Abbreviations: S= Sucrose (10%), PDI=polydispersity index, C=COOH terminated PLGA, E=Ester terminated PLGA, NP= Nanoparticle, ZP= Zeta potential, EE= Encapsulation efficiency

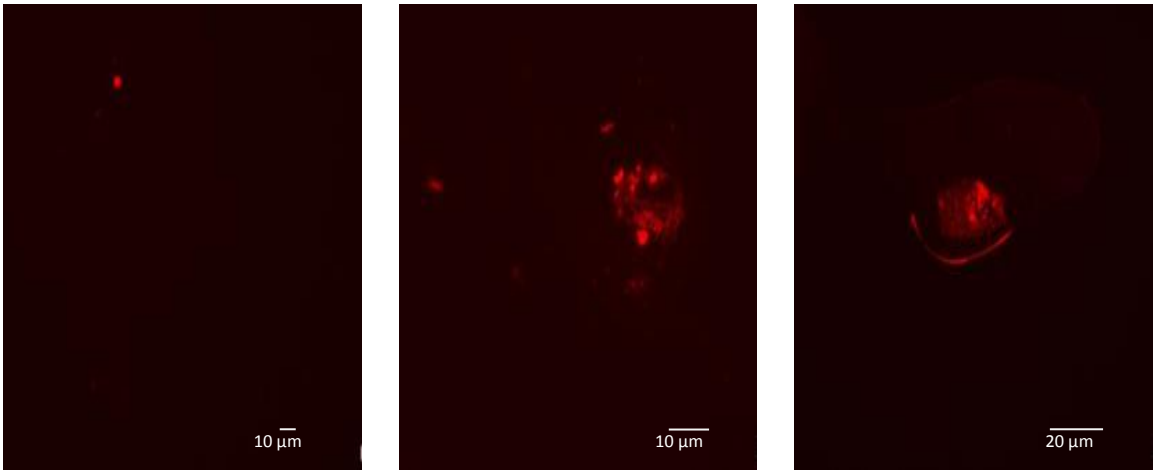


Figure A.2. Fluorescence microscopy images of TMRD loaded 0.18 COOH terminated PLGA NPs at magnification of 10,000 X

**A.4 DC uptake study with TMRD loaded NPs**

For this study, TMRD loaded NPs were used to evaluate their uptake by JAWSII (DC) cell lines. TMRD loaded NPs did not show any significant change in fluorescence which indicated poor uptake by DCs. This might be due to the low TMRD in NPs, which was previously confirmed by percentage of TMRD loading in NPs and fluorescent microscopy images.

Figure A.3 shows the fluorescence intensity changes between untreated and treated cells. The fluorescence intensity was measured for a standard number (10,000) of live cells. The MFI between treated and untreated groups was not significant.

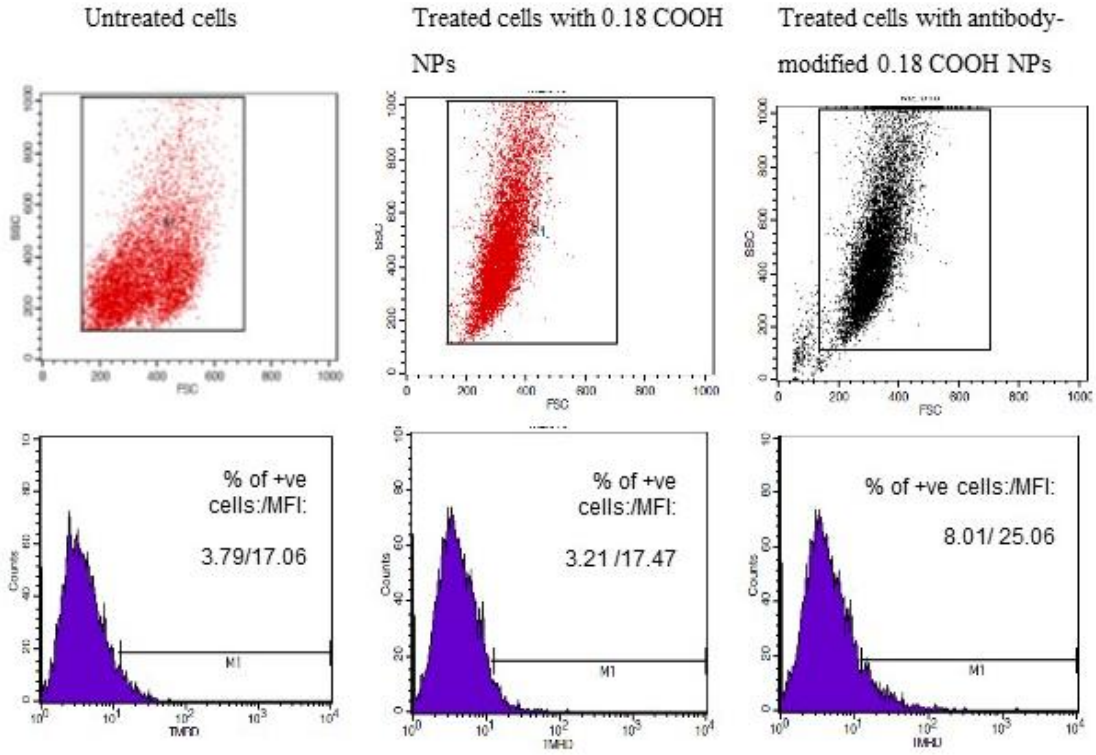


Figure A.3. DC uptake study with TMRD loaded PLGA NPs.

Notes: Dot plots and histograms in left panel represent untreated DCs, middle panel for 0.18C-TMRD-NPs and right panel for 0.18C-TMRD-AD NPs. Histograms show single color analysis of fluorescence. Numbers at the corner of histogram shows the percentage of positive cells for TMRD NPs and MFI. This is representative from triplicate.

### A.5. Discussion on Appendix A

The preparation of NPs loaded with TMRD was successful. The issue was lower loading of TMRD below the detection level in flow cytometry. This could be attributed to various reasons as mentioned below:

- TMRD leaking
- Weak support by the secondary aqueous phase ($W_1/O/W_2$)
- Use of ethyl acetate (polar solvent)

Despite of all these shortcomings, the ultimate solution was using a different fluorescent dye, strong support by the secondary aqueous phase or increasing PVA concentration and using of non-polar solvent, e.g. chloroform, dichloromethane.

Use of ethyl acetate, which is a polar solvent was continued for experiments with coumarin-6 dye. Coumarin-6 is soluble in ethyl acetate, so there is no need to change the concentration of the PVA (outer aqueous phase). Therefore, the chance of dye leaking was minimized. A dye which is soluble in organic phase will preferably remain in that phase along with PLGA. Evaporation of organic solvent will keep the coumarin-6 loaded in PLGA matrix, which is independent of the concentration of PVA. Therefore, an alternate fluorescent dye was used which could easily solubilise in ethyl acetate. Thus, NPs encapsulating coumarin-6 were further formulated to investigate the DC uptake.

# Appendix B

## B.1 Fluorescence microscopy images with coumarin-6 loaded PLGA NPs

Coumarin-loaded NP suspension observed under fluorescence microscope confirmed the presence of dye (figure B.1). This is a qualitative confirmation of presence of higher amount of coumarin-6 compared to TMRD.

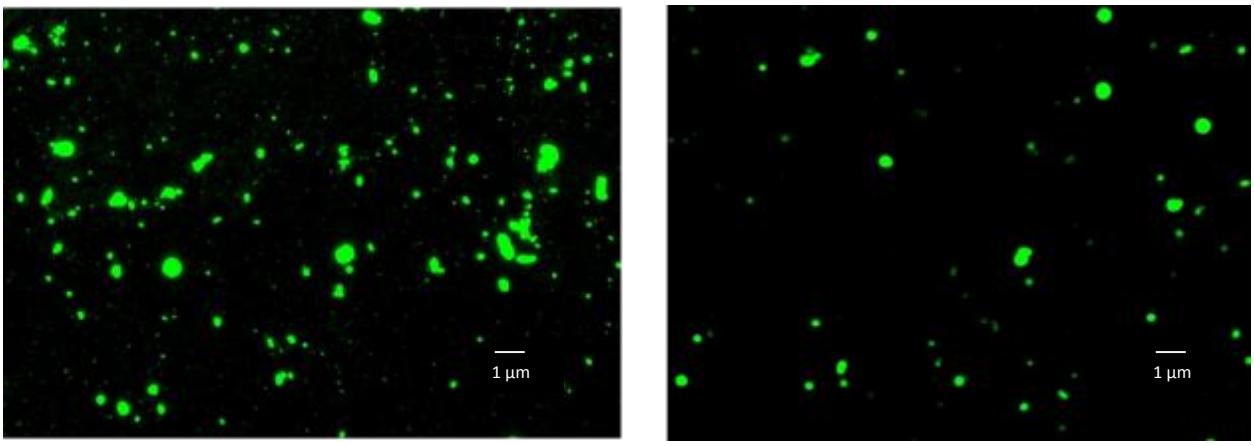


Figure B.1. Fluorescence microscopy images of TMRD loaded 0.18 COOH terminated PLGA NPs at magnification of 10,000 X and 40, 000 X

## B.2. Intracellular localization of coumarin-6 loaded PLGA NPs visualized by fluorescence microscopy

Fluorescence microscopy images were performed with coumarin-6 loaded PLGA NPs. This experiment is a complementary experiment that provides a qualitative assessment of the uptake of the NPs by DCs. On the day of sample preparation, cover slips of adhered cells were washed twice with ice-cold PBS and fixed with 4% paraformaldehyde. After that, the fixed cells were washed twice again with ice-cold PBS and the nuclei of the cells were counterstained with gold anti-fade reagent with DAPI prior to subject in the microscope. Figure B.2 represents the images for untreated and treated groups.

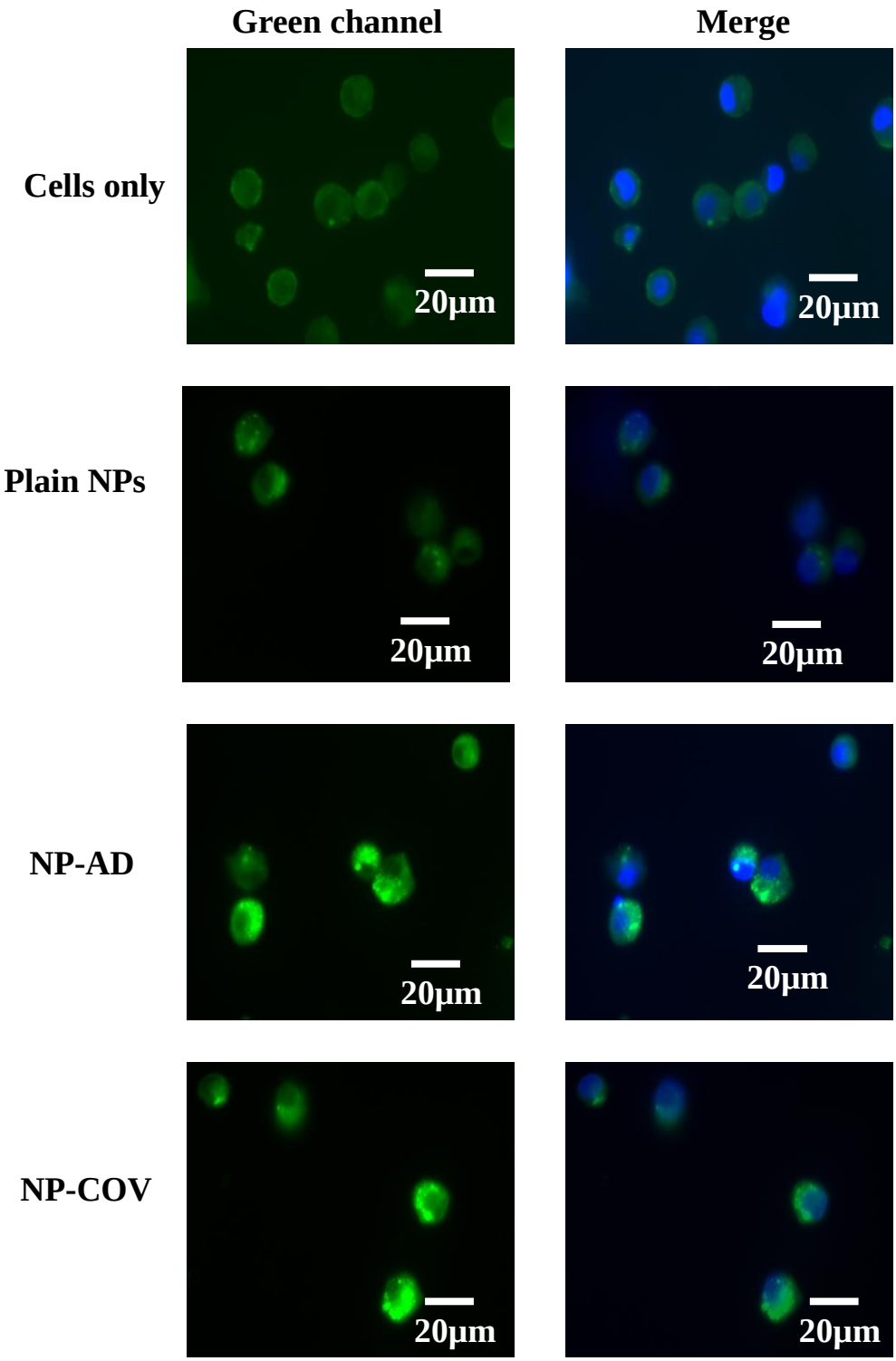


Figure B.2. Representative single stained (CD11c FITC) and double-stained (CD11c FITC and DAPI) fluorescence microscopy images for 0.18C-Cou-NPs. Notes: A) Untreated DCs, B) 0.18C-Cou-NPs, C)

0.18C-Cou-AD NPs, and D) 0.18C-Cou-COV NPs. Blue color represents the DAPI stained nuclei which are encompassed by green fluorescence for the groups treated with coumarin-6 loaded NPs.

# Appendix C

### C.1 Maturation study of DCs with CpG as adjuvant

To do the maturation study, the formulations contain the ovalbumin as a model antigen. The presence of foreign antigen will initiate the immature DCs to mature and trigger the upregulation of DC maturation markers. In order to potentiate and modulate the immune response an adjuvant, cytosine triphosphate guanine (CpG), was also added to the formulation loaded with OVA to compare with OVA-NPs. These NPs were prepared by W/O/W double emulsification solvent evaporation method. The formulations had high loading and encapsulation of OVA. Table C.1 contains the particle size, PDI, ZP, OVA EE and loading of OVA for low viscosity (0.18 iv) COOH terminated NPs. Standard curve equation in figure C.1 was used to determine the OVA content in NPs.

Table C.1. Particle size, PDI, ZP, EE of OVA (%) and OVA loading (μg/mg) of 0.18 iv COOH terminated PLGA NPs before and after Ab attachment (n=3)

| **Formulation** | **Size ± SD (nm)** | **PDI ± SD** | **ZP ± SD (mV)** | **EE of OVA ± SD (%)** | **OVA loading ± SD (μg/mg)** |
|---|---|---|---|---|---|
| 0.18C-OV-NP | 170±35 | 0.31±0.12 | -22.45±0.13 | 50.64±1.67 | 75.2±2.98 |
| 0.18C-OV+S NP | 153±7.56 | 0.30±0.26 | -20.75±0.31 | 51±1.22 | 42.1±1.24 |
| 0.18C-OV- AD NP | 543±23 | 0.48±0.23 | -15.01±0.24 | 44.65±0.43 | 46.4±4.44 |
| 0.18C-OV- AD+S NP | 327±11 | 0.31±0.71 | -10±0.33 | 45.23±0.61 | 40.54±2.67 |
| 0.18C-OV-CpG+S NP | 155±21 | 0.29±0.34 | -21.38±0.61 | 40.34±1.43 | 35.22±2.56 |

Notes: Data are represented as mean±SD

Abbreviations: S= Sucrose (10%), PDI=polydispersity index, C=COOH terminated PLGA, NP= Nanoparticle, ZP= Zeta potential, EE= Encapsulation efficiency, AD=Adsorption, OV=Ovalbumin

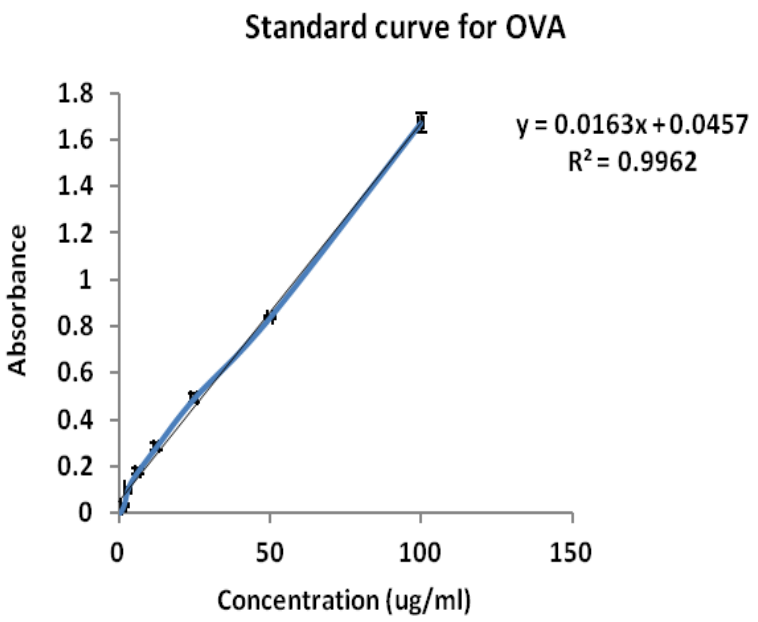


Figure C.1. Standard curve of Ovalbumin in 0.1 M NaOH containing 5% (w/v) SDS. The absorbance of samples and standards were measured at 562 nm in a 96 well plate with microplate reader.

In order to observe the maturation of DCs following the treatment with NP-antigen-adjuvant combination, this study was conducted. Flow cytometry analysis was conducted to investigate the upregulation of CD40, CD86 and MHCII molecules. After 24-hour incubation of cells treated with the formulations, cell suspension of specific number ($2X10^5$ cells/ml) was incubated with titrated amount of anti CD40, CD86 and MHCII with PE conjugated second antibodies. The isotype control of each antibody was used to measure the background fluorescence intensity for the relevant antibody. The gate for FACS analysis was set in such a way to represent the live cells. Figure C.2 represents the upregulation of maturation markers on DCs after 24 hours.

In figure C.2, the upregulation of CD40 marker for sucrose containing plain and modified NPs show 1.2 and 1.7 times increase in expression of CD40 compared to untreated cells, respectively. Figure C.2 shows 2.2 and 2.4 times increase in expression of CD86 on DC surface following the treatment with plain and antibody modified formulation, respectively. For CpG containing NPs the expression of CD86 and CD40

was not very significant. This could be attributed to the low loading of CpG in the NPs. Similarly, for MHCII molecules, the upregulation was 2.7 times for plain OVA containing NPs. In contrast, it was only two times for antibody-modified and CpG containing NPs. Thus, the NPs had poor ability to mature DCs when water-soluble CpG adjuvant was loaded. These results helped us to use an organic solvent soluble adjuvant (MPLA) to be used in the formulations.

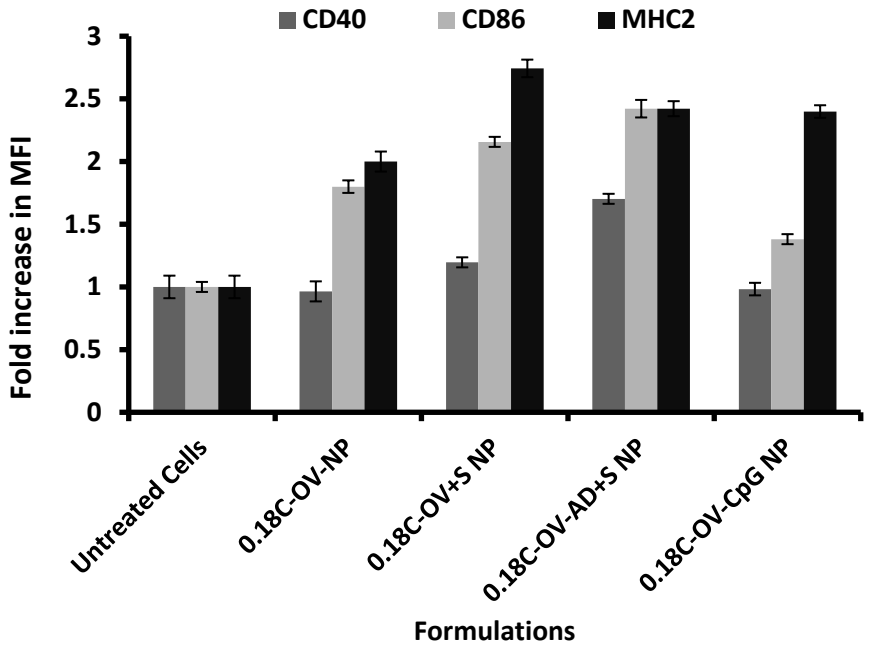


Figure C.2. Bar diagrams representing the fold increase in MFI for DC maturation markers after treatment with 0.18 iv COOH terminated PLGA NPs. Results are representative of at least three experiments.

Figure C.3 is a representation of expression of CD86 marker for untreated as well as treated DCs. The percentage of positive cells increased for plain NPs when compared with untreated cells. Moreover, when plain NPs were compared with antibody modified NPs, the percentage of positive cells did not increase but the MFI increased to 50.86 from 26.25. Similar dot plot and histograms were also obtained for CD40 and MHCII molecules (data not shown).

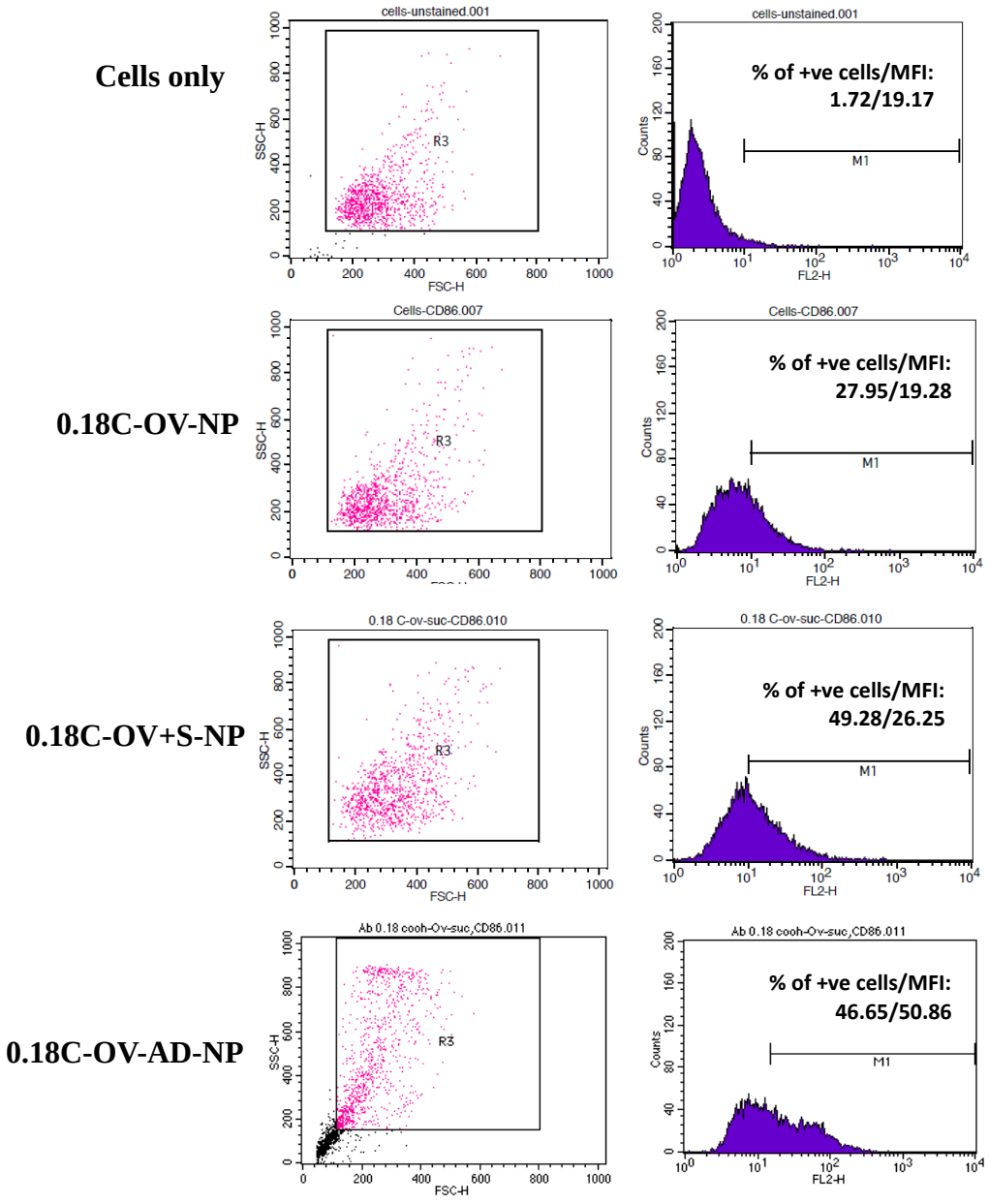


Figure C.3. Representative dot plot and histograms for 0.18C-OV-NPs. Notes: Effect of CD205 antibody modified PLGA NPs on the up-regulation of CD86 upon DC maturation. Untreated DC was used as negative control. After 24 hours of incubation, non-adherent cells were harvested, stained with the antibodies and analyzed by flow cytometry as described in the methods section. The top and bottom numeric values on the histograms represent percentages of positive cells and MFI for CD86 markers.

# Appendix D

**D.1 Maturation study with adjuvant MPLA loaded OVA NPs in presence of BS3**

Chapter 4 contains flow cytometry data for formulations with no BS3. The formulations with BS3 are represented here.

According to figure D.1 (A-D), the upregulation of maturation markers in different treatment groups indicate DC maturation. Specifically, CD86 and MHCII molecules were showing consistent upregulation in all the formulations. However, the higher expression of CD40 was found to vary between targeted and non-targeted NP groups. Therefore, it can be concluded that the presence of TLR4 ligand MPLA triggered the expression of the markers. This synthetic lipid induces strong protective Th1 based immunity with secretion of pro-inflammatory and inflammatory mediators.

Figure D.2 represents the cytokine secretion profile by four PLGA NP groups that contains BS3. There is significant difference in the cytokine secretion level by anti-CD205 Ab modified formulations compared to the control (Cells only and free OVA) ($p<0.05$).

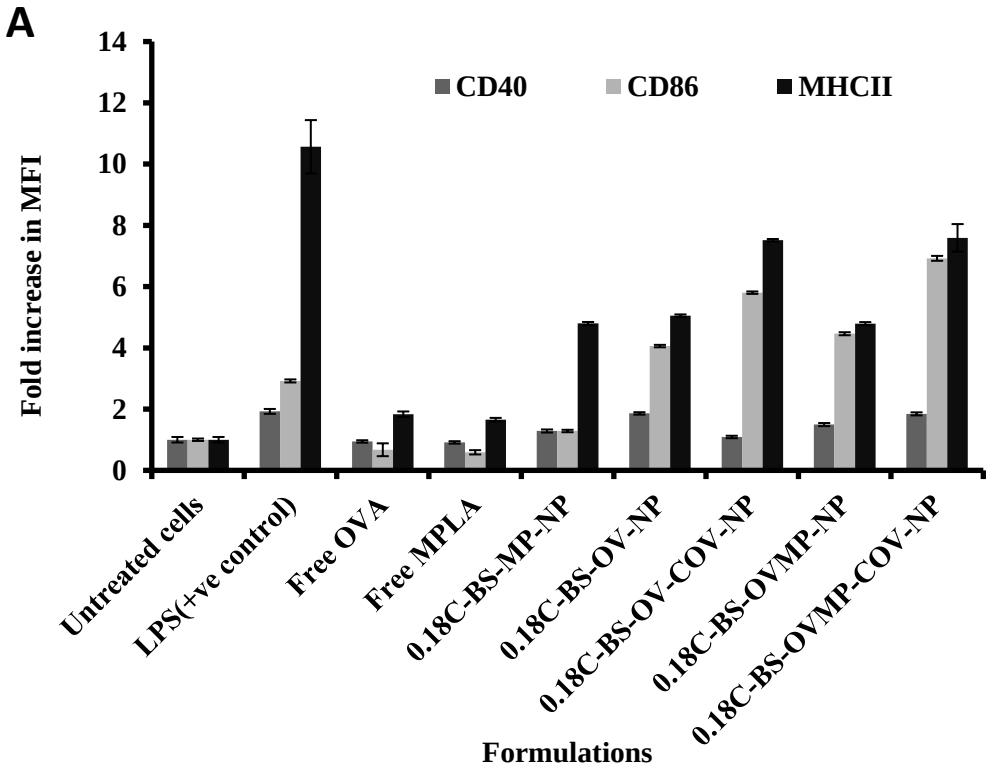

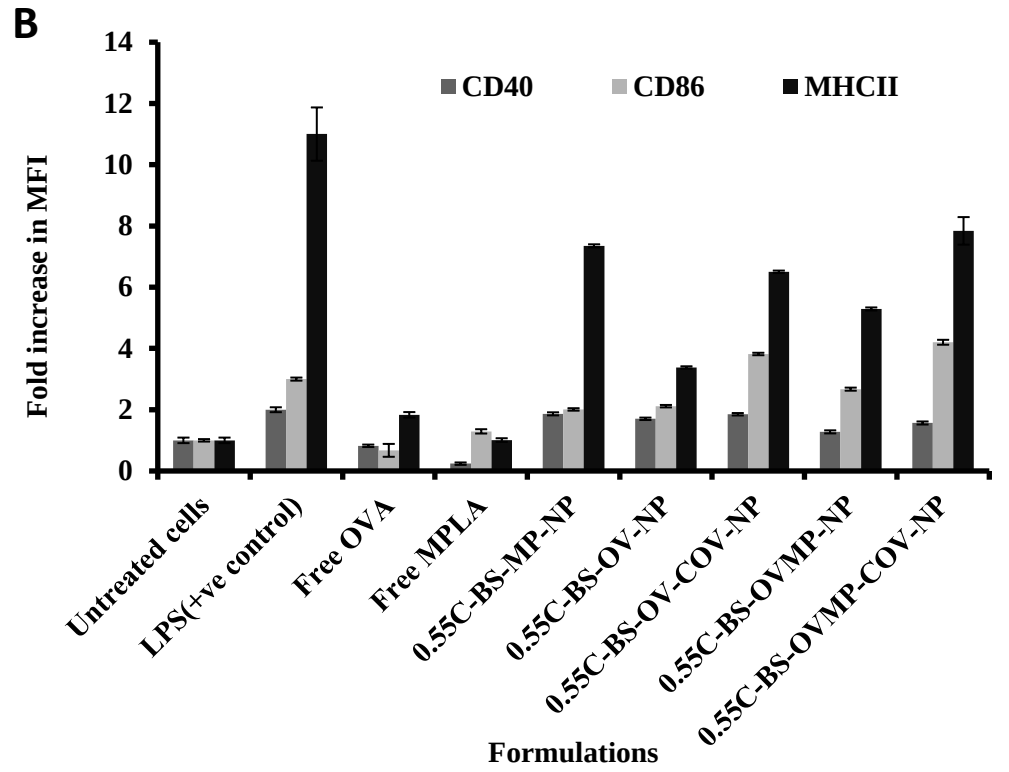
B
CD40
CD86
MHCII
Fold increase in MFI
0
2
4
6
8
10
12
14
Untreated cells
LPS(+ve control)
Free OVA
Free MPLA
0.55C-BS-MP-NP
0.55C-BS-OV-NP
0.55C-BS-OV-COV-NP
0.55C-BS-OVMP-NP
0.55C-BS-OVMP-COV-NP
Formulations

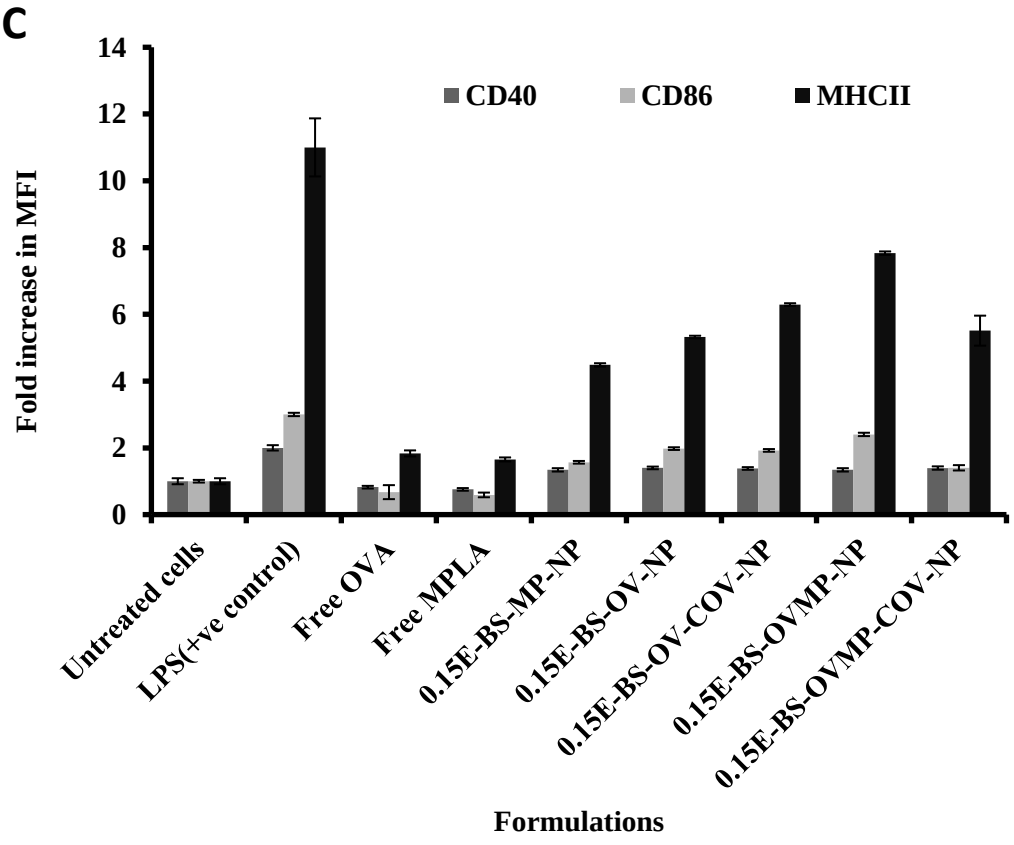
C
CD40
CD86
MHCII
Fold increase in MFI
0
2
4
6
8
10
12
14
Untreated cells
LPS(+ve control)
Free OVA
Free MPLA
0.15E-BS-MP-NP
0.15E-BS-OV-NP
0.15E-BS-OV-COV-NP
0.15E-BS-OVMP-NP
0.15E-BS-OVMP-COV-NP
Formulations

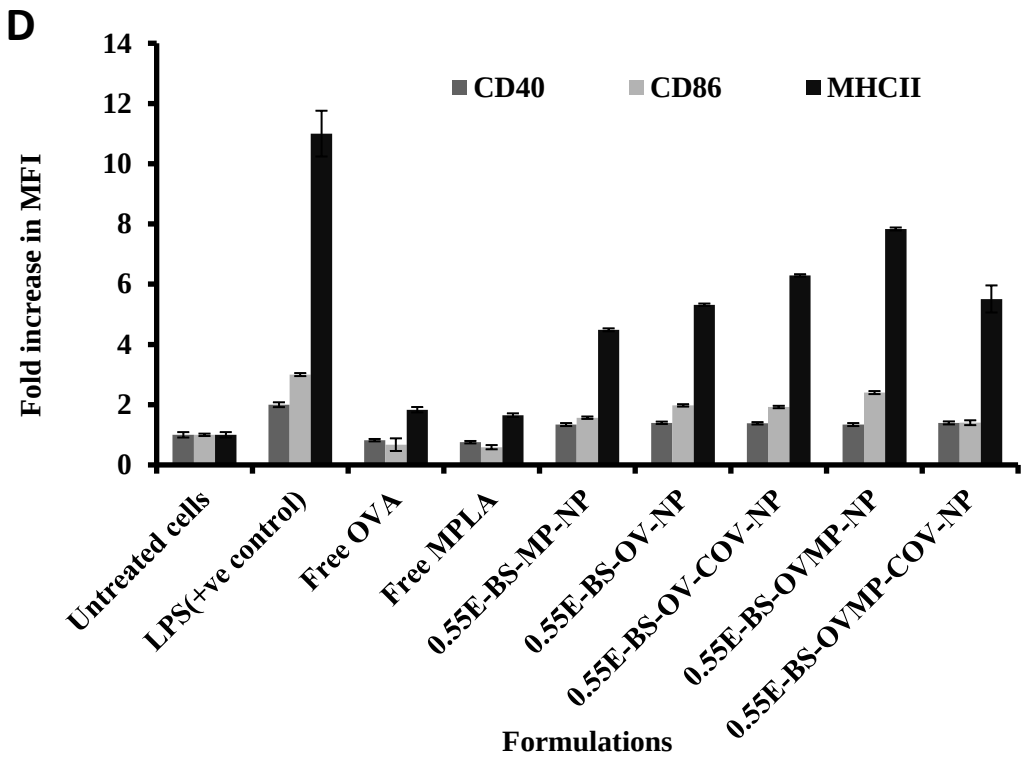


Figure D.1. Bar diagrams representing the fold increase in MFI for DC maturation markers after treatment with 0.18 iv COOH (A), 0.55 COOH (B), 0.15 ester (C), and 0.55 ester (D) terminated PLGA NPs containing BS3. Results are representative of at least three experiments.

Notes: Results are representative of at least three experiments. Fold increase in both cell types was calculated considering MFI of untreated cells (CD40 stained) as control. Each bar represents the mean % ± SD (n=3).

**A)**

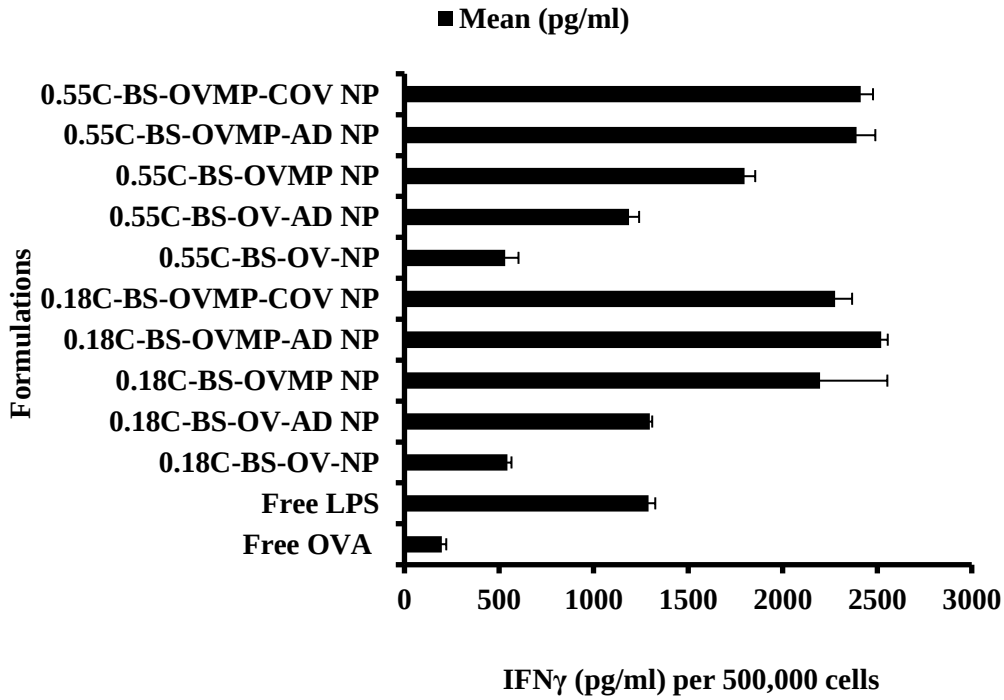
Mean (pg/ml)
0.55C-BS-OVMP-COV NP
0.55C-BS-OVMP-AD NP
0.55C-BS-OVMP NP
0.55C-BS-OV-AD NP
0.55C-BS-OV-NP
0.18C-BS-OVMP-COV NP
0.18C-BS-OVMP-AD NP
0.18C-BS-OVMP NP
0.18C-BS-OV-AD NP
0.18C-BS-OV-NP
Free LPS
Free OVA
Formulations
0
500
1000
1500
2000
2500
3000
IFNγ (pg/ml) per 500,000 cells

**B)**

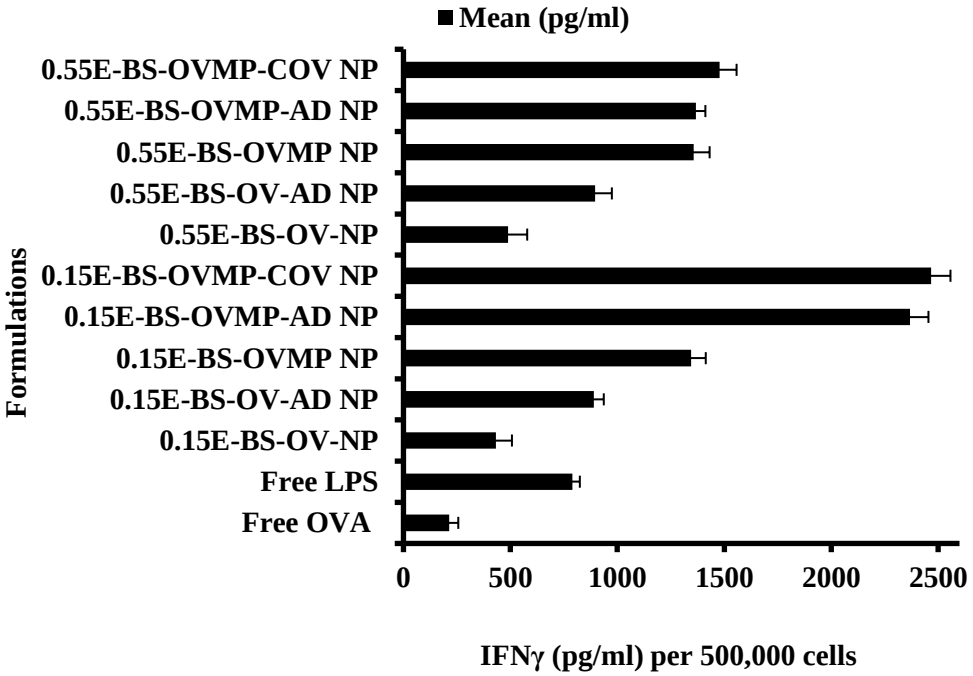
Mean (pg/ml)
0.55E-BS-OVMP-COV NP
0.55E-BS-OVMP-AD NP
0.55E-BS-OVMP NP
0.55E-BS-OV-AD NP
0.55E-BS-OV-NP
0.15E-BS-OVMP-COV NP
0.15E-BS-OVMP-AD NP
0.15E-BS-OVMP NP
0.15E-BS-OV-AD NP
0.15E-BS-OV-NP
Free LPS
Free OVA
Formulations
0
500
1000
1500
2000
2500
IFNγ (pg/ml) per 500,000 cells

C)

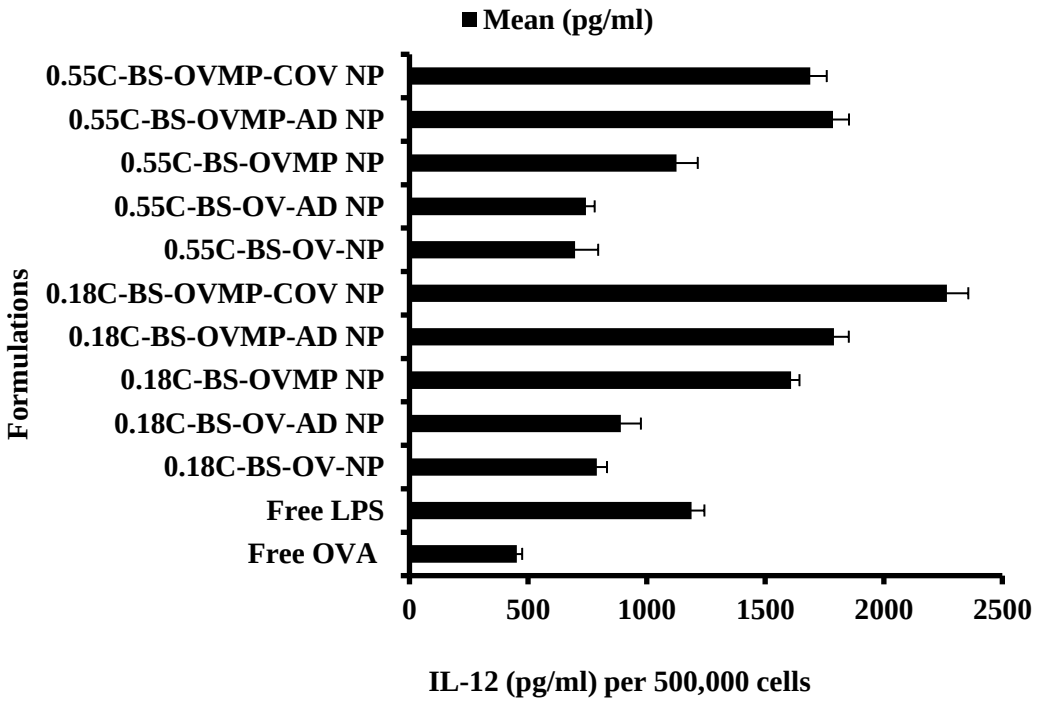
Mean (pg/ml)
0.55C-BS-OVMP-COV NP
0.55C-BS-OVMP-AD NP
0.55C-BS-OVMP NP
0.55C-BS-OV-AD NP
0.55C-BS-OV-NP
0.18C-BS-OVMP-COV NP
0.18C-BS-OVMP-AD NP
0.18C-BS-OVMP NP
0.18C-BS-OV-AD NP
0.18C-BS-OV-NP
Free LPS
Free OVA
Formulations
0
500
1000
1500
2000
2500
IL-12 (pg/ml) per 500,000 cells

D)

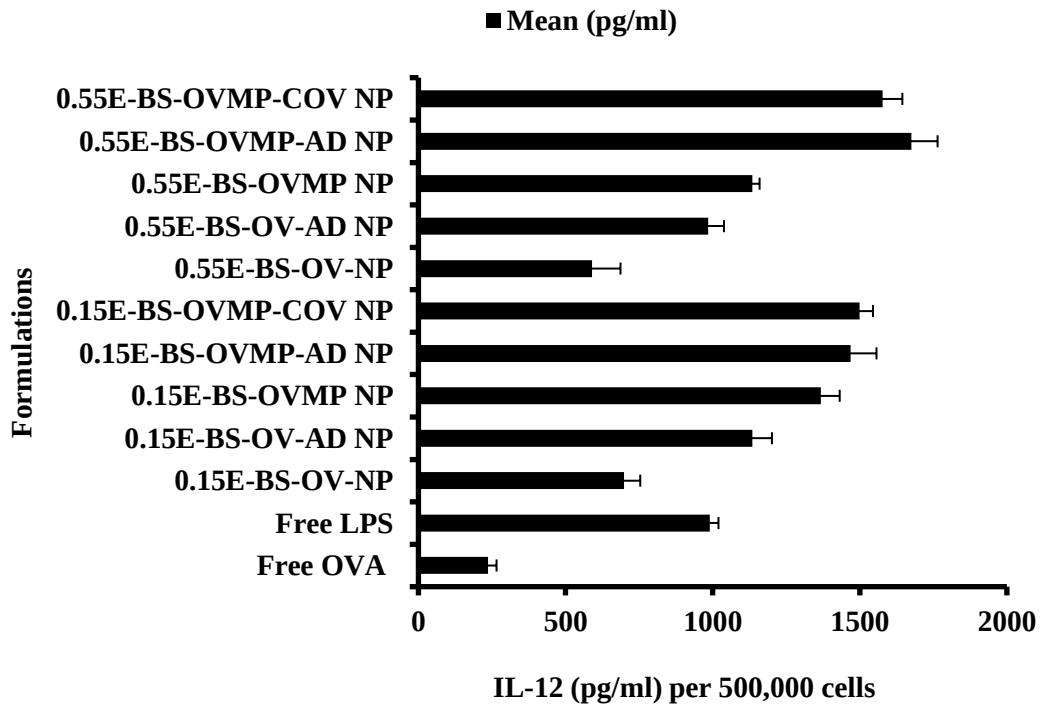
Mean (pg/ml)
0.55E-BS-OVMP-COV NP
0.55E-BS-OVMP-AD NP
0.55E-BS-OVMP NP
0.55E-BS-OV-AD NP
0.55E-BS-OV-NP
0.15E-BS-OVMP-COV NP
0.15E-BS-OVMP-AD NP
0.15E-BS-OVMP NP
0.15E-BS-OV-AD NP
0.15E-BS-OV-NP
Free LPS
Free OVA
Formulations
0
500
1000
1500
2000
IL-12 (pg/ml) per 500,000 cells

**E)**

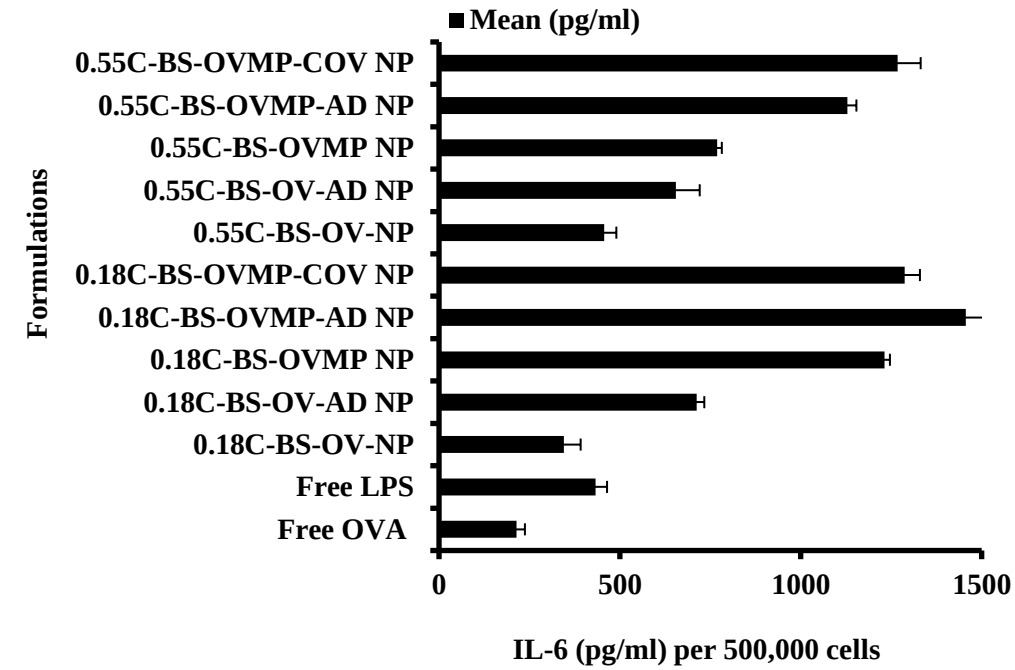
Mean (pg/ml)
0.55C-BS-OVMP-COV NP
0.55C-BS-OVMP-AD NP
0.55C-BS-OVMP NP
0.55C-BS-OV-AD NP
0.55C-BS-OV-NP
0.18C-BS-OVMP-COV NP
0.18C-BS-OVMP-AD NP
0.18C-BS-OVMP NP
0.18C-BS-OV-AD NP
0.18C-BS-OV-NP
Free LPS
Free OVA
Formulations
0
500
1000
1500
IL-6 (pg/ml) per 500,000 cells

**F)**

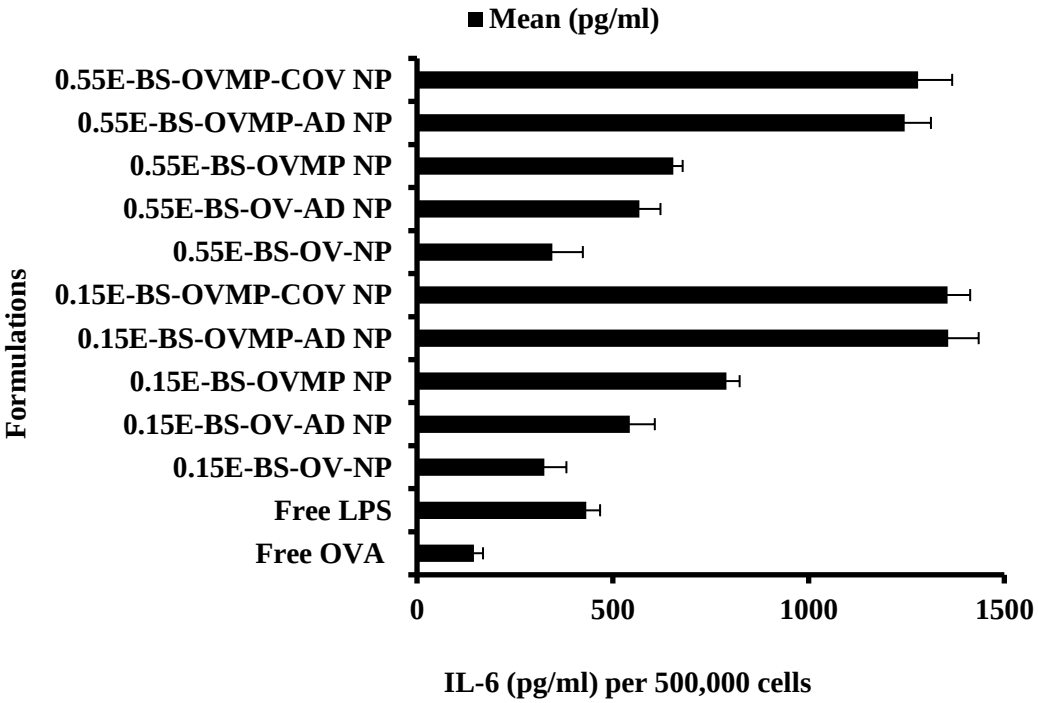
Mean (pg/ml)
0.55E-BS-OVMP-COV NP
0.55E-BS-OVMP-AD NP
0.55E-BS-OVMP NP
0.55E-BS-OV-AD NP
0.55E-BS-OV-NP
0.15E-BS-OVMP-COV NP
0.15E-BS-OVMP-AD NP
0.15E-BS-OVMP NP
0.15E-BS-OV-AD NP
0.15E-BS-OV-NP
Free LPS
Free OVA
Formulations
0
500
1000
1500
IL-6 (pg/ml) per 500,000 cells

G)

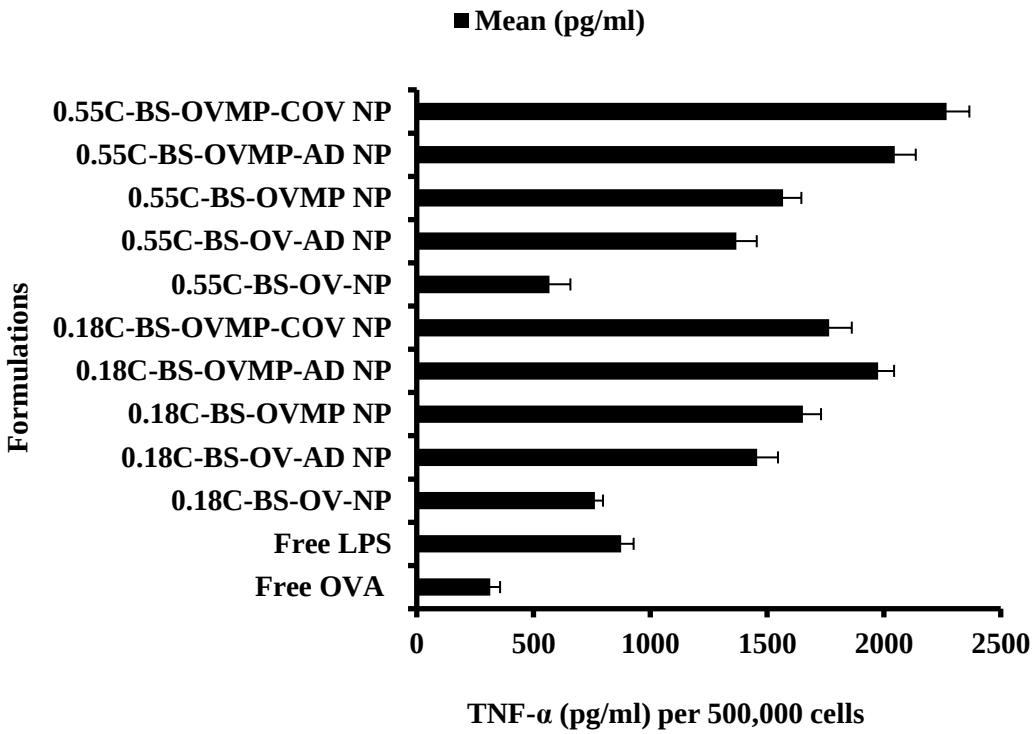
Mean (pg/ml)
0.55C-BS-OVMP-COV NP
0.55C-BS-OVMP-AD NP
0.55C-BS-OVMP NP
0.55C-BS-OV-AD NP
0.55C-BS-OV-NP
0.18C-BS-OVMP-COV NP
0.18C-BS-OVMP-AD NP
0.18C-BS-OVMP NP
0.18C-BS-OV-AD NP
0.18C-BS-OV-NP
Free LPS
Free OVA
Formulations
0
500
1000
1500
2000
2500
TNF-α (pg/ml) per 500,000 cells

H)

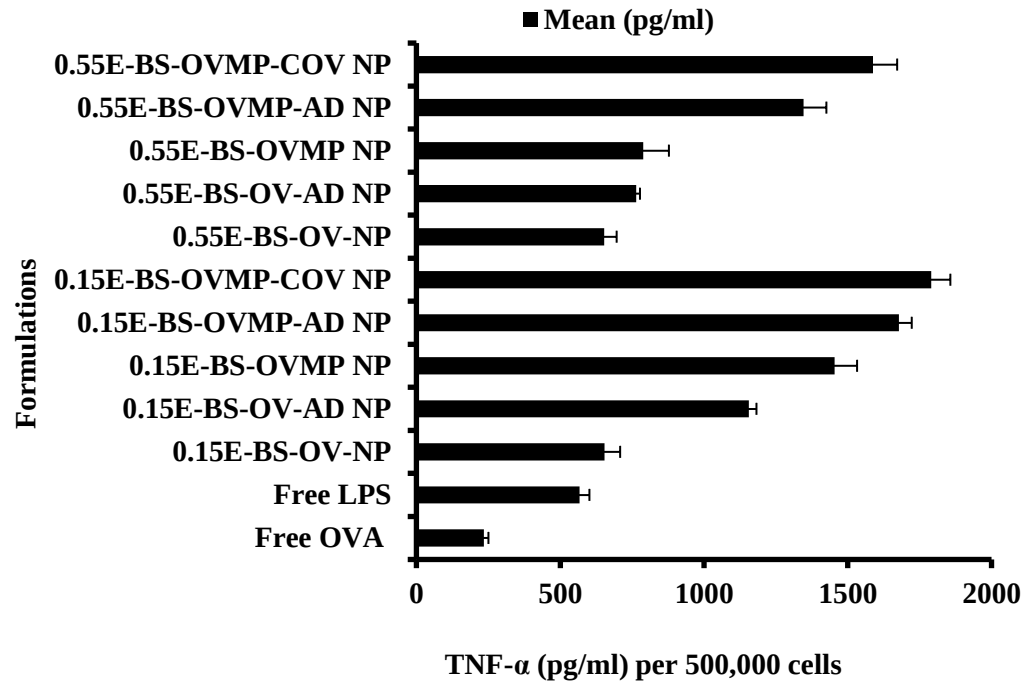
Mean (pg/ml)
0.55E-BS-OVMP-COV NP
0.55E-BS-OVMP-AD NP
0.55E-BS-OVMP NP
0.55E-BS-OV-AD NP
0.55E-BS-OV-NP
0.15E-BS-OVMP-COV NP
0.15E-BS-OVMP-AD NP
0.15E-BS-OVMP NP
0.15E-BS-OV-AD NP
0.15E-BS-OV-NP
Free LPS
Free OVA
Formulations
0
500
1000
1500
2000
TNF-α (pg/ml) per 500,000 cells

Figure D.2: Effect of OVA/OVA-MPLA NPs for cytokines secretion from mature DCs. After 24 hours of incubation, DC culture supernatants were analyzed for IFNγ (A, B), IL-12, (C, D), IL-6 (E, F), and TNF-α (G, H) secretion. This figure is representative for BS3 containing 0.18 iv COOH, 0.55 iv COOH, 0.15 ester, and 0.55 ester terminated plain and anti-CD205 tailored NPs (n=3) ($p<0.05$).

# Appendix E

## E.1 CD spectra of OVA loaded 0.15 iv ester terminated PLGA NPs

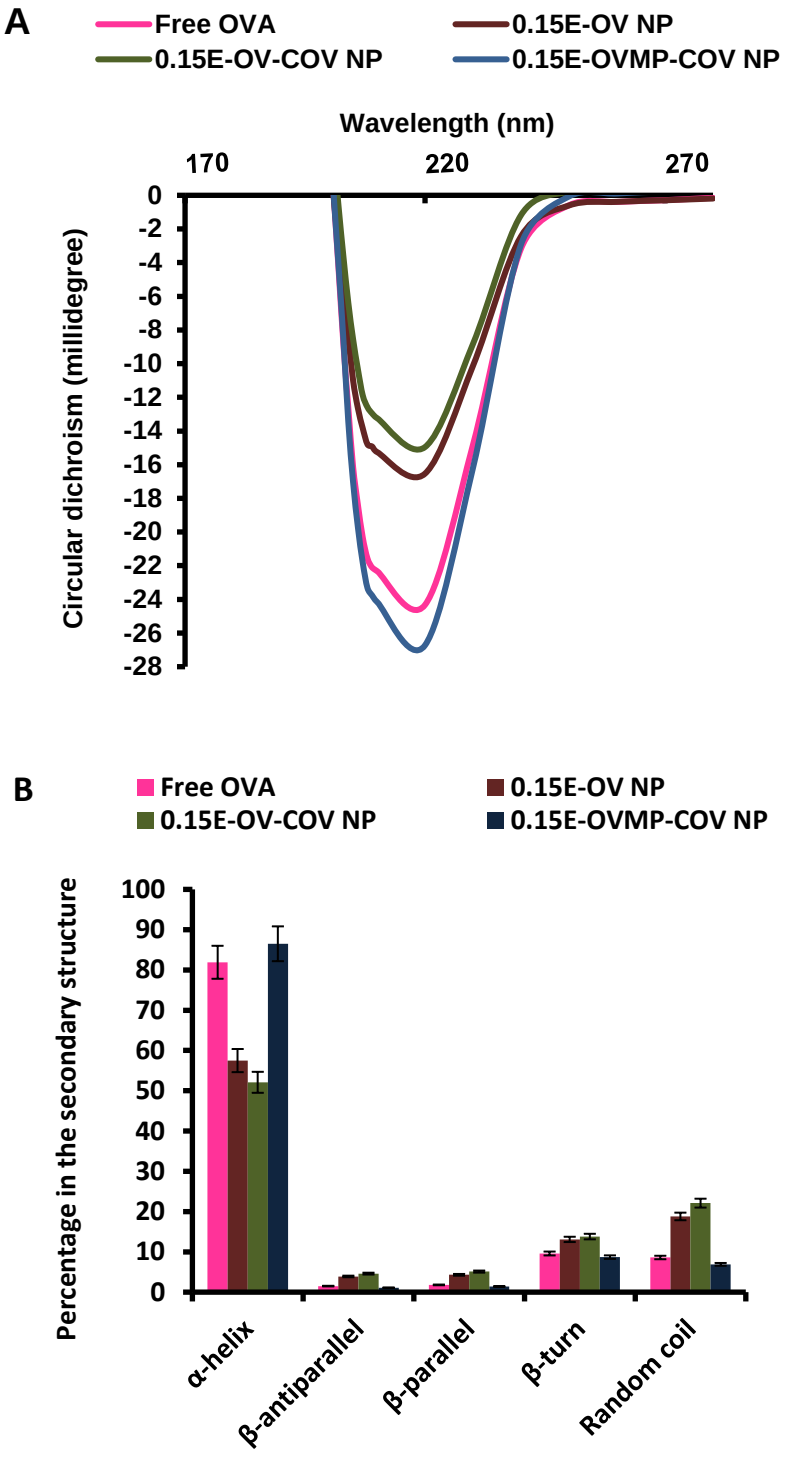

Figure E.1 A) Representative CD spectra of 0.15 ester terminated PLGA NPs. B) Percentages of α-helix, β-anti-parallel, β-parallel, β-turn and random coil of the secondary structure for free OVA, 0.15E-OV-NP, 0.15E-OV-COV NP and 0.15E-OVMP-COV NP after 20 days in PBS media. (n=3)

# Appendix F

## F.1 T cell proliferation study

### F.1.1 Assessment of proliferation with WT balb/c mice by CFSE method

DC and T cell co-culture was assessed with a starting cell number of T cells ($1X10^6$) and DCs ($2X10^5$) for 96 hours. CFSE method was employed to analyze the proliferation of overall T cells. T cells were stained with fluorescent dye CFSE to observe for 4 days. The formulations mentioned here are 0.18 COOH terminated, 0.55 COOH terminated, 0.15 ester terminated and 0.55 ester terminated NPs with OVA and MPLA. The restimulation of the WT mice isolated CD3+T cells with relevant protein (OVAendofit, 20µM) and irrelevant protein (KLH, 20µM) was performed during co-culture (day1).

Figure F.1 (A) represents the histogram for free OVA and free OVMP treated groups. The unimmunized mice show no (0 %) proliferation after 96 hours. IL-2 re-stimulated mice showed 57.1 % cells to be divided with generations (seven) distributed in all stages. Free OVA treated mice T cells showed most of its population in generation 'zero' even after re-stimulation. This was also reflected in cytokine secretion profile. Free OVMP treated mice showed about 51 % divided population within 4 days. There was significant increase in CFSE+CD3+ (96.5 %) in Ovaendo re-stimulated population compared to its non-stimulated group (50.6%). Besides, free OVA (Ovaendo), free OVA (KLH), free OVA (No Ag), and free OVMP (Ovaendo), free OVMP (KLH), free OVMP (No Ag) showed 14.9 %. 8.77 %, 1.56 %, 50.9 %, 15.5 % and 6.54 % proliferating cells, respectively.

The percent divided by 0.18C-OV NP (KLH), 0.18C-OV NP (No Ag), 0.18C-OVMP NP (KLH), 0.18C-OVMP NP (No Ag), 0.18C-OV-AD NP (KLH), 0.18C-OV-AD NP (No Ag), 0.18C-OVMP-AD NP (KLH), 0.18C-OVMP-AD NP (No Ag) was 46.4 %, 55 %, 1.93 %, 3.22 %, 39.1 %, 43.4 %, 5.18 % and 2.95 %, respectively.

The percent divided by 0.55C-OV NP (Ovaendo), 0.55C-OV NP (KLH), 0.55C-OV NP (No Ag), 0.55C-OVMP NP (Ovaendo), 0.55C-OVMP NP (KLH), 0.55C-OVMP NP (No Ag), 0.55C-OV-AD NP (Ovaendo), 0.55C-OV-AD NP (KLH), 0.55C-OV-AD NP (No Ag), 0.55C-OVMP-AD NP (Ovaendo),

0.55C-OVMP-AD NP (KLH), 0.55C-OVMP-AD NP (No Ag) was 12.8 %, 6.54 %, 6.81 %, 15.3 %, 8.87 %, 8.74 %, 13.9 %, 10.7 %, 10.8 %, 15.2 %, 5.39 % and 4.76 %, respectively. Similarly, histograms in figure 59 (I-IV) follows the same trend. This represents histograms for 0.55C-OV-BS-NP, 0.55C-OVMP-BS-NP, 0.55C-OV-COV-NP AND 0.55C-OVMP-COV-NP treated groups.

Figure F.1 (E) represents the histograms for 0.15 ester OVA and OVA-MPLA NPs. 0.15E-OVMP-NP shows higher distribution of cells in different generations in presence of relevant antigen. Whereas, in presence of KLH or no stimulation *in-vitro* the % of positive cells (CFSE-CD3) is limited up to generation 2. The percent divided by 0.15E-OV NP (Ovaendo), 0.15E-OV NP (KLH), 0.15E-OV NP (No Ag), 0.15E-OVMP NP (Ovaendo), 0.15E-OVMP NP (KLH), 0.15E-OVMP NP (No Ag), was 33.2 %, 15.6 %, 67.6 %, 22.4 %, 7.02 % and 46.3 %, respectively.

Figure F.1 (F, G) represents the histograms for 0.55E-OV-NP, 0.55E-OV-MP-NP, 0.55E-OV-AD-NP and 0.55E-OVMP-AD-NP treated groups. There was no consistency in % of fluorescence shift before and after re-stimulation.

The percent divided by 0.55E-BS-OV NP (Ovaendo), 0.55E-BS-OV NP (KLH), 0.55E-BS-OV NP (No Ag), 0.55E-BS-OVMP NP (Ovaendo), 0.55E-BS-OVMP NP (KLH), 0.55E-BS-OVMP NP (No Ag), 0.55E-BS-OV-COV NP (Ovaendo), 0.55E-BS-OV-COV NP (KLH), 0.55E-BS-OV-COV NP (No Ag), 0.55E-BS-OVMP-COV NP (Ovaendo), 0.55E-BS-OVMP-COV NP (KLH), 0.55E-BS-OVMP-COV NP (No Ag) was 13.6 %, 21.1 %, 20.7 %, 10.3 %, 8.56 %, 11.7 %, 85.4 %, 83.4 %, 15.5 %, 17.8 %, 36.7 % and 15 %, respectively.

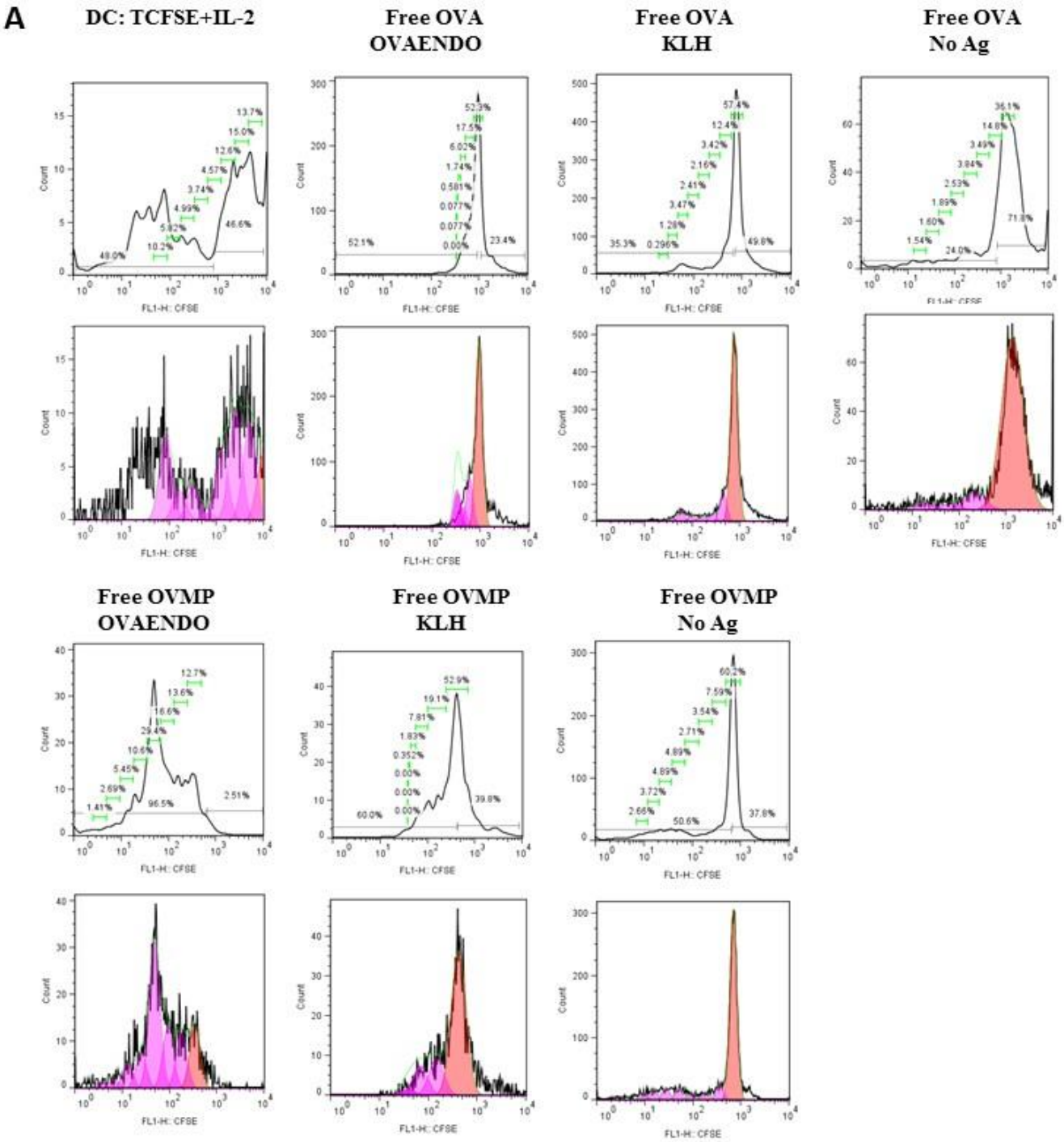
A
DC: TCFSE+IL-2
Free OVA
OVAENDO
Free OVA
KLH
Free OVA
No Ag
Free OVMP
OVAENDO
Free OVMP
KLH
Free OVMP
No Ag
Count
FL1-H: CFSE

**B**

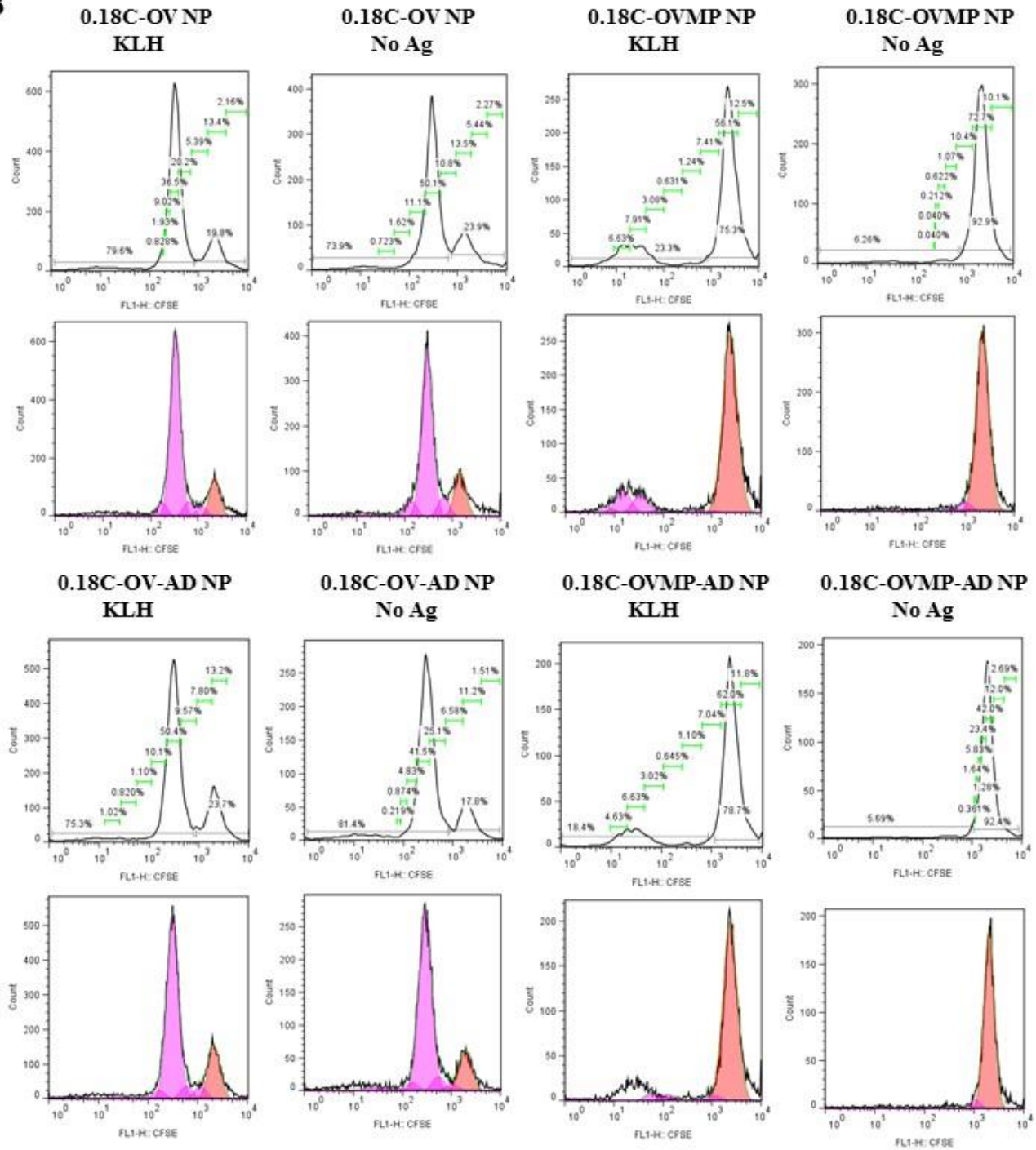
0.18C-OV NP
KLH
0.18C-OV NP
No Ag
0.18C-OVMP NP
KLH
0.18C-OVMP NP
No Ag
0.18C-OV-AD NP
KLH
0.18C-OV-AD NP
No Ag
0.18C-OVMP-AD NP
KLH
0.18C-OVMP-AD NP
No Ag
Count
FL1-H: CFSE

C

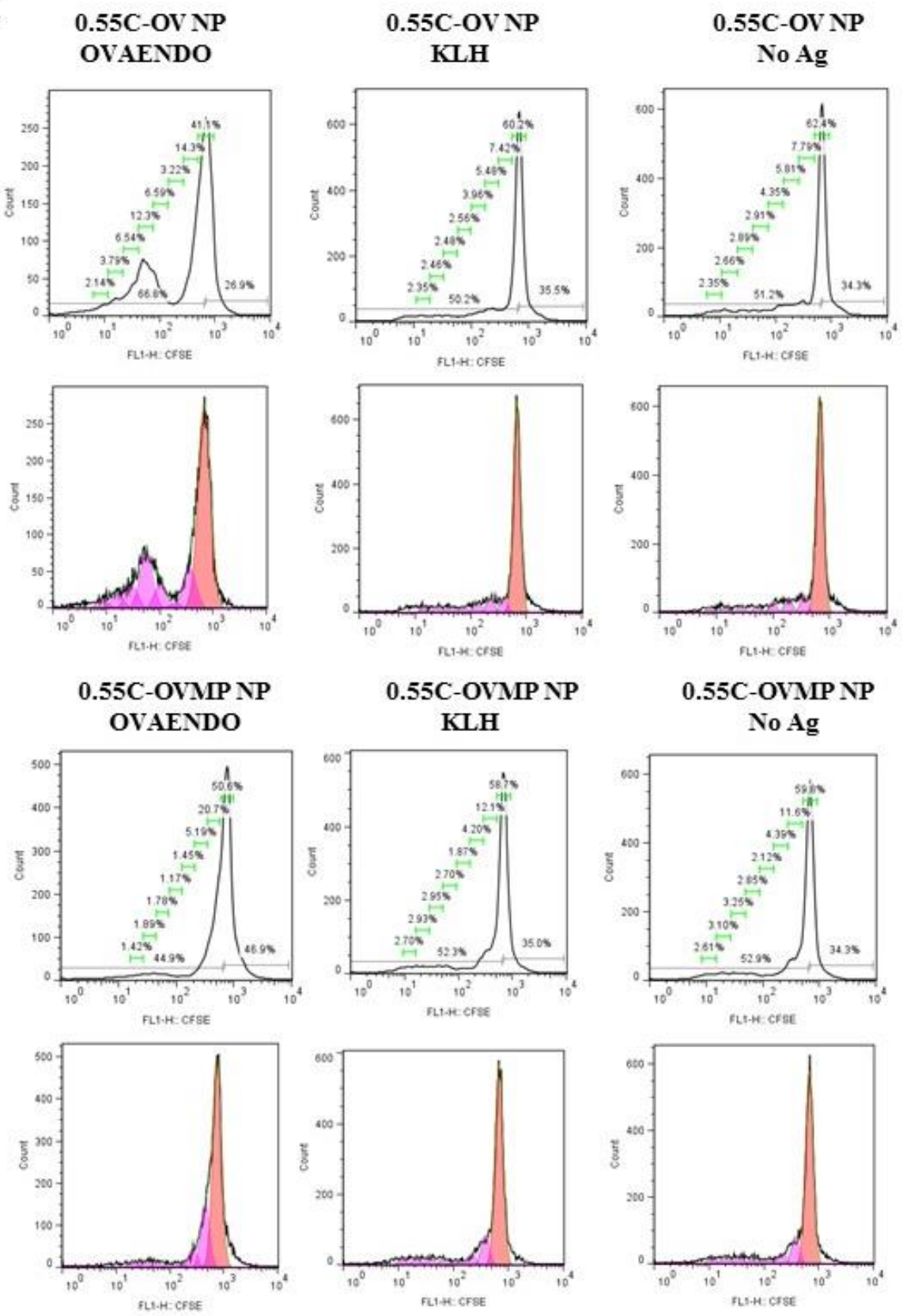
0.55C-OV NP
OVAENDO
0.55C-OV NP
KLH
0.55C-OV NP
No Ag
0.55C-OVMP NP
OVAENDO
0.55C-OVMP NP
KLH
0.55C-OVMP NP
No Ag
Count
FL1-H: CFSE

D

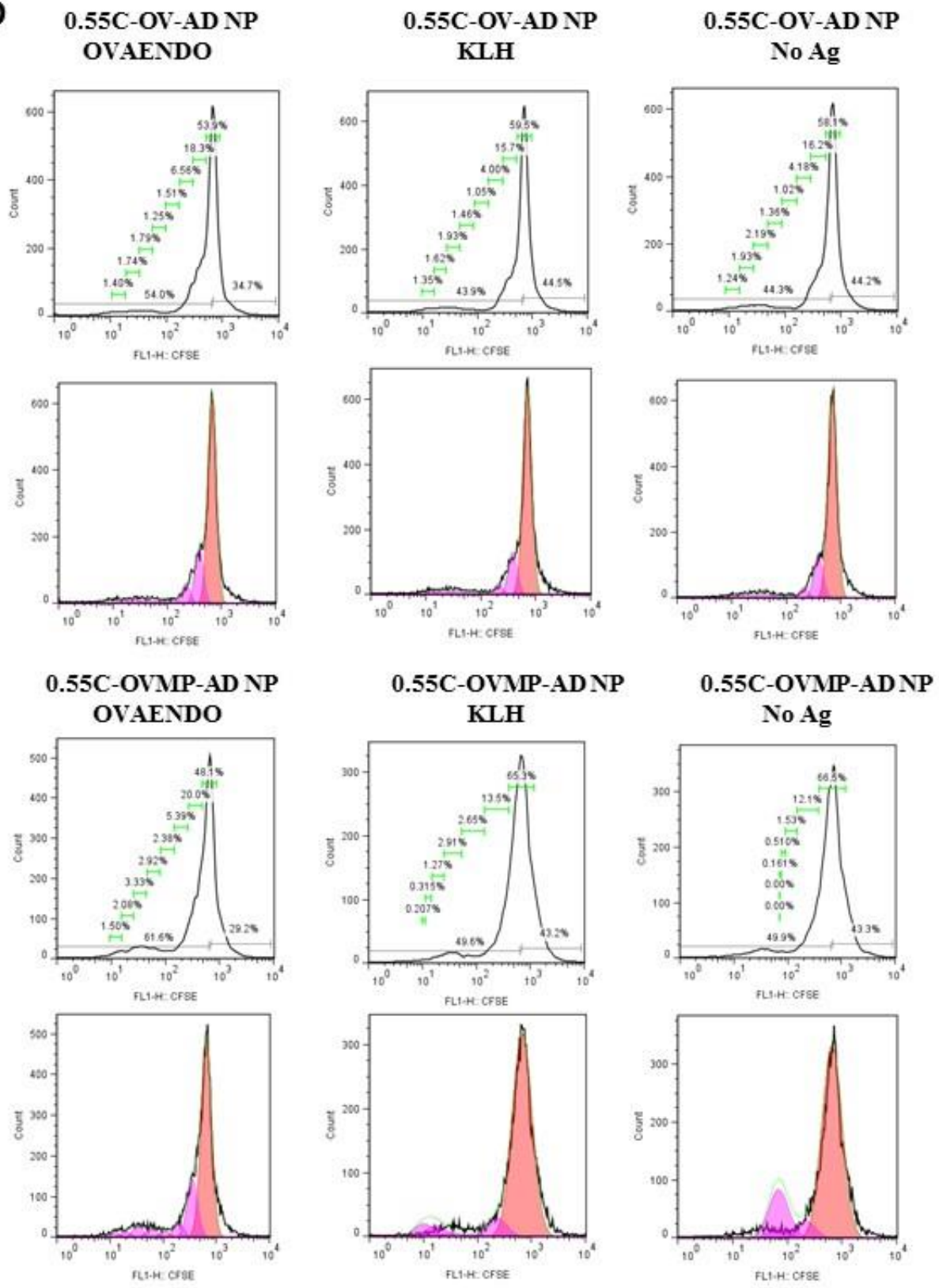
0.55C-OV-AD NP
OVAENDO
0.55C-OV-AD NP
KLH
0.55C-OV-AD NP
No Ag
0.55C-OVMP-AD NP
OVAENDO
0.55C-OVMP-AD NP
KLH
0.55C-OVMP-AD NP
No Ag
Count
FL1-H: CFSE

E

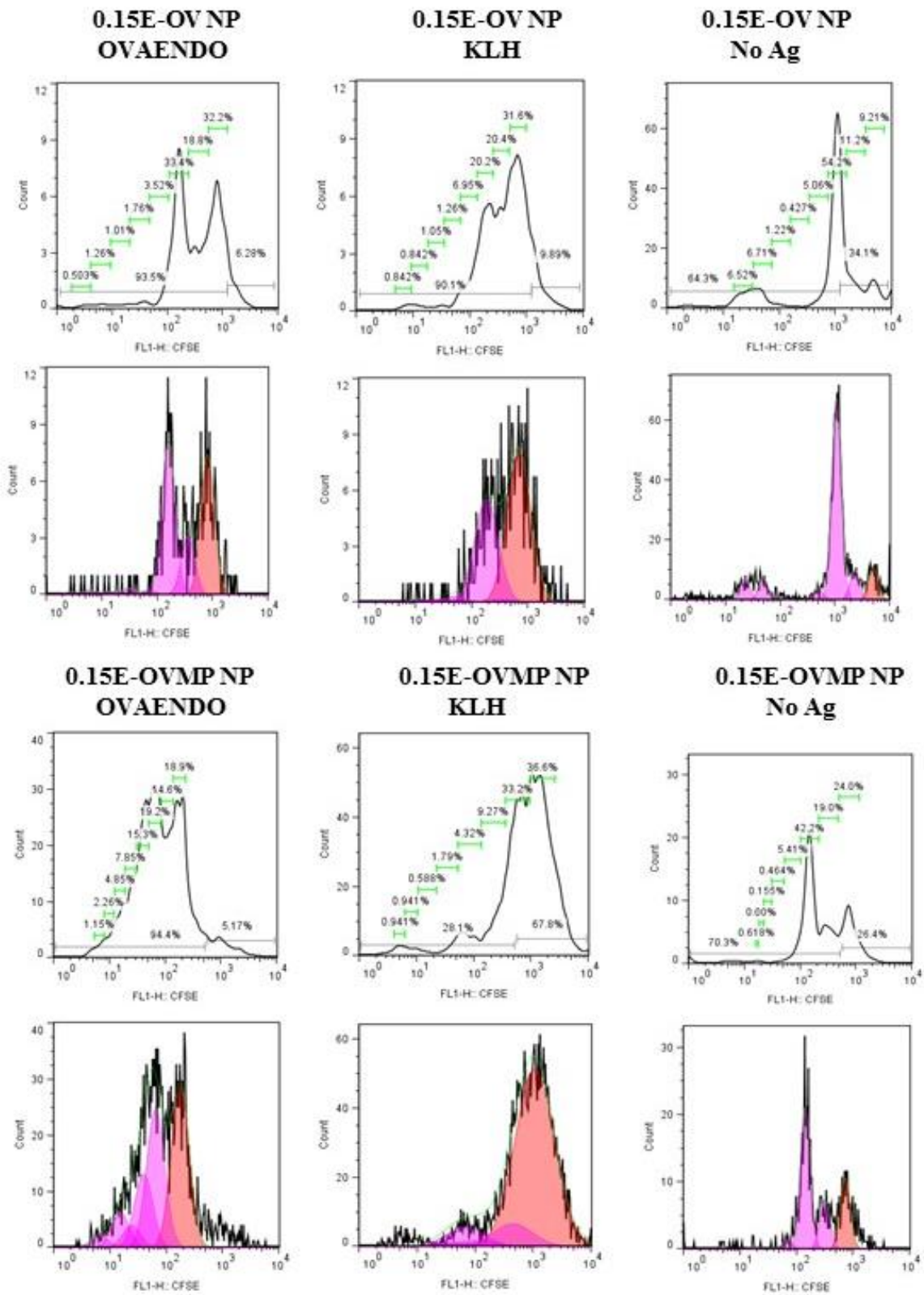
0.15E-OV NP
OVAENDO
0.15E-OV NP
KLH
0.15E-OV NP
No Ag
0.15E-OVMP NP
OVAENDO
0.15E-OVMP NP
KLH
0.15E-OVMP NP
No Ag
Count
FL1-H: CFSE

F

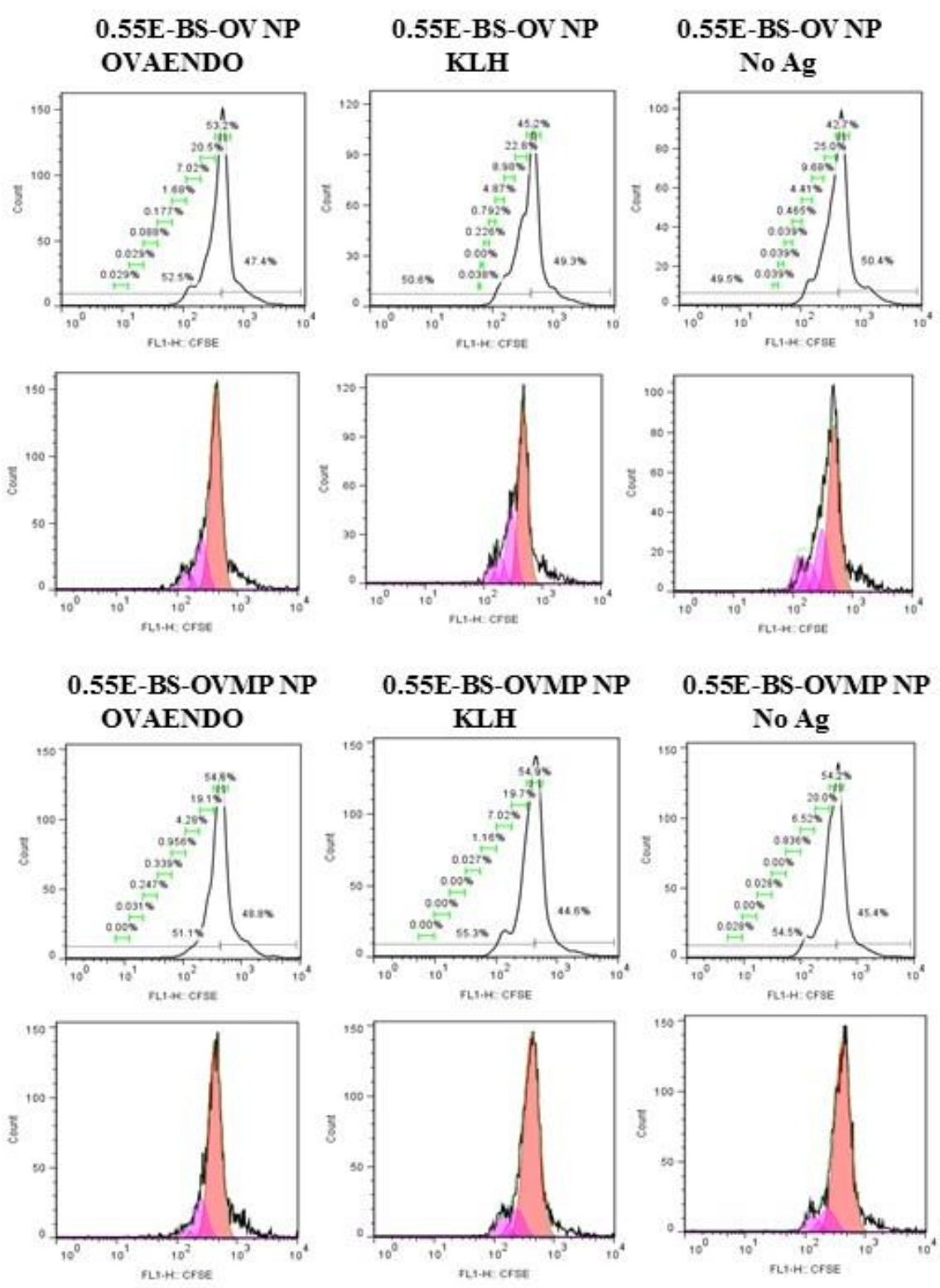
0.55E-BS-OV NP
OVAENDO
0.55E-BS-OV NP
KLH
0.55E-BS-OV NP
No Ag
0.55E-BS-OVMP NP
OVAENDO
0.55E-BS-OVMP NP
KLH
0.55E-BS-OVMP NP
No Ag
Count
FL1-H: CFSE

G

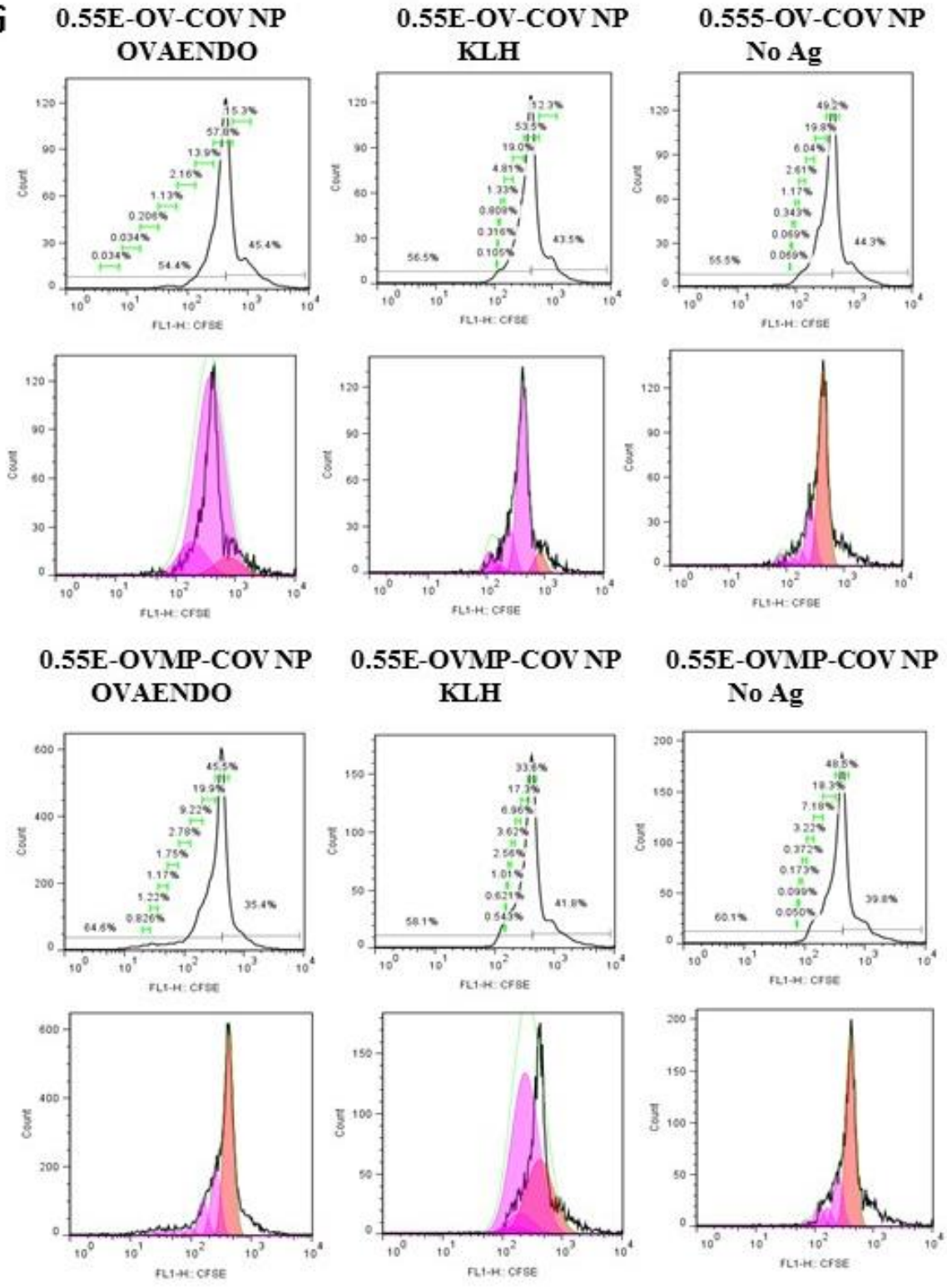
0.55E-OV-COV NP
OVAENDO
0.55E-OV-COV NP
KLH
0.555-OV-COV NP
No Ag
0.55E-OVMP-COV NP
OVAENDO
0.55E-OVMP-COV NP
KLH
0.55E-OVMP-COV NP
No Ag
Count
FL1-H: CFSE

Figure F.1. Overall T cell proliferation assay with WT mice in the vaccination study. Data is represented as histograms and flowjo-analyzed cell-divisions for each group. The groups are controls (A), 0.18C-OV/OVMP NPs (A), 0.55C-OV/OVMP NPs (C, D), 0.15E-OV/OVMP NPs (E) and 0.55E-OV/OVMP NPs (F,G). Briefly, *in-vitro* CFSE-labelled T cells obtained from a specific mice group was co-cultured with irradiated primary DCs. After four days, the cells were harvested, washed and stained with respective antibodies to determine the number of divisions by flow cytometry. In the co-culture there was several groups each restimulated with 20 µM Ovaendofit, or 20 µM KLH or non-stimulated. Abbreviations: NP=Nanoparticle, OV=OVA, MP=MPLA, C=COOH, E=Ester, AD=Adsorption, COV=Covalent binding.

**F.1.2 Assessment of cytokine secretion in WT balb/c T cell and DC co-culture**

Figure F.2 to F.5 represents the cytokine secretion pattern for WT mice after treatment with 0.18 COOH terminated OVA/MPLA NPs. Chapter 5 contains the summary data for the cytokines, whereas, this section contains details of cytokines secreted by each treatment under different conditions. Unimmunized mice were used as negative control and OVMP treated mice were used as positive control in the experiment. Supernatants of the co-culture (DC:T=1:4) were collected after day 4 and kept frozen until use. The cytokines observed were, IFNγ, IL-2, IL-6 and TNF-α. The manufacturer's instructions was followed to perform ELISA for the cytokines.

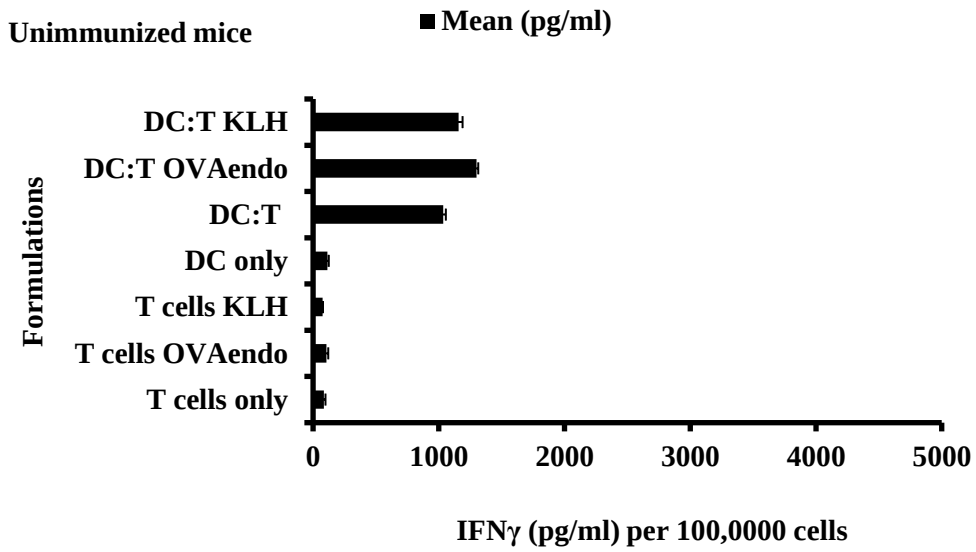
Unimmunized mice
Mean (pg/ml)
Formulations
DC:T KLH
DC:T OVAendo
DC:T
DC only
T cells KLH
T cells OVAendo
T cells only
0
1000
2000
3000
4000
5000
IFNγ (pg/ml) per 100,0000 cells

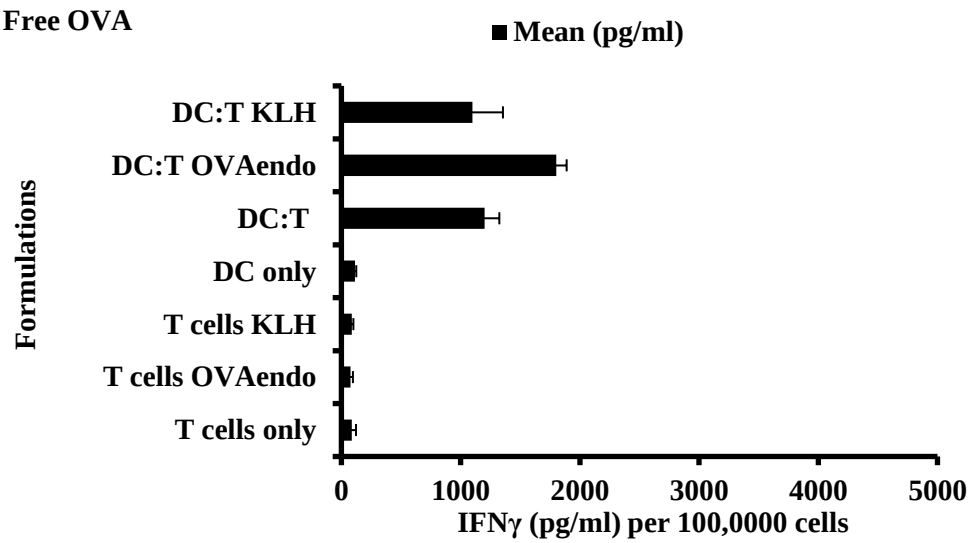
Free OVA
Mean (pg/ml)
Formulations
DC:T KLH
DC:T OVAendo
DC:T
DC only
T cells KLH
T cells OVAendo
T cells only
0
1000
2000
3000
4000
5000
IFNγ (pg/ml) per 100,0000 cells

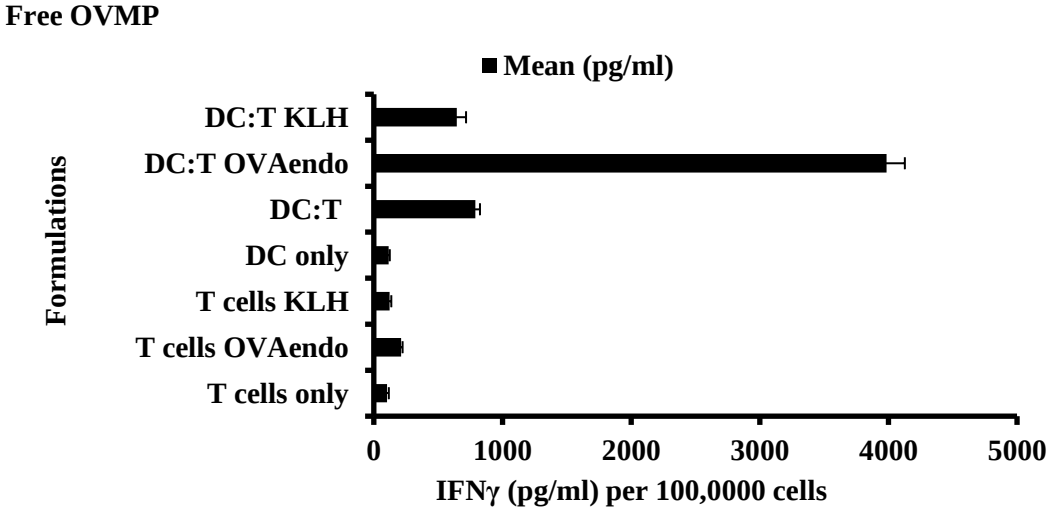
Free OVMP
Mean (pg/ml)
Formulations
DC:T KLH
DC:T OVAendo
DC:T
DC only
T cells KLH
T cells OVAendo
T cells only
0
1000
2000
3000
4000
5000
IFNγ (pg/ml) per 100,0000 cells

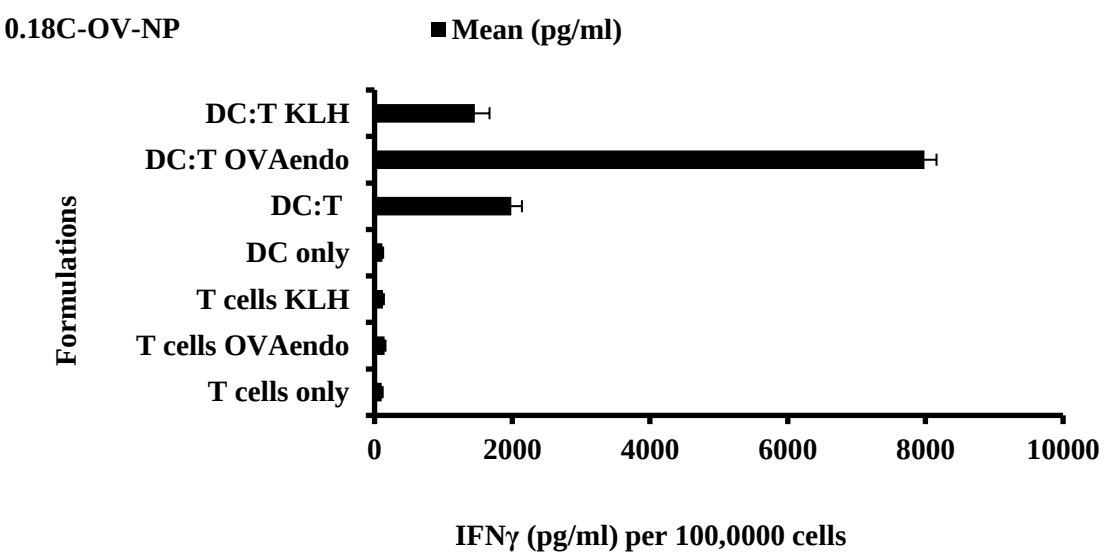
0.18C-OV-NP
Mean (pg/ml)
DC:T KLH
DC:T OVAendo
DC:T
DC only
T cells KLH
T cells OVAendo
T cells only
Formulations
0
2000
4000
6000
8000
10000
IFNγ (pg/ml) per 100,0000 cells

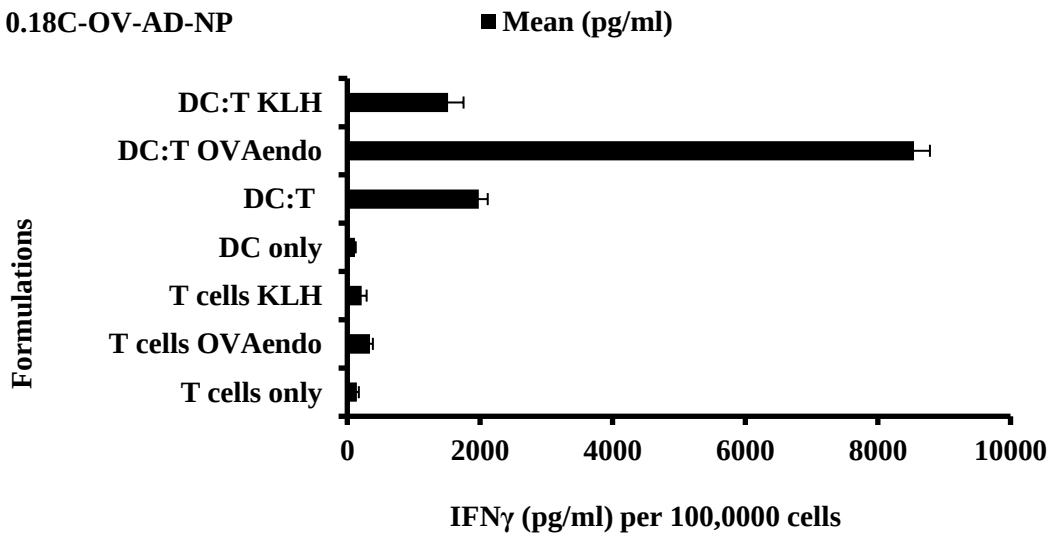
0.18C-OV-AD-NP
Mean (pg/ml)
DC:T KLH
DC:T OVAendo
DC:T
DC only
T cells KLH
T cells OVAendo
T cells only
Formulations
0
2000
4000
6000
8000
10000
IFNγ (pg/ml) per 100,0000 cells

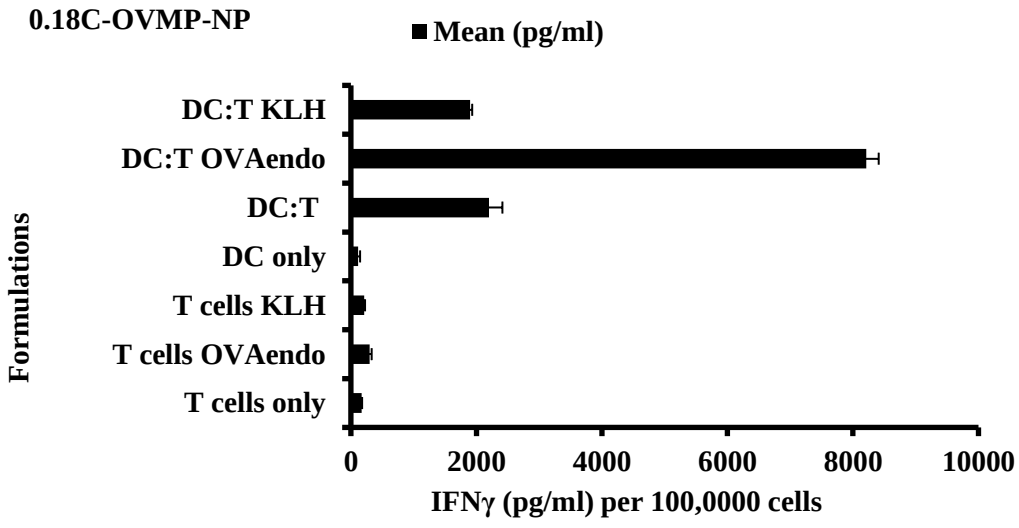
0.18C-OVMP-NP
Mean (pg/ml)
DC:T KLH
DC:T OVAendo
DC:T
DC only
T cells KLH
T cells OVAendo
T cells only
Formulations
0
2000
4000
6000
8000
10000
IFNγ (pg/ml) per 100,0000 cells

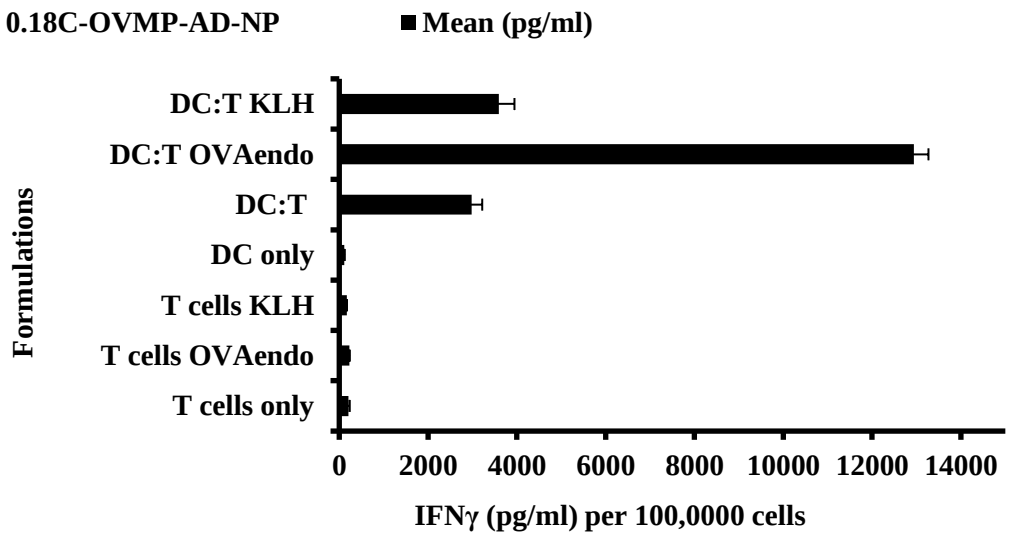


Figure F.2. IFNγ secretion profile of *in-vitro* activated CD3+ T cells after 96 hrs for 0.18 COOH terminated NPs. (n=3) ($p<0.05$)

Notes: CD3 T cells were isolated from WT balb/c mice and co-cultured with primary DCs. Supernatants obtained at the end of 96 hours were collected and analyzed for IFNγ secretion. Treatment groups were unimmunized mice, free OVA, free OVMP, 0.18C-OV-NP, 0.18C-OV-AD-NP, 0.18C-OVMP-NP, and 0.18C-OVMP-AD-NP. Easysep T cell negative isolation kit was used as per manufacturer's suggestion to isolate CD3 positive overall T cells (purity>80 %). T cells were collected, stained with CFSE and co-cultured with pretreated DCs, where T cells were fixed ($1X10^5$) with graded dose of irradiated DCs at a ratio of 1:4. The co-culture was then stimulated with T cell test Ovaendo or irrelevant antigen (KLH). The unstimulated T cells were used as negative control.

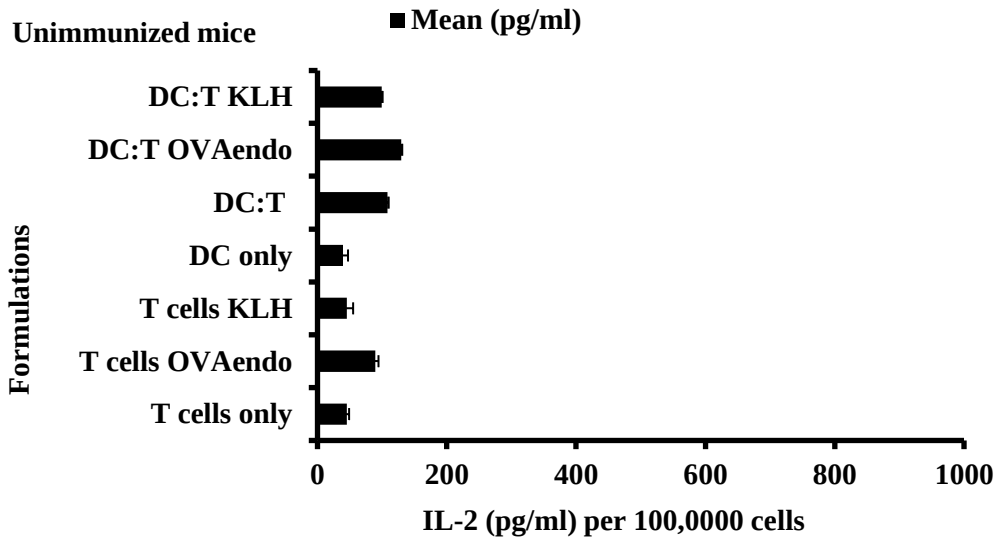
Unimmunized mice
Mean (pg/ml)
DC:T KLH
DC:T OVAendo
DC:T
DC only
T cells KLH
T cells OVAendo
T cells only
Formulations
0
200
400
600
800
1000
IL-2 (pg/ml) per 100,0000 cells

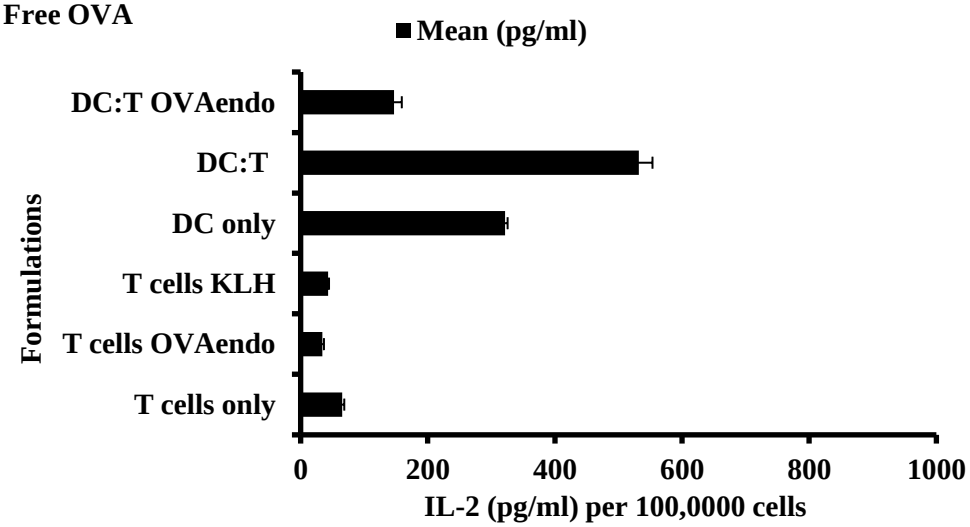
Free OVA
Mean (pg/ml)
DC:T OVAendo
DC:T
DC only
T cells KLH
T cells OVAendo
T cells only
Formulations
0
200
400
600
800
1000
IL-2 (pg/ml) per 100,0000 cells

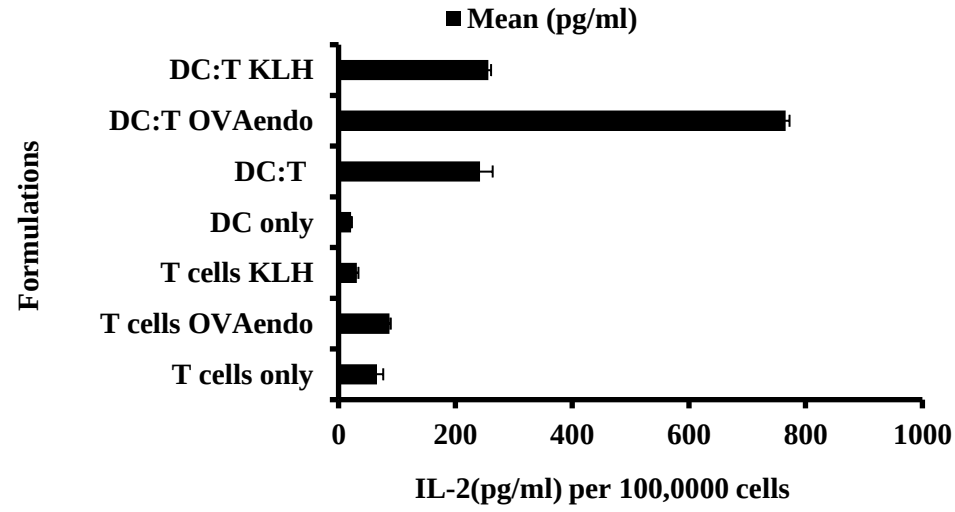
Free OVMP
Mean (pg/ml)
DC:T KLH
DC:T OVAendo
DC:T
DC only
T cells KLH
T cells OVAendo
T cells only
Formulations
0
200
400
600
800
1000
IL-2(pg/ml) per 100,0000 cells

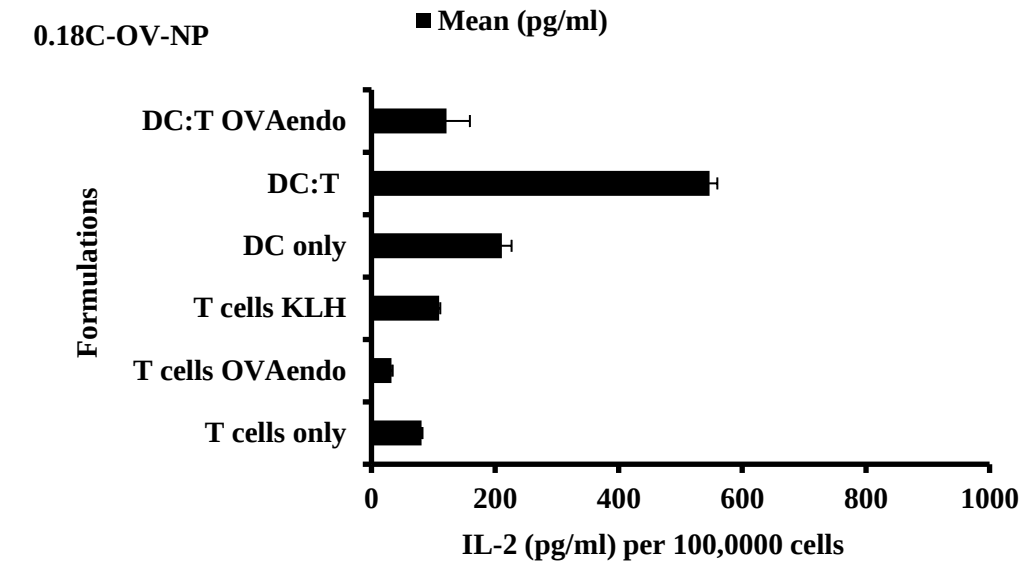
0.18C-OV-NP
Mean (pg/ml)
DC:T OVAendo
DC:T
DC only
T cells KLH
T cells OVAendo
T cells only
Formulations
0
200
400
600
800
1000
IL-2 (pg/ml) per 100,0000 cells

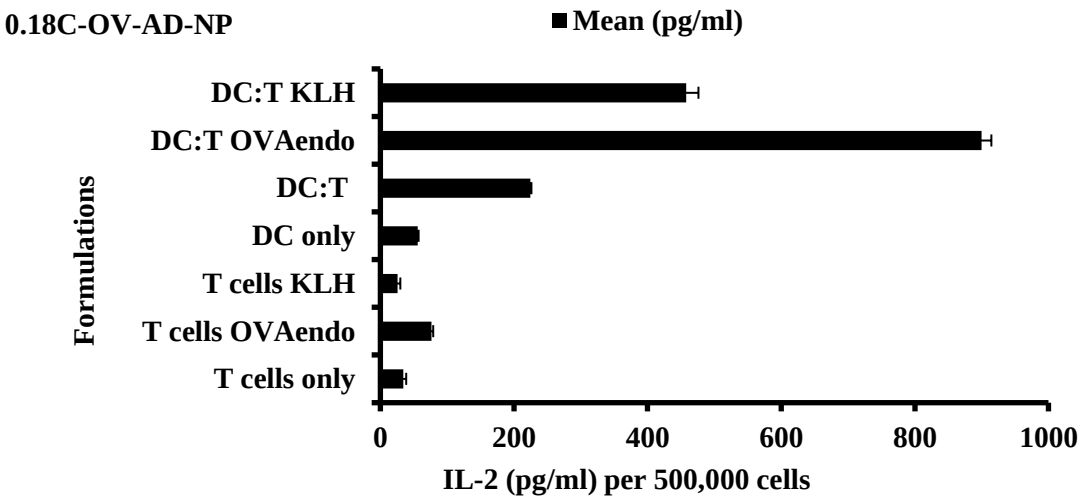
0.18C-OV-AD-NP
Mean (pg/ml)
DC:T KLH
DC:T OVAendo
DC:T
DC only
T cells KLH
T cells OVAendo
T cells only
Formulations
0
200
400
600
800
1000
IL-2 (pg/ml) per 500,000 cells

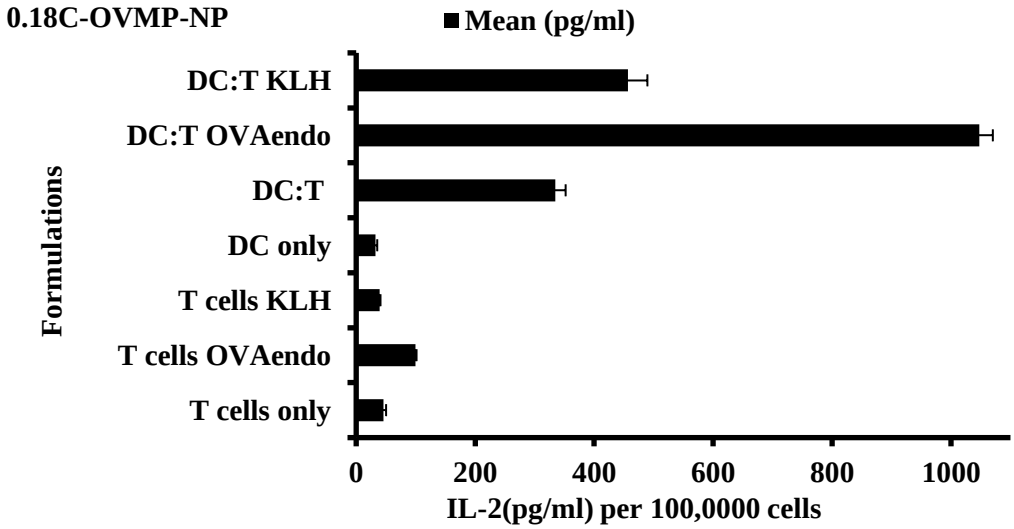
0.18C-OVMP-NP
Mean (pg/ml)
DC:T KLH
DC:T OVAendo
DC:T
DC only
T cells KLH
T cells OVAendo
T cells only
Formulations
0
200
400
600
800
1000
IL-2(pg/ml) per 100,0000 cells

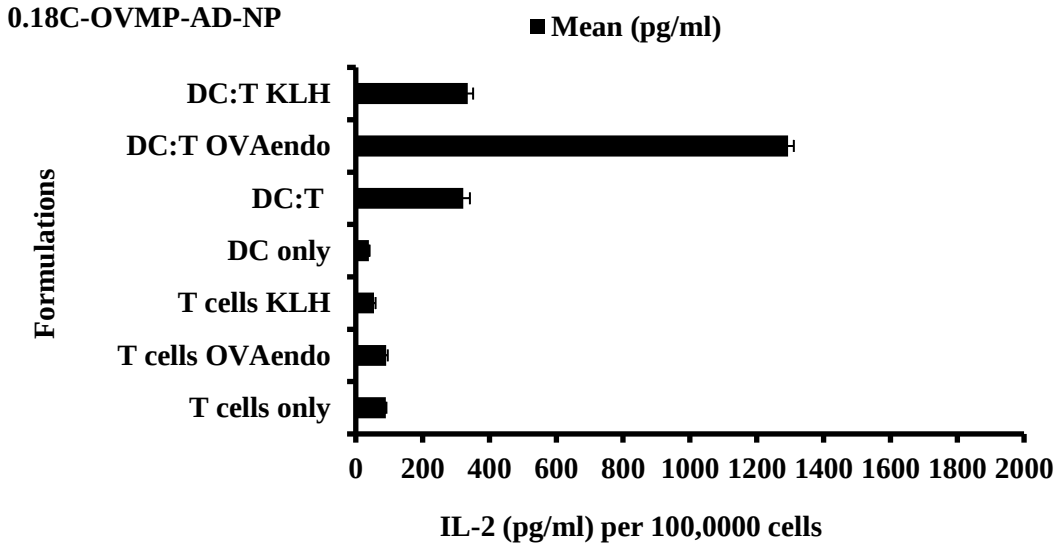


Figure F.3. IL-2 secretion profile of *in-vitro* activated CD3+ T cells after 96 hrs for 0.18 COOH terminated NPs. (n=3) ($p<0.05$)

Notes: CD3 T cells were isolated from WT balb/c mice and co-cultured with primary DCs. Supernatants obtained at the end of 96 hours were collected and analyzed for IL-2 secretion. Treatment groups were unimmunized mice, OVA free, OVMP free, 0.18C-OV-NP, 0.18C-OV-AD-NP, 0.18C-OVMP-NP, and 0.18C-OVMP-AD-NP. Easysep T cell negative isolation kit was used as per manufacturer's suggestion to isolate CD3 positive overall T cells (purity>80 %). T cells were collected, stained with CFSE and co-cultured with pretreated DCs, where T cells were fixed ($1X10^5$) with graded dose of irradiated DCs at a ratio of 1:4. The co-culture was then stimulated with T cell test Ovaendo or irrelevant antigen (KLH). The unstimulated T cells were used as negative control.

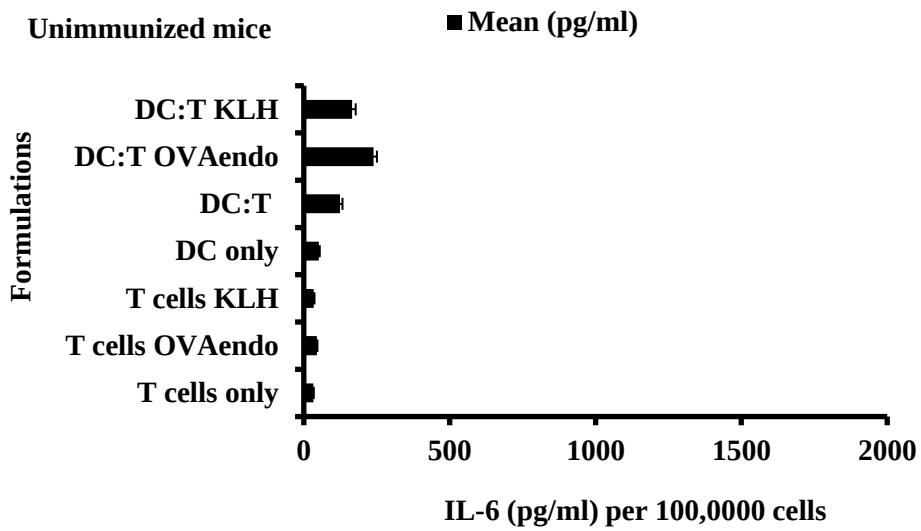
Unimmunized mice
Mean (pg/ml)
Formulations
DC:T KLH
DC:T OVAendo
DC:T
DC only
T cells KLH
T cells OVAendo
T cells only
0
500
1000
1500
2000
IL-6 (pg/ml) per 100,0000 cells

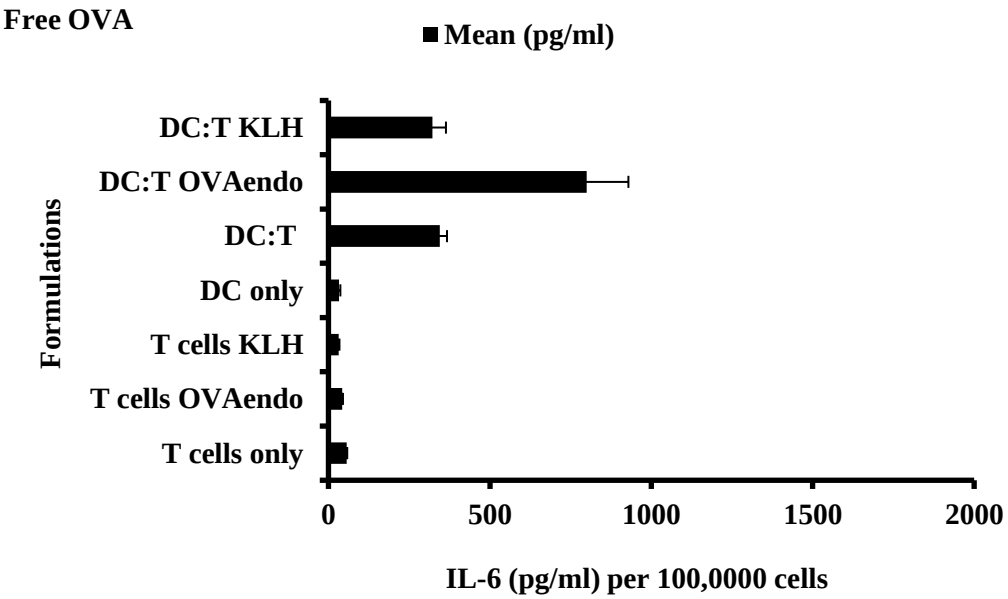
Free OVA
Mean (pg/ml)
Formulations
DC:T KLH
DC:T OVAendo
DC:T
DC only
T cells KLH
T cells OVAendo
T cells only
0
500
1000
1500
2000
IL-6 (pg/ml) per 100,0000 cells

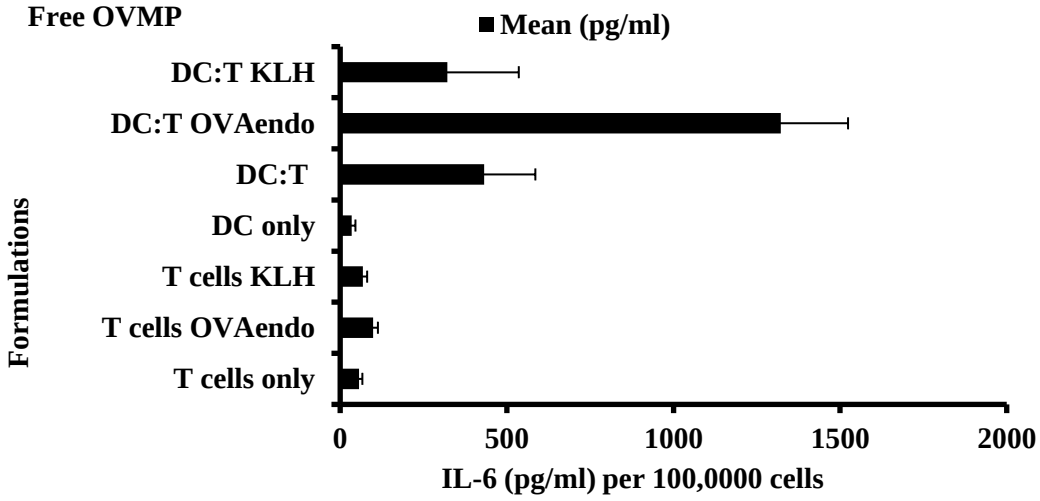
Free OVMP
Mean (pg/ml)
Formulations
DC:T KLH
DC:T OVAendo
DC:T
DC only
T cells KLH
T cells OVAendo
T cells only
0
500
1000
1500
2000
IL-6 (pg/ml) per 100,0000 cells

**0.18C-OV-NP**

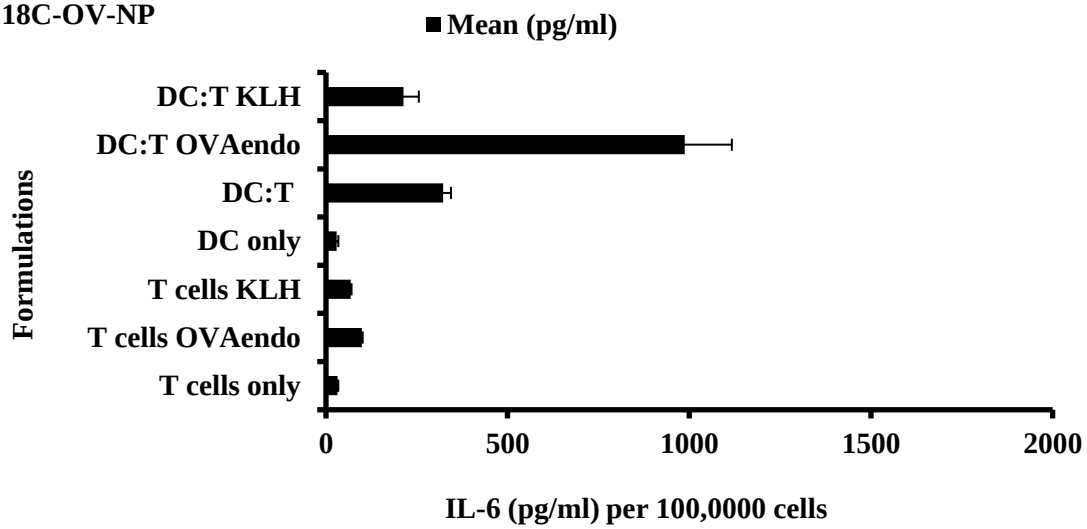


**0.18C-OV-AD-NP**

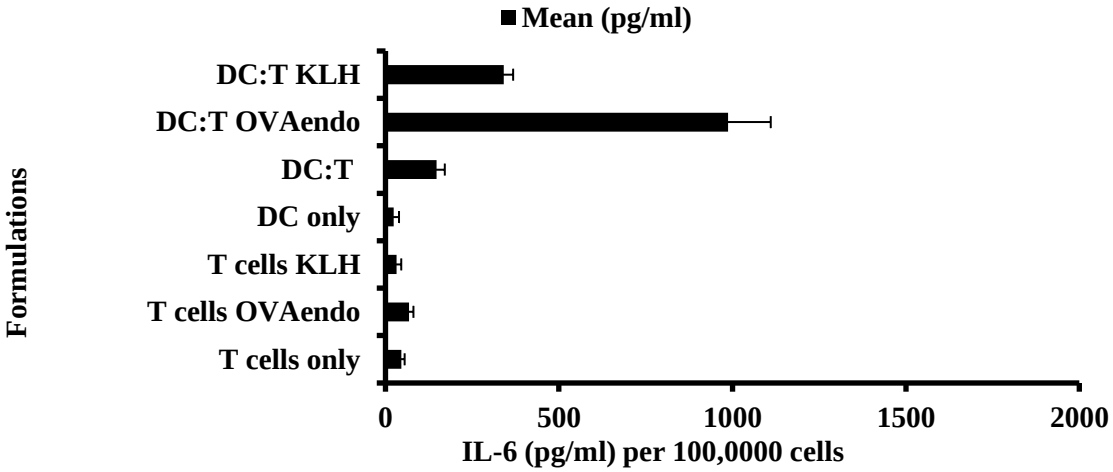


**0.18C-OVMP-NP**

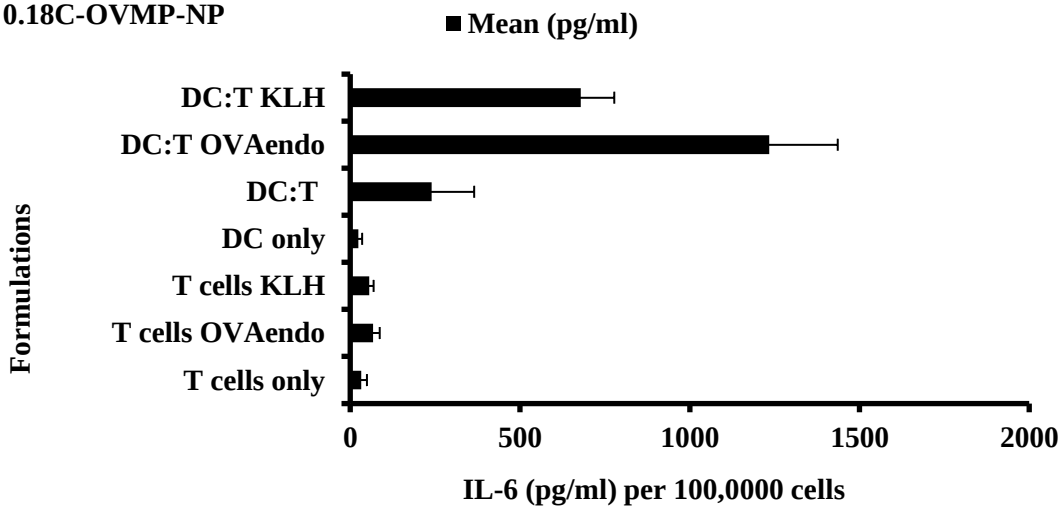

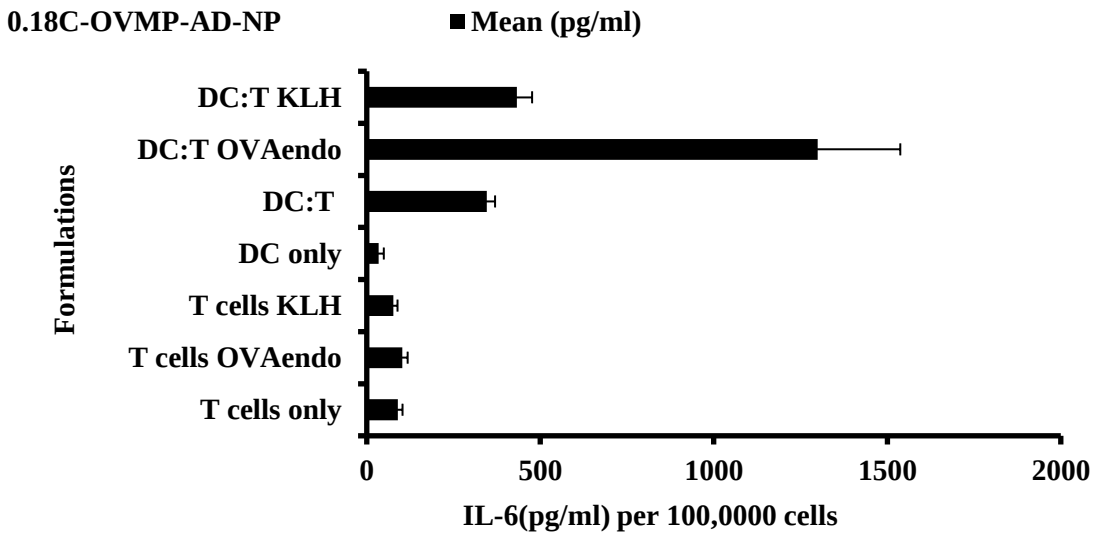


Figure F.4. IL-6 secretion profile of *in-vitro* activated CD3+ T cells after 96 hrs for 0.18COOH terminated NPs. (n=3) ($p<0.05$)

Notes: CD3 T cells were isolated from WT balb/c mice and co-cultured with primary DCs. Supernatants obtained at the end of 96 hours were collected and analyzed for IL-6 secretion. Treatment groups were unimmunized mice, free OVA, free OVMP, 0.18C-OV-NP, 0.18C-OV-AD-NP, 0.18C-OVMP-NP, and 0.18C-OVMP-AD-NP. Easysep T cell negative isolation kit was used as per manufacturer's suggestion to isolate CD3 positive overall T cells (purity>80 %). T cells were collected, stained with CFSE and co-cultured with pretreated DCs, where T cells were fixed ($1X10^5$) with graded dose of irradiated DCs at a ratio of 1:4. The co-culture was then stimulated with T cell test OVAendo or irrelevant antigen (KLH). The unstimulated T cells were used as negative control.

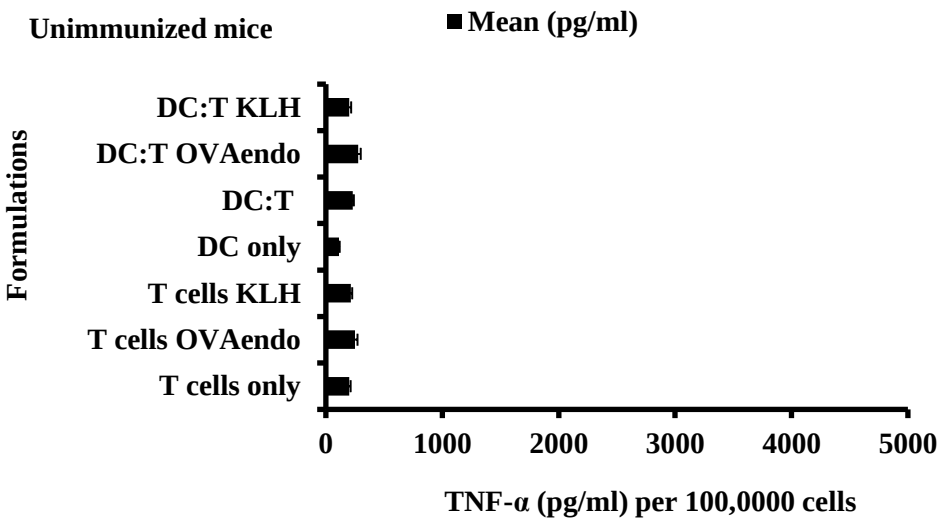
Unimmunized mice
Mean (pg/ml)
Formulations
DC:T KLH
DC:T OVAendo
DC:T
DC only
T cells KLH
T cells OVAendo
T cells only
0
1000
2000
3000
4000
5000
TNF-α (pg/ml) per 100,0000 cells

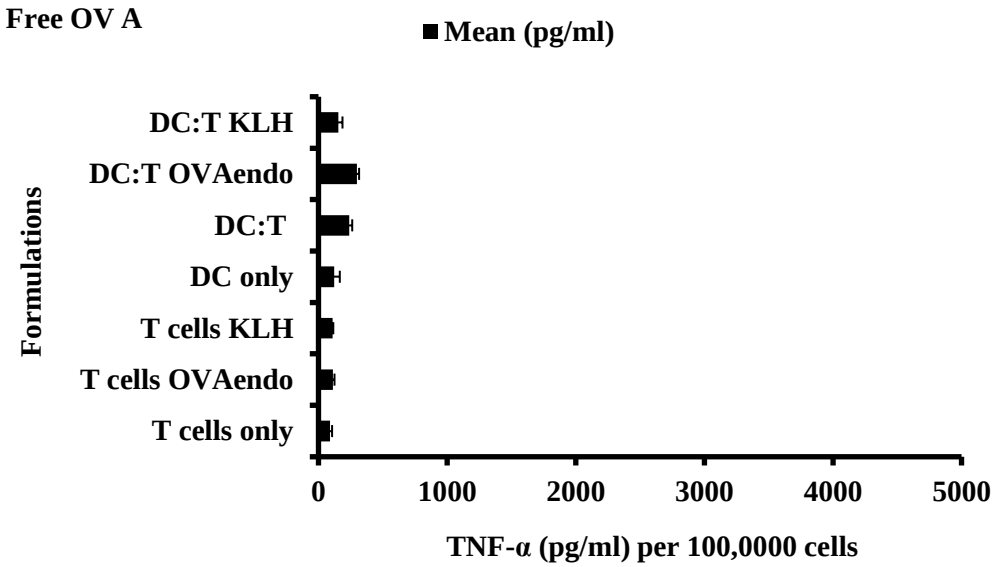
Free OV A
Mean (pg/ml)
Formulations
DC:T KLH
DC:T OVAendo
DC:T
DC only
T cells KLH
T cells OVAendo
T cells only
0
1000
2000
3000
4000
5000
TNF-α (pg/ml) per 100,0000 cells

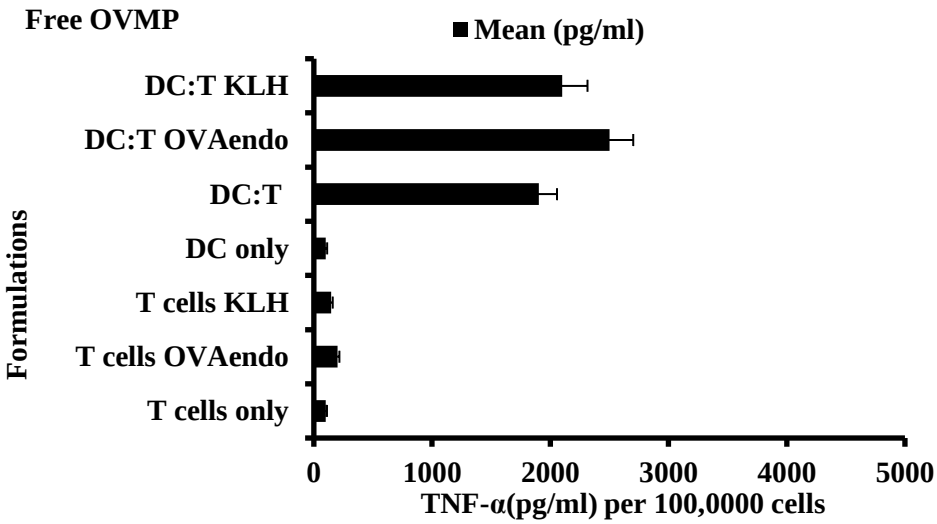
Free OVMP
Mean (pg/ml)
Formulations
DC:T KLH
DC:T OVAendo
DC:T
DC only
T cells KLH
T cells OVAendo
T cells only
0
1000
2000
3000
4000
5000
TNF-α(pg/ml) per 100,0000 cells

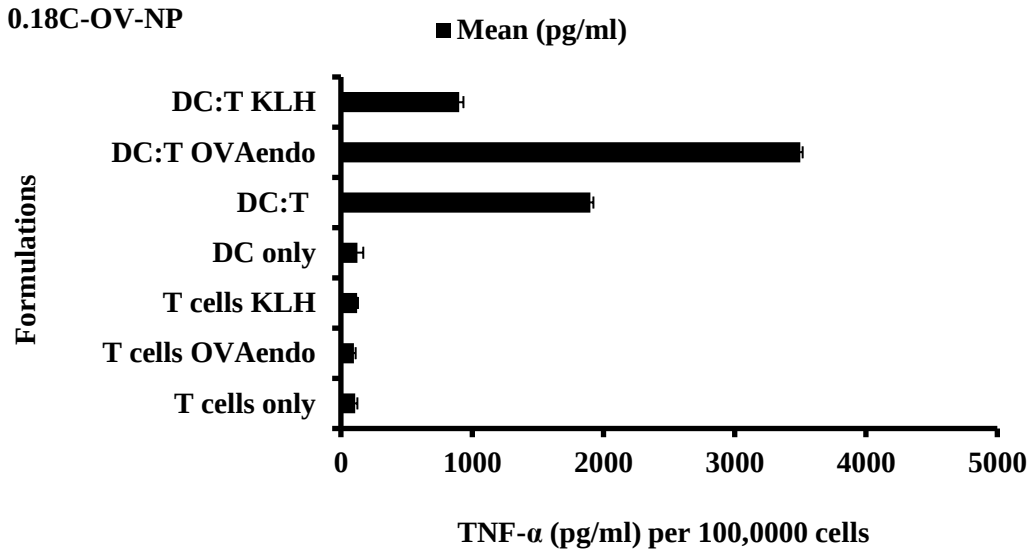
0.18C-OV-NP
Mean (pg/ml)
DC:T KLH
DC:T OVAendo
DC:T
DC only
T cells KLH
T cells OVAendo
T cells only
Formulations
0
1000
2000
3000
4000
5000
TNF-α (pg/ml) per 100,0000 cells

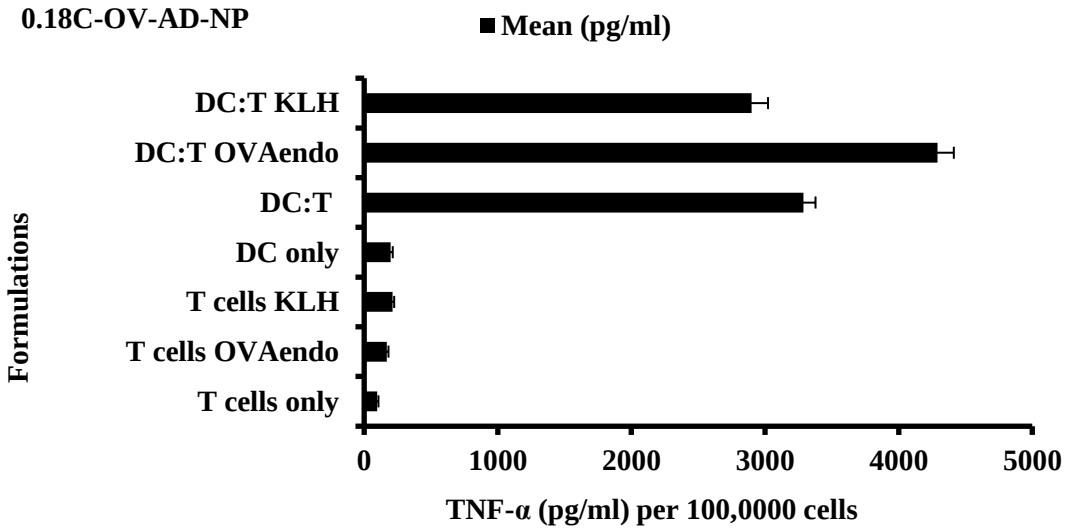
0.18C-OV-AD-NP
Mean (pg/ml)
DC:T KLH
DC:T OVAendo
DC:T
DC only
T cells KLH
T cells OVAendo
T cells only
Formulations
0
1000
2000
3000
4000
5000
TNF-α (pg/ml) per 100,0000 cells

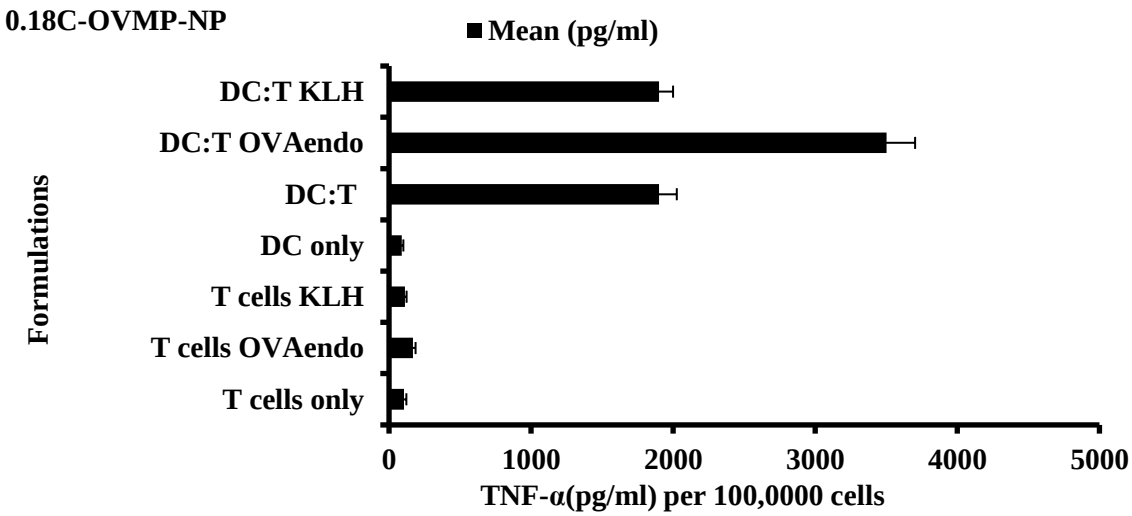
0.18C-OVMP-NP
Mean (pg/ml)
DC:T KLH
DC:T OVAendo
DC:T
DC only
T cells KLH
T cells OVAendo
T cells only
Formulations
0
1000
2000
3000
4000
5000
TNF-α(pg/ml) per 100,0000 cells

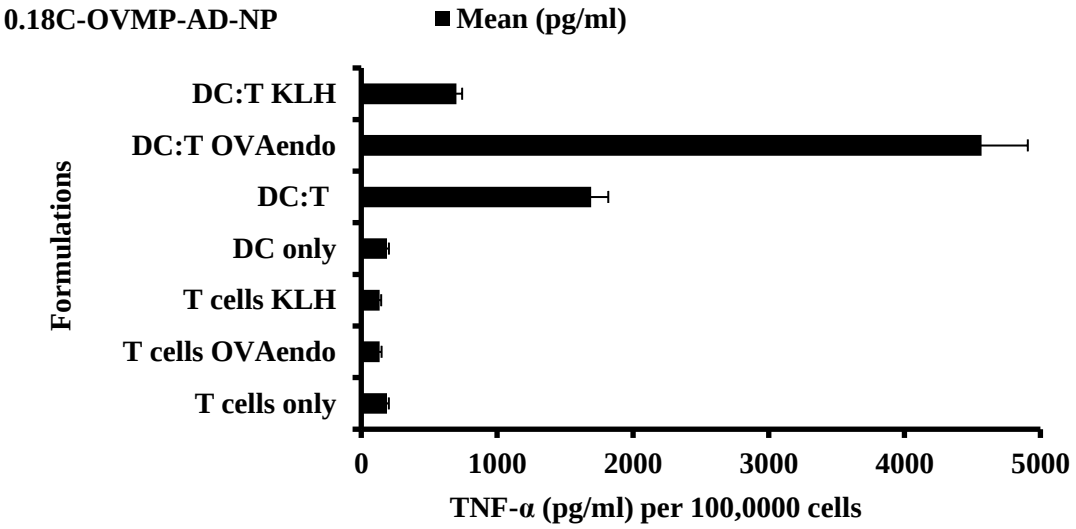


Figure F.5. TNF-α secretion profile of *in-vitro* activated CD3+ T cells after 96 hrs for 0.18 COOH terminated NPs. (n=3) ($p<0.05$)

Notes: CD3 T cells were isolated from WT balb/c mice and co-cultured with primary DCs. Supernatants obtained at the end of 96 hours were collected and analyzed for TNF-α secretion. Treatment groups were unimmunized mice, free OVA, free OVMP, 0.18C-OV-NP, 0.18C-OV-AD-NP, 0.18C-OVMP-NP, and 0.18C-OVMP-AD-NP. Easysep T cell negative isolation kit was used as per manufacturer's suggestion to isolate CD3 positive overall T cells (purity>80 %). T cells were collected, stained with CFSE and co-cultured with pretreated DCs, where T cells were fixed ($1X10^5$) with graded dose of irradiated DCs at a ratio of 1:4. The co-culture was then stimulated with T cell test Ovaendo or irrelevant antigen (KLH). The unstimulated T cells were used as negative control.

### F.1.3 Assessment of T cell proliferation with OT1 mice by CFSE method

CFSE method was employed to analyze the proliferation of CD8+ T cells in OT1 mice. The main objective of this experiment was to confirm the antigen OVA specific response in OT1 mouse. The experiment was optimized based on the results obtained from WT balb/c mice. 0.18 COOH terminated nanoparticles showed the most promising results for both T cell proliferation study as well as cytokines.

The dose of antigen re-stimulation was cut-down in OT1 mice from 20 µM to 1 µM based on some pilot studies performed on them.

DC and T cell co-culture was assessed with a starting cell number of T cells ($1X10^5$). CD8T cells were at a ratio of 1:4 and 1:10. Primary DCs were at $2.5X10^4$ and $1X10^4$ for the corresponding ratios. T cells were stained with fluorescent dye CFSE to observe for 5 days with OVA and MPLA. The restimulation of isolated CD8+T cells was performed with relevant peptide (1 µM) and irrelevant protein (KLH, 1 µM) during co-culture (day1).

OT1 mice were vaccinated twice (week 1 and week 3), spleens and lymph nodes were collected for purification of CD8 T cells. Primary DCs isolated from mouse bone marrow was irradiated before co-culture. DCs were co-cultured with CD8 T cells and re-stimulated with either CD8 peptide or KLH irrelevant antigen. Figure E.6 shows the proliferation study of CFSE labelled T cells after 5 days of co-culture. Unimmunized mice were used as negative control. Free OVA-MPLA treated mice were used as positive control.

The percent divided by DC: $T_{CFSE}$ (KLH), DC: $T_{CFSE}$ (No Ag), free OVA (KLH). free OVA (No Ag), free OVMP (KLH), free OVMP (No Ag), 0.18C-BS-OV NP (KLH), 0.18C-BS-OV NP (No Ag), 0.18C-BS-OVMP NP (KLH), 0.18C-BS-OVMP NP (No Ag), 0.18C-OV-AD NP (KLH), 0.18C-OV-AD NP (No Ag), 0.18C-OV-COV NP (KLH), 0.18C-OV-COV NP (No Ag), 0.18C-OVMP-AD NP (KLH), 0.18C-OVMP-AD NP (No Ag), 0.18C-OVMP-COV NP (KLH), 0.18C-OVMP-COV NP (No Ag) was 2.29 %, 0.085 %, 19.1 %, 13.2 %, 19.7 %, 66.2 %, 22 %, 24.7 %, 8.61, 11.6 %, 14.7 %, 33.6 %, 15.9 %, 6.8 %, 71.4 %, 43.5 %, 23.4 % and 20.5 % respectively.

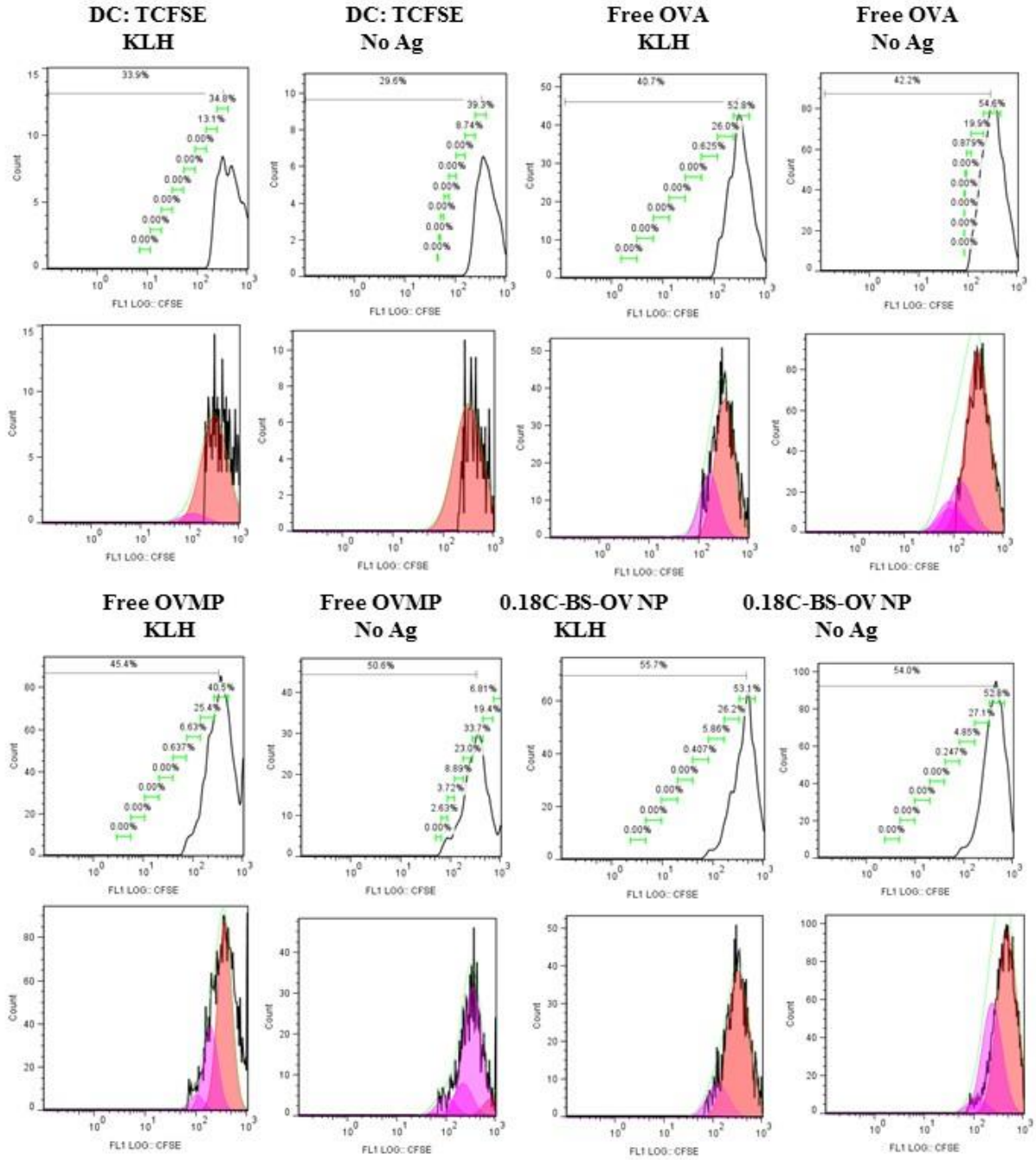
DC: TCFSE
KLH
DC: TCFSE
No Ag
Free OVA
KLH
Free OVA
No Ag
Free OVMP
KLH
Free OVMP
No Ag
0.18C-BS-OV NP
KLH
0.18C-BS-OV NP
No Ag
Count
FL1 LOG: CFSE

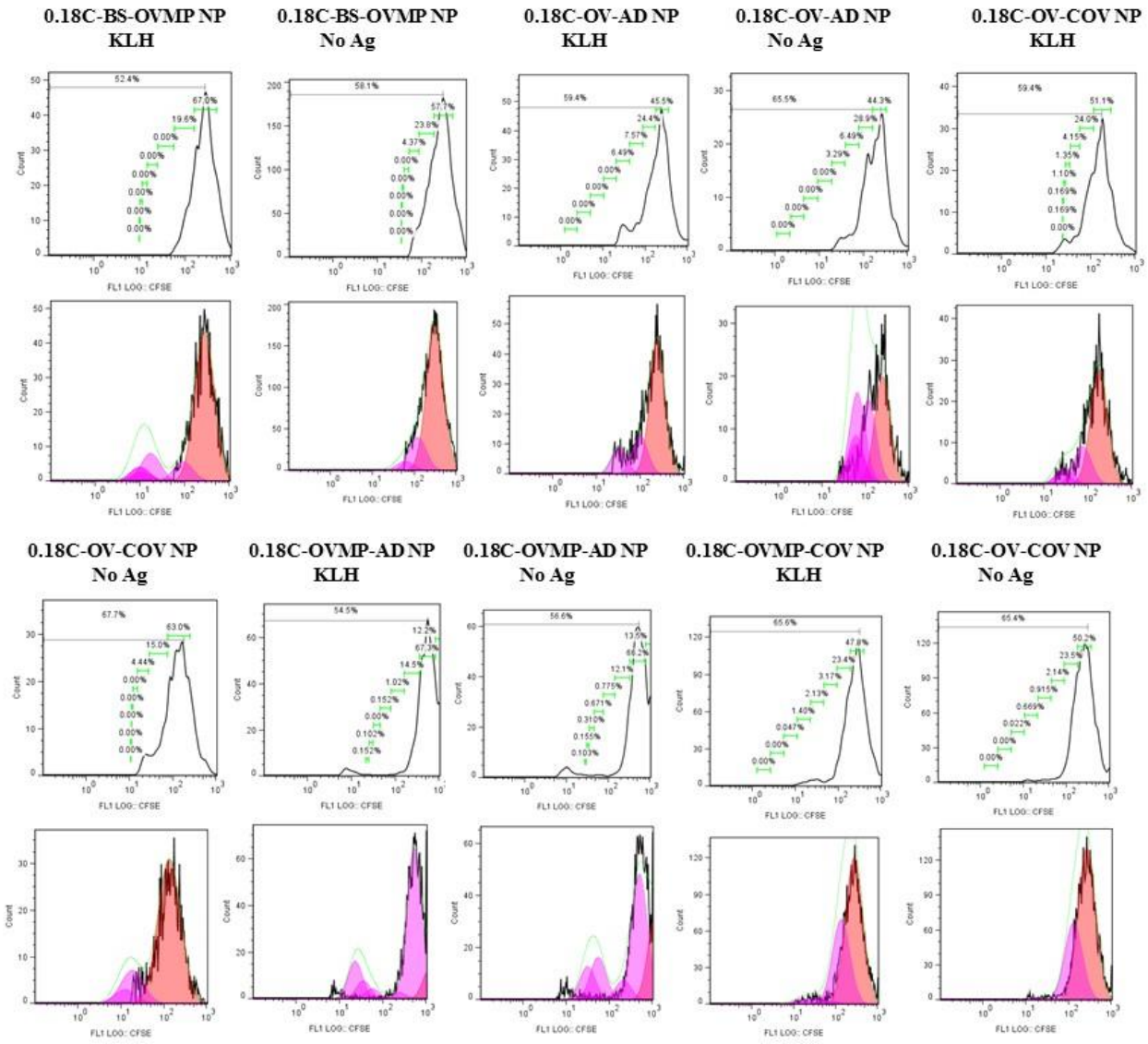


Figure F.6. Representative histogram for CD8 T cells proliferation after 96 hours of co-culture by flow cytometry for 0.18 COOH terminated nanoparticles (1-9). In brief, OT-1 mouse (3-4/group) was vaccinated twice, sacrificed to collect spleens and lymph nodes after 21 days. DC (irradiated) was co-cultured with CD8 T cells after purification using isolation kit. Several groups were included in the study that was either re-stimulated with relevant SIINFEKL peptide or KLH (irrelevant) or kept unstimulated. After five days, T cells were harvested, washed, stained with CD8 antibody and data was acquired in flow cytometer.

Notes: 1. Unimmunized cells, 2. Free OVA, 3. Free OVMP, 4. 0.18C-OV-BS3-NP, 5. 0.18C-OVMP-BS3-NP, 6. 0.18C-OV-AD-NP, 7. 0.18C-OV-COV-NP, 8. 0.18C-OVMP-AD-NP AND 9. 0.18C-OVMP-COV-NP. Left side histogram shows different proliferative generations represented in percentage. All histogram shows up to seven generations. Left side histogram represents the proliferative generations in graded color of pink. Data is analyzed using flowjo software version 7.6.5.

**F.1.4 Assessment of cytokine secretions in OT-1 mice T cell and DC co-culture**

Figure F.7 to F.10 (1-9) represents the cytokine secretion pattern in the co-colture supernatant of OT-1 mouse and primary DCs. Supernatants were collected after day 5 and kept frozen until use. The cytokines observed were IFNγ, IL-2, IL-6 and TNF-α. The manufacturer's instructions was followed to perform ELISA for the cytokines.The cytokine secretion is assessed per 500, 000 cells. Two ratios of DC:T cells are represented here for cytokine secretion. DC:T at 1:4 and 1:10 was evaluated. Individual results of LN derived CD8 T cells and Dc co-culture are also mentioned for some of the formulaitons. The amount of cytokine secretion is comparatively higher than the WT mice.

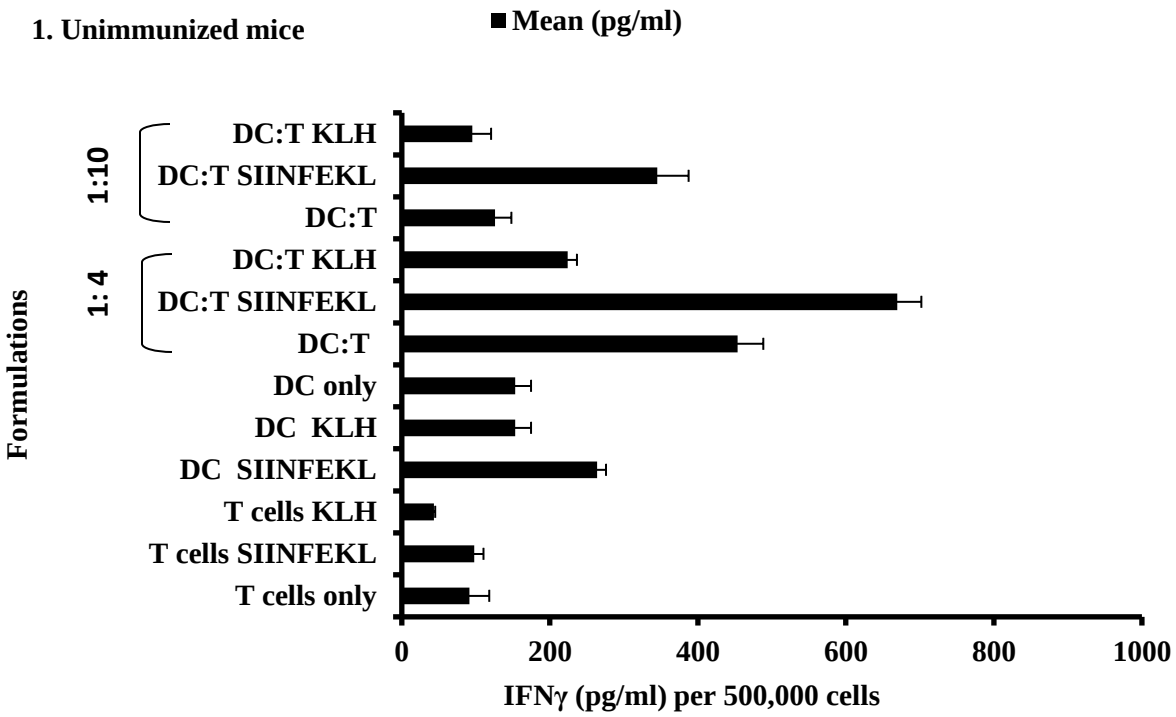
1. Unimmunized mice
Mean (pg/ml)
Formulations
1:10
1: 4
DC:T KLH
DC:T SIINFEKL
DC:T
DC:T KLH
DC:T SIINFEKL
DC:T
DC only
DC KLH
DC SIINFEKL
T cells KLH
T cells SIINFEKL
T cells only
0
200
400
600
800
1000
IFNγ (pg/ml) per 500,000 cells

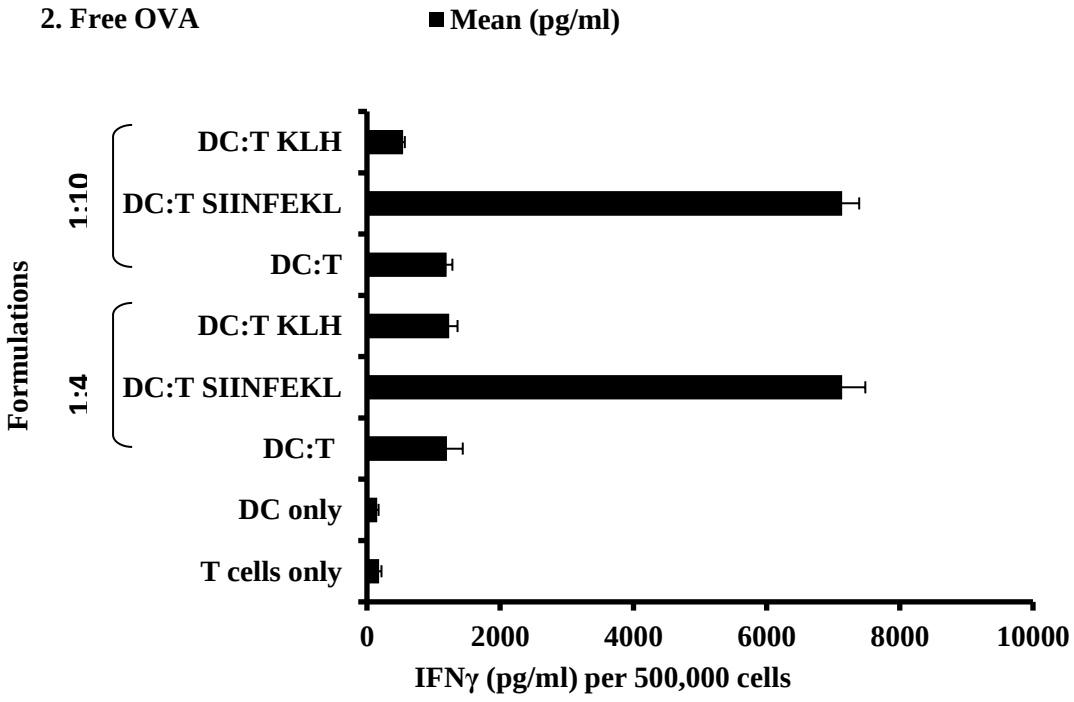
2. Free OVA
Mean (pg/ml)
Formulations
1:10
1:4
DC:T KLH
DC:T SIINFEKL
DC:T
DC:T KLH
DC:T SIINFEKL
DC:T
DC only
T cells only
0
2000
4000
6000
8000
10000
IFNγ (pg/ml) per 500,000 cells

**3. Free OVMP**

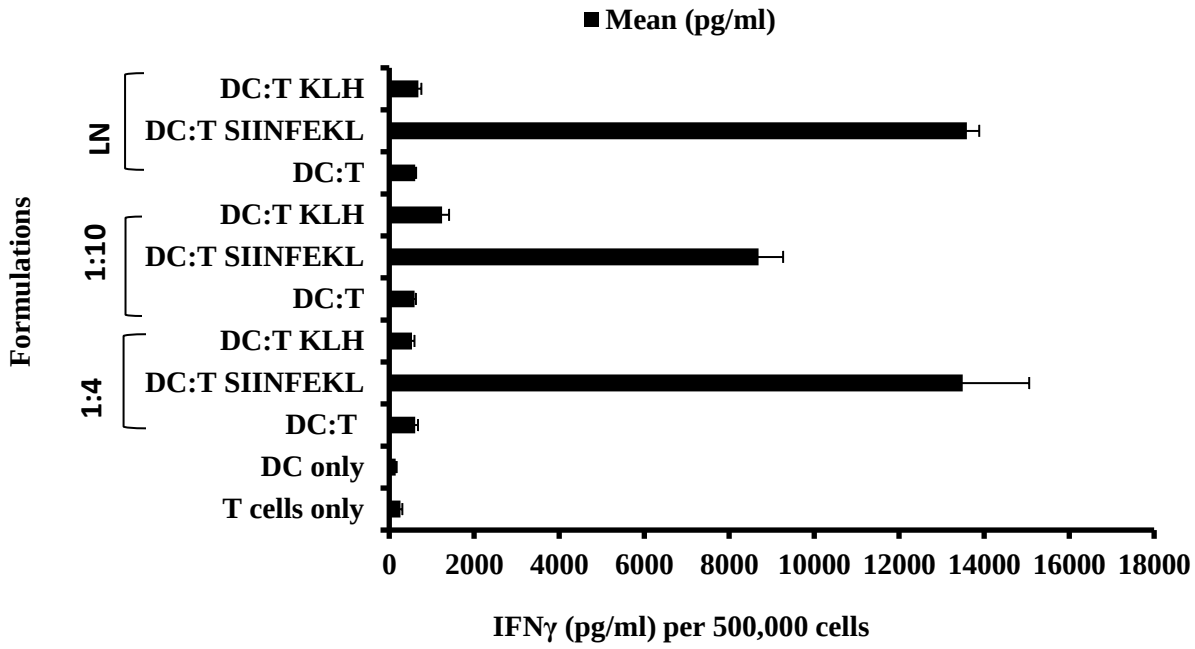


**4. 0.18C-OV-BS3-NP**

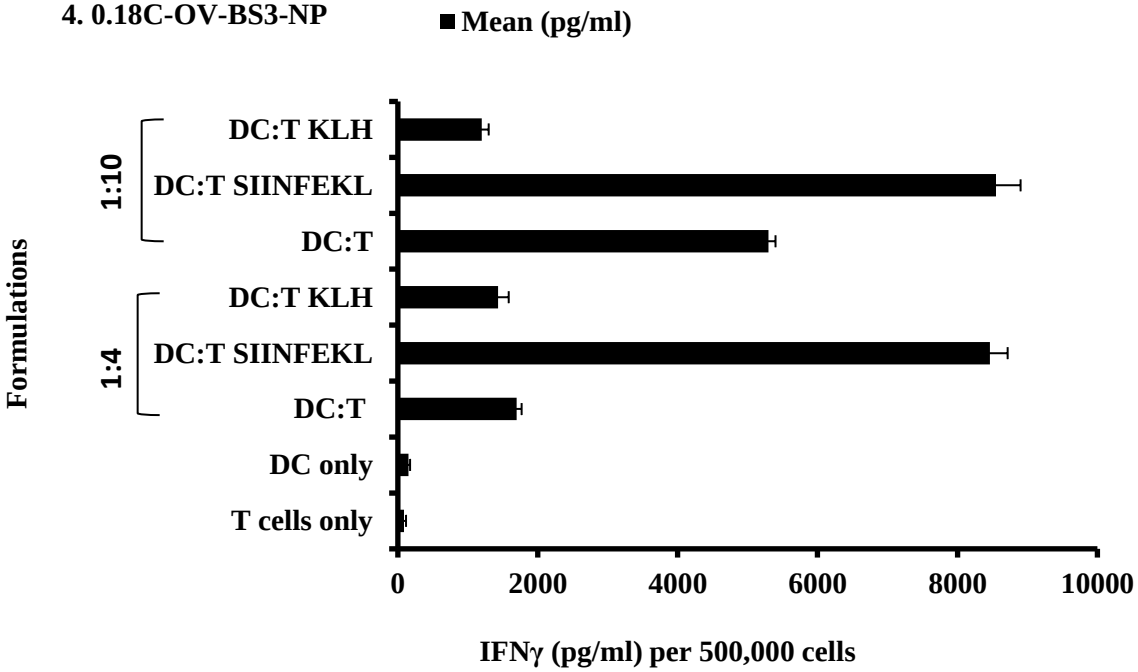

**5. 0.18C-OVMP-BS3-NP**

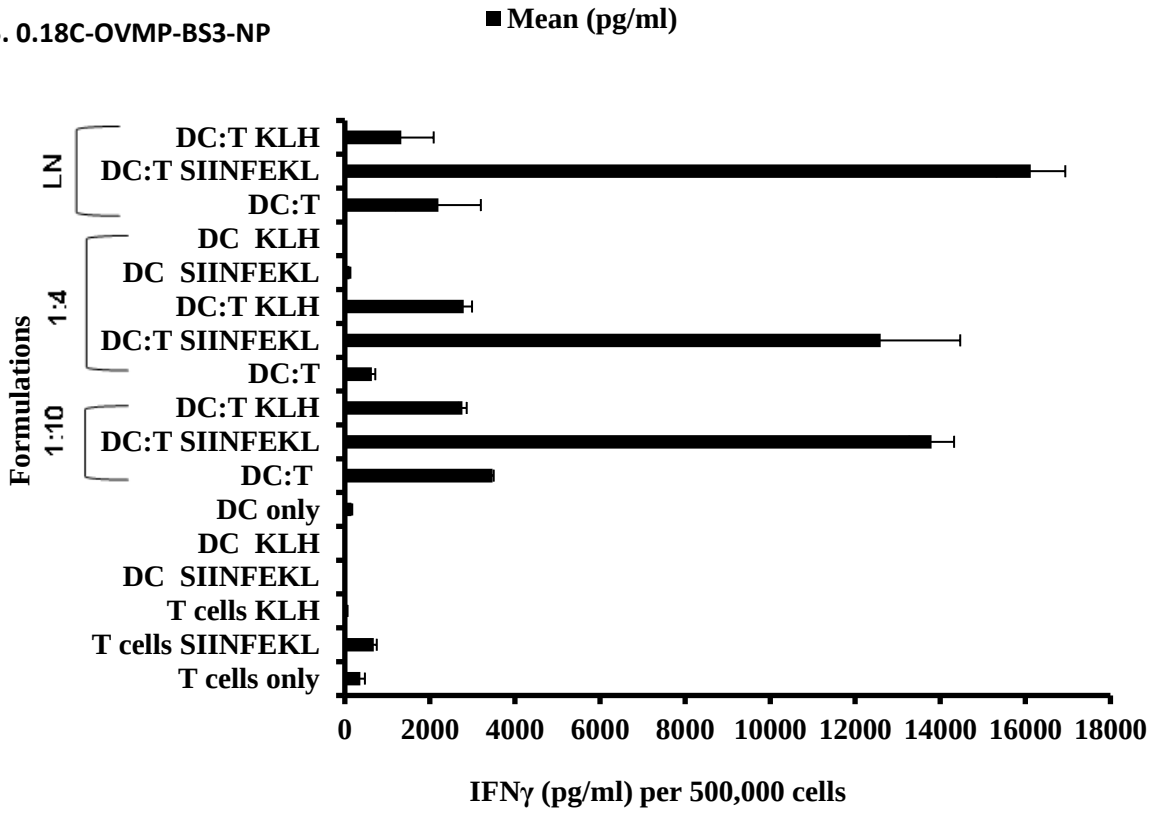


**6. 0.18C-OV-AD-NP**

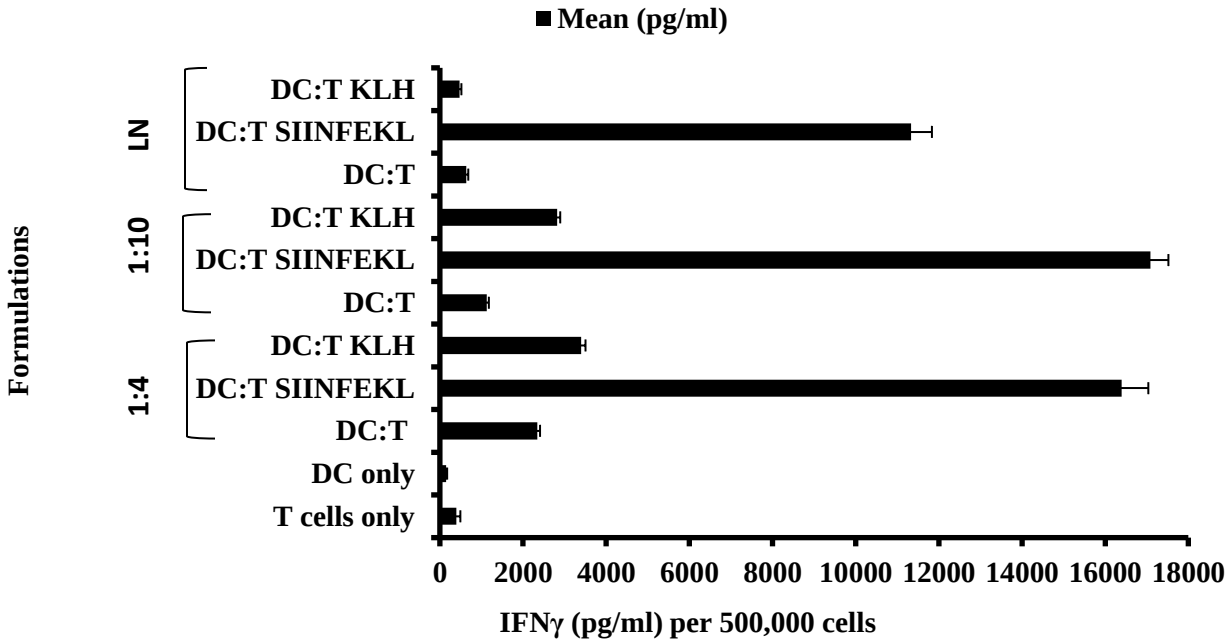

**7. 0.18C-OV-COV-NP**

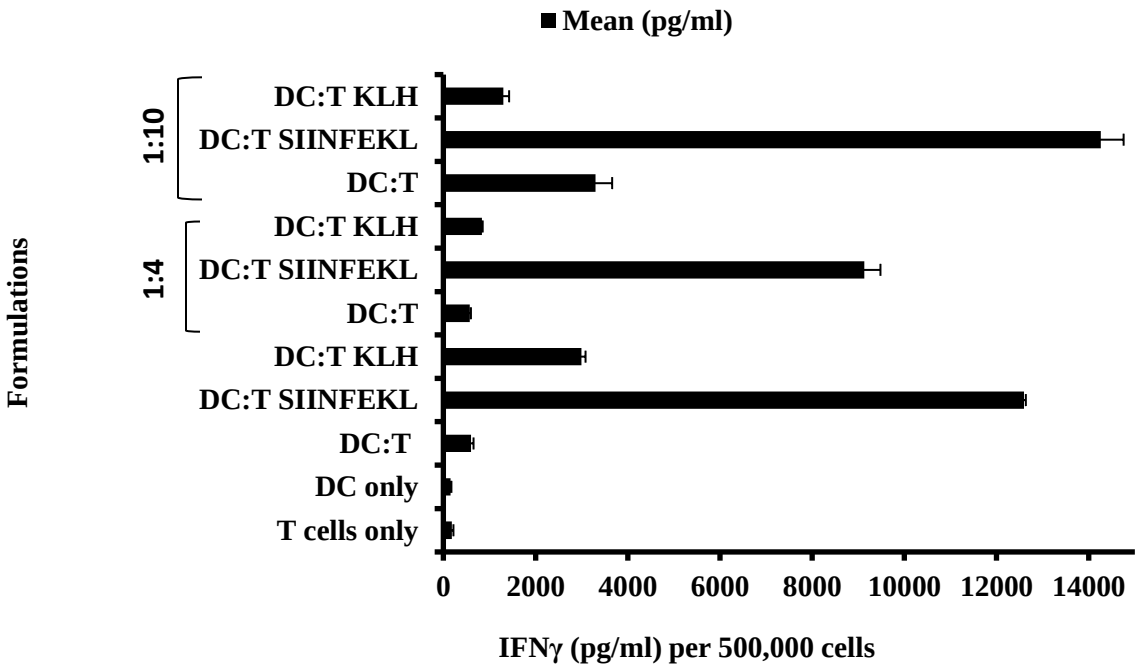


**8. 0.18C-OVMP-AD-NP**

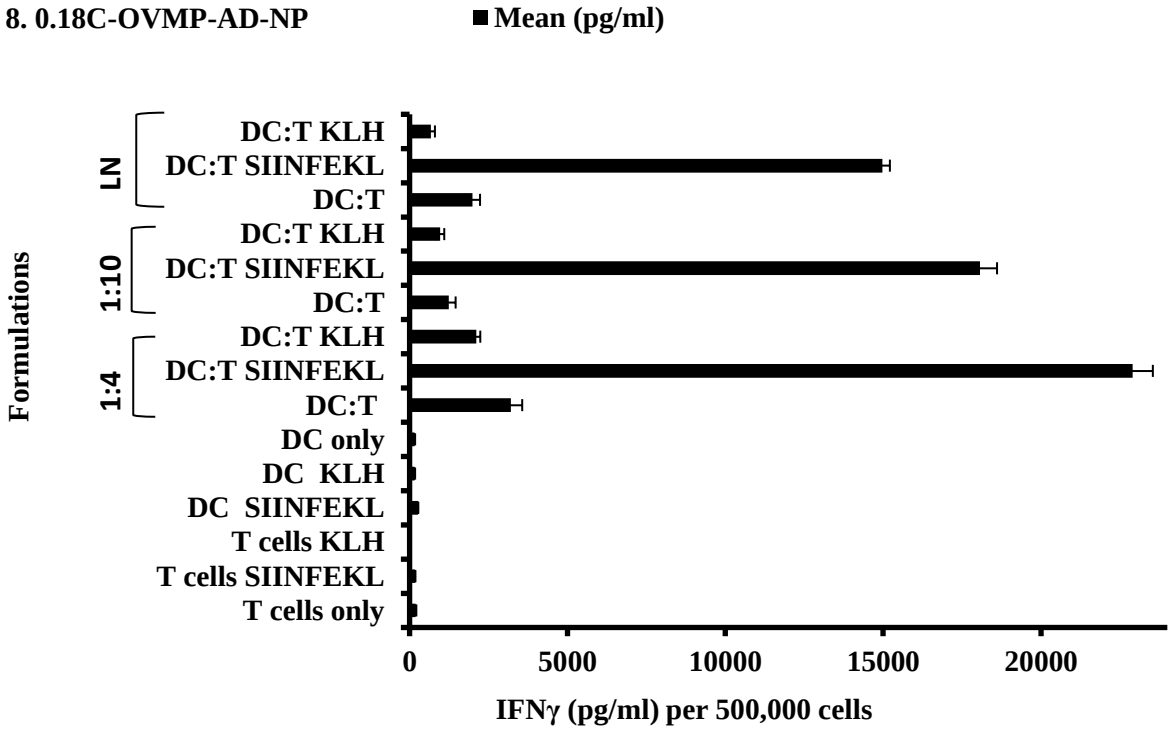

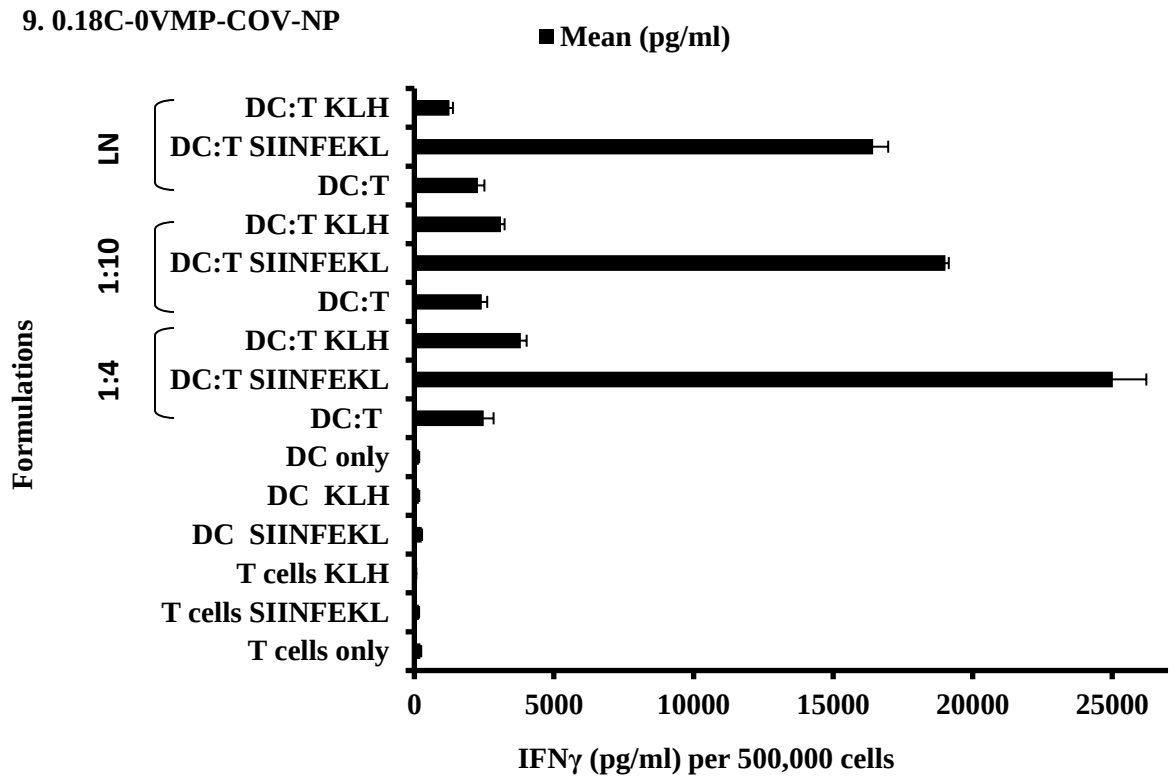


Figure F.7 (1-9): Effect of OVA/OVA-MPLA NPs for IFNγ secretion in DC: T co-culture supernatant on day 5. The ratio of DC: T was 1:4 and 1:10 where T cells was $1X10^5$ and DCs were $2.5X10^4$ and $1X10^4$. These T cells were isolated from splenocytes. Lymph node (LN) derived CD8 T cells were plated with DCs at 1:4 ratio (DC: T). After five days' incubation, culture supernatants were collected, stored and analyzed for IFNγ secretion. This figure is representative for nine groups as numbered above. (n=3) ($p<0.05$)

**1.Unimmunized mice**

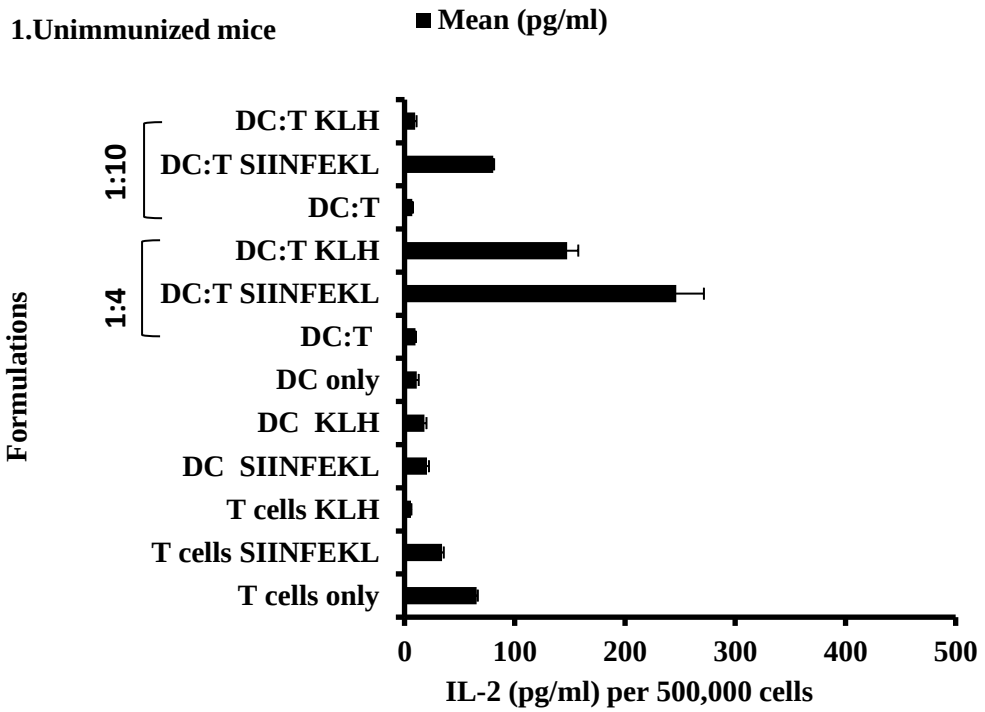


**2. Free OVA**

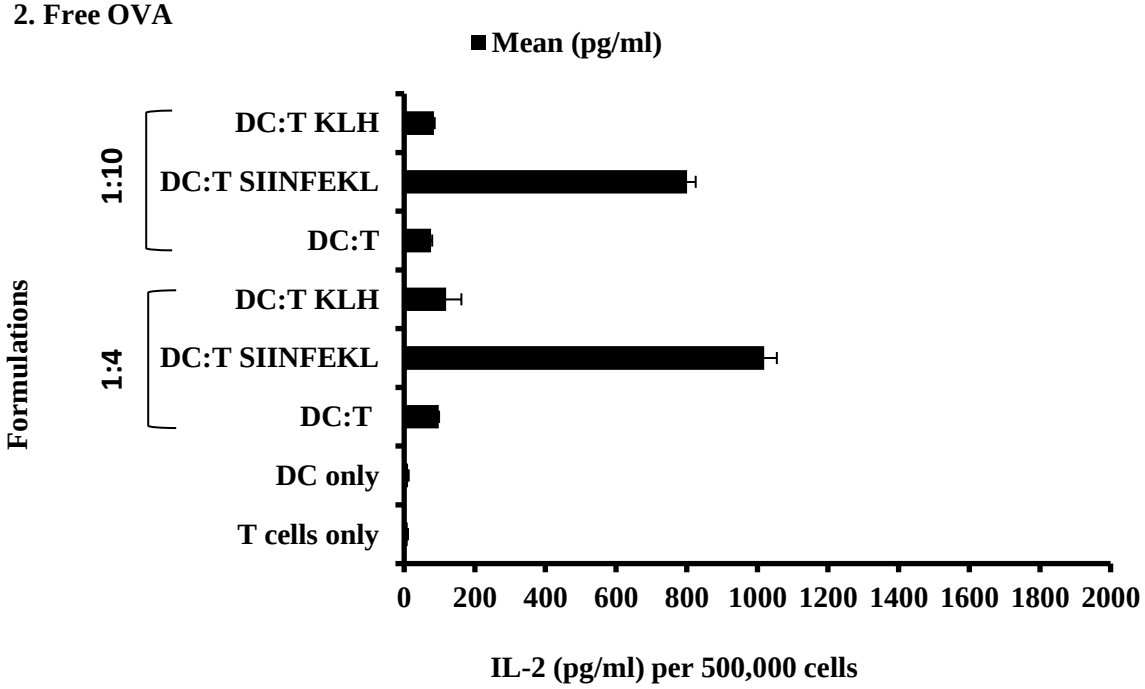

**3.Free OVMP**

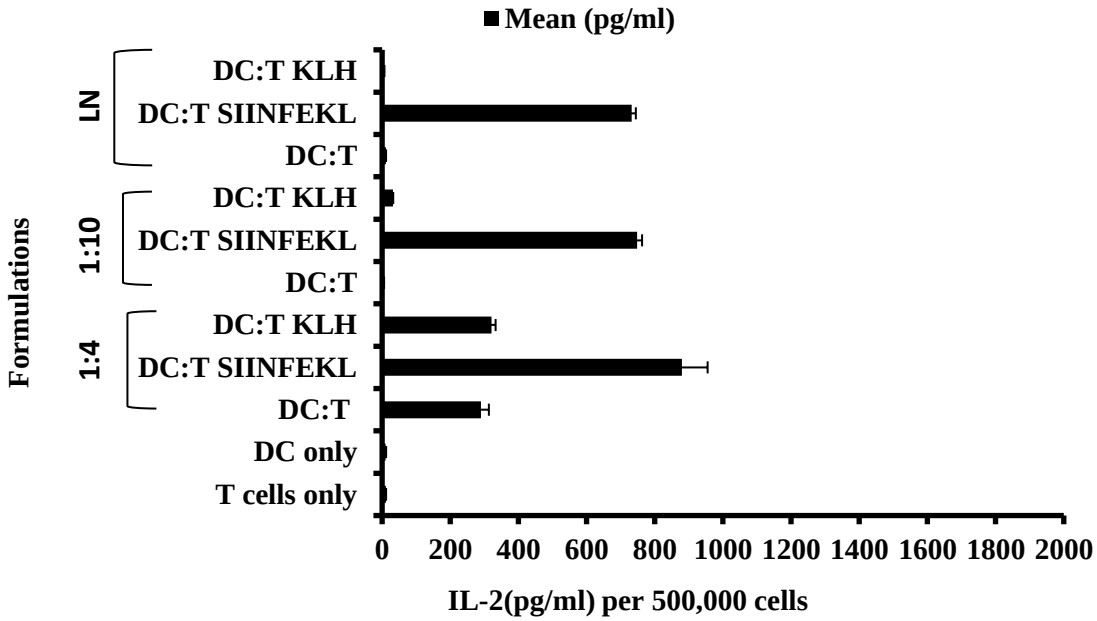


**4. 0.18C-OV-BS3-NP**

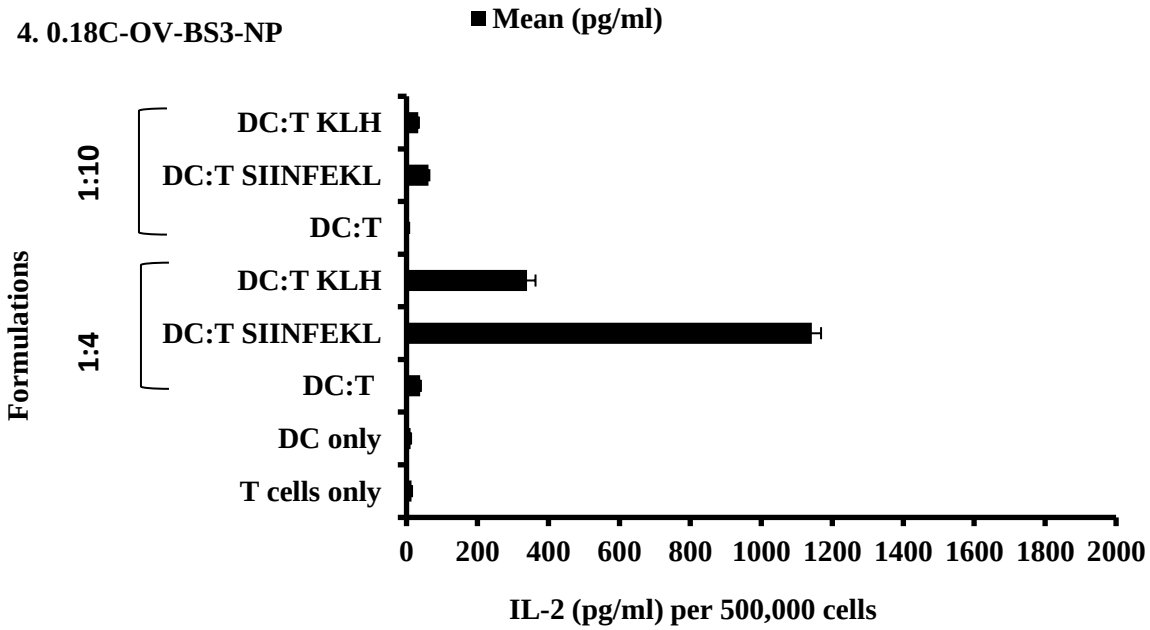

**5. 0.18C-OVMP-BS3-NP**

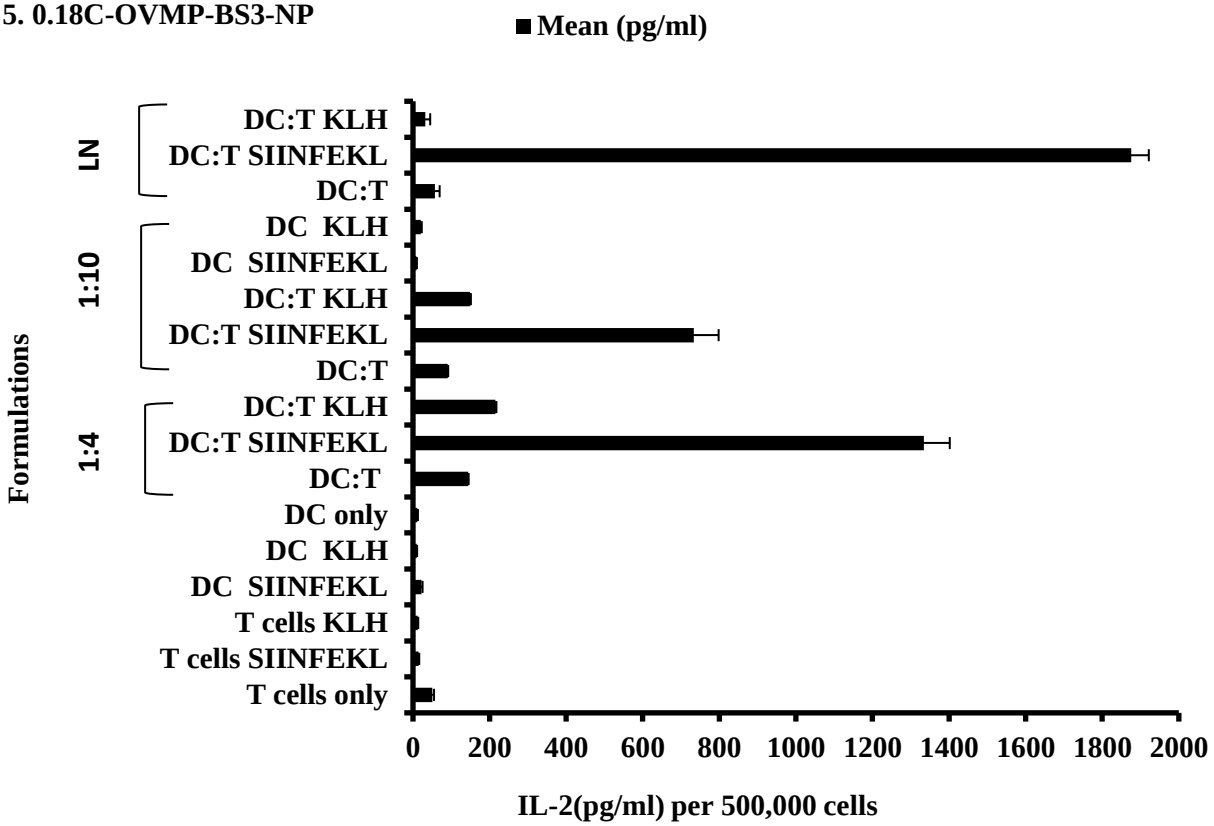


**6. 0.18C-OV-AD-NP**

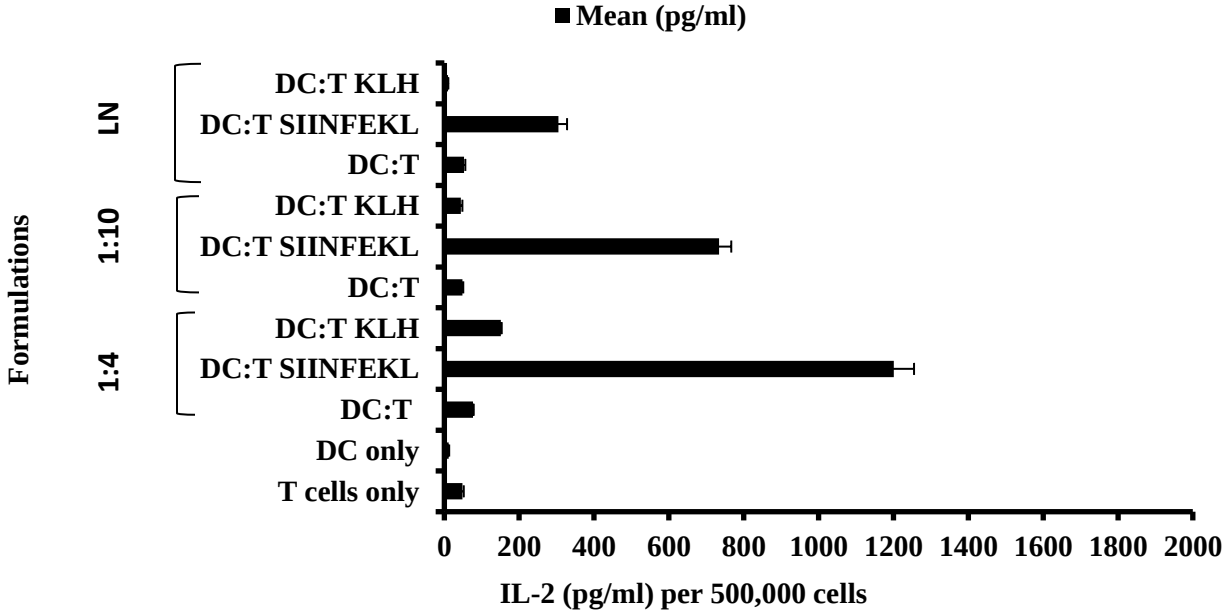

**7. 0.18C-OV-COV-NP**

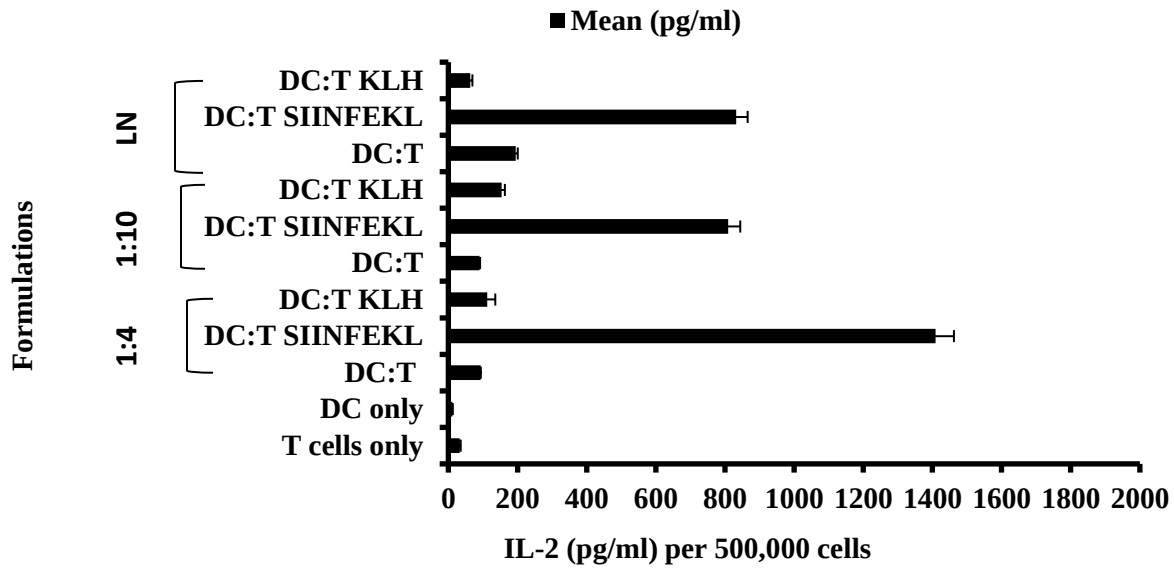


**8. 0.18C-OVMP-AD-NP**

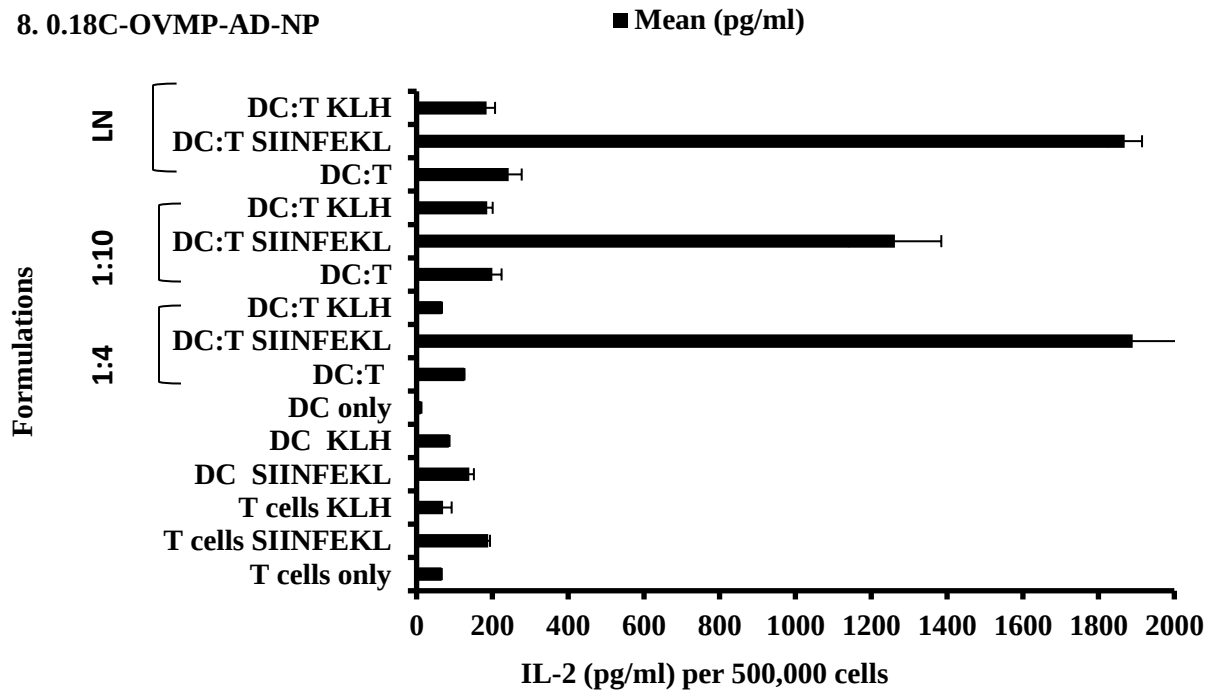

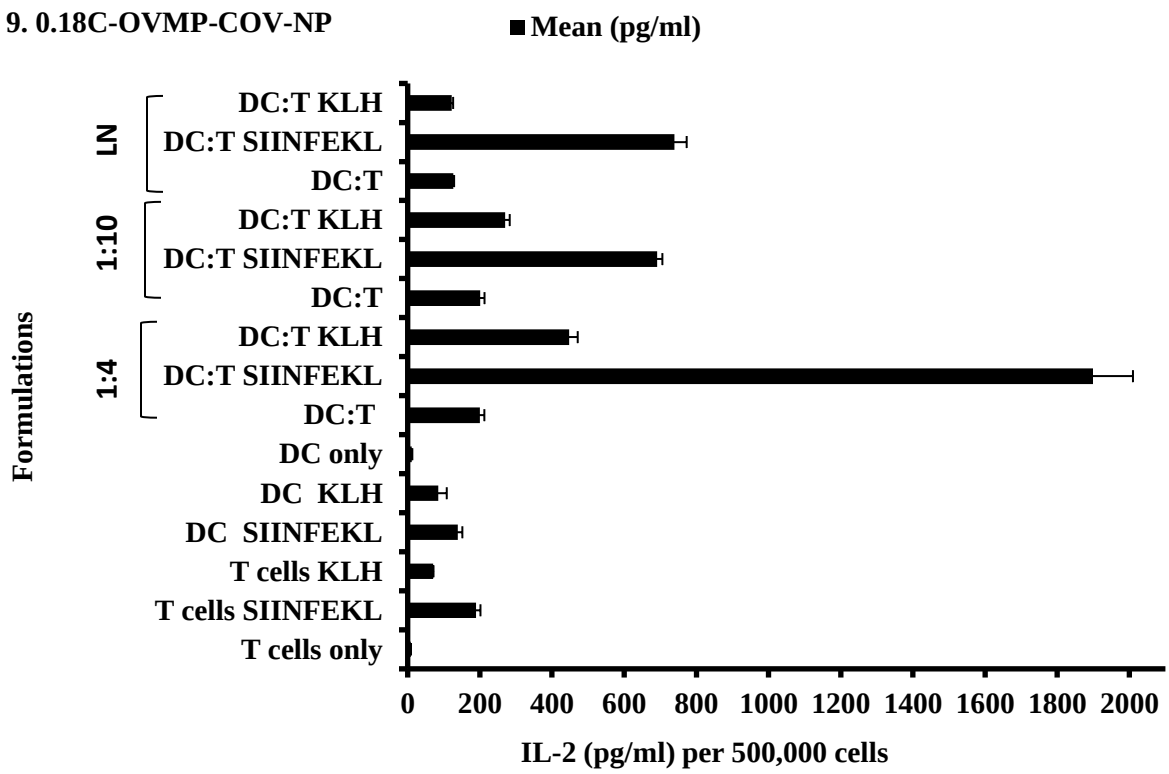


Figure F.8 (1-9): Effect of OVA/OVA-MPLA NPs for IL-2 secretion in DC: T co-culture supernatant on day 5. The ratio of DC: T was 1:4 and 1:10 where T cells was $1X10^5$ and DCs were $2.5X10^4$ and $1X10^4$. These T cells were isolated from splenocytes. Lymph node (LN) derived CD8 T cells were plated with DCs at 1:4 ratio (DC: T). After five days' incubation, culture supernatants were collected, stored and analyzed for IL-2 secretion. This figure is representative for nine groups as numbered above. (n=3) ($p<0.05$)

**1. Unimmunized mice**

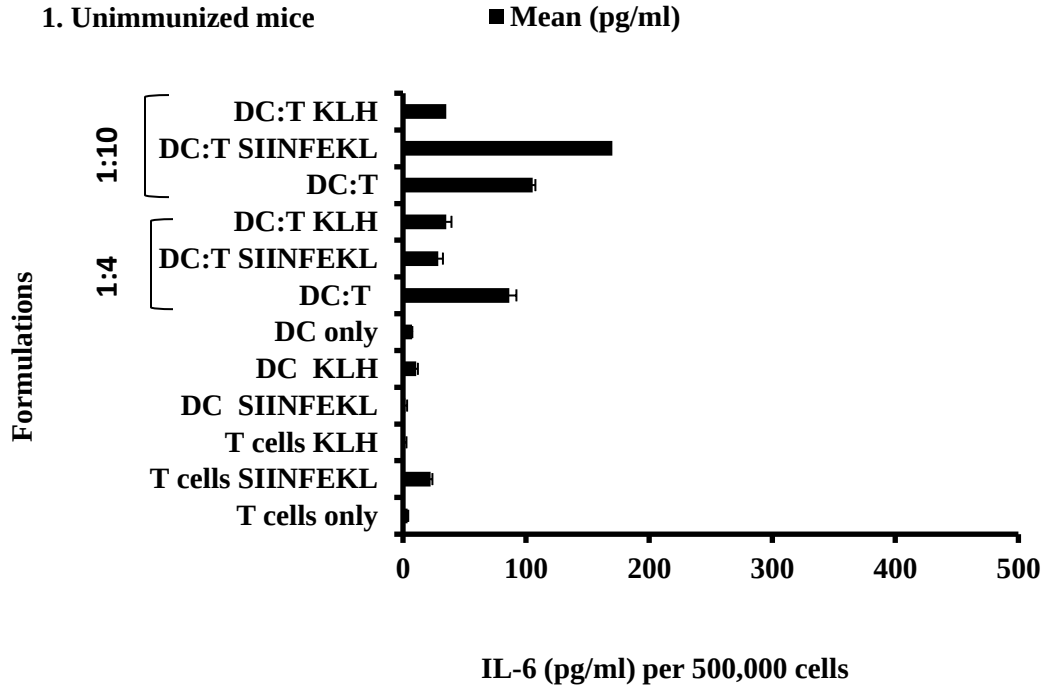


**2. Free OVA**

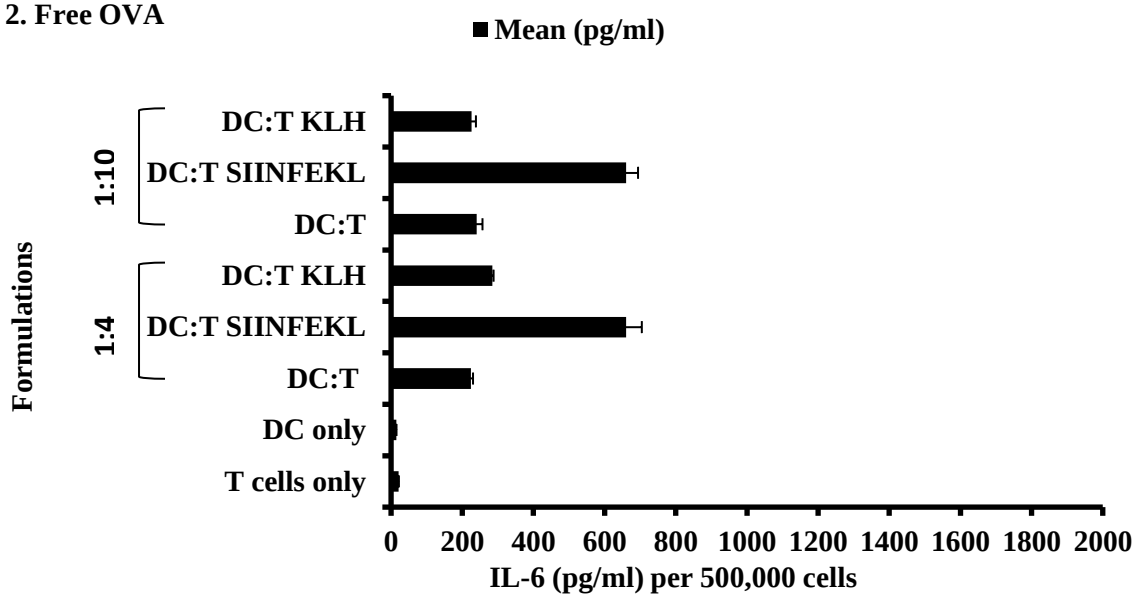

**3. Free OVMP**

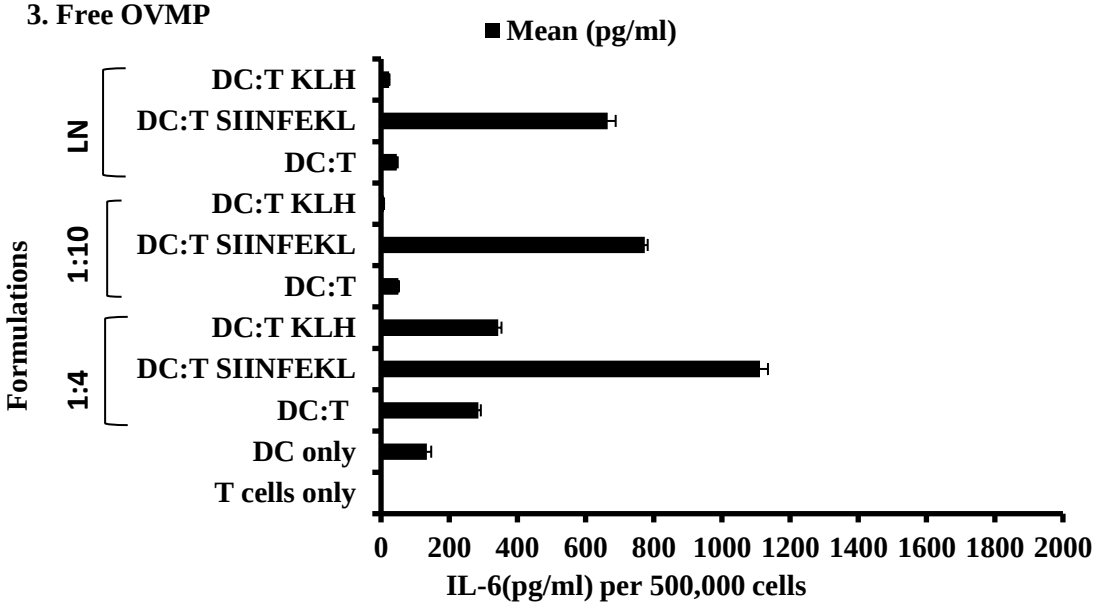


**4. 0.18C-OV-BS3-NP**

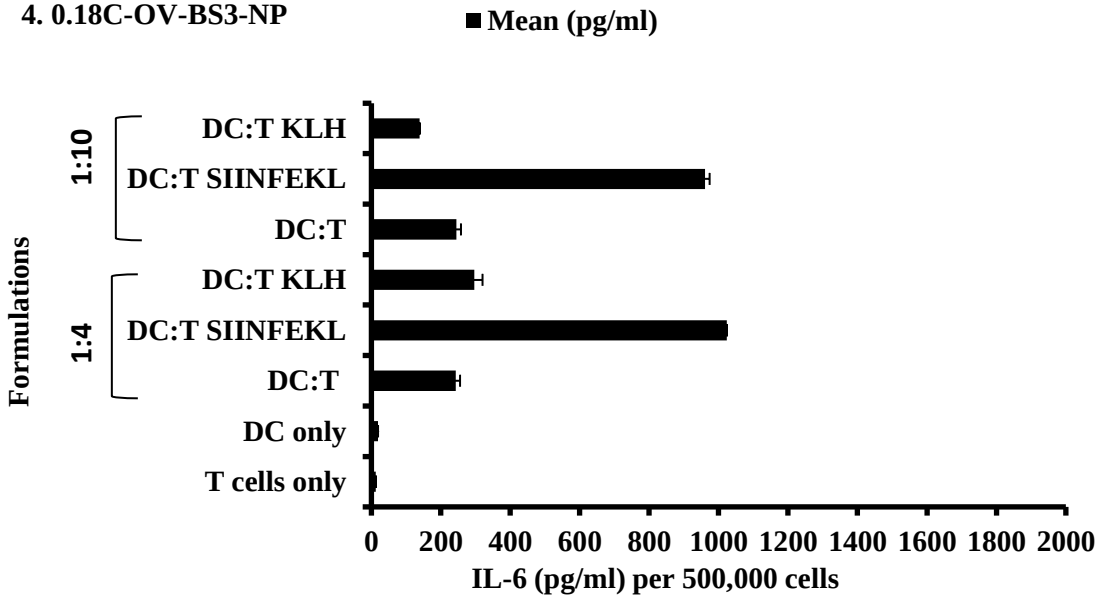

**5. 0.18C-OVMP-BS3-NP**

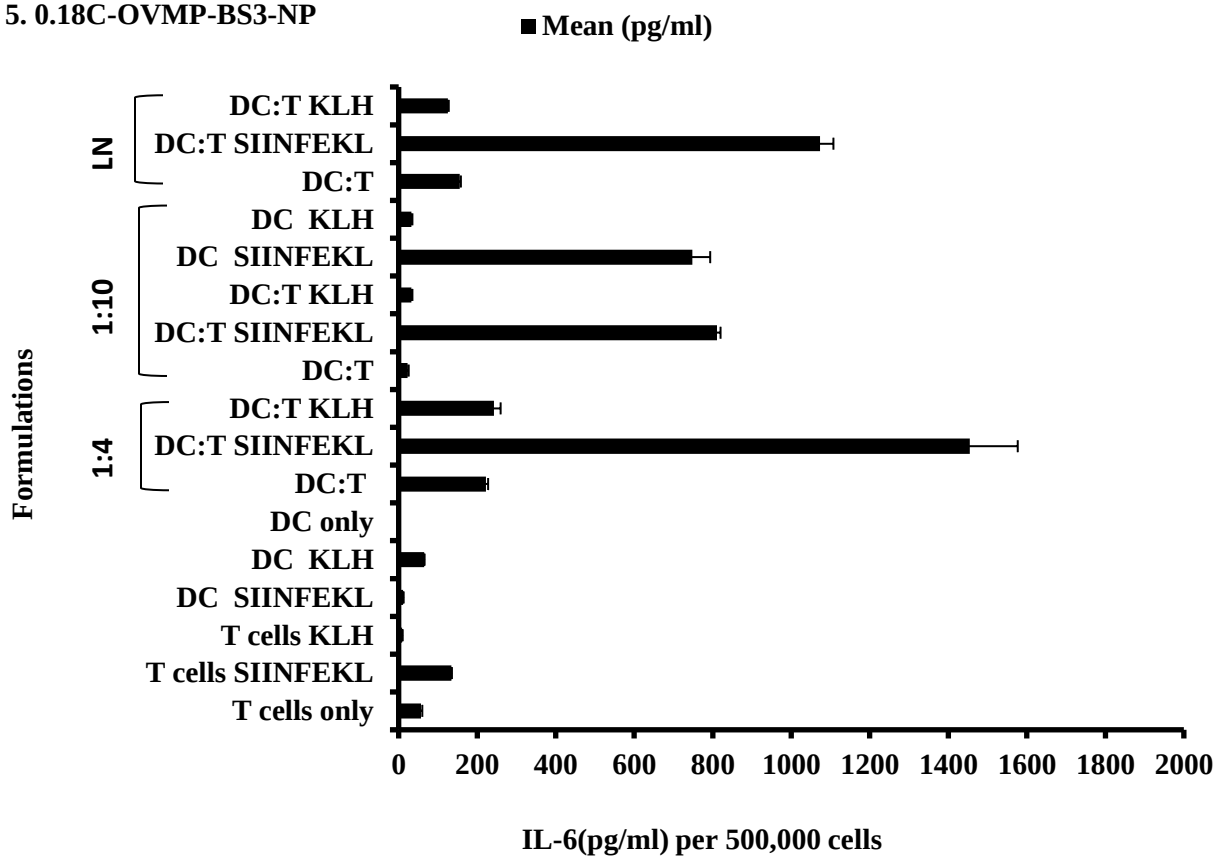


**6. 0.18C-OV-AD-NP**

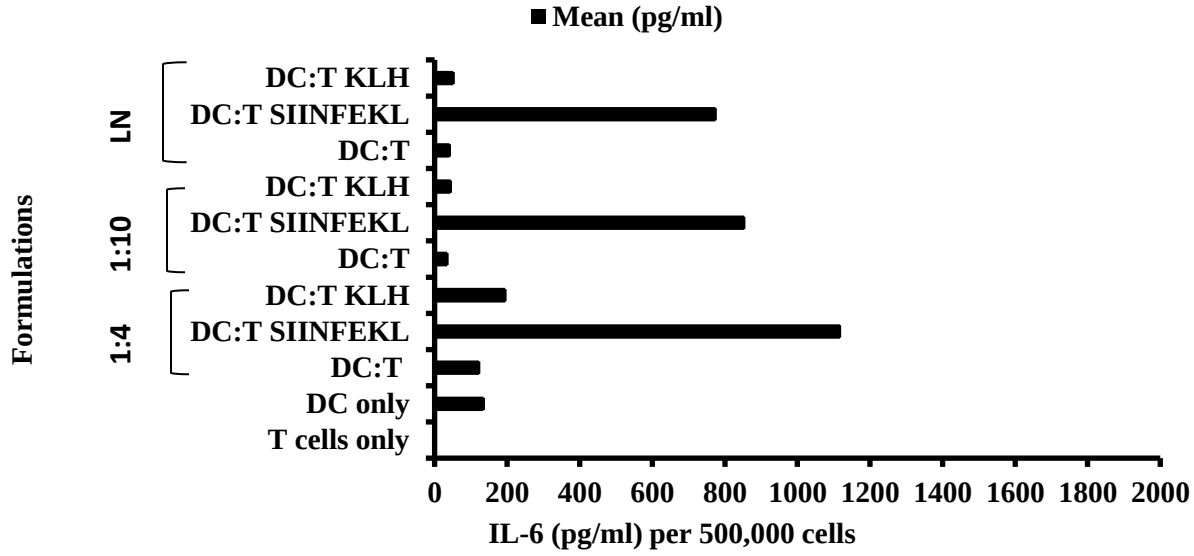

**7. 0.18C-OV-COV-NP**

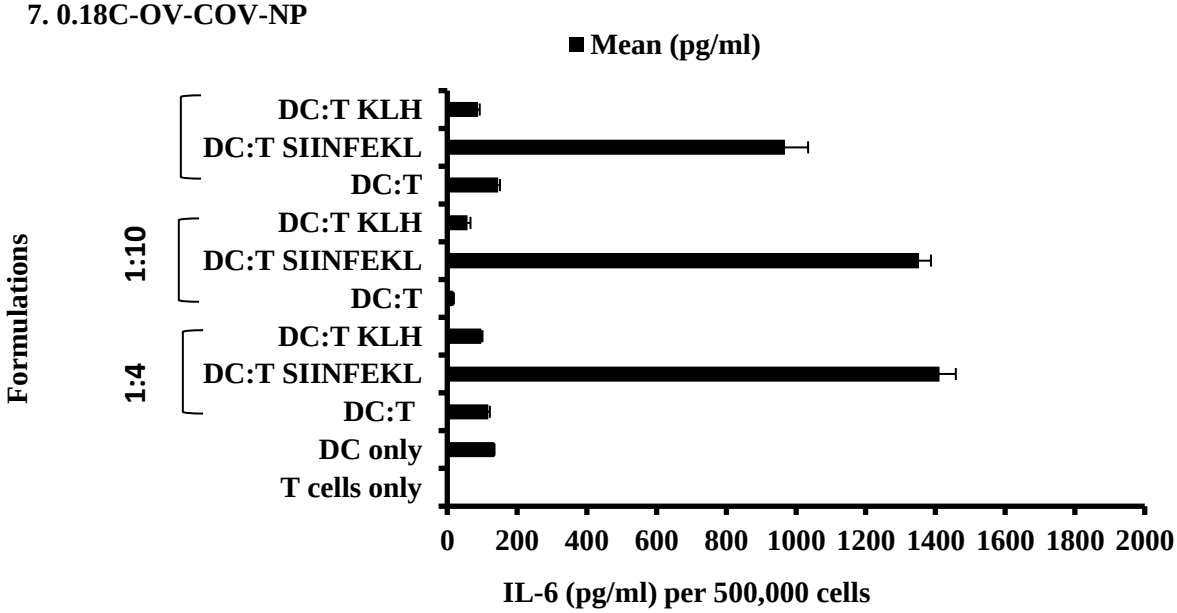


**8. 0.18C-OVMP-AD-NP**

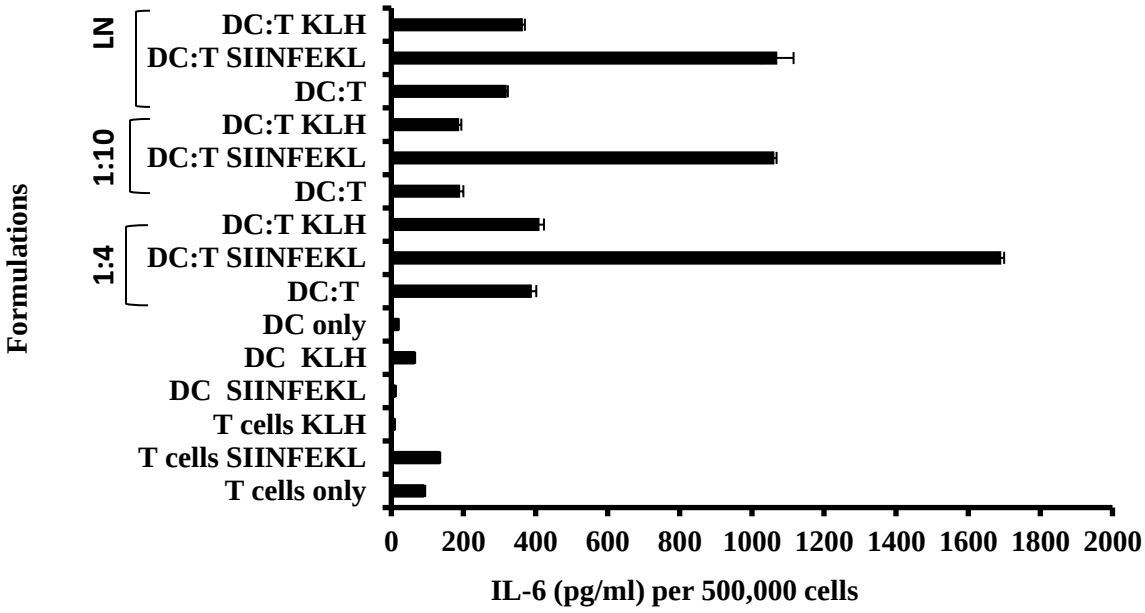

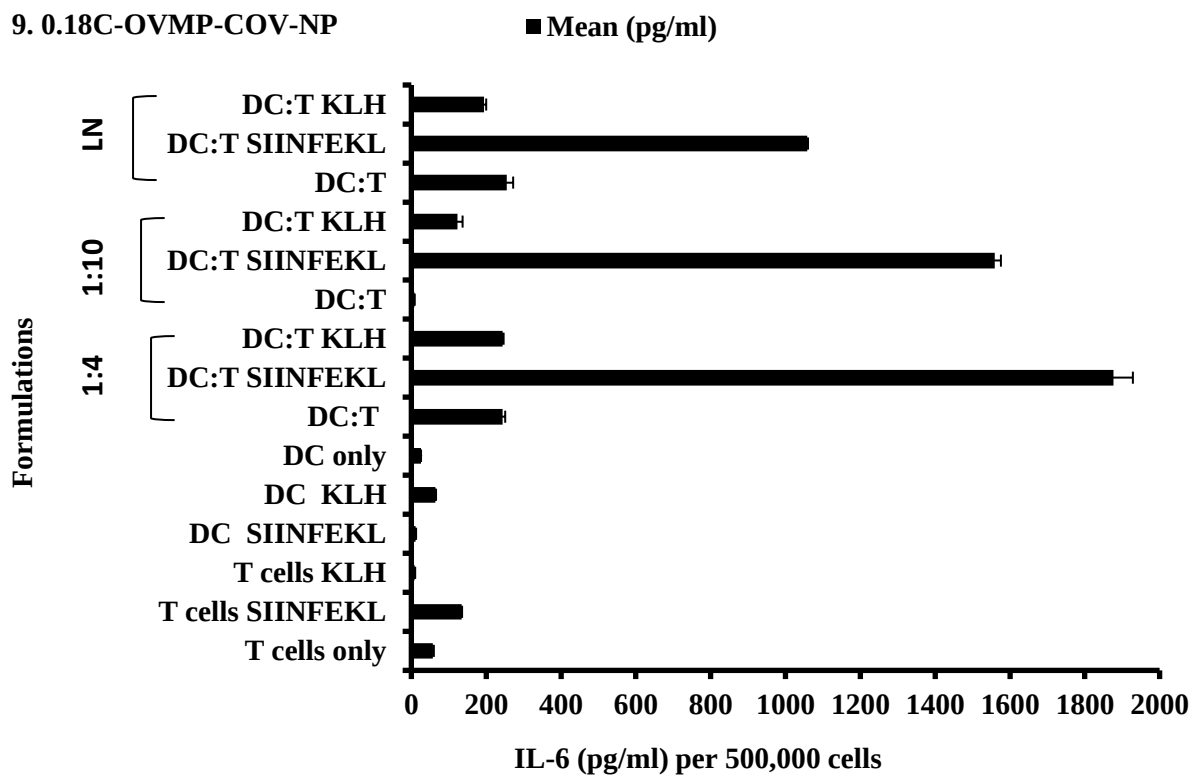


Figure F.9 (1-9): Effect of OVA/OVA-MPLA NPs for IL-6 secretion in DC: T co-culture supernatant on day 5. The ratio of DC: T was 1:4 and 1:10 where T cells was $1X10^5$ and DCs were $2.5X10^4$ and $1X10^4$. These T cells were isolated from splenocytes. Lymph node (LN) derived CD8 T cells were plated with DCs at 1:4 ratio (DC: T). After five days' incubation, culture supernatants were collected, stored and analyzed for IL-6 secretion. This figure is representative for nine groups as numbered above. (n=3) ($p<0.05$)

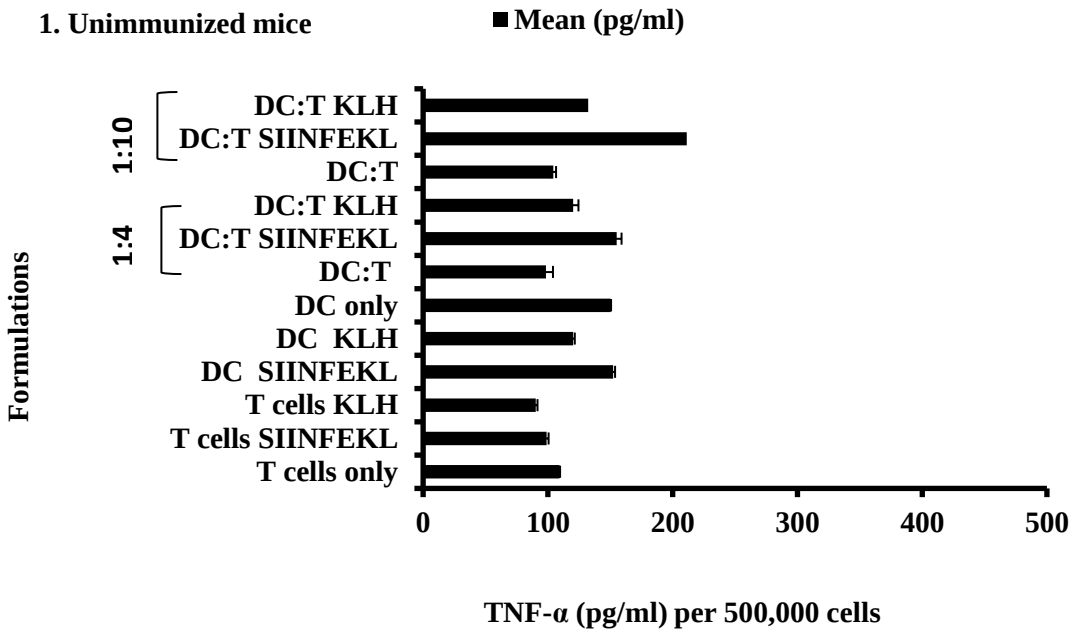
1. Unimmunized mice
Mean (pg/ml)
Formulations
1:10
1:4
DC:T KLH
DC:T SIINFEKL
DC:T
DC:T KLH
DC:T SIINFEKL
DC:T
DC only
DC KLH
DC SIINFEKL
T cells KLH
T cells SIINFEKL
T cells only
0
100
200
300
400
500
TNF-α (pg/ml) per 500,000 cells

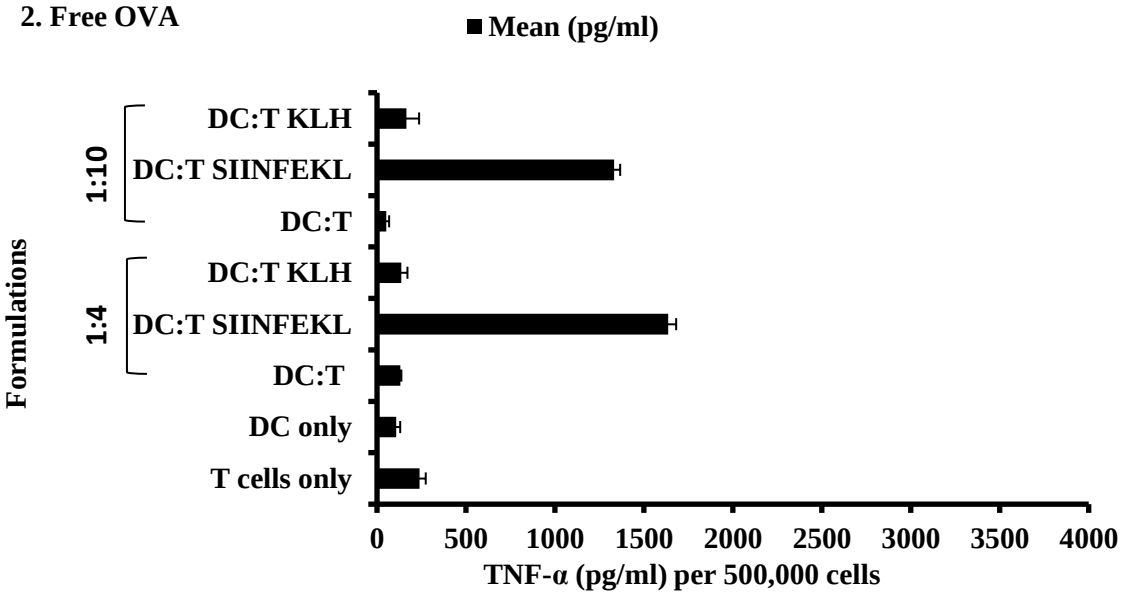
2. Free OVA
Mean (pg/ml)
Formulations
1:10
1:4
DC:T KLH
DC:T SIINFEKL
DC:T
DC:T KLH
DC:T SIINFEKL
DC:T
DC only
T cells only
0
500
1000
1500
2000
2500
3000
3500
4000
TNF-α (pg/ml) per 500,000 cells

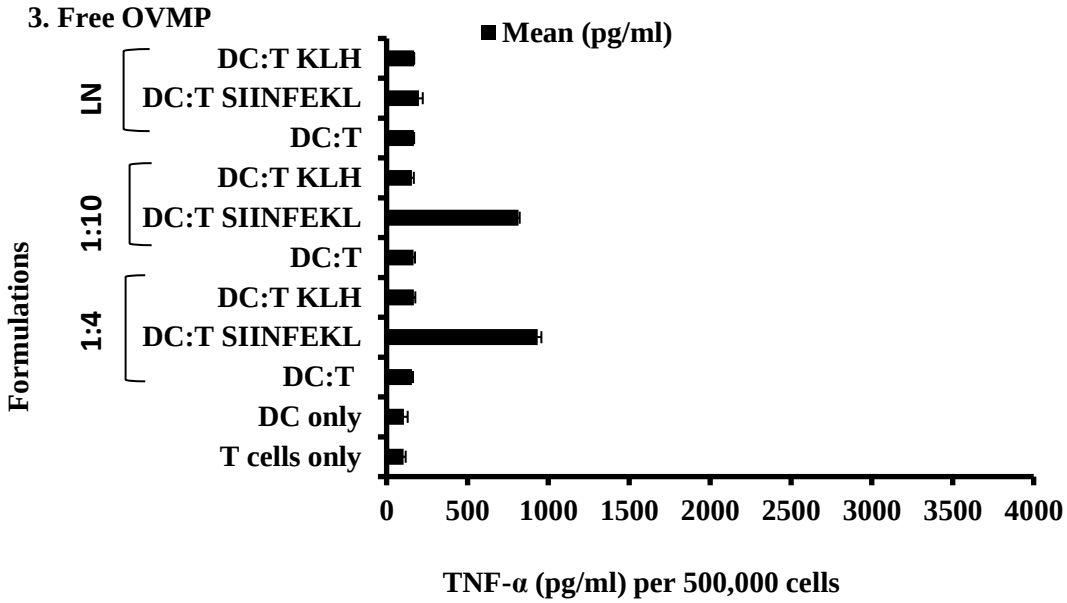
3. Free OVMP
Mean (pg/ml)
DC:T KLH
DC:T SIINFEKL
DC:T
DC:T KLH
DC:T SIINFEKL
DC:T
DC:T KLH
DC:T SIINFEKL
DC:T
DC only
T cells only
LN
1:10
1:4
Formulations
0
500
1000
1500
2000
2500
3000
3500
4000
TNF-α (pg/ml) per 500,000 cells

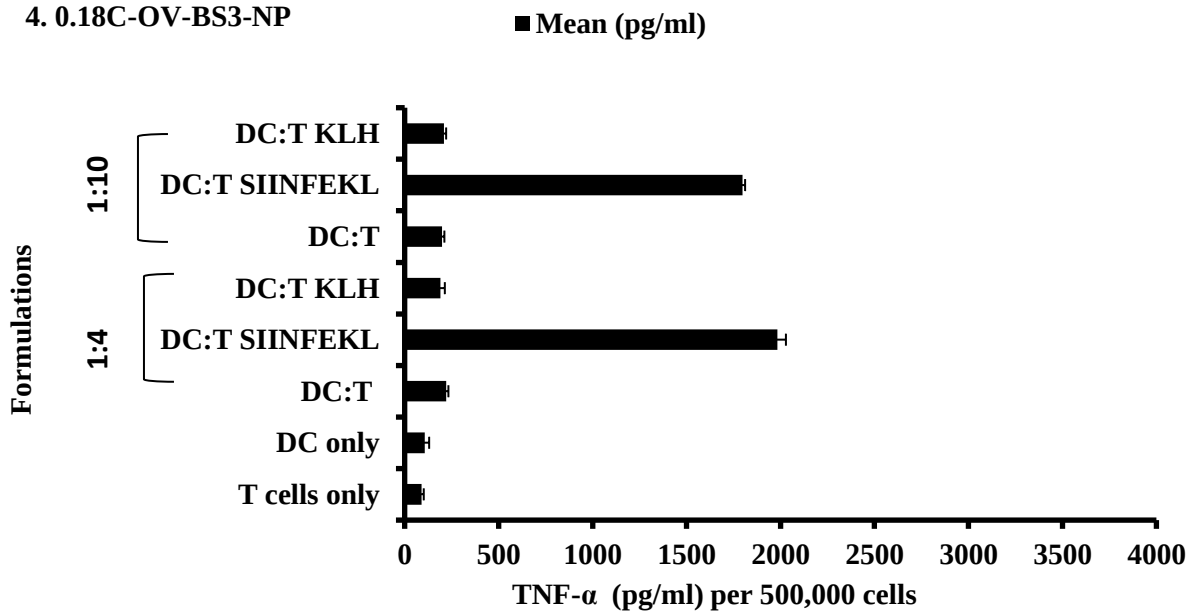
4. 0.18C-OV-BS3-NP
Mean (pg/ml)
DC:T KLH
DC:T SIINFEKL
DC:T
DC:T KLH
DC:T SIINFEKL
DC:T
DC only
T cells only
1:10
1:4
Formulations
0
500
1000
1500
2000
2500
3000
3500
4000
TNF-α (pg/ml) per 500,000 cells

**5. 0.18C-OVMP-BS3-NP**

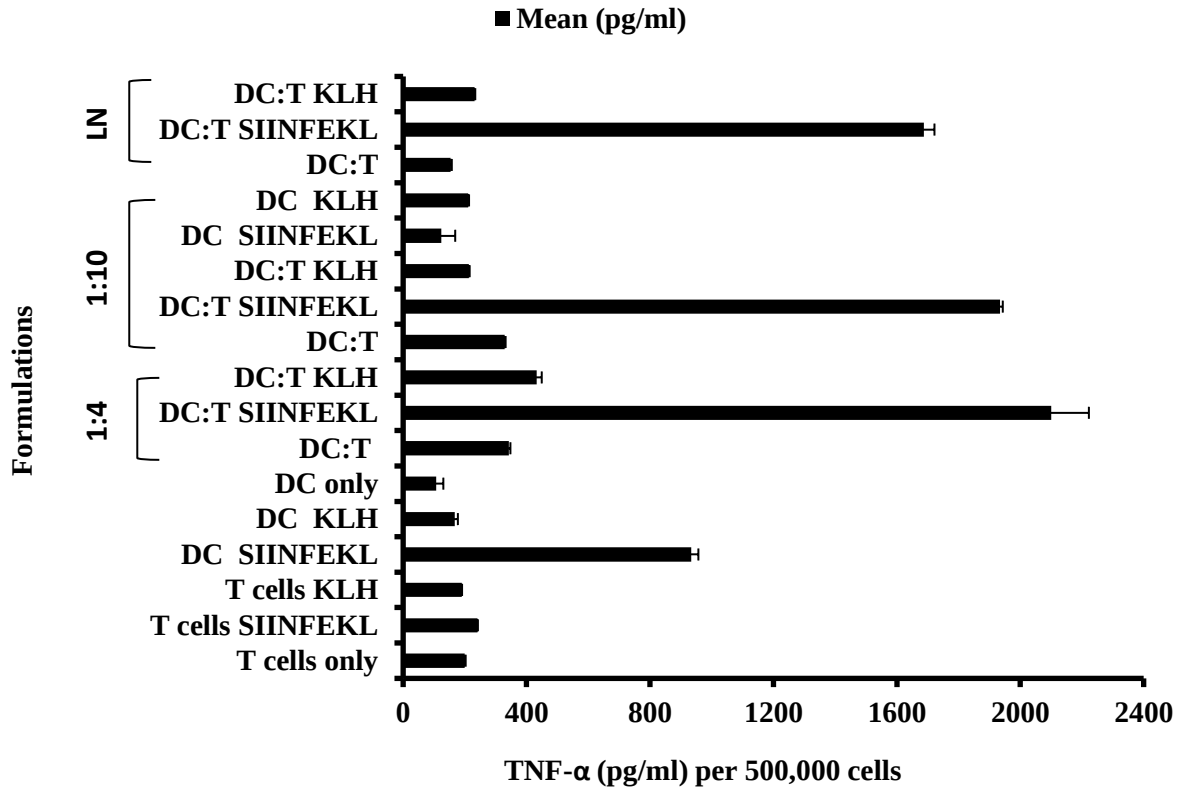


**6. 0.18C-OV-AD-NP**

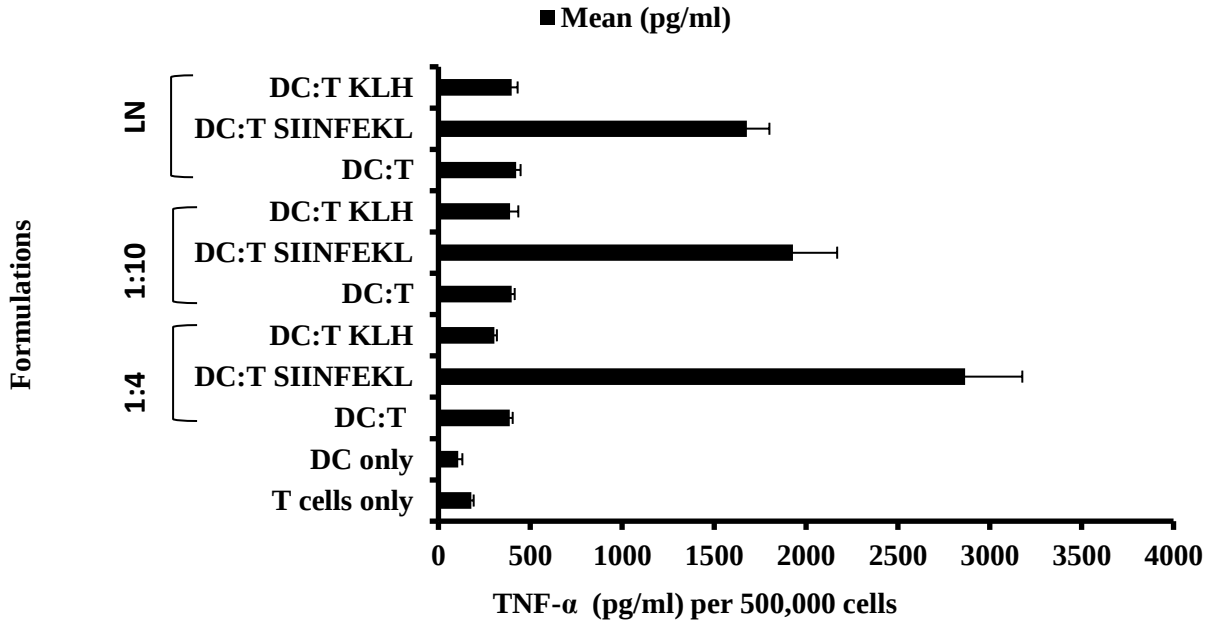

**7. 0.18C-OV-COV-NP**

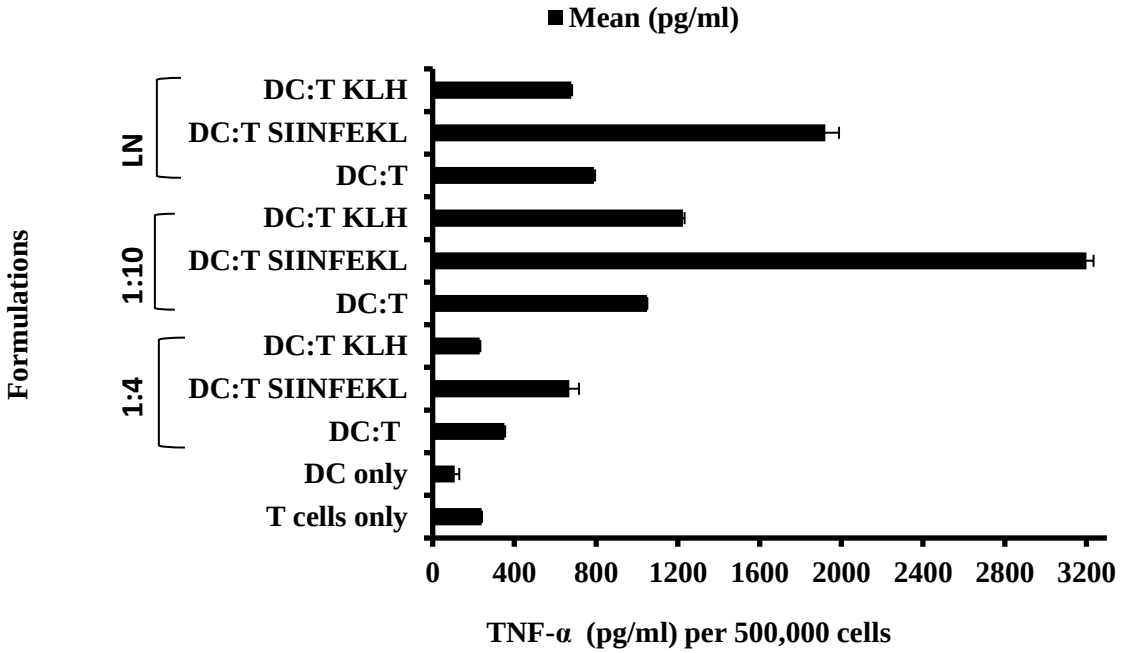


**8. 0.18C-OVMP-AD-NP**

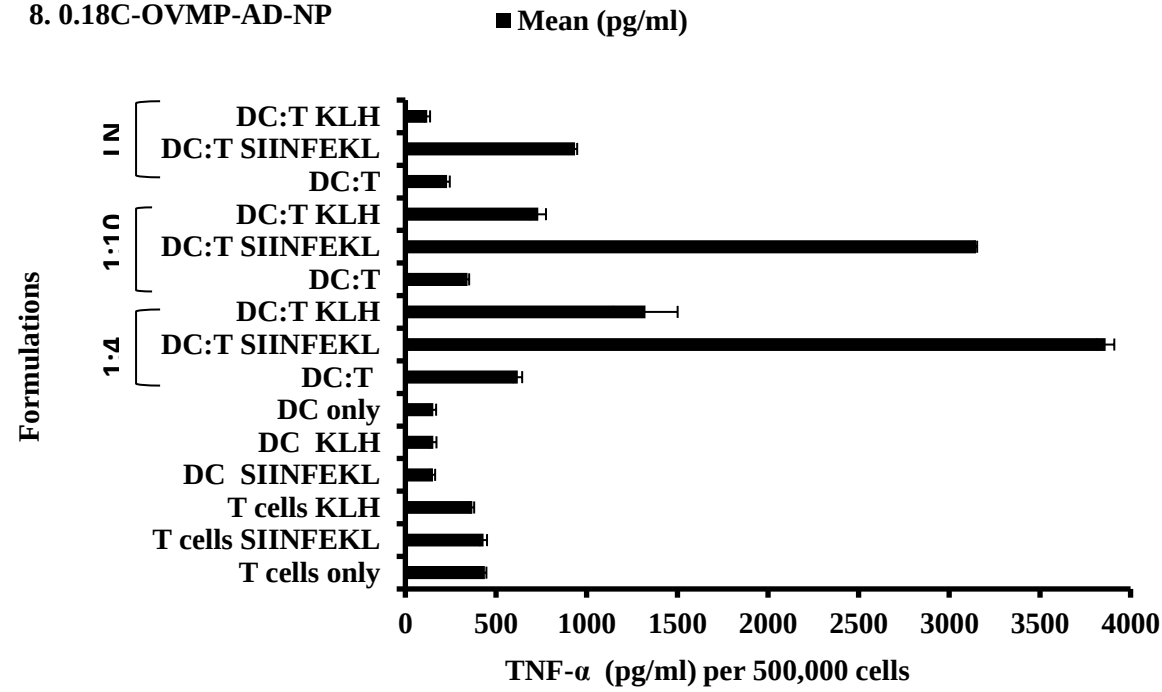

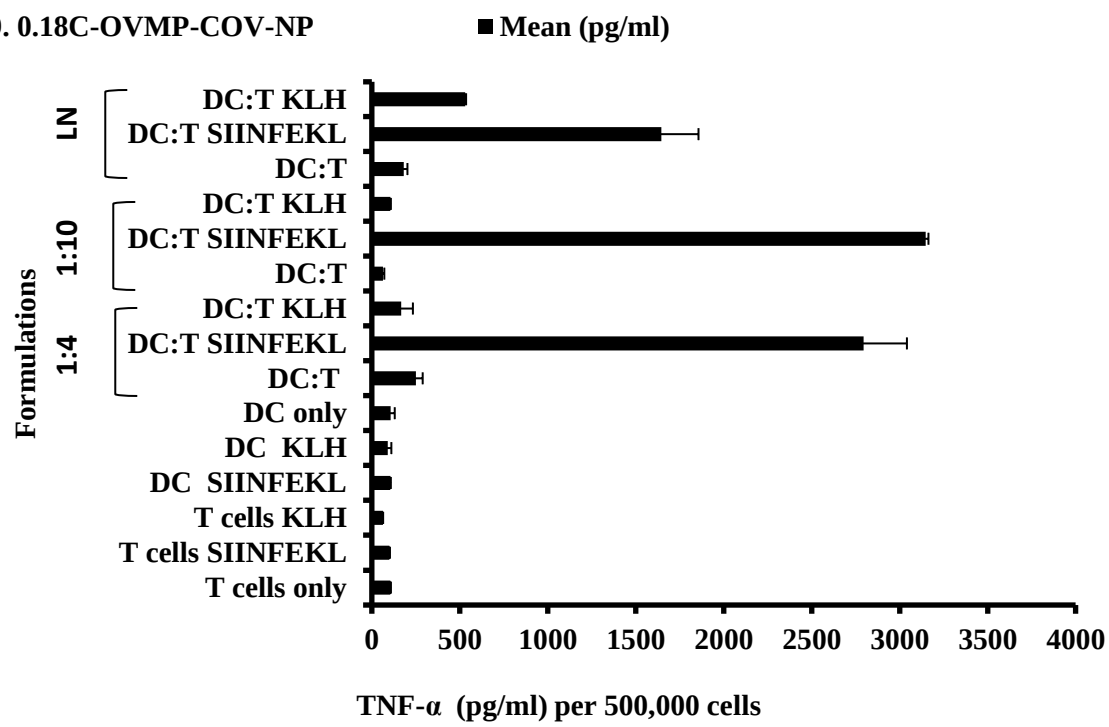


Figure F.10 (1-9): Effect of OVA/OVA-MPLA NPs for cytokines secretion in DC: T co-culture supernatant on day 5. Notes: The ratio of DC: T was 1:4 and 1:10 where T cells was $1X10^5$ and DCs were $2.5X10^4$ and $1X10^4$. These T cells were isolated from splenocytes. Lymph node (LN) derived CD8 T cells were plated with DCs at 1:4 ratio (DC: T). After five days' incubation, culture supernatants were collected, stored and analyzed for TNF-α secretion. This figure is representative for nine groups as numbered above. (n=3) ($p<0.05$)

# Appendix G

# Permission to reprint published paper

(Investigation and optimization of formulation parameters on preparation of targeted anti CD205 tailored PLGA nanoparticles)

## Dove Medical Press update on your published paper

1 message

**Tania Olliver** <tania@dovepress.com> Tue, Apr 26, 2016 at 5:49 PM
To: Tasnim Jahan <stj885@mail.usask.ca>

Dear Mrs Jahan

Thank you for your email.

You may use your paper in your thesis as long as you properly cite it, and the online version is linked to the original paper. Please see the information on the website http://www.dovepress.com/author_guidelines.php?content_id=696

Kind regards

Tania

**Tania Olliver**

**Editorial Manager, Dove Medical Press Ltd**

44 Corinthian Drive, Albany, Auckland, New Zealand

PO Box 300-008, Albany, Auckland, 0752, New Zealand

**p** +649 443 3060 (Extn 201) **f** +649 443 3061 **e** tania@dovepress.com

**Live Chat** http://www.dovepress.com/live_help.t

**Facebook** https://www.facebook.com/DoveMedicalPress

**Twitter** http://twitter.com/DovePress

**From:** tjahan123@gmail.com [mailto:tjahan123@gmail.com] **On Behalf Of** Tasnim Jahan
**Sent:** Wednesday, 27 April 2016 9:27 a.m.

**To:** Tania Olliver <tania@dovepress.com>
**Subject:** Re: Dove Medical Press update on your published paper

Hi,

I want to include my journal "Investigation and optimization of formulation parameters on preparation of targeted anti CD205 tailored PLGA nanoparticles" in my PhD thesis dissertation. What is the process to get permission to include this paper as a section?

Regards
Sheikh Tasnim Jahan
PhD candidate
Division of Pharmacy
College of Pharmacy and Nutrition
University of Saskatchewan.